# The American Mineralogist

*Journal of the Mineralogical Society of America*

Vol. 36 JANUARY-FEBRUARY, 1951 Nos. 1 and 2

## *Contents*





Published bi-monthly by the Society

# Mineralogical Society of America

ASSOCIATED WITH THE GEOLOGICAL SOCIETY OF AMERICA

*President:* Adolf Pabst, University of California, Berkeley, California.
*Vice President:* Michael Fleischer, U. S. Geological Survey, Washington 25, D. C.
*Secretary:* C. S. Hurlbut, Jr., Harvard University, Cambridge, Massachusetts.
*Treasurer:* Earl Ingerson, U. S. Geological Survey, Washington 25, D.C.
*Editor:* Walter F. Hunt, University of Michigan, Ann Arbor, Michigan.
*Councilors:* Clifford Frondel, Harvard University, Cambridge, Massachusetts.
Lewis S. Ramsdell, University of Michigan, Ann Arbor, Michigan.
E. F. Osborn, School of Mineral Industries, Pennsylvania State College, Pennsylvania.
George T. Faust, U. S. Geological Survey, Washington 25, D. C.
George Tunell, University of California at Los Angeles, California.

---

The enlarged issues of this journal for 1951 are made possible by a grant from the Penrose Fund of the Geological Society of America.


## The American Mineralogist—Journal of the Mineralogical Society of America

A journal containing articles on mineralogy, crystallography, petrography, and allied sciences, issued every two months. Contributions are invited from everyone.


Office of Publication, Mineralogical Laboratory, Ann Arbor, Mich.


The general conduct of the journal is in the hands of the Editor, **Walter F. Hunt**, Ann Arbor, Michigan. The council of the Mineralogical Society has appointed the following board of associate editors, to whom should be sent articles dealing with the special subjects indicated:

Michael Fleischer, U. S. Geological Survey, Washington, D.C., *New minerals.*
Esper S. Larsen, U. S. Geological Survey, Washington, D.C., *Optical crystallography*
Austin F. Rogers, Stanford University, California, *Geometrical crystallography.*
M. N. Short, University of Arizona, Tucson, Arizona, *Mineralography.*
George Tunell, University of California at Los Angeles, *Structural crystallography.*

Contributors of leading articles are given without charge 100 reprints (without covers) of their article. If additional reprints are desired these can be purchased at the following rates:

| *Pages* | *1–4* | *5–8* | *9–12* | *13–16* | *17–20* | *21–24* | *25–28* | *29–32* | *Covers* |
|---|---|---|---|---|---|---|---|---|---|
| *Copies* | | | | | | | | | |
| 25 | $3.50 | $5.00 | $ 8.00 | $ 9.50 | $11.00 | $13.00 | $15.00 | $16.00 | $4.90 |
| 50 | 3.80 | 5.55 | 8.80 | 10.40 | 12.10 | 14.20 | 16.40 | 17.50 | 5.50 |
| 75 | 4.10 | 6.10 | 9.60 | 11.30 | 13.20 | 15.40 | 17.80 | 19.00 | 6.10 |
| 100 | 4.40 | 6.65 | 10.40 | 12.20 | 14.30 | 16.60 | 19.20 | 20.50 | 6.70 |
| Addl. C's | 1.20 | 2.20 | 3.20 | 3.60 | 4.40 | 4.80 | 5.60 | 6.00 | 2.40 |

Cover Composition $1.55.


Sent to all members and fellows of the Mineralogical Society of America. Subscription price, $4.00 per year (single copies of normal issues, $1.00 plus postage).

Entered as second class matter at the post office at Menasha, Wis., under Act of March 3, 1879. Acceptance for mailing at the special rate of postage provided for in section 1103, Act of Oct. 3, 1917, paragraph 4 section 429 P. L. & R. authorized March 13, 1922.

Notices of change of address, orders, and remittances should be sent to Dr. Earl Ingerson, U.S. Geological Survey, Washington 25, D. C.

Printed by the George Banta Publishing Company, Menasha, Wisconsin

# THE AMERICAN MINERALOGIST

JOURNAL OF THE MINERALOGICAL SOCIETY OF AMERICA

Vol. 36 JANUARY-FEBRUARY, 1951 Nos. 1 and 2


## THE URANIUM MINERALS FROM THE HILLSIDE MINE, YAVAPAI COUNTY, ARIZONA*


JOSEPH M. AXELROD, FRANK S. GRIMALDI, CHARLES MILTON, AND K. J. MURATA

*U. S. Geological Survey, Washington, D. C.*



ABSTRACT

Coating gypsum on the 300-foot level of the Hillside Mine, Yavapai County, Arizona, was a small deposit in which were found several hitherto unknown uranium minerals, together with schroeckingerite, which had been previously known only from Wyoming and Czechoslovakia. The new species are named andersonite, swartzite, and bayleyite; they are, respectively, hydrous uranyl carbonates of sodium and calcium, of calcium and magnesium, and of magnesium, all of general formula $X_4UO_2(CO_3)_3 \cdot nH_2O$, where $X_4$ represents respectively, $Na_2Ca$, CaMg, and $Mg_2$, and $n$, respectively, 6, 12, and 18. With these minerals occur two other new substances, naturally occurring dehydration products of swartzite and bayleyite, respectively, whose definitive properties are not well enough known to propose them as valid species. Andersonite, swartzite, and bayleyite, previously unknown either as minerals or synthetic compounds, have been synthesized. Analyses, optical data, $x$-ray patterns, and crystallographic data of these new species are given, with $x$-ray patterns of the dehydration products above mentioned. Schroeckingerite also has been analyzed and its formula found to differ from that given in the older accounts in the literature; our analysis agrees closely with that of the Wyoming schroeckingerite recently reported by Jaffe, Sherwood, and Peterson.[1] The various uranium carbonate minerals recorded in the literature are briefly considered. Of them, liebigite (=uranothallite) and schroeckingerite are well established. Voglite is almost certainly valid; randite certainly, and rutherfordine probably, are to be discredited; sharpite may be valid; the status of studtite and diderichite is very doubtful.


### LOCATION AND GEOLOGICAL SETTING

Dr. Charles A. Anderson, geologist of the U. S. Geological Survey, who first observed and collected the material in which the uranium minerals here described occur, has given us the following information concerning the Hillside Mine. It is located in Yavapai County, west-central Arizona, $3\frac{1}{2}$ miles north of Bagdad, and 43 miles by airline from Prescott. The mine produces gold, silver, lead, and zinc from a vein several feet


* Published by permission of the Director, U. S. Geological Survey.


[1] References are listed by numbers at end of this paper.

thick. Faulting, post- and pre-mineralization, has occurred. Sulfides present in the vein include pyrite, arsenopyrite, galena, sphalerite, chalcopyrite, tetrahedrite, and argentite; minerals of the oxidation zone include silver, cerargyrite, cerussite, anglesite, smithsonite, and hemimorphite. The country rock is pre-Cambrian mica-schist, intruded by pre-Cambrian granite. The age of the mineralization is thought to be Cretaceous or early Tertiary because, in the lower levels of the mine, the vein is reported to cut porphyry dikes, as at Bagdad.

Uranium minerals were found in only one place, as a coating about $\frac{1}{8}$ inch thick on gypsum, in the oxidized zone, and about forty feet above the water level. The source of the uranium is not known; it may be related to small aplite-pegmatite dikes in the pre-Cambrian schist that are associated with the granite, or it may have been deposited with the ore vein. In any case, the uranium carbonate minerals are clearly of secondary origin, and were deposited on the walls of the drift. Subsequent mining operations have completely obliterated the occurrence of the secondary uranium minerals.

No published data appear to exist on the Hillside Mine, and a recent publication listing the known minerals of Arizona does not mention any uranium minerals as occurring in Arizona.[2]

Very recently a specimen of uranium-bearing ore from the 400′ level has been received by us, and is now under investigation. An altogether different uranium mineralogy is present, the minerals johannite (hydrous copper uranium sulfate), pitchblende, and a probably new zinc uranium sulfate having been recognized thus far. A further account of these minerals will appear in a subsequent issue of the *American Mineralogist.*

## Appearance of Specimens

Adhering to the micaceous schist are scattered green rosettes of schroeckingerite, with sulfur-yellow bayleyite. Overlying this schist is a layer of snow-white granular gypsum containing small clusters of vivid green swartzite. Coating gypsum is a mass of yellow bayleyite, most of it now altered to a pale-yellow powder. The rare andersonite is easily overlooked; superficially, it resembles swartzite, but when the two minerals are seen together, the distinctive characters are apparent. In general, the several uranium minerals are intergrown with one another and with the gypsum and schist minerals; only schroeckingerite can be easily obtained in relatively large masses (about a pin-head in size) of a fair degree of purity.

In the mine, bayleyite crystals are sharp and well faceted. In the drier atmosphere of Washington, they soon become dull, losing their luster and finally disintegrate to a yellow powder. Swartzite behaves

similarly to a lesser extent; andersonite is stable. The stability is inverse to the degree of hydration.

Typical crystals of swartzite and andersonite are illustrated in Figs. 1 and 2. No natural bayleyite was available for the reason above stated. However, synthetic bayleyite (Figs. 3*a* and 3*b*) is illustrated.

## Method of Study

The study of the minerals from the Hillside Mine involved special difficulties, and at first sight it seemed almost impossible to separate the components of the specimens. However, the separation was made; and in order that other workers, who may encounter material of like nature in the future, may not be unduly discouraged in undertaking similar investigations, our methods of separation, identification, and analysis are presented in more detail than they would otherwise be.

The individual mineral crystals are very small, usually almost microscopic; the largest seldom exceed a millimeter in length, except schroeckingerite, which occurs in fairly pure rosette-like aggregates of flat plates a few tenths of a millimeter in diameter. Moreover, the various minerals occur more or less mixed, surrounded by and intergrown with the minerals of the mica schist and with gypsum. To obtian reasonably pure material for study it was therefore necessary to crush—not grind—the aggregate, to sift out the dust and coarse particles, and to pick out with a needle under a binocular microscope, particle by particle, the several samples to be analyzed—a tedious process, but the only course feasible. At first, before becoming familiar with the varied habit of the individual minerals, and their rather subtle variations in shades of yellow and green, it was also necessary to check the hand-picking frequently by examination under ultra-violet light making use of the characteristic fluorescence (see below) of the several species. After a suitable quantity of material had been thus obtained, a further selection from the picked material was made of the clearest possible crystals, which were spectrographically analyzed. The data thus obtained were invaluable in planning the quantitative analysis, for, because of the small sample available for many determinations, modifications of customary methods had to be devised. Furthermore, this pilot spectrographic analysis on the purest possible material indicated which of the minor constituents in the quantitatively analyzed sample were present as contaminants and not as essential constituents of the mineral. Later, synthesis of the minerals from C.P. chemicals checked the conclusions drawn from the spectrographic and quantitative analyses. At the same time that the spectrographic study was in progress, the individuality of the analyzed materials was established by their *x*-ray diffraction patterns.

## Physical and Chemical Data

The physical data are given in Table 1 and the chemical data in Table 2.

### *Fluorescence, optics and other physical properties*

The fluorescence of the minerals was examined under two kinds of mercury vapor lamps, one providing "short ultraviolet" radiation (Mineralight, model V-41) and the other, "long ultraviolet" radiation (Hanovia Inspectolight). Spectrograms of the radiation emitted by these lamps have already been published.[3] The relative brightness and color of the fluorescence of each mineral were the same under both lamps.

Table 1. Optical and Physical Data on Andersonite, Swartzite, Bayleyite, and Dehydration Products

| | Andersonite | Swartzite | Bayleyite |
|---|---|---|---|
| $\alpha$ | 1.520 ($\omega$) colorless | 1.465 colorless | 1.455 pinkish? |
| $\beta$ | 1.540 ($\epsilon$) pale yellow | 1.51 yellow | 1.490 pale yellow |
| $\gamma$ | | 1.540 yellow | 1.500 pale yellow |
| color (daylight) | bright yellow-green | green | yellow |
| habit | pseudo-cubic | prismatic | prismatic |
| symmetry | rhombohedral | monoclinic | monoclinic |
| extinction | | | $c:\alpha = 15°$ |
| sign | (+) | (−) | (−) |
| 2V (calc.) | 0° | 40° | 30° |
| density (measured) | 2.8 | 2.3 | 2.05 |
| (calc.) | 2.86 | 2.32 | 2.06 |
| solubility in water | easy | easy | easy |
| fluorescence | bright whitish-green | bright yellowish-green | weak, color uncertain |
| formula | $Na_2CaUO_2(CO_3)_3 \cdot 6H_2O$ | $CaMgUO_2(CO_3)_3 \cdot 12H_2O$ | $Mg_2UO_2(CO_3)_3 \cdot 18H_2O$ |
| | | Dehydration product | Dehydration product |
| $\alpha$ | | | 1.502 |
| $\gamma$ | | | 1.551 |
| color | | whitish dull-yellow | whitish |
| habit | | pseudomorphous after swartzite | pseudomorphous after bayleyite |
| fluorescence | | weak, color uncertain | moderate whitish-green |

The fluorescent colors observed were greens and yellows, typical of secondary uranium minerals. As is well known, this fluorescence is due to the uranyl ion, and consists of five or more discrete bands of wave lengths distributed throughout the visible spectrum. The wave length ranges and relative intensities of these bands vary slightly from mineral to mineral, resulting in a range of color of fluorescence between green and yellow. A thorough study of the fluorescence of secondary uranium minerals, therefore, requires precise spectrographic measurements. This study was not possible with the minerals described in this paper because of the small amounts of pure samples available.

In lieu of a spectrographic study, the fluorescence of the different

TABLE 2. ANALYTICAL DATA

ANALYSES OF URANIUM MINERALS FROM ARIZONA (AND SYNTHETIC ANDERSONITE)

| | Andersonite (*a*) | Synthetic Andersonite | Swartzite | Bayleyite (*d*) | |
|---|---|---|---|---|---|
| MgO | 0.5±0.1(*b*) | — | 5.24 | 9.03 | 8.97 |
| CaO | 8.9±0.5 | 8.80 | 8.40 | 3.42 | 2.75 |
| $Na_2O$ | 9.3±0.5 | 9.61 | .25 | — | .19 |
| $K_2O$ | — | — | .47 | — | .09 |
| $UO_3$ | 43.4±1.5 | 44.27 | 37.19 | 30.80 | 32.42 |
| Total $H_2O$ | 16.7(*c*) | 16.50 | 29.31 | 35.19 | 36.60 |
| $CO_2$ | 19.6±0.5 | 20.61 | 17.16 | 14.60 | 15.36 |
| $SO_3$ | 1.6±0.3 | | 1.98 | 4.43 | 3.95 |
| F | — | — | — | — | — |
| Acid insol., Ignited | — | — | .30 | 2.27 | .45 |
| Total | 100.0 | 99.79 | 100.30 | 99.74 | 100.78 |
| Formula | $Na_2CaUO_2(CO_3)_3 \cdot 6H_2O$ | | $CaMgUO_2(CO_3)_3 \cdot 12H_2O$ | $Mg_2UO_2(CO_3)_3 \cdot 18H_2O$ | |
| Sp. Gr. (determined) | 2.8 | | 2.3 | 2.06 | 2.05 |
| (calculated) | 2.86 | | 2.32 | | 2.06 |
| *Analyst* | F. S. Grimaldi | Marie Eiland | F. S. Grimaldi | F. S. Grimaldi | |

(*a*) Only 3.8 mg. of andersonite was available for the complete analysis.
(*b*) Spectrographically by K. J. Murata.
(*c*) By difference.
(*d*) The two analyses were made on separate samples.

TABLE 2 (continued)

ANALYSES OF SCHROECKINGERITE ("DAKEITE")

| | *Arizona* | *Wyoming* | *Wyoming* | *Joachimsthal* |
|---|---|---|---|---|
| | | $SiO_2$ .95<br>$R_2O_3$ .08 | | |
| MgO | 0.63 | — | — | — |
| CaO | 18.44 | 18.14 | 18.31 | 19.1 |
| $Na_2O$ | 3.19 | 3.63 | 7.31 | n.d. |
| $K_2O$ | .23 | — | — | — |
| $UO_3$ | 31.28 | 31.44 | 30.27 | 32.4 |
| $H_2O$ | 20.20 | 20.15 | 19.95 | 20.2 |
| $CO_2$ | 14.67 | 14.20 | 13.71 | n.d. |
| $SO_3$ | 9.24 | 9.17 | 9.61 | 9.1 |
| F | 2.09 | 2.15 | — | — |
| Insol. | 1.53 | | 1.05 | .4 |
| | 101.50 | 99.91 | 100.22 (Sic) | |
| O=F | .88 | .90 | | |
| | 100.62 | 99.01 | | |
| Sp. Gr. | 2.5 | | | |
| *Analyst* | F. S. Grimaldi | A. M. Sherwood[1] | F. Gonyer[4] | R. Novácek[5] |

[1,4,5] See references at end of paper.

minerals was characterized visually according to the following scheme. Two readily available minerals, schroeckingerite and autunite, were selected as standards for comparison of fluorescent colors. The fluorescent

color of schroeckingerite under the Mineralight lamp was designated *bright whitish-green;* that of autunite, *bright greenish-yellow*. The fluorescent colors of the minerals studied were close to one or the other, but one (that of swartzite) was definitely intermediate. This was called *yellowish green*. This three-step classification, though rather crude, was found adequate for the purpose, and it has the important advantage that the colors are defined in terms of standards that can be reproduced easily by other investigators. The results of our observations are included in Table 1.

The colors of the natural and synthetic andersonites are distinctly different, the former being bright yellow-green and the latter greenish yellow; and likewise the fluorescence differs, that of natural andersonite being whitish green and that of the synthetic compound yellow-green and weaker. Whether or not this variation is to be ascribed to the 0.5% MgO found in the natural andersonite is not known. The relation of green and yellow color in the uranium compounds to cation or other variables is an interesting question.

*Methods of analysis*

The weight of each mineral available for chemical analysis was: andersonite 3.8 mg., swartzite 0.25 g., bayleyite 0.5 g., and schroeckingerite, several grams. With the exception of schroeckingerite it would have been desirable if more material had been available for analysis.

In general, U, Ca, Mg, the alkalies, and acid insoluble, were determined on one portion; $CO_2$ and $SO_3$ on another; and F and $H_2O$ on separate portions. The sample weights in grams taken for analysis are given in Table 2A. For andersonite all the determinations reported were made on the total sample of 3.8 mg.

TABLE 2A. SAMPLE WEIGHTS IN GRAMS, TAKEN FOR ANALYSIS

| | Swartzite | Bayleyite | Schroeckingerite |
|---|---|---|---|
| Insol., U, Ca, Mg, Na, K | 0.1 | 0.2 | 0.3 |
| $CO_2$, $SO_3$ | .05 | .1 | .15 |
| $H_2O$ | .06 | .1 | .15 |
| F | | | .02 |

Accepted standard procedures were used in the analyses and for this reason only a very brief description of the procedures is given below. The analysis of andersonite involved a few unusual procedures and these are described separately.

PROCEDURES:

1. *Determination of insoluble material, U, Ca, Mg, Na, K*

Dilute HCl was added to the sample in a platinum dish and the mixture was digested on the steam bath for 30 minutes. The solution was then evaporated to dryness. It was taken up in hydrochloric acid and evaporated to dryness again. Dilute HCl was next added and the solution digested a few minutes. The insoluble material was filtered off, washed with dilute HCl, ignited, and weighed. The filtrate was boiled gently to insure the removal of carbon dioxide and a double precipitation with a slight excess of redistilled ammonia was then made. The $R_2O_3$ group obtained was filtered off, ignited, and weighed. The $R_2O_3$ group was then fused with $K_2S_2O_7$ and the melt dissolved in 50 ml. of dilute $H_2SO_4$ (7+93). After cooling to room temperature, the solution was passed through a small Jones reductor. It was then aerated and titrated with standard $KMnO_4$. The $U_3O_8$ figure obtained by titration agreed very closely with the weight of the ignited $R_2O_3$ precipitate obtained previously. The titrated solution was then concentrated to 50 ml. by evaporation and the reduction and titration repeated as a check.

The filtrate from the ammonia precipitate was treated with oxalic acid and the calcium oxalate obtained after double precipitation was ignited to CaO and weighed.

Magnesium was determined in the filtrate from the calcium oxalate by first destroying ammonium salts and oxalate, precipitating magnesium with 8-hydroxy-quinoline, igniting the precipitate under cover of oxalic acid to MgO, and weighing. The filtrate from the magnesium was taken to dryness and the ammonium salts and organic matter were destroyed by gentle ignition. Sulfuric acid was added to the residue, the solution evaporated on the steam bath and then on hot plate to remove the excess sulfuric acid. The sulfates obtained were ignited (temp. about 750°) and then weighed as $Na_2SO_4+K_2SO_4$. Potassium was then determined as potassium chloroplatinate and the sodium determined by difference.

2. *Determination of $CO_2$ and $SO_3$*

Carbon dioxide was determined, using a standard absorption train. The $SO_3$ content was obtained gravimetrically as $BaSO_4$ on the solution from the $CO_2$ determination.

3. *Determination of fluorine*

The fluorine was distilled with perchloric acid and then titrated with standard thorium nitrate after the solution was adjusted to a pH of 3.0 with monochloracetic acid-sodium monochloracetate buffer. Sodium alizarin sulfonate was used as indicator.

4. *Determination of total water*

Water was determined by the Penfield method after first mixing the sample with dry $Na_2WO_4$ to hold back oxides of sulfur. Before weighing and after the water was collected in the tube, the tube was inclined at an angle of about 45° for 30 minutes, open end down to allow the carbon dioxide released by the sample to be replaced by air.

*Analysis of andersonite*

The sample was weighed and transferred to a platinum dish. About 5 ml. of water was added and carbon dioxide was determined by titrating the sample with standard 0.01*N* HCl to the methyl orange end-point. This method for the determination of carbon dioxide was used after testing the more abundant bayleyite by titration and absorption train. The two methods gave good agreement in the results for carbon dioxide. After the titration a drop of concentrated HCl was added and the solution boiled gently. It was then cooled and 5 drops of dilute barium chloride solution were added. The cloud of $BaSO_4$ was then matched against standards and the value for $SO_3$ was thus obtained. The $BaSO_4$ was then

digested for some time and allowed to settle overnight. This was filtered off and rejected. In the filtrate uranium was precipitated as before, and after fusion of the ignited ammonia precipitate in $K_2S_2O_7$ it was determined colorimetrically with $NaOH\text{-}H_2O_2$.

The filtrate from the ammonia precipitate was taken to dryness and the ammonium salts destroyed. Calcium was precipitated again as the oxalate but from very small volume. It was filtered off and ignited to CaO. The CaO was then titrated with standard 0.01*N* HCl. A check on the calcium figure was obtained as follows: Oxalic acid was added to the titrated solution and the mixture was evaporated on the steam bath to remove chloride. The dish was then heated gently over a flame to remove the oxalate and finally the sample was ignited to CaO. The residue was then titrated with standard HCl. Bromthymol blue is recommended for acid-base titrations with 0.01*N* solutions.

The filtrate from the calcium oxalate was taken to dryness and the ammonium salts destroyed. The alkalies were weighed as sulfates and then sodium was determined by precipitating with zinc uranyl acetate.

DISCUSSION OF THE ANALYSES. *Contamination with gypsum*

Andersonite, swartzite, and bayleyite contained $CaSO_4 \cdot 2H_2O$ (gypsum) as impurity.

| *Sample* | *Impurity (% of Sample)* | *To be subtracted from the analysis* |
|---|---|---|
| Andersonite | 3.4% $CaSO_4 \cdot 2H_2O$ | 1.6% $SO_3$, 1.1% CaO, 0.7% $H_2O$ |
| Swartzite | 4.26% $CaSO_4 \cdot 2H_2O$ | 1.98% $SO_3$, 1.39% CaO, 0.89% $H_2O$ |
| Bayleyite | 8.45% $CaSO_4 \cdot 2H_2O$ | 3.93% $SO_3$, 2.75% CaO, 1.77% $H_2O$ |

The contamination of these minerals was to be expected in view of their intimate association with gypsum. Only the schroeckingerite, which occurs in relatively large homogeneous aggregates, appears to be essentially free from gypsum. That the contaminant was gypsum was shown by optical examination. Further, it appeared that, by synthesizing the several substances in the absence of sulfate ion, the $SO_3$ of the analyses was not part of these minerals. *X*-ray diffraction patterns did not reveal the gypsum, as it was in too small a quantity.

In Table 3 are the analyses with the constituents of the admixed gypsum deducted. The molecular ratios are then computed to obtain the formulas of the new minerals. The $SO_3$ of the analyses was the basis for allotment of CaO and $H_2O$ to $CaO \cdot SO_3 \cdot 2H_2O$, gypsum; a reasonable and proper assumption, inasmuch as andersonite, swartzite, and bayleyite contain no $SO_3$; and the analyzed schroeckingerite, which does contain $SO_3$, was known to be free from admixed gypsum.

*Notes on analytical data*

Although the analysis indicates 17.43 molecules of water in the bayleyite formula, there is a strong presumption that 18 is the correct figure, and that the lower value indicates that spontaneous dehydration of bayleyite had already commenced before the water determination was made. The 12 and 6 molecules of water present in swartzite and ander-

sonite, respectively, suggest that a similar multiple of 6, that is 18, is more likely than an odd number such as 17. Furthermore, the density calculated for 18 $H_2O$ agrees better with the measured density. For these reasons, the higher water content is assumed to be the correct one.

Except for bayleyite, specific gravities were obtained by suspending one or two grains of the mineral in a liquid of the same gravity.

TABLE 3. COMPUTATION OF FORMULAS FROM ANALYSES

| | Andersonite | Gypsum | Remainder | Ratio | |
|---|---|---|---|---|---|
| MgO | 0.5 | | 0.5 | 0.12 | 1.50× 1.0 |
| CaO | 8.9 | 1.1 | 7.8 | 1.39 | |
| $Na_2O$ | 9.3 | | 9.3 | 1.50 | 1.50× 1.0 |
| $UO_3$ | 43.4 | | 43.4 | 1.52 | 1.50× 1.0 |
| $H_2O$ | 16.7 | 0.7 | 16.0 | 8.88 | 1.50× 5.9 |
| $CO_2$ | 19.6 | | 19.6 | 4.45 | 1.50× 3.0 |
| $SO_3$ | 1.6 | 1.6 | | | |
| | 100.0 | 3.4 | 96.6 | | |

Deduced formula $CaO \cdot Na_2O \cdot UO_3 \cdot 3CO_2 \cdot 6H_2O$
or $Na_2Ca(UO_2)(CO_3)_3 \cdot 6H_2O$. As indicated, a slight replacement of calcium by magnesium may exist.

The formula of andersonite also can be computed from the analysis of the synthetic material:

| | Andersonite (synthetic) | Ratio | |
|---|---|---|---|
| CaO | 8.80 | 1.57 | 1.55× 1.01 |
| $Na_2O$ | 9.61 | 1.55 | 1.55× 1.00 |
| $UO_3$ | 44.27 | 1.55 | 1.55× 1.00 |
| $H_2O$ | 16.50 | 9.17 | 1.55× 5.91 |
| $CO_2$ | 20.61 | 4.69 | 1.55× 3.03 |
| | 99.79 | | |

Deduced formula $CaO \cdot Na_2O \cdot UO_3 \cdot 3CO_2 \cdot 6H_2O$
or $Na_2Ca(UO_2)(CO_3) \cdot 6H_2O$

| | Swartzite | Gypsum | Remainder | Ratio | |
|---|---|---|---|---|---|
| MgO | 5.24 | | 5.24 | 1.30 | 1.30× 1.00 |
| CaO | 8.40 | 1.39 | 7.01 | 1.25 | 1.30× .96 |
| $Na_2O$ | .25 | | .25 | .04 | 1.30× .03 |
| $K_2O$ | .47 | | .47 | .05 | 1.30× .04 |
| $UO_3$ | 37.19 | | 37.19 | 1.30 | 1.30× 1.00 |
| $H_2O$ | 29.31 | .89 | 28.42 | 15.80 | 1.30×12.15 |
| $CO_2$ | 17.16 | | 17.16 | 3.90 | 1.30× 3.00 |
| $SO_3$ | 1.98 | 1.98 | | | |
| Insol. | .30 | | | | |
| | 100.30 | 4.26 | 95.74 | | |

TABLE 3 (continued)

Deduced formula $MgO \cdot CaO \cdot UO_3 \cdot 3CO_2 \cdot 12H_2O$
or $MgCa(UO_2)(CO_3)_3 \cdot 12H_2O$

| | Bayleyite | Gypsum | Remainder | Ratio | |
|---|---|---|---|---|---|
| MgO | 8.97 | | 8.97 | 2.220 | 1.11× 2.00 |
| CaO | 2.75 | 2.75 | | | |
| $Na_2O$ | .19 | | .19 | .03 | |
| $K_2O$ | .09 | | .09 | .01 | |
| $UO_3$ | 32.42 | | 32.42 | 1.133 | 1.11× 1.02 |
| $H_2O$ | 36.60 | 1.77 | 34.83 | 19.350 | 1.11×17.43 |
| $CO_2$ | 15.36 | | 15.36 | 3.491 | 1.11× 3.15 |
| $SO_3$ | 3.95 | 3.93 | .02 | | |
| Insol. | .45 | | | | |
| | 100.78 | 8.45 | 91.88 | | |

Deduced formula $2MgO \cdot UO_3 \cdot 3CO_2 \cdot 18H_2O$
or $Mg_2(UO_2)(CO_3)_3 \cdot 18H_2O$

| | Schroeckingerite | Ratio | |
|---|---|---|---|
| MgO | .63 | .16 | |
| CaO | 18.44 | 3.29 | 1.09× 3.02 |
| $Na_2O$(Na) | 3.19 (2.36) | (1.03) | 1.09× .95 |
| $K_2O$ | .23 | .02 | |
| $UO_3$ | 31.28 | 1.09 | 1.09× 1.00 |
| $H_2O$ | 20.20 | 11.22 | 1.09×10.29 |
| $CO_2$ | 14.67 | 3.33 | 1.09× 3.05 |
| $SO_3$ | 9.24 | 1.16 | 1.09× 1.06 |
| F | 2.09 | 1.10 | 1.09× 1.01 |
| Insol. | 1.53 | | |
| | 101.50 | | |
| Less O=F | .88 | | |
| | 100.62 | | |

The deduced formula is $Ca_3Na[UO_2(CO_3)_3SO_4F] \cdot 10H_2O$, which is the same as that derived by Jaffe, Sherwood, and Peterson.

In view of the small quantity (3.8 milligrams) of andersonite available for analysis, it was thought proper to verify the calculated formula by means of a second analysis made on synthetic material. Mrs. Marie Eiland, chemist of the U. S. Geological Survey, kindly made this analysis. Both analyses are given in Table 2 above, and it is evident that the agreement is satisfactory.

The analysis of the Arizona schroeckingerite was made before the publication of the study of the Wyoming schroeckingerite by Jaffe, Sherwood, and Peterson.[1] In these circumstances, it is gratifying to note that the two analyses agree closely. Better agreement could hardly be

expected, considering that the respective samples are from different localities, were analyzed by different chemists, and are substances of complex composition. The agreement is of special significance in that the deduced formula $Ca_3Na[UO_2(CO_3)_3(SO_4)F]\cdot 10H_2O$ (which may be rewritten $3CaCO_3\cdot NaF\cdot (UO_2)SO_4\cdot 10H_2O$) independently obtained by Jaffe, Sherwood, Peterson, and by ourselves differs from the formula hitherto ascribed to dakeite (=schroeckingerite) by Larsen and Gonyer[4] namely $3CaCO_3\cdot Na_2SO_4\cdot UO_3\cdot 10H_2O$, in having only half as much $Na_2O$, and in containing essential fluorine.

Dr. Clifford Frondel[6] of Harvard University has observed (personal communication) that there is a difference in size of the unit cells of the Bohemian and the two American schroeckingerites. Both of the latter agree closely in *x*-ray pattern as well as chemical composition. If a similarly good analysis of the Bohemian mineral were available, a significant difference in composition might be shown.

*Spectrographic Data*

Table 4. Spectrographic Study

| | Major elements >1% | Minor elements <1% | Not found |
|---|---|---|---|
| Schroeckingerite | U, Ca, Na | Mg, Al, Fe, K, Mn | Sr and* |
| Bayleyite | U, Mg, Ca(3%) | Al | Fe, Mn, Na, K, Sr, and* |
| Bayleyite (purer sample) | U, Mg, Ca(1%) | Al | Fe, Mn, Na, K, Sr, and* |
| Andersonite | U, Ca(14%), Na(11%) | Al, Mg(0.5%) | Fe, Mn, K, Sr, and* |
| Swartzite | U, Ca(14%), Mg(5%) | Al, Sr | Fe, Mn, Na, K, and* |
| Dehydration product of bayleyite and of swartzite (mixture) | U, Mg, Ca(1%) | Al, Fe | Mn, Na, K, Sr, and* |

* Not found in any: Be, B, Pb, Cu, Mo, W, As, Sb, Sn, Tl, Zn, Cd, Co, Ni, Ge, In, Cr, V, Y, La, Bi, Ag, Li, Rb, Cs, Ti, Zr, Ba, Th.

The numbers in parentheses indicate the spectrographically estimated percentages; they indicate order of magnitude rather than exact percentages, and are thus in reasonable agreement with Grimaldi's analytical figures.

The minor elements detected spectrographically are referred to impurities—in part, the "insoluble" of the analyses. A possible exception is the 0.5% Mg found in the andersonite.

The notably less Ca in the purer sample of bayleyite indicates that the Ca present is not a constituent of the mineral.

## Synthesis of the New Minerals

The synthesis of these compounds was undertaken in order to verify beyond question that the *x*-ray diffraction patterns were those of com-

pounds of the deduced chemical compositions, and, also, in the case of the andersonite to have an analysis free from the uncertainty arising from the minute quantity of natural substance available. The literature did not show that they had been previously prepared, but the homologous substances listed below had been.[7]

| | |
|---|---|
| $(NH_4)UO_2(CO_3)_3 \cdot 2H_2O$ | (The indicated $H_2O$ content, or its absence, |
| $Na_4UO_2(CO_3)_3$ | is of doubtful validity.) |
| $K_4UO_2(CO_3)_3$ | |
| $Ag_4UO_2(CO_3)_3$ | |
| $Tl_4UO_2(CO_3)_3$ | |
| $Ca_2UO_2(CO_3)_3$ | |
| $Ba_2UO_2(CO_3)_3$ | |

The methods given for preparing these compounds were successfully employed by us to prepare synthetic andersonite, swartzite, and bayleyite.

Details of the synthesis follow:

For bayleyite, $Mg_2UO_2(CO_3)_3 \cdot 18H_2O$.
Proportions used of starting materials:

| | *Mol. Ratio* | *Weights* |
|---|---|---|
| $Mg(NO_3)_2 \cdot 6H_2O$ | 2 | 5.13 gm. |
| $UO_2(NO_3)_2 \cdot 6H_2O$ | 1 | 5.02 gm. |
| $K_2CO_3$ | 3 | 4.14 gm. |

Add slowly the uranium nitrate solution to the $K_2CO_3$ solution in the presence of phenolphthalein as indicator. If the indicator decolorizes, add $K_2CO_3$ solution until the indicator is just barely pink. Now add magnesium nitrate solution. If the phenolphthalein decolorizes, add $K_2CO_3$ solution until the indicator is just barely pink. Allow to crystallize at room temperature.

Bayleyite also was synthesized by first preparing the insoluble silver uranyl carbonate, reacting an excess of the silver uranyl carbonate with magnesium chloride, filtering off the precipitate of AgCl and excess silver uranyl carbonate, and allowing the filtrate to crystallize. Sometimes a gelatinous mass formed on drying, but by "seeding" this mass crystallized nicely (Figs. 3*a* and 3*b*). The reaction is $Ag_4UO_2(CO_3)_3 + 2MgCl_2 + 18H_2O \rightarrow$ bayleyite $+ 4AgCl$.

Andersonite was synthesized similarly to bayleyite.

| | *Molecular Ratio* | *Weights* |
|---|---|---|
| $Ca(NO_3)_2 \cdot 4H_2O$ | 1 | 2.36 gm. |
| $NaNO_3$ | 2 | 1.62 gm. |
| $K_2CO_3$ | 3 | 4.14 gm. |
| $UO_2(NO_3)_2 \cdot 6H_2O$ | 1 | 5.02 gm. |

Again the uranium solution was added to $K_2CO_3$ solution and the

acidity was adjusted with $K_2CO_3$ until the phenolphthalein was just pink. Then a solution of $NaNO_3$ and $Ca(NO_3)_2$ was added, the acidity was adjusted as before and the mixture was allowed to crystallize at room temperature.

At first there was some difficulty in synthesizing swartzite by similar procedures; on evaporating a solution of the constituents a greenish-yellow glass, or better, gel, of refractive index near 1.53 forms, but on "seeding" with a fragment of the natural mineral, excellent crystals develop.

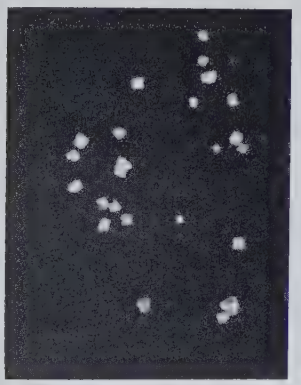

FIG. 1 ×15
Swartzite $CaMgUO_2(CO_3)_3 \cdot 12H_2O$
Yavapai County, Arizona

FIG. 2 ×15
Andersonite $Na_2CaUO_2(CO_3)_3 \cdot 6H_2O$
Yavapai County, Arizona

FIG. 3*a* ×38 FIG. 3*b*
Bayleyite $Mg_2UO_2(CO_3)_3 \cdot 18H_2O$ (Synthetic)
The synthetic preparations yield acicular crystals; the natural bayleyite was stubby prismatic, with good terminal faces.

## Remarks on the Homologous $X_4UO_2(CO_3)_3 \cdot nH_2O$ Series

As already mentioned, numerous synthetic compounds of the above general formula are known, in which $X_4$ may represent four univalent ions, two similar divalent, or, as in the naturally occurring minerals,

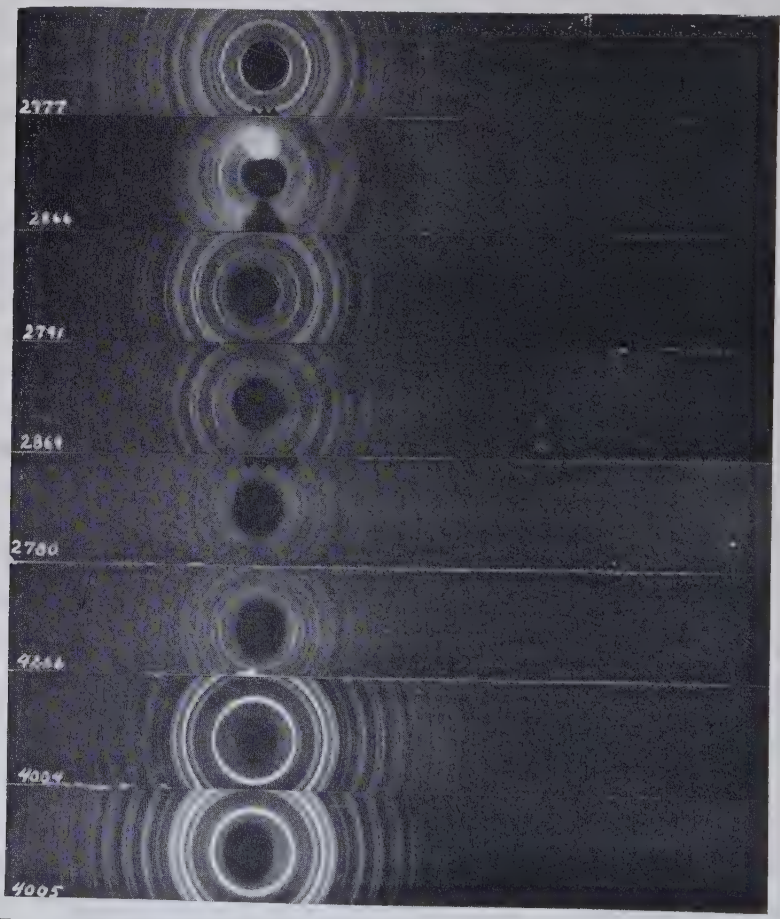


Fig. 4. Powder patterns of uranium minerals and synthetic preparations (filtered copper radiation)

2777 Bayleyite, Arizona
2866 Bayleyite, Synthetic
2791 Andersonite, Arizona
2869 Andersonite, Synthetic
2780 Swartzite, Arizona
4266 Swartzite, Synthetic
4004 Dehydration product of bayleyite, Arizona
4005 Dehydration product of bayleyite, Synthetic

two different divalent, or two univalent and one divalent, ions. It would be of interest to determine how extensively the series extends, whether a univalent and a trivalent ion, or a single quadrivalent ion could function as $X_4$. The varying value of $n$, determined for a large number of the compounds, should be of interest from a theoretical structural viewpoint. Also, the variation in fluorescence of the naturally occurring compounds with varying states of hydration, now an unexplained feature of this class of substances, could perhaps be clarified by a study of a large number of these homologues, in which the variations in cation and water content are known factors.

## X-ray Investigation

*X*-ray powder and Weissenberg diffraction patterns were made of andersonite, swartzite, and bayleyite. Powder patterns were made of the dehydration products of swartzite and bayleyite, and also of schroeckingerite. "Randite" (=β-uranotile), uranothallite (=liebigite), "voglite" (often actually liebigite), "rutherfordine" (=an undescribed calcium uranium silicate) also were studied by their powder patterns.

### *Data from powder patterns*

Table 5 gives the powder pattern data on the new minerals.

The error figures are estimates. The diffraction data for andersonite and swartzite were inconclusive as to the presence of a center of symmetry, so piezoelectric tests were made through the kindness of Paul L. Smith at the Naval Research Laboratory in Washington. The crystals showed no piezoelectricity, so that this test also was inconclusive. None of the crystals had enough faces to determine the crystal class from morphology or good enough faces to make etch tests practicable.

## The New Mineral Names

Andersonite is named after Charles A. Anderson, geologist of the United States Geological Survey, who first observed and collected the material from which these minerals were isolated and identified.

Swartzite is named for Charles K. Swartz (1861–1949), professor of geology and mineralogy at The Johns Hopkins University, an inspiring teacher of many generations of students.

Bayleyite is named in honor of William S. Bayley (1861–1943), for many years professor of mineralogy and geology at the University of Illinois, and geologist with the United States Geological Survey.

The naturally formed dehydration products of bayleyite and swartzite are not proposed as species. Although the dehydration product of the bayleyite, at least, yields a characteristic and definite *x*-ray diffraction-

TABLE 5. POWDER PATTERN DATA (FILTERED COPPER RADIATION)
$\lambda = 1.5418$ Å

| Andersonite, Arizona | | | Swartzite, Arizona | | |
|---|---|---|---|---|---|
| *d* | *I* | *hkl* | *d* | *I* | *hkl* |
| 13.0 | 10 | 100 | 8.76 | 10 | 110 |
| 9.51 | 3 | 101 | 7.31 | 9 | 020 |
| 7.97 | 10 | 111 | 6.37 | 5 | 001 |
| 6.56 | 2 | 200 | 5.83 | 1 | 011 |
| 5.68 | 10 | $10\bar{2}$, 112 | 5.50 | 10 | $11\bar{1}$, 200 |
| 5.22 | 10 | $\bar{1}12$, $11\bar{2}$ | 5.13 | 1 | 210 |
| 4.35 | 6 | $\bar{1}22$ | 4.82 | 8 | 111, 021 |
| 4.19 | 6 | 103 | 4.62 | 2 | $12\bar{1}$ |
| 4.04 | 4 | 113, $10\bar{3}$, 222 | 4.46 | 2 | $20\bar{1}$, 130 |
| 3.82 | 3 | $11\bar{3}$ | 4.37 | 2 | 220 |
| 3.71 | 8 | 203, $\bar{2}22$ | 3.85 | 2 | 201 |
| 3.49 | 2 | $\bar{1}23$ | 3.66 | 7 | 040, 230 |
| 3.34 | 2 | 223 | 3.53 | 5 | 310 |
| 3.15 | 5*b* | 303, $\bar{2}23$, $22\bar{3}$ | 3.39 | 1 | 221 |
| 3.00 | 7 | $\bar{1}33$, $11\bar{4}$, $30\bar{3}$ | 3.31 | 1 | $23\bar{1}$, $31\bar{1}$ |
| 2.79 | 6 | | 3.25 | 1 | 320 |
| 2.45 | 5 | | 3.19 | 7 | $10\bar{2}$, 002 |
| 2.39 | 5 | | 3.11 | 2 | $32\bar{1}$ |
| 2.36 | 4 | | 3.04 | 1 | 240, 231 |
| 2.21 | 7 | | 2.91 | 8 | 022, $21\bar{2}$, 311 |
| 2.04 | 4 | | 2.82 | 2 | |
| 2.01 | 4 | | 2.61 | 5 | |
| 1.977 | 4 | | 2.28 | 4 | |
| 1.957 | 4 | | 2.23 | 3 | |
| 1.933 | 4 | | 2.19 | 2 | |
| 1.895 | 4 | | 2.10 | 2 | |
| 1.852 | 6 | | 2.06 | 8 | |
| 1.749 | 5 | | 1.817 | 5 | |
| 1.684 | 3 | | 1.707 | 8 | |
| 1.573 | 4 | | 1.375 | 2 | |
| 1.393 | 3 | | 1.268 | 2 | |
| 1.344 | 3 | | 1.217 | 3 | |
| 1.262 | 3 | | .9615 | 2 | |
| 1.232 | 3 | | | | |
| 1.038 | 2 | | | | |
| .9803 | 2 | | | | |
| .9505 | 2 | | | | |
| .8192 | 2 | | | | |
| .8011 | 2 | | | | |

(The dehydration product of swartzite is amorphous to *x*-rays)

*b:* Broad

TABLE 5 (continued)

| Bayleyite, Arizona | | | Dehydration product of bayleyite, Arizona | |
|---|---|---|---|---|
| *d* | *I* | *hkl* | *d* | *I* |
| 13.1 | 9 | 200, 110 | 8.27 | 10 |
| 7.66 | 10 | 310, 020 | 7.25 | 2 |
| 6.53 | 4 | 400, 220, 001 | 6.24 | 1 |
| 5.85 | 4*b* | 201, 111, 11$\bar{1}$ | 5.54 | 1 |
| 5.08 | 4 | 311 | 5.34 | 5 |
| 4.89 | 4 | 021, 31$\bar{1}$, 401 | 5.13 | 3 |
| 4.71 | 1 | 221, 22$\bar{1}$ | 4.77 | 9 |
| 4.54 | 2 | 40$\bar{1}$ | 4.62 | 2 |
| 4.41 | 2 | 330, 600 | 4.51 | 3 |
| 3.83 | 6 | 620, 040 | 4.42 | 3 |
| 3.70 | 2 | 331, 710, 530, 240 | 4.23 | 7 |
| 3.26 | 4 | 002 | 4.00 | 3 |
| 3.15 | 2 | 11$\bar{2}$, 212 (*n.r.*) | 3.75 | 2 |
| 3.05 | 2 | 312 (*n.r.*), 730, 911 | 3.56 | 2 |
| 2.96 | 2 | | 3.49 | 3 |
| 2.88 | 4 | | 3.20 | 3 |
| 2.69 | 5 | | 3.11 | 4 |
| 2.42 | 2 | | 3.07 | 3 |
| 2.37 | 2 | | 3.02 | 3 |
| 2.30 | 2 | | 2.89 | 2 |
| 2.21 | 5 | | 2.86 | 2 |
| 2.12 | 4 | | 2.76 | 3 |
| 1.908 | 3*b* | | 2.71 | 3 |
| 1.796 | 2*b* | | 2.64 | 4 |
| 1.754 | 2*b* | | 2.47 | 2 |
| 1.682 | 1 | | 2.44 | 3 |
| 1.378 | 1 | | 2.32 | 4 |
| 1.247 | 1 | | 2.26 | 3 |
| | | | 2.14 | 3 |
| | | | 2.12 | 3 |
| | | | 2.08 | 2 |
| | | | 2.05 | 3 |
| | | | 1.973 | 2 |
| | | | 1.881 | 4 |
| | | | 1.848 | 3 |
| | | | 1.811 | 2 |
| | | | 1.787 | 3 |
| | | | 1.752 | 2 |
| | | | 1.695 | 3 |
| | | | 1.578 | 3 |
| | | | 1.551 | 2 |
| | | | 1.352 | 2*b* |

*n.r.*: Not recorded on any Weissenberg film
*b*: Broad

TABLE 6. CRYSTALLOGRAPHIC DATA FROM SINGLE CRYSTAL WEISSENBERG X-RAY STUDY

*Andersonite:* $Na_2CaUO_2(CO_3)_3 \cdot 6H_2O$

$a = 13.11 \pm .02$ Å — Space group: $R\bar{3}(C_{3i}^2)$ or $R3$ $(C_3^4)$, rhombohedral
$\alpha = 86°56' \pm 30'$ — $Z = 6$.
For the hexagonal description:
$a = 18.04 \pm .05$ Å — $Z = 18$
$c = 23.90 \pm .05$ Å
$c/a = 1.325$. — Calculated density = 2.86 (2.8 measured).

*Swartzite:* $CaMgUO_2(CO_3)_3 \cdot 12H_2O$

$a = 11.12 \pm .05$ Å — Space group: $P2_1/m(C_{2h}^2)$ or $P2_1(C_2^2)$, monoclinic
$b = 14.72 \pm .05$ Å — $Z = 2$
$c = 6.47 \pm .02$ Å. — Calculated density = 2.32 (2.3 measured).
$\beta = 99°26' \pm 30'$

*Bayleyite:* $Mg_2UO_2(CO_3)_3 \cdot 18H_2O$

$a = 26.65 \pm .05$ Å — Space group: $P2_1/a(C_{2h}^5)$, monoclinic
$b = 15.31 \pm .05$ Å — $Z = 4$
$c = 6.53 \pm .02$ Å. — Calculated density = 2.06 (2.05 measured).
$\beta = 93°4' \pm 20'$.

pattern, this is not considered sufficient grounds for establishing a new mineral species, for the pattern may be that of a mixture.

## SYNOPSIS OF URANIUM CARBONATE MINERALS

A tabulation of the known uranium carbonate minerals is given below in Table 7, followed by more detailed discussion of the status of the several species.

TABLE 7. URANIUM-CARBONATE MINERALS

| Species | Year Discovered | Composition (reported) | Color | Remarks |
|---|---|---|---|---|
| liebigite | 1848 | $CaUO_2(CO_3)_2 \cdot 20H_2O$ (erroneous) see uranothallite below | apple-green | established species |
| voglite | 1853 | contains Ca, Cu, $H_2O$ | emerald-green to bright grass-green | =liebigite? (in part) |
| schroeckingerite[8] | 1873 | $NaCa_3UO_2(CO_3)_3SO_4F \cdot 10H_2O$ | green | well-established species |
| randite | 1878 | "hydrous Ca-U carbonate" | yellow | is impure $\beta$-uranotil |
| uranothallite | 1853–1882 | $Ca_2U(CO_3)_4 \cdot 10H_2O$ | siskin-green | liebigite has priority |
| rutherfordine | 1906 | $UO_2CO_3$ | yellow | dubious (not a carbonate) |
| sharpite | 1938 | $6UO_3 \cdot 5CO_2 \cdot 8H_2O$ | yellow-green | needs further study |
| studtite | 1947 | U–Pb?–$H_2O$–$CO_2$ | yellow | needs further study |
| diderichite | 1947 | U–$H_2O$–$CO_2$ | yellow-green | needs further study |
| andersonite | 1948 | $Na_2CaUO_2(CO_3)_3 \cdot 6H_2O$ | green | |
| swartzite | 1948 | $CaMgUO_2(CO_3)_3 \cdot 12H_2O$ | green | |
| bayleyite | 1948 | $Mg_2UO_2(CO_3)_3 \cdot 18H_2O$ | yellow | |

*Liebigite*

Considerable confusion has existed in the past as to the status of liebigite. In 1848 J. Lawrence Smith[9] described a mineral under this name from Adrianople, Turkey, as a hydrous carbonate of calcium and uranium. He computed a formula $CaCO_3 \cdot (UO_2)CO_3 \cdot 20H_2O$. Later, in 1851,[10] he mentioned another occurrence of the same mineral from Johanngeorgenstadt. In 1853 the same mineral (as established by Evans and Frondel[11] in 1949) was described by Vogl[12] from Joachimsthaal under the name Uran-Kalk-Carbonate. Finally, in 1882, Schrauf[13] determined that Vogl's Joachimsthaal mineral differed in composition from that given by Smith, being $Ca_2U(CO_3)_4 \cdot 10H_2O$, and proposed the name uranothallite. Smith's original analysis of liebigite is therefore erroneous, but as Evans and Frondel have shown that his mineral is the same as the correctly determined uranothallite, Smith's name, liebigite, has priority. Weisbach[14] in 1875 proposed the name flutherite, which under the circumstances has no standing.

*Voglite*

Voglite was first described by Vogl[12] in 1853, from Joachimsthaal, as a copper calcium uranium hydrous carbonate. The name voglite was proposed by Haidinger in a footnote to the original description by Vogl. There is no reason to question its validity as a species, although, as noted by Frondel,[11] "Most specimens so labelled are uranothallite," i.e., liebigite. Such was the case with U. S. National Museum specimen R2763 from Joachimsthaal (Roebling collection).

*Schroeckingerite*

Schroeckingerite is discussed above.

*Randite*

Randite was first described by August Koenig[15] in 1878 as a canary-yellow incrustation of acicular tufts on granite, at Frankford, near Philadelphia, Pa. An analysis of 47 milligrams of impure material is cited by *Dana*, System, 6th Ed. p. 309, as indicating a hydrous calcium uranium carbonate. It differed from liebigite and voglite in color, being yellow, whereas these two are green. An imperfect analysis gave a formula $Ca_5U_2C_6O_{20} \cdot 3H_2O$. The author proposed the name randite, with a reservation that the mineral needed further study before acceptance as a new species.

A specimen from the United States National Museum R2765 (Roebling Collection) of so-called randite shows a thin waxy crust of green-

ish yellow color. Microscopically, extremely small needles with ill-defined optics can be seen, but it was impossible to obtain enough for quantitative analysis.

However, from Dr. Frondel it was learned that the original randite "is a gross mixture of β-uranotil, tyuyamunite, kaolin, and calcite, with the β-uranotil dominant and representing the acicular crystals. . . . "[16] Further, Frondel observes, "An authentic specimen of randite from Sam Gordon proved to be tyuyamunite. Other specimens labelled randite were β-uranotil."[17] The National Museum randite above mentioned (R2765) gave an $x$-ray powder pattern similar to that of β-uranotil from Joachimsthaal (H7644 from the Harvard collection).

The suggestion of Ramdohr[18] that randite may be uranothallite, is therefore untenable.

A definitive study of randite by Frondel[19] published recently shows it to be a mixture of known minerals, it is therefore to be discredited as a species.

*Uranothallite*

Uranothallite is discussed above.

*Rutherfordine*

Rutherfordine was described in 1906 by W. Marckwald[20] from German East Africa with the formula $UO_2 \cdot CO_3$. We have studied the U. S. National Museum specimen 93291 so labelled, and found its $x$-ray diffraction pattern to be the same as that of a presumably new calcium uranium silicate from Mitchell Co., N. C., in the Harvard collection (personal communication from Clifford Frondel). The species is therefore not to be included among the uranium carbonates.

*Sharpite*

Sharpite was described in 1938 by J. Melon[21] from Shinkolobwe, Belgian Congo, as $6UO_3 \cdot 5CO_2 \cdot 8H_2O$. No $x$-ray data are available, but its identity as a species rests on an analysis and optical data.

*Studtite and diderichite*

Studtite and diderichite were described in 1947 by J. Vaes[22] from Shinkolobwe, Belgian Congo, as possibly uranium carbonates. The comment of Michael Fleischer[23] on these proposed names is justified: "It is to be regretted that new names were given to these very poorly characterized minerals. . . . It would be better to hold up publication of descriptions like these until enough data at least were obtained so that future workers could recognize the minerals from the descriptions."

Acknowledgments

Our thanks are due Michael Fleischer and Earl Ingerson of the United States Geological Survey who have read and instructively commented on the manuscript of this paper. Professor Clifford Frondel of Harvard University has kindly checked the several *x*-ray patterns of the new uranium minerals against the extensive file at Harvard, and we have borrowed freely from his detailed knowledge of the uranium minerals, in particular with reference to randite, liebigite, and rutherfordine. Dr. L. J. Spencer of the British Museum has advised us as to nomenclature of the new species. Judith Weiss Frondel of the United States Geological Survey helped in checking the literature of recorded uranium minerals. George Switzer of the United States National Museum furnished specimens of type material on which comparative studies could be made. Paul L. Smith of the Naval Research Laboratory made tests for piezo-electricity.

References

1. Jaffe, Howard W., Sherwood, Alexander M., and Peterson, Maurice J., New data on schroeckingerite: *Am. Mineral*, **33,** 152–157 (1948).
2. Galbraith, Frederic William, 3rd, Minerals of Arizona (2n ed. revised): *Arizona Bureau of Mines, Bulletin* **153** (1947).
3. Murata, K. J., and Smith, R. L., Manganese and lead as coactivators of red fluorescence in halite: *Am. Mineral.*, **31,** 530 (1946).
4. Larsen, E. S., Jr., and Gonyer, F. A., Dakeite, A new uranium mineral from Wyoming: *Am. Mineral.*, **22,** 561–563 (1937).
5. Nováček, R., The identity of dakeite and schroeckingerite; *Am. Mineral.*, **24,** 317–323 (1939).
6. Letter, Clifford Frondel to Charles Milton, January 27, 1948.
7. Hedvall, J. A., Beitrag zur Kenntniss der komplexen Uranyl Carbonate: *Z. f. anorg. Chem.*, **146,** 225–229 (1925).
8. Schrauf, A., Schroeckingerite, ein neues Mineral von Joachimsthaal: *Min. Mitt., Heft* **II,** 137–138 (1873).
9. Smith, J. L., Two new minerals-medjidite (sulphate of uranium and lime)—liebigite (carbonate of uranium and lime): *Am. Jour. Sci.*, **5,** 336 (1848).
10. Smith, J. L., Liebigite: *Am. Jour. Sci.*, **11,** 259 (1851).
11. Evans, Howard, and Frondel, Clifford, Studies on Uranium Minerals (II): Liebigite and Uranothallite, *Am. Mineral.*, **35,** 251–254 (1950).
12. Vogl, J. F., Drei neue Mineral-Vorkommen von Joachimsthaal: *Jb. Geol. Reichs.* (Vienna), **4,** 220–223 (1853).
13. Schrauf, A., Uranothallit, false Liebigite, von Joachimsthaal: *Zeit. f. Kr.*, **6,** 410–413 (1882).
14. Weisbach, A., *Syn. Min.* p. 48, 1875 (referred to in Hintze, Carl, Handbuch der Mineralogie I, No. 26, 3056, 1929).
15. Koenig, August, Mineralogical notes—randite: *Proc. Acad. Philadelphia*, **30,** 408 (1878).
16. Letter, Clifford Frondel to Michael Fleischer, July 11, 1946.
17. Letter, Clifford Frondel to Michael Fleischer, June 19, 1946.
18. Ramdohr, Paul, Klockmann's Lehrbuch der Mineralogie, p. 469, Stuttgart (1948).

19. Frondel, Clifford, Studies of Uranium minerals (1): Parsonsite and Randite, *Am. Mineral.*, **35,** 245–250 (1950).
20. Marckwald, W., Ueber Uranerze aus Deutsch-Ostafrika: *Centrallblatt f. Min., Geol., u. Pal.*, **24,** 761–763 (1906).
21. Melon, J., La sharpite, nouveau carbonate d'uranyl du Congo belge: *Bull. Sean. Inst. Roy. Colon. Belge*, **9,** 333–336 (1938).
22. Vaes, J. F., Six nouveau mineraux d'urane provenant de Shinkolobwe (Katanga): *Bull. Soc. Belge Geol.*, **70, B,** 212–225 (1947).
23. Fleischer, Michael, New mineral names: *Am. Mineral.*, **33,** 385 (1948).

*Manuscript received*
*April 8, 1950*

# DIFFERENTIAL THERMAL ANALYSIS OF NATURAL HYDROUS FERRIC OXIDES

J. Laurence Kulp, *Columbia University, New York, N. Y.*, and Albert F. Trites*

Abstract

Differential thermal analysis and *x*-ray diffraction have been applied to nearly 100 specimens of hydrous ferric oxide aggregates.

The thermal curves of goethite and lepidocrocite are sufficiently different to permit semi-quantitative estimation of these minerals in natural mixtures. The common occurrence of lepidocrocite in most aggregates of natural hydrous ferric oxides (limonite) is surprising.

Thermal curves of artificial mixtures of these minerals are given and are used to interpret the natural mixtures. Synthetic hydrous ferric oxide of two types was prepared and the thermal curves discussed.

## Introduction

Since the hydrous iron oxides are of considerable significance in geology, it is of interest to define the thermal curves for these minerals and the mineral aggregates in which they occur. Blanchard (1944) has studied the mineralogical composition of certain limonite specimens but made no thermal study. Systematic variations in the concentration of one of these minerals may be of considerable use in analyzing the nature of depositional sequence and areal extent. Such data may also be important in the study of the weathered part of hydrothermal deposits. Locke (1926) has shown that it is possible to identify certain types of mineralization by color differences and textures of "gossans" or "iron caps." A quantitative analysis of the mineral composition of such occurrences should yield information useful in scientific prospecting. Finally, the geochemistry of iron can be more fully appreciated if the substitution relationships in these common supergene minerals are determined.

This investigation was undertaken with the primary purpose of establishing the type differential thermal curves for goethite and lepidocrocite. A large number of representative specimens containing these minerals were analyzed. The effects of purity and grain-size on the thermal curves were studied by means of artificial mixtures of these hydrous iron oxide minerals with foreign constituents common to natural mixtures.

Precipitates of hydrous ferric oxide were prepared in the laboratory under various conditions and examined by thermal and *x*-ray technique.

The authors wish to express their appreciation to Professors Paul F. Kerr and Ralph J. Holmes and Mr. H. D. Holland for helpful criticisms and suggestions.

* Present address: U. S. Geol. Survey, Denver, Colorado.

Mineral specimens were obtained from the mineral collection of the Department of Geology, Columbia University.

## Equipment and Procedure

The experimental procedures used in this investigation included differential thermal analysis, *x*-ray diffraction, and optical examination.

The differential thermal analysis equipment and technique used is described by Kerr and Kulp (1948, 1949).

The theory of differential thermal analysis has been treated in several papers (Speil et al. 1945), (Kerr and Kulp 1948). A dual-terminal thermal couple is used, one terminal inserted in a thermally inert material, the other in the mineral to be tested. The rate of heating is maintained constant. Results are shown by plotting temperature-difference of the dual couple against temperature. Reactions involving heat change are indicated by characteristic deviations from a straight base line. The nature of the heat changes determines the direction and amplitude of the deviation. Loss of adsorbed or lattice water, decomposition, or changes in structure all may produce peaks.

All specimens were prepared for thermal analysis by grinding to 180–200 mesh to minimize variations due to particle size.

Debye powder patterns of the samples were taken with iron radiation. In general, the component of mixtures of iron oxide minerals could not be detected by *x*-ray technique unless their concentration was greater than 10%.

Artificial mixtures were prepared from ground samples of the pure components. The components were weighed with an analytical chemical balance and thoroughly mixed prior to (thermal) testing.

## The Hydrous Ferric Oxides

### 1. *Hydrous Ferric Oxide Minerals*

Descriptions of the naturally occurring hydrous iron oxides have resulted in a sizeable list of mineral names. The members of the group have included turgite, goethite, lepidocrocite, hydrogoethite, limonite, xanthosiderite, hydrohematite, ehrenwerthite, kaliophite, hypoxanthite, melanosiderite, avasite, esmeraldaite and limnite.

Dehydration and *x*-ray studies of both natural and synthesized material have shown most of the former "minerals" to be invalid. Posnjak and Merwin (1919) have shown that no series of iron oxide hydrates exists, and their results have been substantiated by other investigators.

Only goethite ($HFeO_2$) and lepidocrocite FeO(OH) have been accepted as minerals of the hydrous iron oxides in the 7th Edition of Dana's *System of Mineralogy*. Considerable information is available on

the physical and chemical properties of these minerals, but a detailed thermal structural study has not been published.

2. *Chemistry of Hydrous Ferric Oxides*

Thermal curves of individual specimens labelled goethite or lepidocrocite have been published by Grim and Rowland (1942) and by Speil et. al (1945).

The hydrous iron oxide occurrences found as gossans are the result of the weathering of sulfide ore bodies. These characteristically have moderate to high iron content but negligible aluminum. Therefore, aluminum ions would not be present in any abundance during the formation of the hydrous iron oxide mineral and would not be observed as a substitution product.

The hydrous basic iron oxides, which are colloidally transported, are later precipitated as goethite or lepidocrocite. Aluminum is usually transported as colloidal clay particles (kaolinite, montmorillonite, or illite). These colloids have sufficiently different properties from the hydrous iron oxide colloids that they tend to be separated in precipitation. Moreover, free aluminum ions are not present for reaction during sedimentation and diagenesis.

The result is that the geochemical conditions generally separate iron and aluminum in weathering processes even though from a structural point of view substitution seems feasible.

Hydrous ferric oxide may be easily prepared by adding a soluble base, such as ammonium hydroxide, to a solution containing ferric ions. The precipitate formed will be of extremely small particle size. This can be attributed to the very low solubility of ferric oxide which produces a high degree of supersaturation preceding precipitation. A large quantity of water is entrained in these particles.

The *x*-ray diffraction patterns of such precipitates fail to indicate crystallinity.

However, if this "amorphous" material is aged under water for a sufficiently long time, crystallinity will appear accompanying the process of dehydration. This emphasizes the instability of form of hydrous ferric oxide gel and its general absence in nature.

Weiser and Milligan (1934, 1935) aged precipitates prepared by adding ammonium hydroxide to ferric chloride solution and examined the resulting material by *x*-ray diffraction methods. At room temperature, lines began to appear only after five months, and in order to obtain good patterns, aging for one year was found necessary. At 100° C., the transformation was visible after only one hour, and the lines were sharp after seventeen hours. The color changed from brown to red and, in every case, the

final product was alpha-$Fe_2O_3$. This led Weiser and Milligan to conclude that the brown gel was nothing more than particles of alpha-$Fe_2O_3$ of a size below *x*-ray detection, containing absorbed water.

The polymorphs of the monohydrate of iron are:

1. Alpha-$Fe_2O_3 \cdot H_2O$ (goethite), gives alpha-$Fe_2O_3$ (hematite) on dehydration.
2. Beta-$Fe_2O_3 \cdot H_2O$ (not known in nature) also gives alpha-$Fe_2O_3$ on dehydration.
3. Gamma-$Fe_2O_3 \cdot H_2O$ (lepidocrocite), gives gamma-$Fe_2O_3$ (ferromagnetic) on dehydration.

Alpha-$Fe_2O_3 \cdot H_2O$ may be formed by the aging of the brown gel formed by the oxidation of ferrous compounds or slow hydrolysis of most ferric salts. A more hydrous form of alpha-$Fe_2O_3 \cdot H_2O$ may be formed by the oxidation of ferrous bicarbonate solution with peroxide, oxygen, or air at room temperature. This hydrous material will lose its absorbed water if heated in a stream of dry air at 100° C. for 48 hours, changing to the same composition as alpha-$Fe_2O_3 \cdot H_2O$.

The simplest method for preparing alpha-$Fe_2O_3 \cdot H_2O$ is by the slow hydrolysis of certain iron salts, such as ferric acetate, nitrate, bromide, and oxalate.

Gamma-$Fe_2O_3 \cdot H_2O$ is synthesized by the oxidation of freshly prepared hydrous $Fe_3O_4$, hydrous $2Fe_2O_3 \cdot 3FeO$, $Fe_2S_3$, and FeS, and ferrous chloride, the latter in the presence of pyridine or sodium azide in a solution with a pH of 2.0 to 6.5.

It is of interest to note that direct neutralization of ferric iron solutions results in hydrous ferric oxide which upon aging transforms to hematite rather than either to goethite or to lepidocrocite.

The color of hydrous and anhydrous oxides of iron is of interest. The red and the yellow hydrates have been found in nature side by side. It was once thought that the yellow type was the more unstable form and, upon dehydration produced the red monohydrate. Posnjak and Merwin (1919) believed both monohydrates to be stable at any possible normal surface temperature of the earth. The color differences appear to be largely determined by particle size.

## Experimental Results

### *Goethite*

Figure 1 shows the differential thermal curves of some of the purest goethite specimens tested. The curve for pure goethite is apparently characterized by a single endothermic peak between 385 and 405° C. This endothermic reaction is due to the decomposition of the goethite lattice. All of the specimens are characterized by coarse crystallinity. The observed habits of these specimens included: fibrous, with fibers in concentric radial growth; fibrous, forming bands with the fibers arranged

normal to the band; platy, with a tendency toward radial growth. The dense massive or light porous variety are not represented in this group.

The more brightly colored fibrous specimens have the lower peak temperatures. This is probably to be related to the smaller crystallite size. The average peak temperature for these high purity goethite specimens is 395° C. Since the experimental error in the determination of this temperature from one run to the next is of the order of 5° C., the range of peak temperatures for these specimens is probably 390–400° C.

Since goethite gave no reaction between 500 and 1000° C., most of the later thermal curves were not continued above 600° C.

To study the effect of particle size on the thermal curve of a single specimen, a series of samples were thermally analyzed.

The results are shown in Table 1. All six samples gave thermal curves with very similar shapes except the powdered material which started decomposing at about 300° C. instead of 340° C. (See Figure 1.)

Table 1. Particle Size Study—Cornwall, England

| Particle Size | Peak Temperature |
|---|---|
| Coarser than 50 mesh | 405° C |
| 50–80 mesh | 405 |
| 80–100 mesh | 400 |
| 100–120 mesh | 400 |
| 120–200 mesh | 395 |
| Powdered | 390 |

50–80 mesh goethite was intimately mixed with similarly ground hematite in various proportions. The hematite acted as an inert impurity, since it undergoes no decomposition or phase change in the temperature interval used. The calibration curve obtained by plotting height of reaction peak against concentration of goethite can be used to estimate the percentage of coarsely crystalline goethite in natural mixtures. Since hematite is a common constituent, the mixture was suitable. To a first approximation, other thermally inert constituents in a natural mixture would affect the goethite curve similarly.

Figure 2 shows the effect of the hematite on the goethite curve. Hematite, alone produces no distinctive thermal peaks as seen in the last curve. The peak temperature of the goethite was reduced from 405° C. to 375° C. when diluted with 90% hematite. The amplitude of the reaction decreased with the depression of the peak temperatures.

It is doubtful that this factor influenced the peak temperature of the goethite curves shown in Fig. 1, since the impurities were less than 5% of the volume of the material tested.

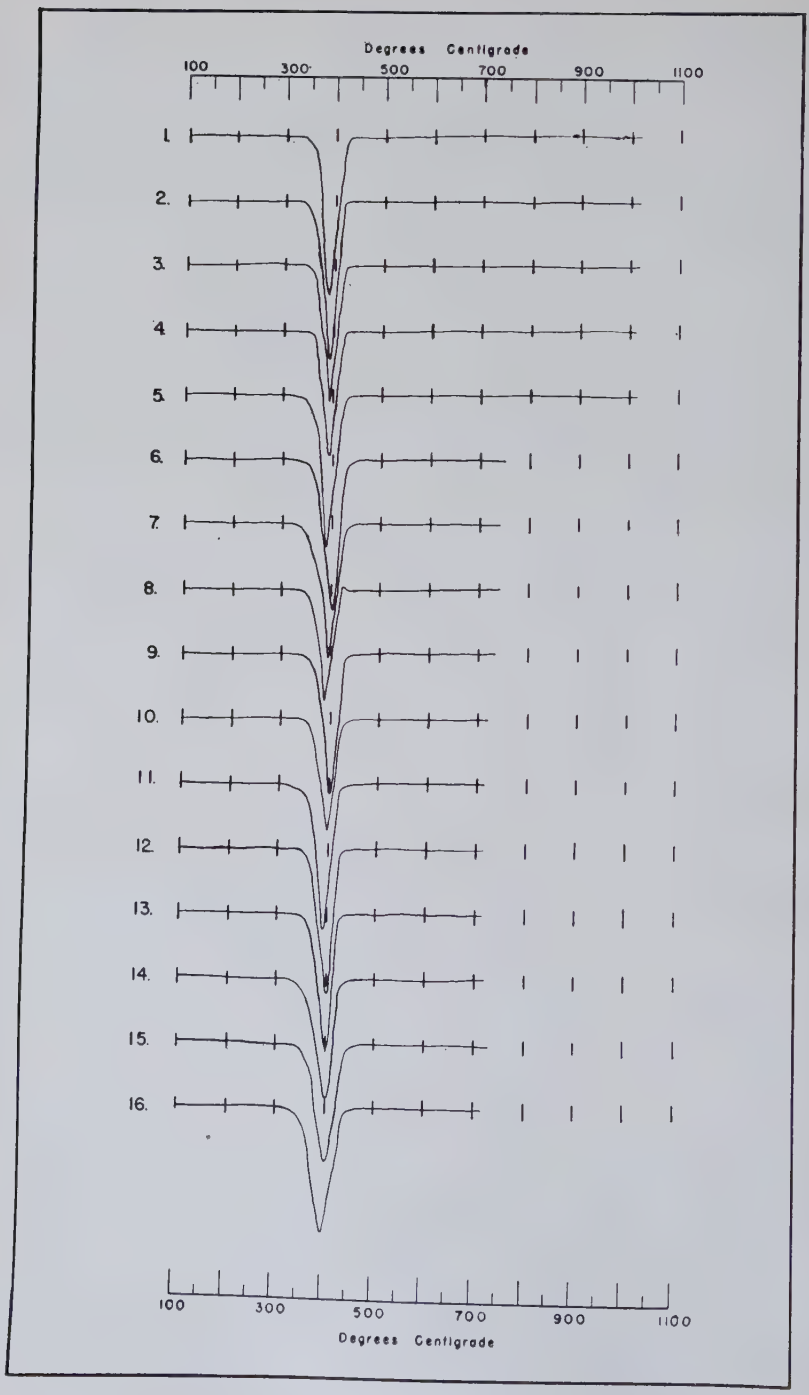


FIG. 1. For legend see top p. 29.

FIG. 1. Goethite specimens.*

| Curve No. | Museum Label | Locality |
|---|---|---|
| 1–1 | 442-2 Limonite and hematite | Lake Superior |
| 1–2 | 32-2 Limonite | Lake Superior |
| 1–3 | 185-5 Limonite (Fibrous) | Lake Superior |
| 1–4 | 185-6 Limonite (Fibrous) | Lake Superior |
| 1–5 | 160-1 Goethite | Superior Mine, Mich. |
| 1–6 | 160-5 Goethite | Ironwood, Mich. |
| 1–7 | 33-5 Goethite | Negaumee, Mich. |
| 1–8 | 430-1 Goethite | Needle Ironstone, Jackson Mine, Mich. |
| 1–9 | 162-1 Goethite | Cornwall, England |
| 1–10 | 162-2 Goethite | Restormed Mine, Cornwall, England |
| 1–11 | 169-5 Limonite | Schwartzenburg, Saxony |
| 1–12 | 430-3 Goethite | Friedrichsrode, Thuringia |
| 1–13 | 430-2 Goethite | Brazil |
| 1–14 | 430-4 Goethite | Pikes Peak |
| 1–15 | 430-5 Goethite | Pikes Peak |
| 1–16 | 430-6 Goethite | Tavistock, Devonshire |

* All specimens were *x*-rayed and showed only goethite lines.

*Lepidocrocite*

Figure 3 shows the thermal curves of specimens which were largely lepidocrocite. These curves have a number of interesting features. In general, lepidocrocite yields a thermal curve which has an endothermic reaction which begins between 250 and 300° C., culminates in a peak at 350° C. and is followed by a variable exothermic peak. There is no further reaction to 1000° C.

Pure lepidocrocite is represented by curves (Fig. 3) 2, 3, 4, 5, 6, 7, 8, 9, 10, 11, 12, 13. In these specimens it is noted that the initial break ranges from about 260° C. to 300° C. It is believed that this variation is a function of particle size. The peak temperature does not appear to be as sensitive to this factor as the temperature of the initial break. The width of the peak appears to be related to the particle (or better, crystallite) size distribution. The most uniform specimen was 3-4 (Ore Hill) which produced one of the sharpest peaks. The variations in the shape and temperature of the exothermic peak are numerous. It seems probable that if the removal of $H_2O$ after the decomposition were sluggish, the presence of a small amount of water vapor would catalyze the transition from gamma-$Fe_2O_3$ to alpha-$Fe_2O_3$ (hematite).

The contrast of the goethite and lepidocrocite thermal curves is readily explained in terms of their structures (Bragg 1937). While they both have the same chemical composition ($Fe_2O_3 \cdot H_2O$), they differ structurally in the nature of the bonding of the hydrogen atom. In goethite the hydrogen atoms act as cations between oxygen atoms in two-fold coordination.

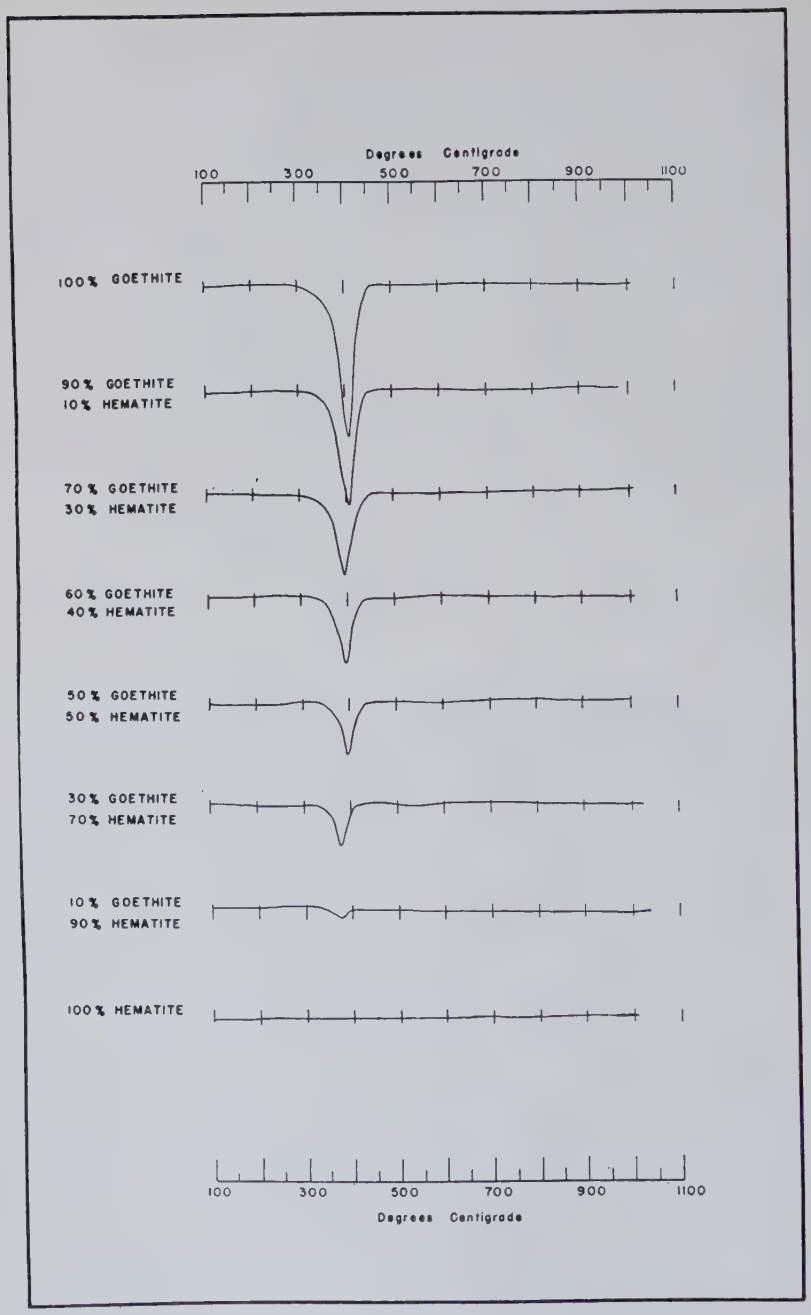


FIG. 2. Goethite-hematite artificial mixtures (50–80 mesh).

Lepidocrocite has the hydrogen atom in a discrete OH group. As might be expected, the former situation is more stable, hence the decomposition of lepidocrocite occurs at a lower temperature than goethite. While lepidocrocite decomposes to yield gamma-$Fe_2O_3$, goethite decomposing at a higher temperature gives alpha-$Fe_2O_3$ directly. The exothermic reaction in the lepidocrocite curve is due to the phase transformation of gamma-$Fe_2O_3$ to alpha-$Fe_2O_3$. This is also consistent with the observed facts that the goethite is harder and tends to be better crystallized than lepidocrocite. It is also noteworthy that the aluminum analogs, diaspore and boehmite show the same difference in decomposition temperature.

The differential thermal curve peak occurs, of course, at a temperature considerably higher than the equilibrium dehydration temperature. Gruner (1931) believes the equilibrium decomposition temperature to be between 140° C. and 200° C. for goethite. Tunell and Posnjak (1931) state that the decomposition temperature lies between 100° C. and 140°C. In either case, the rate must be very slow until about 350° C. at which temperature the reaction is detectable on the differential thermal curve.

These minerals apparently do not absorb much water since even the limonite mixture curves (Figs. 6, 7, 8) do not show the effect which such water would cause.

The grain size, purity, and physical structure are also important in determining the temperature of decomposition.

Generally speaking, a decrease in grain size tends to lower the peak temperature, but does not affect the area under the curve.

Impurities may also be expected to produce a downward shift in the temperature of the peak with an accompanying decrease in amplitude (Speil, et al. 1945).

The high purity specimens 3-2 and 3-3 show the highest peak temperatures. These were the coarsest specimens analyzed. Specimens 3-14 and 3-15 contain considerable inert impurity. 3-14 also contains some goethite, 3-1 is a mixture of goethite and lepidocrocite. In general, pure lepidocrocite shows an endothermic peak at 350° C. The shape of the low temperature side of the endothermic peak may also be used to detect the presence of a mixture. In the case of 3-1, the goethite present is a minor constituent and has very small particle size.

Known mixtures of lepidocrocite and goethite were prepared and analyzed thermally. The particle size was 100–120 mesh. Figure 4 shows the results of this analysis. It can be seen that a double peak exists in every percentage mixture, from 80% goethite and 20% lepidocrocite to 20% goethite and 80% lepidocrocite. The peak temperature of goethite is lowered from 400° C. to 384° C., while lepidocrocite was reduced from 357° C. down to 348° C.

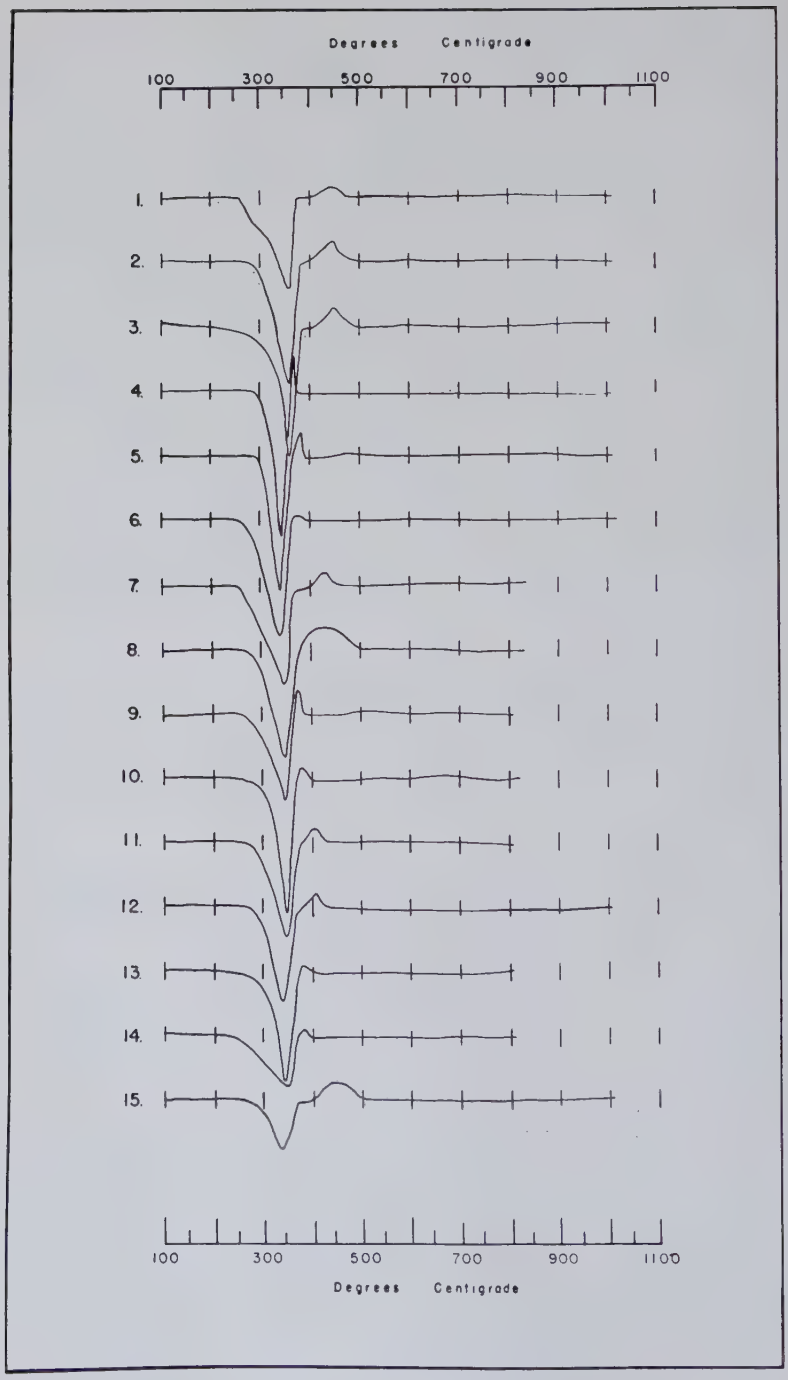


FIG. 3. For legend see top p. 33.

FIG. 3. Lepidocrocite specimens.

| Curve No. | Museum Label | Locality | X-Ray Identification |
|---|---|---|---|
| 3-1 | 34-2 Lepidocrocite | Easton, Pa. | Lepidocrocite, Goethite |
| 3-2 | 431-3 Lepidocrocite | Easton, Pa. | Lepidocrocite |
| 3-3 | 507-3 Lepidocrocite | Northampton, Pa. | — |
| 3-4 | 452-1 Limonite | Ore Hill, Salisbury | Lepidocrocite |
| 3-5 | 452-2 Limonite | Roxbury, Conn. | — |
| 3-6 | 442-1 Limonite | Rimon Valley, Duchess County, N. Y. | — |
| 3-7 | 34-4 Lepidocrocite | Richmond, Mass. | Lepidocrocite |
| 3-8 | 185-3 Limonite | Gaston County, N. C. | Lepidocrocite |
| 3-9 | 163-1 Limonite | Michigan | Lepidocrocite |
| 3-10 | 169-1 Limonite | Camaria, Jahsio, Mexico | — |
| 3-11 | 169-2 Limonite | Englenho, Velho, Brazil | Lepidocrocite |
| 3-12 | 184-2 Limonite | Steiberg, Sweden | Lepidocrocite |
| 3-13 | 185-1 Limonite | Schwartzenberg, Saxony | Lepidocrocite |
| 3-14 | 32-1 Limonite | Sasa, Saxony | Lepidocrocite, Hematite |
| 3-15 | 34-1 Xanthosiderite | Huttenholz, Thuringia | — |

To show the effect of inert constituents on mixtures of lepidocrocite and goethite, artificial mixtures of lepidocrocite, goethite, and hematite, in various proportions were prepared and analyzed thermally. Figure 5 shows these results. The peak of the goethite is lowered from 400° C. to 394° C., and the lepidocrocite from 357° C. to 350° C. It is of interest that hematite alone lowered the peak of goethite more than a mixture of hematite and lepidocrocite. It is also important to note the relative amplitudes of the goethite and lepidocrocite peaks. These thermal curves (Figs. 4 and 5) may be used to estimate the concentration of goethite and lepidocrocite from thermal curves of natural mixtures. Caution must be exercised to take into account particle size effects.

*Natural Aggregates*

Figures 6, 7, and 8 give the thermal curves of natural aggregates of hydrous ferric oxide. In each case the museum label name has been included so that the correlation of the actual mineral composition with common hand specimen identification may be appreciated.

Figure 6 shows curves of specimens which are composed of both goethite and lepidocrocite, with or without additional inert impurities. Comparison of these curves with Figs. 4 and 5 will permit estimation of the composition. They range from dominantly goethite (6-15) to dominantly lepidocrocite (6-13). These specimens (mostly labelled "limonite") were not selected for lepidocrocite content. They show rather strikingly the importance of lepidocrocite in these natural aggregates.

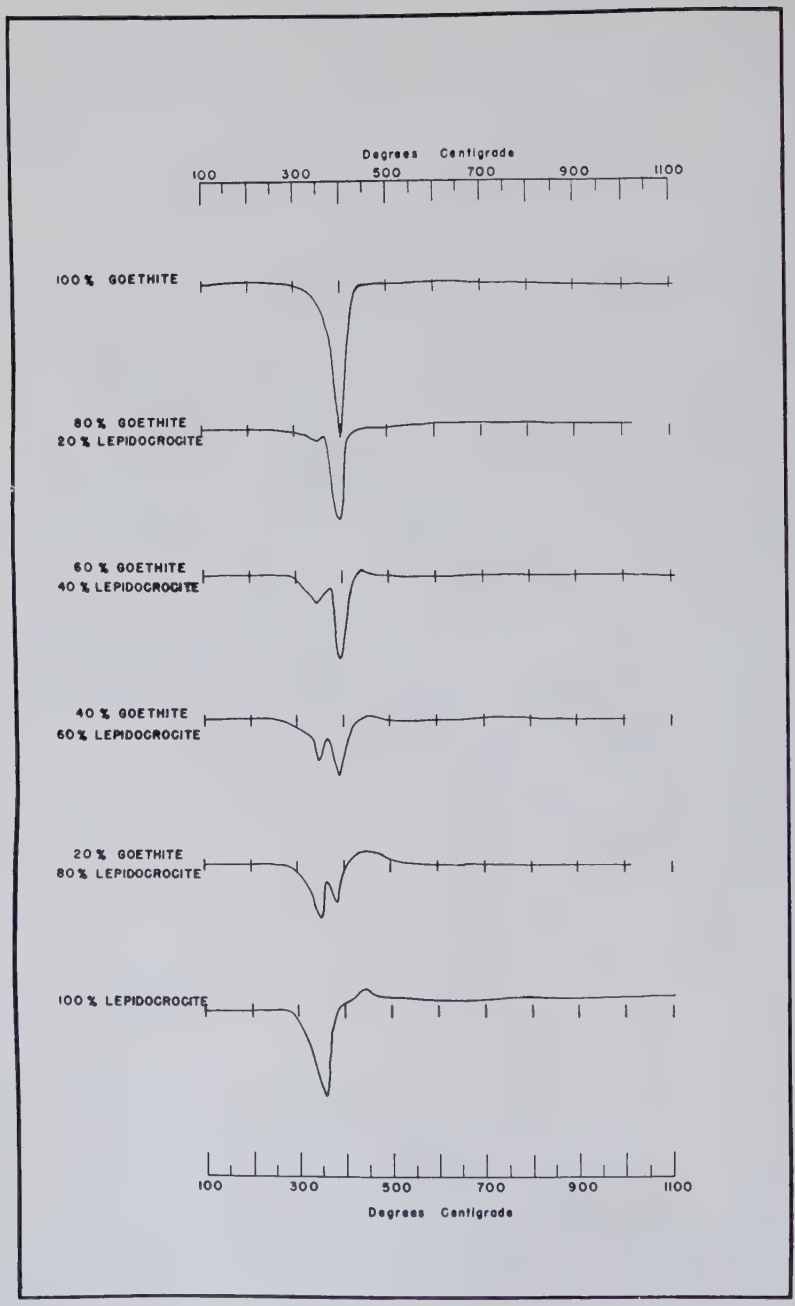


FIG. 4. Goethite, lepidocrocite, artificial mixtures (50–80 mesh).

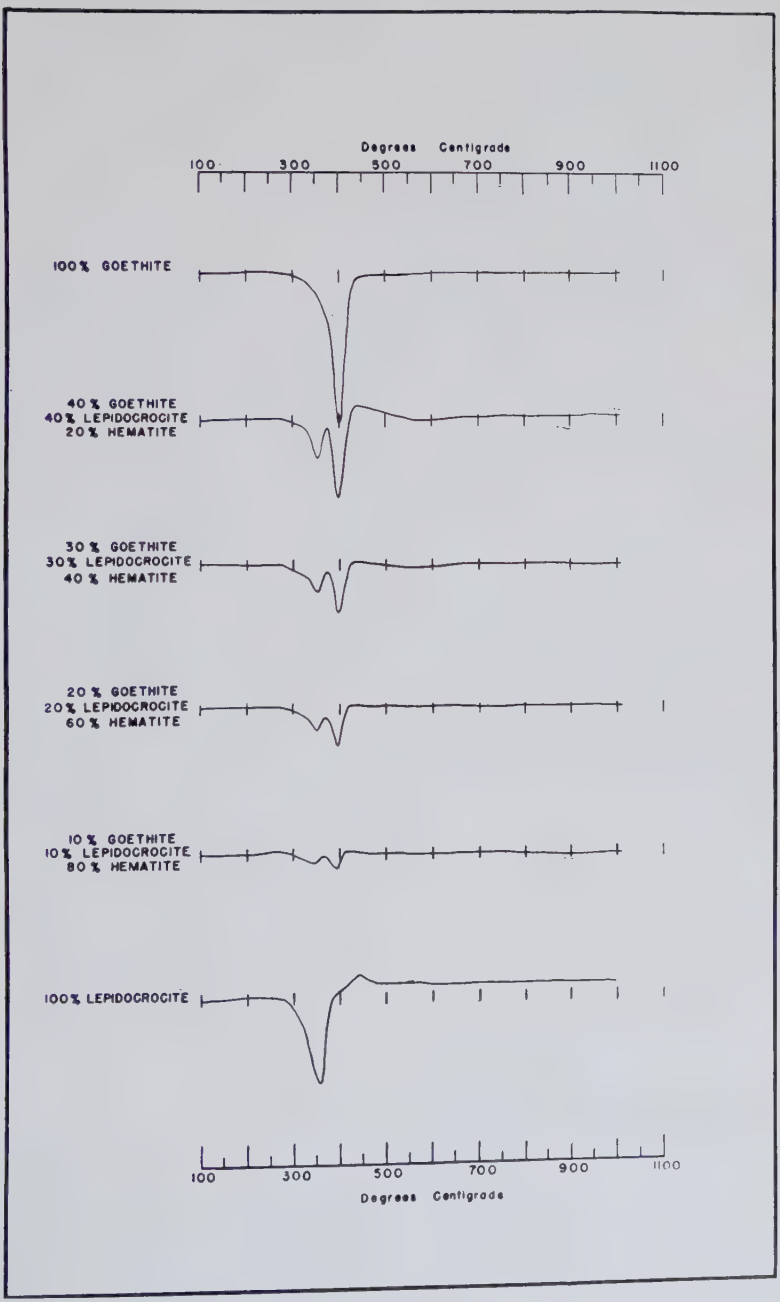


FIG. 5. Goethite, lepidocrocite, hematite artificial mixtures (50–80 mesh).

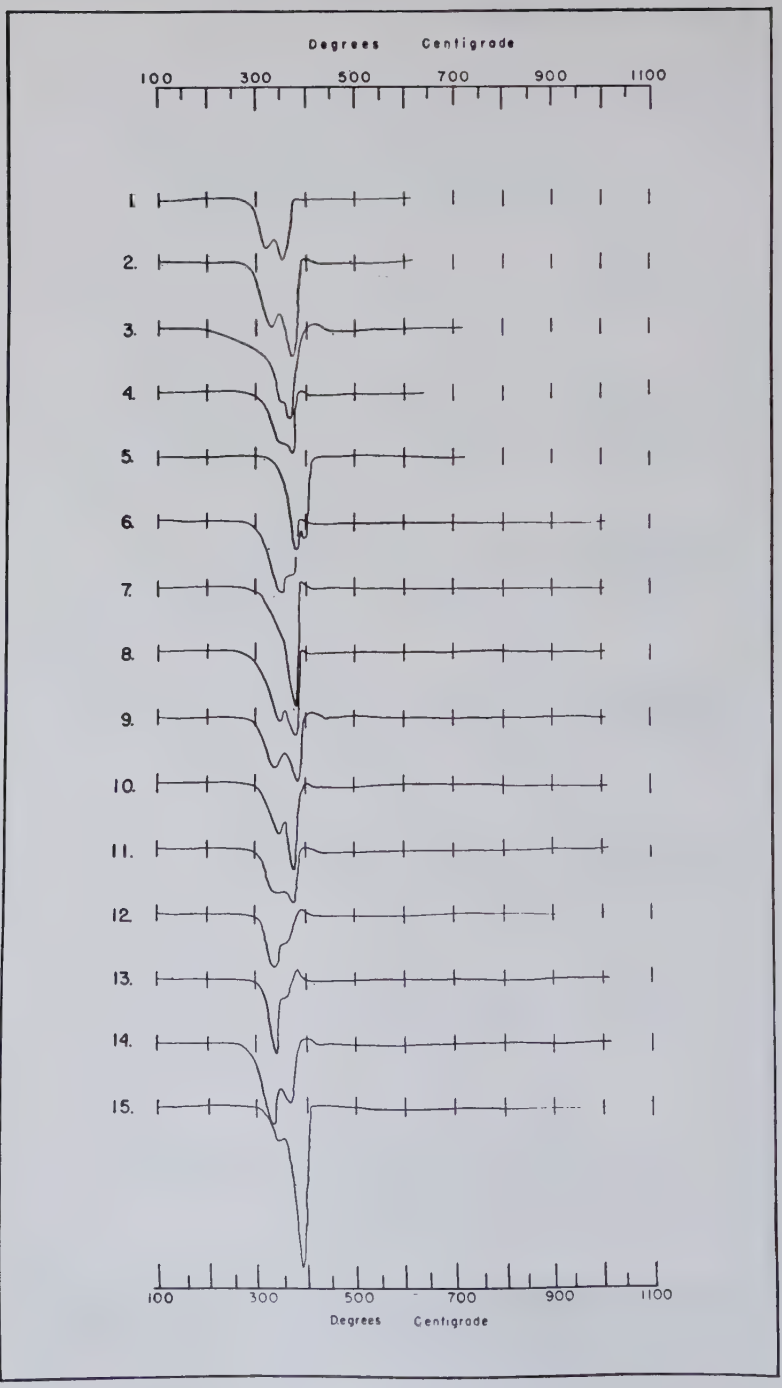


FIG. 6. For legend see top p. 37.

FIG. 6. Natural hydrous ferric oxide aggregates (mostly goethite and lepidocrocite).

| Curve No. | Museum Label | Locality | *X*-Ray Identification |
|---|---|---|---|
| 6-1 | 160-2 Goethite | Siegen, Prussia | Lepidocrocite, Goethite, Hematite |
| 6-2 | 182-3 Limonite | Siegen, Prussia | Lepid., Goethite |
| 6-3 | 431-5 Goethite | Herdorf, Siegen | Lepid., Goethite |
| 6-4 | 162-6 Limonite | Gaston County, N. C. | Lepid., Goethite, Hematite |
| 6-5 | 162-5 Limonite | Antonio Perciea, Brazil | Goethite |
| 6-6 | 33-2 Goethite | Roxbury, Conn. | — |
| 6-7 | 33-1 Goethite | Lake Superior | — |
| 6-8 | 36-2 Limonite | Easton, Pa. | Lepid., Goethite |
| 6-9 | 34-5 Limonite | Northampton, Pa. | Lepid., Goethite, Hematite |
| 6-10 | 32-3 Limonite | Woodstock, Ala. | — |
| 6-11 | 32-5 Limonite after Pyrite | Brunleya, Va. | Lepid., Goethite, Hematite |
| 6-12 | 185-2 Limonite | Wilson, Wis. | — |
| 6-13 | 184-1 Limonite | Salisbury, Conn. | — |
| 6-14 | 182-6 Limonite | Salisbury, Conn. | Lepid., Goethite |
| 6-15 | 184-3 Limonite | Llano County, Texas | Goethite, Lepid. |

Figures 7 and 8 show the curves of some additional specimens labelled "limonite" and "goethite," as well as those labelled "lepidocrocite" and "turgite." In general, most of these specimens proved to be high in hematite. (7-7) apparently contains a small percentage (15%) of kaolinite in addition to 30–40% each of lepidocrocite and goethite. (7-13) is a typical lepidocrocite curve. (8-8) is the curve of a high purity goethite. The common occurrence of lepidocrocite is again noteworthy. (8-13) is a specimen consisting of hematite and quartz.

*Substitution*

An examination of the thermal curves of Figs. 1 and 3 does not reveal evidence of substitution. This is consistent with the facts derived from *x*-ray diffraction and semi-quantitative analysis. No shifts of the high angle lines indicative of cation substitution were observed. Semi-quantitative chemical analysis of a large number of these specimens showed no important contributors from such common ions as aluminum, magnesium, manganese or titanium. These might be expected on the basis of the crystal structure if substitution does occur. The ionic radius of aluminum ion is near that of ferric ion and both form common minerals. The structures of goethite and diaspore are the same as are the structures of lepidocrocite and boehmite. One must conclude that the absence of

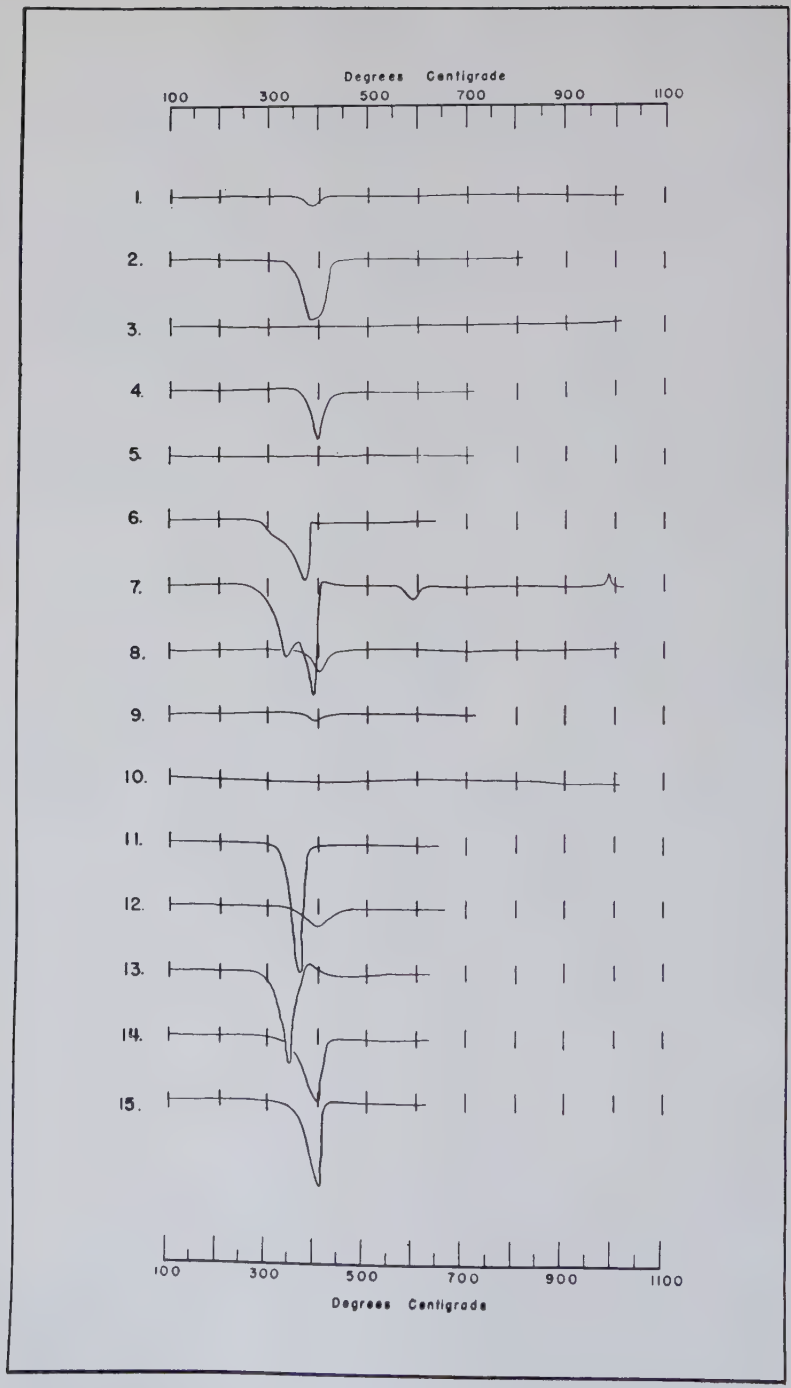


FIG. 7. For legend see top p. 39.

FIG. 7. Natural hydrous ferric oxide aggregates.

| | | | |
|---|---|---|---|
| 7-1 | 34-3 Lepidocrocite | Rossbach, Siegen | Goethite, Hematite |
| 7-2 | 36-5 Goethite | Přizbram, Bohemia | — |
| 7-3 | 36-3 Turgite | Woodstock, Ala. | Hematite |
| 7-4 | 431-1 Goethite | Jackson Mine, Mich. | Goethite, Hematite |
| 7-5 | 431-2 Goethite | Marquette, Mich. | — |
| 7-6 | 160-6 Goethite | Marquette, Mich. | — |
| 7-7 | 507-2 Lepidocrocite | Siegen | Lepid., Goethite, Kaolinite |
| 7-8 | 507-5 Goethite | Rossbach, Siegen | — |
| 7-9 | 507-6 Goethite | Přizbram, Bohemia | — |
| 7-10 | 452-3 Turgite | Lehigh County, Pa. | Hematite |
| 7-11 | 452-4 Turgite | Shelby County, Ala. | Goethite |
| 7-12 | 452-5 Turgite & Limonite | Lancaster County, Pa. | — |
| 7-13 | 161-1 Goethite | California | Lepidocrocite |
| 7-14 | 161-2 Goethite | Pikes Peak | Goethite, Hematite |
| 7-15 | 161-5 Goethite | Gotha, Germany | |

substitution of ferric ion by aluminum is due to the geochemical separation of these ions in the process of weathering and deposition.

In the case of ordinary rock weathering the aluminum is generally locked up in the clay minerals. In gossans the iron is released from sulfide minerals essentially in the absence of free aluminum ions. Thus the chemical environment is not favorable to the formation of substituted goethite or lepidocrocite. The absence of evidence for substitution in these numerous natural aggregates is consistent with this concept.

*Prepared Hydrous Ferric Oxides*

An interesting set of thermal curves was obtained from the precipitation of ferric iron as the hydrous oxide under different laboratory conditions. The results of these experiments are shown on Fig. 9.

The first determination (1) was made on the iron precipitated by adding saturated $FeCl_3$ solution dropwise to a concentrated $NH_4OH$ solution. The dense precipitate which was formed was filtered, washed once with dilute $NH_4OH$ and allowed to dry at room temperature. Formation therefore took place under the conditions of rapid precipitation at a pH of 10 and a temperature of 25° C. The dried precipitate was analyzed thermally.

Its first endothermic reaction occurs slightly under 200° C., and is probably caused by the release of water adsorbed on the colloidal material. The major asymmetric exothermic peak at 490° C. is due to the recrystallization of the amorphous $Fe_2O_3$ to alpha-$Fe_2O_3$ (hematite). This was proved by *x*-ray patterns taken at 450° C. and 550° C. The slight dip prior to the major exothermic peak is attributed to the sublimation

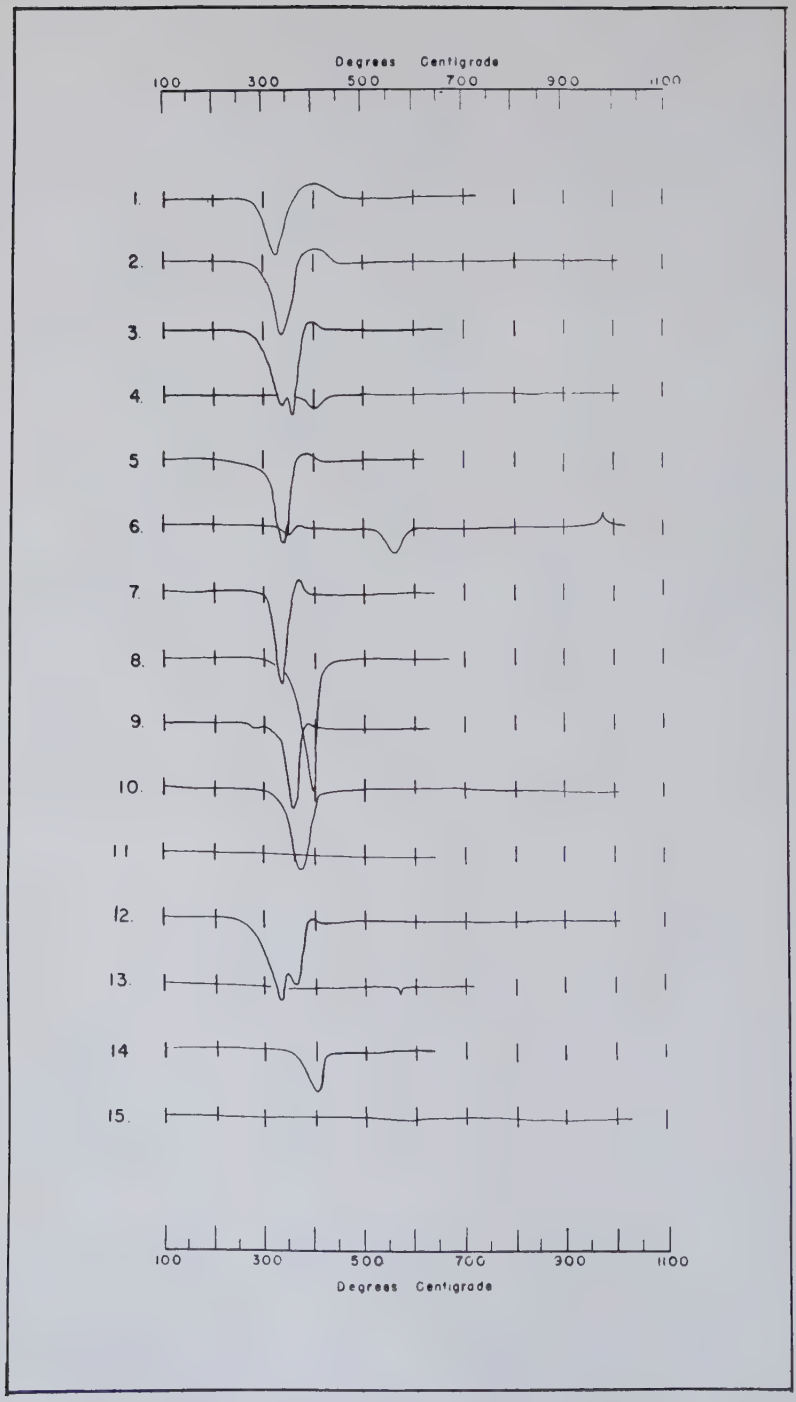


FIG. 8. For legend see top p. 41.

FIG. 8. Natural hydrous ferric oxide aggregates.

| Curve No. | Museum Label | Locality | X-Ray Identification |
|---|---|---|---|
| 8-1 | 183-5 Limonite | Terra do Curral, Brazil | Lepid, Hematite |
| 8-2 | 183-6 Limonite | Pico de Italina, Brazil | — |
| 8-3 | 431-6 Lepidocrocite | Herdorf, Siegen | Lepid., Goethite |
| 8-4 | 186-1 Limonite | L'Ause, Lake Superior | — |
| 8-5 | 442–3 Limonite | Osmond Mine, Kings Mtn., N. C. | Lepidocrocite |
| 8-6 | 442-4 Limonite | Easton, Pa. | Goethite, Hematite, Kaolinite |
| 8-7 | 442-5 Limonite | New York | Lepidocrocite |
| 8-8 | 442-6 Limonite | Roxbury, Conn. | Goethite |
| 8-9 | 182-1 Limonite | Salzburg, Austria | — |
| 8-10 | 182-2 Limonite | Brazil (yellow) | — |
| 8-11 | 182-4 Limonite | Brazil (brown) | Hematite |
| 8-12 | 182-5 Limonite | Lenox, Mass. | Lepid., Goethite |
| 8-13 | 33-3 Goethite | Přizbram, Boehmia | Hematite, quartz |
| 8-14 | 33-4 Goethite | Pikes Peak | — |
| 8-15 | 507-1 Turgite | Lake Superior | — |

of $NH_4OH$. Thus, as might be expected, this method of preparation simply yielded colloidal $Fe_2O_3 \cdot xH_2O$ which dehydrates to hematite.

Curve 2 shows the thermal record of material prepared by adding concentrated $NH_4OH$ dropwise to a saturated solution of $FeCl_3$. At the end of the precipitation the solution was faintly acid to litmus. The rapid precipitation took place at a pH of 5 and a temperature of 25° C. The color of the precipitate was a much lighter brown than that of the material obtained by the former method at a pH of 10. The precipitate was washed thoroughly with water.

The first large endothermic reaction at 178° C. is almost identical to that of Curve 1, but of slightly smaller amplitude. The exothermic peak at 278° C. is to be attributed to the recrystallization of amorphous $Fe_2O_3$ to hematite. This reaction is apparently catalyzed by the presence of hydrogen ions. A small endothermic kick is found at 400° C. which is due to a trace of $NH_4OH$ not removed in the washing.

These experiments strongly suggest that in nature hematite is generally formed by the autodehydration of the hydrous ferric oxide gel which is a result of direct neutralization of a ferric ion solution. Goethite and lepidocrocite are not formed under these conditions but rather by the slow oxidation of certain ferrous compounds and the slow hydrolysis of ferric salts (goethite) or oxidation of iron sulfides and hydrous $Fe_3O_4$ gels (lepidocrocite).

The remaining curves represent mixtures of prepared hydrous ferric oxides precipitated in the presence of kaolinite. The reduced peaks of the

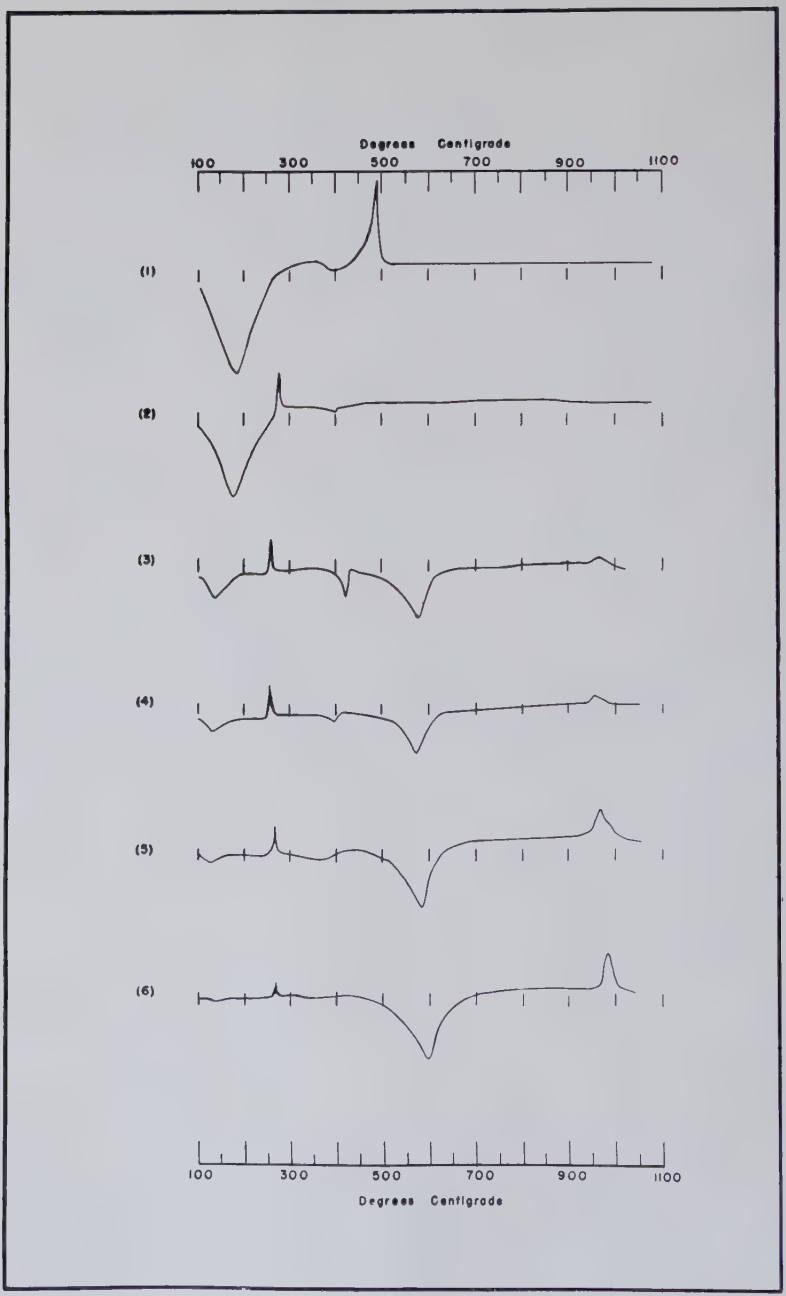


FIG. 9. For legend see top p. 43.

FIG. 9. Prepared hydrous ferric oxides.

| Curve No. | Conditions |
|---|---|
| 9-1 | Precipitation at pH10; 25° C, thorough washing with dil. $NH_4OH$ |
| 9-2 | Precipitation at pH5; 25° C, thorough washing with $H_2O$ |
| 9-3 | Precipitation at pH5; 25° C, 40 gms. $FeCl_3$, 40 gms. kaolinite |
| 9-4 | Precipitation at pH5; 25° C, 25 gms. $FeCl_3$, 40 gms. kaolinite |
| 9-5 | Precipitation at pH5; 25° C, 15 gms. $FeCl_3$, 40 gms. kaolinite |
| 9-6 | Precipitation at pH5; 25° C., 5 gms. $FeCl_3$, 40 gms. kaolinite |

kaolin may be seen at 579° C. and 952° C. The hydrous ferric oxides were prepared by adding $NH_4OH$ dropwise to a solution containing $FeCl_3$ and kaolinite. The solution was acid to litmus during the precipitation. The precipitate was filtered, washed with water, and dried at room temperature for 3 days. In these experiments, the washing was not as thorough as in the case of curve (2). Note the decrease in the $NH_4OH$ peak with the hydrous ferric oxide concentration.

This type of experiment could be profitably carried out with synthetic goethite and lepidocrocite. It would appear that considerable information of the geochemical condition which determine the relative concentration of these minerals could be ascertained in this way. The products of both the oxide formed in the acid and basic solutions gave alpha-$Fe_2O_3$ lines. Thus it appears that under these conditions colloidal hydrous iron oxide formed directly which goes over to hematite on dehydration.

## CONCLUSIONS

The typical differential thermal curve of goethite seems characterized by a single endothermic reaction. For a heating rate of 12° C. per minute the peak on the thermal curve appears at 395° C. $\pm$ 10° C. depending somewhat on the crystallite size.

The typical lepidocrocite thermal curve also has a single endothermic reaction which seems to have a peak temperature close to 350° C. This is followed by an exothermic peak, due to the phase change of gamma to alpha-$Fe_2O_3$.

It is possible, then, to distinguish between goethite and lepidocrocite on the basis of their thermal curves.

Analysis of a large number of natural hydrous ferric oxide aggregates shows the presence of both lepidocrocite and goethite. Lepidocrocite appears to be much more common than is generally appreciated.

It is possible to estimate the percentage composition of the hydrous iron oxide minerals in these natural mixtures.

Inert impurities are effective in lowering the peak temperature of these

minerals and frequently cause a broadening of the peaks, and a decrease of the amplitude.

Differences in particle size affect the peak temperatures. It was found that the smaller particle sizes produced lower peak temperatures. The difference in the temperature of the peaks may be as much as 25° C. when coarsely crystalline goethite is ground to pass 300 mesh.

Substitution of iron by other common cations was not detected in this study. This is related to the geochemical environment in which they are formed.

Artificially prepared hydrous ferric oxides gave thermal curves which depended on the pH of the solution in which they were formed. The presence of hydrogen ion catalyzes the recrystallization to hematite.

Differential thermal analysis appears applicable to a systematic study of gossans, since both goethite and lepidocrocite may be estimated semi-quantitatively. Systematic variations in the hydrous iron oxide mineral with position of an ore body or with type of ore mineral present might be expected. Such variations would certainly reflect changing geochemical conditions.

## References

Blanchard, Roland (1944), Chemical and mineralogical composition of typical limonites: *Am. Mineral.*, **29,** 111–114.

Bragg, W. L. (1937), Atomic Structure of Minerals, Cornell Univ. Press, Ithaca, N. Y.

Grim, R. E., and Rowland, R. A. (1942), Differential thermal analysis of clay minerals and other hydrous materials: *Am. Mineral.*, **27,** 746–761; 801–818.

Gruner, J. W. (1931), The stability relations of goethite and hematite: *Econ. Geol.*, **26,** 442–445.

Kerr, P. F., and Kulp, J. L. (1948), Multiple differential thermal analysis: *Am. Mineral.*, **33,** 387–419.

Kulp, J. L., and Kerr, P. F. (1949), Improved differential thermal analysis apparatus: *Am. Mineral.*, **34,** 839–845.

Locke, A. (1926), Leached outcrops as guides to copper ore: Williams and Wilkins, Baltimore.

Palache, C., Berman, H., and Frondel, C. (1944), Dana's System of Mineralogy, 7th Ed., John Wiley and Sons.

Posnjak, E., and Merwin, H. E. (1919), The hydrated ferric oxides: *Am. Jour. Sci.*, **47,** 311–348.

Speil, S., Berkelhamer, L. H., Pask, J. A., and Davies, B., (1945), Differential thermal analysis. Its application to clays and other aluminous minerals: *U. S. Bur. of Mines, Tech. Paper* **664.**

Tunell, G., and Posnjak, E. (1931), The stability relation of goethite and hematite: *Econ. Geol.*, **26,** 337–343.

Weiser, H. B., (1935), Inorganic Colloid Chemistry, Vol. **2,** The Hydrous Oxides and Hydroxides.

Weiser, H. B., and Milligan, W. O. (1934), *X*-ray studies of the hydrous oxides: *Jour. Phys. Chem.*, **38,** 513–519.

*Manuscript received*
*March 8, 1950*

# THE NORTONITE FALL AND ITS MINERALOGY

Carl W. Beck* and Lincoln LaPaz† *Department of Geology and Department of Mathematics and Astronomy, The University of New Mexico, Albuquerque, New Mexico.*

Abstract

A brief summary is given of the circumstances attending the observation of, the search for, and the recovery of the achondrites that fell on February 18, 1948 in Kansas and Nebraska. The main mass of this achondritic fall is not only the largest known aerolite in the world but also the largest meteorite of any type of witnessed fall. The weight of the principal mass is inferred to be at least 2360 pounds and the integrated weight of the recoveries so far made is estimated as in excess of 2500 pounds. The recovered achondrites serve as the type stone of a new achondritic subclass, the nortonites, intermediate between the aubrites and the Cumberland Falls whitleyite.

Brief details are given on the distribution of nortonite recoveries, on the apparent and corrected radiant of the shower, and on the real path of the fireball.

The mineralogy of the nortonites is discussed. Megascopically, this achondrite resembles a rhyolite porphyry in which the "phenocrysts" are grayish cleavage enstatite and glassy enstatite, and the fine-grained "groundmass" seems to be solely enstatite. Closer inspection reveals inclusions of nickel-iron pellets; abundant, small flakes of graphite; diallage; and iron-rust stains. Microscopic examination in thin sections and oil immersions confirms the megascopic examination, and reveals that olivine is fairly abundant. Clinoenstatite is intergrown with enstatite in some crystals. Optical constants are given for enstatite and olivine. The meteorite has a fusion rind ranging from 0.2 mm. to at least 17.7 mm. The rind is holocrystalline and is very fine grained.

A polished section of one nickel-iron inclusion was studied. The metallic phase is made up of kamacite and schreibersite. Small amounts of troilite were noted in other metallic inclusions but none in the polished specimen.

Chemical and spectrographic analyses of the stony and metallic phases are given. Tests have been run at the Institute for Nuclear Studies of the University of Chicago on nortonite samples in an effort to detect radioactivities induced by exposure to cosmic radiation. To date, no evidence of such radioactivities has been obtained.

The recovery of this achondrite gives strong support to the "meteorite-planet" hypothesis favored by Boisse, Farrington, and Harrison Brown.

Eight figures and two tables are given.

## Introduction

Shortly before 4:56 p.m. C.S.T. on February 18, 1948, a large and brilliant detonating fireball fell near the common boundary of Norton County, Kansas, and Furnas County, Nebraska. Initial reports describing this incident as the fall of an airplane in flames southeast of the airbase at McCook, Nebraska, were transmitted to the Institute of Meteoritics of the University of New Mexico shortly before 6:00 p.m. M.S.T.

* Research Associate, Institute of Meteoritics, The University of New Mexico.
† Director, Institute of Meteoritics, The University of New Mexico.

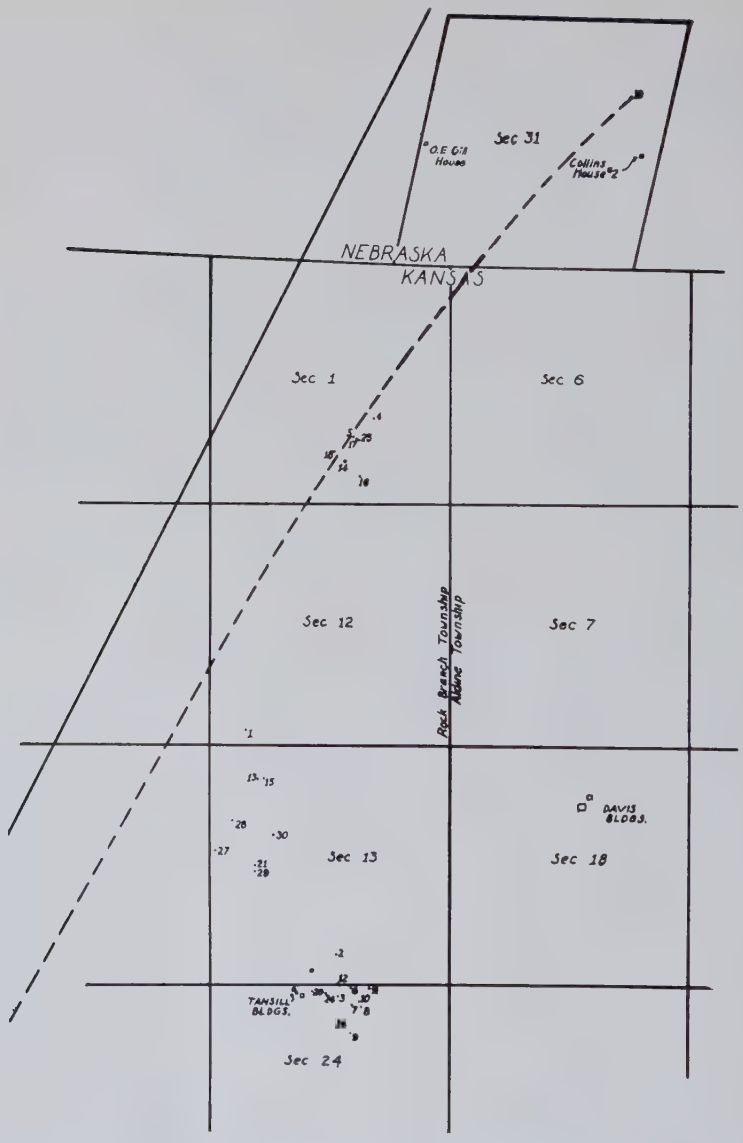


FIG. 1. Distribution of recovered fragments of the Norton County, Kansas-Furnas County, Nebraska meteorite fall of February 18, 1948. No. 18, the 131½-pound meteorite; no. 19, the 2360-pound meteorite. Solid line is the projection of the original path of the meteorite; dashed line is the projection of the real path of the meteorite veering to the east.

Within the next few hours much additional information was secured by means of interrogations conducted through Civil Air Patrol and other channels.

The best observations of the fall were so concordant that by March 3 calculations at the Institute had led to the determination of a provisional "strewn-field" location. This field was elliptical in shape, with major and minor axes of eight and four miles, respectively. The major axis, the direction of which was about N. 25° E., extended from a point about four miles south of the Kansas-Nebraska line, and almost exactly on the 100° meridian, to a point about four miles north of the state line.

A search party from the Institute entered the strewn-field on March 24, 1948. Heavy snowfall rendered effective search impossible, but this first party obtained valuable testimony from eye witnesses and secured many transit measurements of the azimuth and elevation of points on the apparent path of the fire ball. These instrumental measurements confirmed the provisional strewn-field, and gave every indication that the main mass had fallen in the northern end of the fall area in Furnas County, Nebraska. A second Institute party entered this area on April 27, 1948, and searched that portion of the elliptical strewn-field situated in Nebraska. Although the concordant testimony of eyewitnesses in this area completely substantiated the conclusion that the main mass had fallen in Furnas County, no trace of its point of impact could be found.

On revisiting the area canvassed by the first Institute party, the news was received that on April 6 a "strange stone" had been found. This stone turned out to be a fine achondritic mass. An all-out search of the southern half of the strewn-field resulted in more and more finds, culminating in the discovery on May 1 of a deeply buried achondrite weighing $131\frac{1}{2}$ pounds (LaPaz, 1948). However, in spite of all efforts, the main mass of the shower remained undiscovered until, on July 3, a caterpillar tractor started to capsize into the six-foot crater produced by impact of the chief fragment of the fall. Excavations conducted by the Institute of Meteoritics and the University of Nebraska, which had jointly acquired possession of the main mass, showed that this impact crater was over ten feet deep. The locations of the various recoveries are shown in Fig. 1.

Under the direction of Dr. C. B. Schultz, University of Nebraska State Museum, and Professor E. F. Schramm, University of Nebraska, the ponderous and fragile main mass of the achondritic fall was encased in burlap, plaster of paris, and boards and trucked to the Institute of Meteoritics. In spite of the fragile nature of the achondritic material, the sheathing prevented damage to even the sharpest knife edges separating contiguous piezoglyphs (Fig. 2).

## Characteristics of the Achondrite and Its Real Path

The stone has an irregular shape; however, a close approximation to its true volume was obtained by treating the achondrite as made up of several regular geometric solids. By this method Mr. Frank Lane, De-

partment of Mathematics and Astronomy, University of New Mexico, found that the volume of the Furnas County stone was approximately 11.8 cubic feet. Adopting the smallest admissible value of the density of the achondrite (3.18), this volume corresponds to a weight of 2360 pounds. The integrated weight of all the fragments so far recovered from the shower has been estimated conservatively as in excess of 2500 pounds.

In view of the relative rarity of achondrites—this class of meteorite constitutes only 9 per cent of the aerolitic falls of the world and makes up

FIG. 2. The main mass of the achondrite, showing piezoglyphs.

an even smaller proportion of the recoveries on a weight basis (Leonard, 1943 and 1946)—the extraordinary nature of the shower of February 18, 1948, as regards magnitude, can be appreciated. However, it is not alone in size that this fall is exceptional. The material recovered in Kansas and Nebraska differs sufficiently from all known achondrites to justify adopting it as the type stone of a new achondritic subclass (Beck and LaPaz, 1949). The role played by the Norton-Furnas achondrite is that of a second link in the chain connecting the aubrites (Au) and the enstatite-achondrites (Cen). The first link is the whitleyite (Merrill, 1921) as shown in the classificational sequence of Leonard (1948). Following Leonard (1948 and 1949), this fall would be assigned the nomenclature $A_2$no, would occupy a position between the aubrites and the whitleyite, and would be called *nortonite*.

The projection of the path of the achondrite before it was affected by air resistance is shown by the solid line in Fig. 1. The projection of the real path of the meteorite in the atmosphere is shown by the dashed line in Fig. 1. A veering of the real path toward the east, similar to but more pronounced than that shown in Fig. 1, has been found for other well-observed meteorite falls; for example, the recently reported meteorite-crater producing fall of February 12, 1947, in the Maritime Province of the USSR (LaPaz, 1949). The nortonite meteorite exploded at least twice during its visible flight and these explosions produced huge clouds of meteoritic dust.

Calculations from the known time of occurrence of the nortonite shower, the coordinates of the apparent radiant point, and velocity estimates give the following: (1) the geocentric velocity of the fireball was only 5.75 miles/second; and (2) the corrected radiant point had a right ascension of 11°50′ and a declination of −29°01′.

## Mineralogy

*Megascopic Examination.* The main mass of the achondrite, the outside of which exhibits fusion crusts ranging in thickness from less than 0.2 mm. to at least 17.7 mm., is beautifully pitted with flight markings, or piezoglyphs (Fig. 2). The color of the fusion rind ranges from white to black, with most of it being a brownish-gray or grayish-brown, putty color. That the fusion was incomplete during its flight through the atmosphere is shown by the trapped angular fragments imbedded in the fusion crust. The appearance of the unfused, main mass of the meteorite suggests a rhyolite porphyry. The "groundmass" is of a grayish-white color, fine grained in texture. The "phenocrysts" are enstatite of two different types. One type is a light-gray enstatite exhibiting the usual pyroxenic cleavage at angles of 88° and 92°, and resembling a weathered feldspar in a porphyry. The other type is a clear, glassy enstatite with no apparent cleavage; this is not unlike the appearance of quartz in a porphyry. The cleavage enstatite reaches a length of 25 mm., and the glassy enstatite occurs in broken fragments of equal length. A closer examination reveals abundant, small flakes of graphite; iron rust stains; a brown, platy mineral identified in thin section as diallage; and, haphazardly scattered through the mass, rounded, superficially oxidized included pellets of nickel-iron ranging in size from very small to at least dimensions of 50 by 35 by 20 mm. (Fig. 3). Local, small slickensided surfaces are present. On the slickensided surfaces observed there seems to be a particular concentration of graphite and iron stain. The largest of such surfaces covered an area of 9 square centimeters.

An interesting, and unprecedented, phenomenon developed on the large mass of the meteorite after its arrival at the Institute of Meteoritics.

When part of the plaster of paris coating was removed, the meteorite grew a "beard;" *i.e.*, a white, fibrous growth appeared on the surface of the meteorite, covering an area of more than 2000 square centimeters. The fibers reached a length of about 5 cm. A qualitative chemical test of the "beard" showed abundant magnesium, water, and carbon dioxide with traces of iron and aluminum. The material effervesced readily in

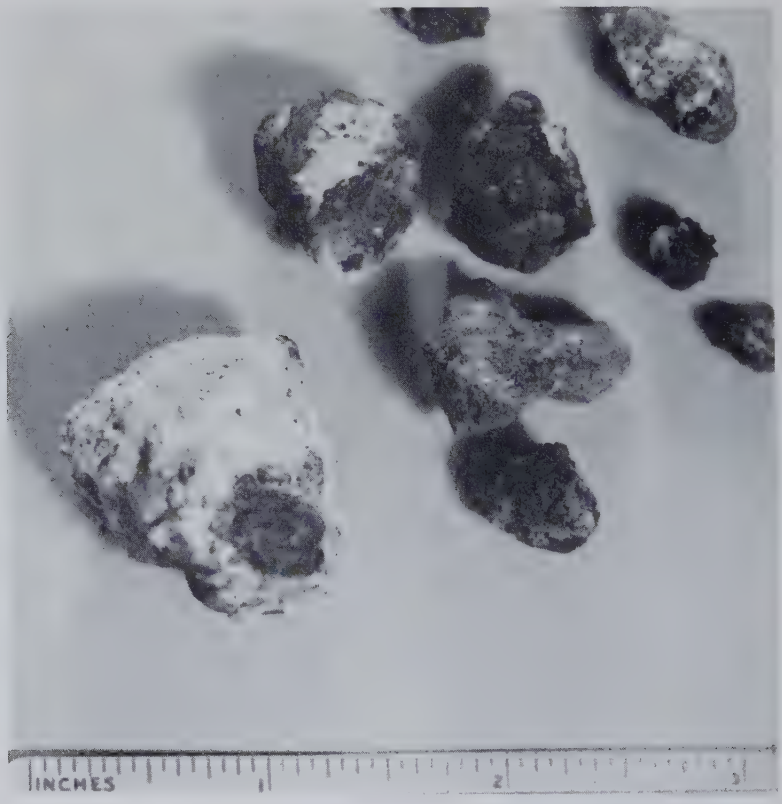


FIG. 3. Collection of nickel-iron inclusions.

dilute cold HCl; it is apparently a hydrated magnesium carbonate. The meteorite had lain in the moist Nebraska soil from February to August, during which time water containing carbon dioxide had penetrated into the interstices of the stone. In Albuquerque, with a higher altitude and drier climate, the water was drawn back out of the tiny openings in the stone, evaporated, and deposited material dissolved from the interior of the meteorite.

The specific gravities of the various components of the achondrite varied from 3.06 to 6.11. The specific gravity of the cleavage enstatite is 3.18 (Jolly balance).

*Microscopic Examination.* In thin section the cleavage enstatite is seen to make up the main mass of the meteorite, both the "groundmass" and the "phenocrysts." The enstatite ranges from large, well-formed crystals to fine-grained interstitial material (Fig. 4), giving a seriate porphyry texture. Some of the enstatite (the glassy enstatite referred to above) gives an undulatory extinction and a distorted abnormal interference figure, evidence that it is under strain. Other grains of the glassy enstatite

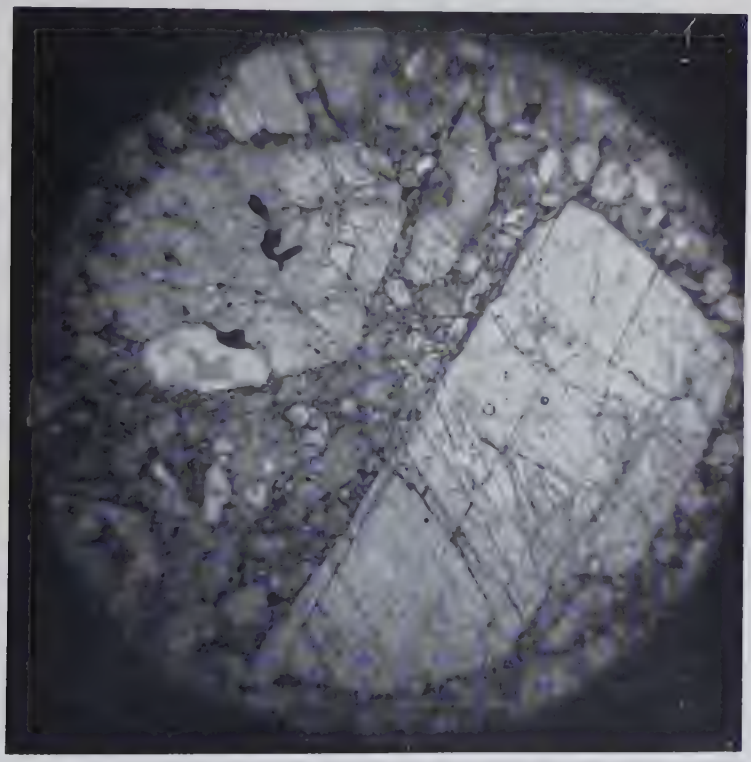

FIG. 4. Photomicrograph of well-developed enstatite crystals. ×200.

give an undulatory extinction but a distinct interference figure. In such cases the optic angle is 80–85°, compared with an optic angle of 40° for the cleavage enstatite. As shown below, this is the only difference in the optical constants of the two types of enstatite. Therefore, the authors have been forced to the conclusion that the difference in the axial angle is a function of the strain. In a few crystals of the cleavage enstatite the appearance in crossed nicols is noteworthy. An enstatite crystal appears homogeneous in plane polarized light, but the same crystal in crossed nicols shows narrow, pinched out bands reminiscent of polysynthetic twinning in feldspars (Fig. 5). The main mass gives the parallel extinction

of enstatite; the bands give an inclined extinction up to 20°. There is no noticeable difference in the indices of refraction nor in the interference color, so that the authors have concluded such crystals represent an intergrowth of enstatite and clinoenstatite. Merrill (1921) recognized the same phenomenon in the Cumberland Falls achondrite. Figure 6 shows the same intergrowth of the two pyroxenes, but in this one case the clinoenstatite is in vermicular intergrowth with the host enstatite.

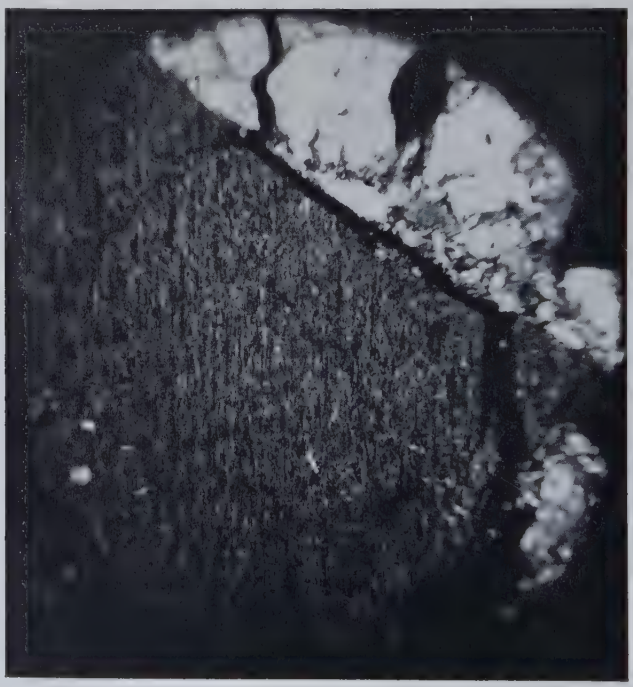

FIG. 5. Intergrowth of enstatite and clinoenstatite, crossed nicols. ×200.

Olivine is fairly abundant intermixed with enstatite in the finer grained portions of the meteorite, and, occasionally, there is a fairly large grain. Most of the olivine is remarkably fresh; only occasionally does one see a slight alteration to serpentine. Some of the olivine is poikilitic in the enstatite. Graphite flakes are abundant. Diallage is scattered throughout the mass in small amounts. In thin section the fusion rind is seen to be holocrystalline and very fine grained. In a few places there are some colorless, clear blebs of glass.

By the oil immersion method the following optical constants were obtained for the cleavage type of enstatite: $\alpha = 1.652$, $\beta = 1.654$, $\gamma = 1.660$; optical character, positive; axial angle = 40°; dispersion, $r < v$, weak;

optical orientation, $X=a$, $Y=b$, $Z=c$; the axial plane is {010}; cleavage is {110} at 88° and 92°; parting is {010} and is unusually well developed judging from the number of centered biaxial flash figures and the ease

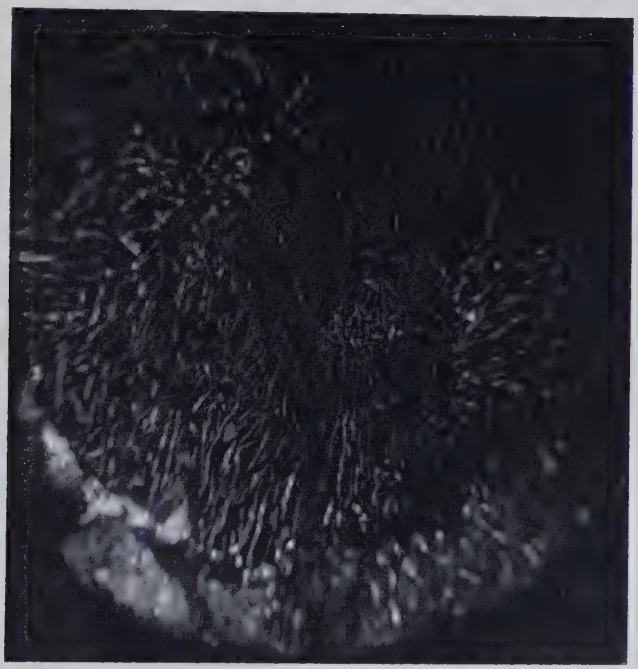

FIG. 6. Intergrowth of enstatite and vermicular clinoenstatite, crossed nicols. ×200.

with which they can be obtained; the cleavage traces are length slow; and the extinction is parallel. The above constants check very well with those of pure artificial enstatite (Larsen and Berman, 1934, p. 118). The small amount of iron in the chemical analysis (below) corroborates the purity of the enstatite.

The glassy enstatite gives the same constants as for the cleavage enstatite, with two exceptions. The glassy enstatite does not cleave or part; rather, it explodes with a conchoidal fracture. Both in thin section and in oil immersion this glassy enstatite is seen to be under considerable internal strain. The other, and more surprising, difference is that the axial angle for the glassy enstatite is 80–85°. Ordinarily, this axial angle would indicate an enstatite with about 9 per cent $FeSiO_3$; but this mineralogical composition would result in higher indices of refraction (approximately, $\alpha=1.665$, $\beta=1.669$, $\gamma=1.674$) than those actually observed. Inasmuch as the glassy enstatite differs optically from the cleavage enstatite only

in being under strain, the authors have concluded that the difference in axial angles is a function of the strain.

Isolated grains of olivine gave the following optical constants: $\alpha = 1.645$, $\beta = 1.663$, $\gamma = 1.683$; optical character, positive; axial angle $= 85°$; $r < v$, weak; optical orientation, $X = b$, $Y = c$, $Z = a$; axial plane is {001}.

The microscopic examination of the fusion rind in an oil immersion shows it to be holocrystalline, very fine grained, and to have an average index of refraction of 1.656.

*Polished Section.* Photomicrographs of a polished metallic inclusion

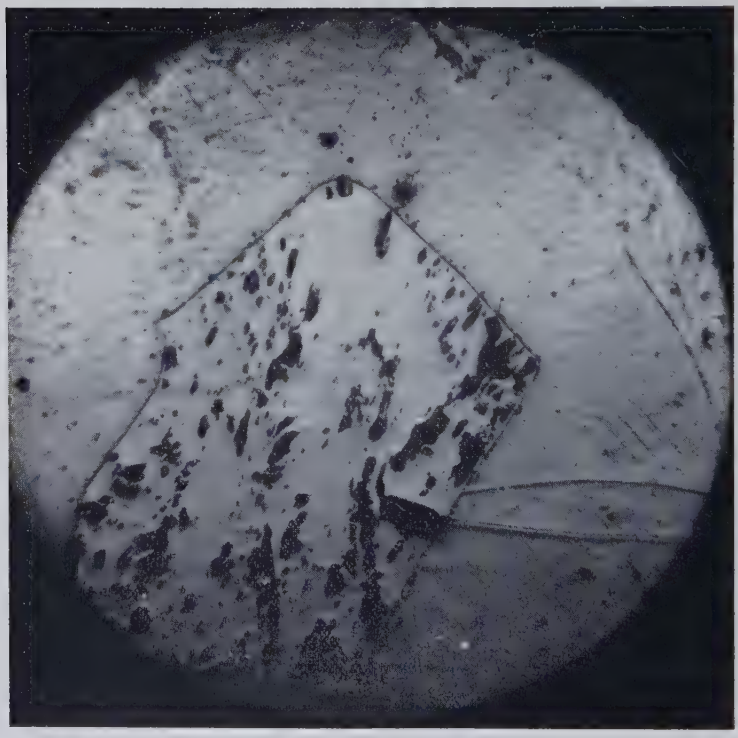

FIG. 7. Photomicrograph of etched surface of nickel-iron polished section. Schreibersite crystal surrounded by kamacite. Nital, 30 seconds. ×200.

from the achondrite are shown in Figs. 7 and 8. The composition of the metallic nodule chosen for polishing is mostly kamacite with conspicuous schreibersite. The schreibersite appears as elongate crystals with sharp grain boundaries; as rounded, elongate bodies; and as tiny, irregular inclusions scattered throughout the kamacite. In the latter case the schreibersite always has an area of lighter colored kamacite concentric about

each particle. The cause of these halos is unknown. They may be due to radioactivity or strain. After etching with 5 per cent Nital, the halos disappear. The same etching brings out a fine Neumann structure (Fig. 8).

Small amounts of troilite were noted in two of the metallic nodules, but none in the polished section. Neither the spectrographic nor chemical

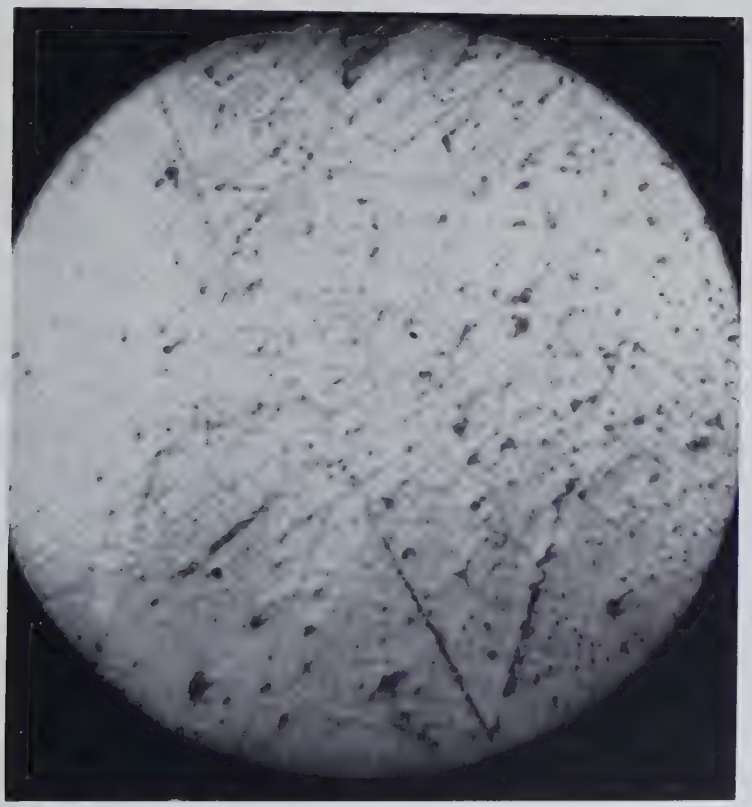

FIG. 8. Photomicrograph of etched kamacite showing Neumann lines. Nital, 30 seconds. ×200.

analyses revealed any sulfur. The small amount of sulfur present presumably concentrated selectively as troilite in some of the metallic nodules.

## ANALYSES

Combined chemical and spectrographic analyses of the metallic and stony phases of the meteorite are shown in Tables 1 and 2. For comparison with the stony phase of the nortonite, chemical analyses of Cumberland Falls (Merrill, 1921), Bustee (Maskelyne, 1870), Bishopville (Smith,

1864), and Shalka (Maskelyne, 1870) are also listed in Table 2.

The metallic phase of nortonite, on the basis of mineralogical and chemical composition, is classified as a normal hexahedrite (*H*). This is consistent with the mineralogical composition of homogeneous kamacite (showing Neumann lines), schreibersite, and troilite, and with the chemical composition, particularly the percentage of nickel.

Table 1. Combined Chemical and Spectrographic Analysis of the Metallic Phase of the Norton County, Kansas-Furnas County, Nebraska, Achondrite

| Constituent | Per cent |
|---|---|
| Fe | 91.16 |
| Ni | 5.82 |
| $SiO_2$ | 0.07 |
| P | 0.015 |
| Al | 1.00 |
| Co | 0.37 |
| Cr | 0.061 |
| Cu | 1.20 |
| Mo | N.D. <0.02 |
| Pb | N.D. <0.02 |
| Sn | N.D. <0.02 |
| Ag | N.D. <0.02 |
| Bi | N.D. <0.02 |
| V | N.D. <0.02 |
| Total | 99.696 |

N.D.: not detected.

$$\text{Molecular ratio } \frac{\text{Fe}}{\text{Ni}} = 16.46$$

$$\text{Molecular ratio } \frac{\text{Fe}}{\text{Ni} + \text{Co}} = 15.48$$

The stony phase of the nortonite is richer in magnesia and poorer in iron than any of the other achondrites. In addition, the nortonite contains more silica than any of the others save Bishopville. The analyses of the nortonite are in accord with the purity and abundance of enstatite as noted under the optical considerations. Assuming, on the basis of the indices of refraction of the enstatite, that the FeO is in the olivine, and considering only $SiO_2$, MgO, and FeO, the authors calculated a norm for the nortonite as follows:

| | |
|---|---|
| Enstatite | 91.00% |
| Olivine | 9.00% |

On this basis the olivine is 90.56 per cent forsterite, 9.44 per cent fayalite.

From the microscopic examinations and the chemical analyses, the nortonite resembles most closely the whitleyite save the nortonite contains no inclosures of chondritic material. It differs from the bustite in

TABLE 2. COMBINED CHEMICAL AND SPECTROGRAPHIC ANALYSIS OF THE STONY PHASE OF NORTONITE COMPARED WITH CHEMICAL ANALYSES OF THE SAME PHASE OF CUMBERLAND FALLS, BUSTEE, BISHOPVILLE, AND SHALKA METEORITES

| Constituent | Nortonite | Cumberland Falls | Bustee | Bishopville | Shalka |
|---|---|---|---|---|---|
| $SiO_2$ | 56.61 | 55.172 | 52.73 | 57.034 | 52.51 |
| MgO | 39.34 | 38.734 | 37.22 | 33.506 | 28.35 |
| CaO | 1.66 | 1.586 | 1.18 | 2.016 | 0.89 |
| $Al_2O_3$ | 0.71 | 0.382 | — | 1.706 | 0.66 |
| FeO | 0.60 | 2.916 | 4.28 | 1.265 | 16.81 |
| $Na_2O$ | 0.10 | 0.157 | — | 1.027 | 0.22 |
| $K_2O$ | 0.26 | 0.150 | — | 0.089 | — |
| $TiO_2$ | 0.06 | — | — | — | — |
| Cl | 0.08 | 0.028 | 2.35 | — | — |
| $P_2O_5$ | 0.07 | 0.034 | — | — | trace |
| MnO | 0.38 | 0.112 | 0.01 | 0.189 | — |
| S | 0.00 | 0.784 | — | 0.297 | 0.14 |
| C | 0.00 | 0.164 | 0.92 | — | — |
| $Cr_2O_3$ | 0.117 | 0.062 | — | — | 1.25 |
| NiO | 0.043 | 0.123 | 0.78 | 0.538 | — |
| CoO | 0.005 | trace | — | trace | — |
| CuO | 0.033 | 0.003 | — | — | — |
| $MoO_3$ | 0.003 | — | — | — | — |
| PbO | 0.008 | — | — | — | — |
| $SnO_2$ | 0.001 | — | — | — | — |
| Ignition loss | 0.10 | 0.167 | — | 1.995 | — |
| Totals | 100.180 | 100.574 | 99.47 | 99.662 | 100.83 |
| $m=$ | 118.02 | 23.91 | 15.65 | 47.68 | 3.04 |

$$m = \frac{\frac{\%\text{MgO}}{\text{mol. wt. MgO}}}{\frac{\%\text{ FeO}}{\text{mol. wt. FeO}}}$$

having no oldhamite, osbornite, nor plagioclase. It differs from the chladnites in the high magnesia content. This evidence confirms the conjecture that the nortonite has no counterpart among known achondrites (LaPaz, 1948; Beck and LaPaz, 1949), and justifies its adoption as the type stone of a new subclass of achondrites.

*Radioactivities Induced by Cosmic Rays.* The Institute for Nuclear

Studies of the University of Chicago subjected samples of the nortonite to radioactivity tests. Counts on the nortonite samples as a whole, as well as on several elements isolated from the sample, using a thin end window counter which should have permitted most of the beta rays to pass through had they been present, revealed no trace of activity other than that attributable to uranium, thorium, and potassium.

## Theoretical Considerations

The recovery of the Norton County, Kansas-Furnas County, Nebraska, achondrite gives strong support to the "meteorite-planet" hypothesis originated in 1850 by Boisse and advanced independently by Farrington in 1901. More recently, Brown (1948) has applied thermodynamics to the problem of the composition of meteorites and has given further approval to the hypothesis that meteorites had their origin in a planet roughly the size of Mars. This meteorite-planet was disrupted in some unknown manner—by collision with another planet, by internal explosion, or by tidal disintegration—in the space enclosed by the orbits of Mars and Jupiter. Brown (1948) holds that " . . . the greater the metal-phase content of a meteorite, the further from within the depths of the disrupted planet did it arise. The planet possessed a core of nickel-iron and a mantle of silicate phase containing dispersed metal." The small amount of nickel-iron inclusions in nortonite would argue that this achondrite came from near the surface of the meteorite-planet. The Norton County-Furnas County achondrite shows such dynamic metamorphism as Merrill (1921) had in mind when he described the Cumberland Falls meteorite as supplying "direct evidence of the destruction of some pre-existing planet."

In this sense, the importance from the cosmogonic viewpoint of the recently recovered nortonite is at least as great as that which Merrill assigned to the long famous whitleyite.

## References

Beck, Carl W., and LaPaz, Lincoln (1949), Preliminary report on the mineralogy of the Norton County, Kansas-Furnas County, Nebraska, achondrite: *C.M.S., P.A.*, **57,** No. 2, 85–88.

Brown, Harrison (1948), Meteorites, relative abundances, and planet structures: *Scientific Monthly*, **67,** No. 6, 383–389.

LaPaz, Lincoln (1948), The Norton County, Kansas meteorite: *Science*, **107,** No. 2786, 543.

LaPaz, Lincoln (1949), The reported crater-producing meteoritic fall of 1947, February 12, in Eastern Siberia: *C.M.S., P.A.*, **57,** No. 2, 88–92.

Larsen, E. S., and Berman, Harry (1934), The microscopic determination of the non-opaque minerals: *U. S. Geol. Survey, Bull.* **848,** 118.

Leonard, Frederick C. (1943), Statistical studies of the meteoritic falls of the World; 4. Their classificational distribution: *C.S.R.M.*, **3,** 65–70; *P.A.*, **51,** 44–49.

Leonard, Frederick C. (1946), Statistical studies of the meteoritic falls of the World; 7. Numbers and per cents of observed and unobserved falls of all classes: *C.S.R.M.*, **3,** 235–239; *P.A.*, **54,** 44–48.

Leonard, Frederick C. (1948), The Furnas County stone of the Norton County, Kansas-Furnas County, Nebraska, achondritic fall (1000, 400): *C.M.S.*, *P.A.*, **56,** No. 8, 434–437. A simplified classification of meteorites and its symbolism: *C.M.S.*, *P.A.*, **56,** No. 8, 437–442.

Leonard, Frederick C. (1949), On naming new subclasses of meteorites: *C.M.S.*, *P.A.*, **57,** No. 3, 137–138.

Maskelyne, N. Story (1870), *Phil. Trans. Royal Soc. London*, 160, 206, 367. Taken from Farrington, O. C. (1915), Meteorites: The Lakeside Press, 174.

Merrill, G. P. (1921), The Cumberland Falls, Whitley County, Kentucky, meteorite: *Proc. U. S. National Museum*, **57,** 97–105.

Smith, J. Lawrence (1864), Chladnite of the Bishopville meteoric stone proved to be a magnesian pyroxene: *Am. Jour. Sci.*, **38,** 2nd series, 225–226.

# HUTTONITE, A NEW MONOCLINIC THORIUM SILICATE

A. Pabst,
*University of California, Berkeley, California.*

## WITH AN ACCOUNT OF ITS OCCURRENCE, ANALYSIS, AND PROPERTIES

C. Osborne Hutton, *Stanford University, California.*

Abstract

The name huttonite is given to a mineral of composition $ThSiO_4$, isostructural with monazite. It has been isolated in minute grains from beach sands of South Westland, New Zealand. It is monoclinic; sp. gr. 7.1; $\alpha=1.898$, $\beta=1.900$, $\gamma=1.922$; dispersion $r<v$, moderate; $2V=25°$; $Y\|b$, Z near $c$; colorless to very pale cream. Space group $C_{2h}^5$—$P2_1/n$; $a_0=6.80$Å, $b_0=6.96$, $c_0=6.54$, $\beta=104°55'$; cell content $4(ThSiO_4)$.

### *X*-Ray Examination

Professor Hutton turned over to the writer a portion of a new mineral which he had concentrated from the sands of Gillespie's Beach, South Westland, New Zealand. The material received consisted of several hundred minute grains, none more than 0.2 mm. in maximum dimension, weighing a few hundredths of a gram altogether. The grains were all anhedral, mostly bounded by more or less conchoidal fractures and in part by smoother surfaces taken to be parting or rudimentary cleavage. These surfaces were invariably found to be parallel to the *b*-axis. Several somewhat platy fragments were found to be flattened nearly parallel to the (100) plane. The distinct cleavage nearly normal to the acute bisectrix, reported by Hutton, was only seen in a few grains.

From this material both powder and single crystal diffraction patterns were obtained. The single crystal patterns required very long exposures due to the minute size of the crystals. All crystals had to be mounted with the aid of the polarizing microscope. The first fragment was mounted with the rotation axis parallel to a prominent parting surface and at right angles to Y. When finally adjusted after several trial runs the rotation axis proved to be the *c* axis. Thereafter it was possible to set crystals for rotation on a desired axis fairly well if fragments could be found yielding a suitable interference figure. Eventually rotation and zero and first layer Weissenberg patterns were obtained on both the *c* and *b* axes.

The cell dimensions, obtained from the best lines of the indexed powder pattern and checking closely with values derived from single crystal patterns, calibrated by quartz, are:

| | | |
|---|---|---|
| $a_0=6.80\pm0.03$ Å | | |
| $b_0=6.96\pm0.03$ Å | $\beta=104°55'\pm10'$ | $Y\|\|b$ |
| $c_0=6.54\pm0.03$ Å. | | Z near $c$. |

All patterns were made with copper radiation. The wave length of the unresolved Cu-$K_\alpha$ radiation was taken to be 1.542 Å.

Assuming a cell content of $4(ThSiO_4)$ the calculated density becomes 7.18, to be compared with the value 7.1, found by Hutton.

Systematic extinctions unambiguously indicate the space group to be $C2_h^5 - P2_1/n$.

These findings show the thorium silicate found and described by Hutton to be a new mineral, distinct from the tetragonal form of this compound long familiar as the mineral thorite. It is proposed to call this new mineral *huttonite*.

## Systematic Relations

The cell dimensions of huttonite are very close to those of monazite, the cell content is analogous and the space group is the same. The optical character and orientation are also similar. As may be seen from Tables 1 and 2 and from Fig. 1 there is close correspondence of both rotation and powder patterns of the two minerals.

Reports on the cleavage of monazite are conflicting, but {100} and {001} are sometimes recognized as cleavage or parting directions. Rather obscure or imperfect cleavage or parting close to these directions is also noted in huttonite.

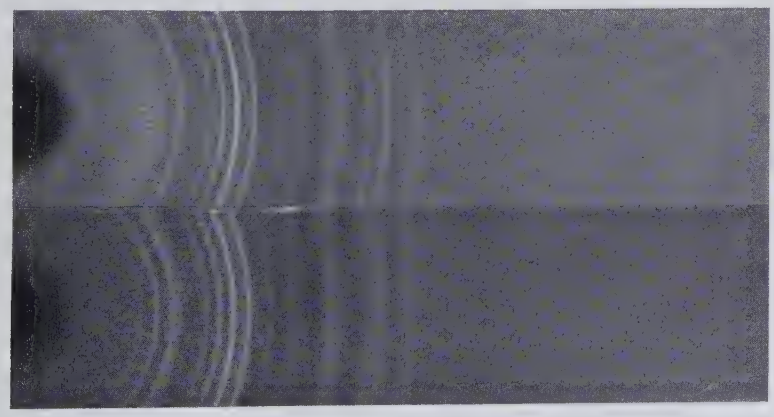

Fig. 1. Powder patterns CuK rays, Ni filter. Camera diameter 114.6 mm. Top—monazite; bottom—huttonite.

The finding of a close relation of huttonite to monazite has been foreshadowed to some extent by the finding of a substantial $ThO_2$ and $SiO_2$ content in many monazites. In a number of cases these "impurities" are present in the proportion of $ThSiO_4$. This led some mineralogists to the supposition that these monazites were contaminated by mechanical

TABLE 1. COMPARISON OF ZERO LAYER LINES OF *c*-AXIS ROTATION PATTERNS OF HUTTONITE AND MONAZITE

| *Huttonite* Gillespie's Beach, South Westland, New Zealand | | | *Monazite*‡ "Turnerit," Perdatsch, Switzerland, as reported by S. von Gliszczynski in Table 1, *Zeit. Kr.*, **101,** 4 (1939). | | |
|---|---|---|---|---|---|
| *hkl* | *Intensity* | *Spacing* | *hkl* | *Intensity* | *Spacing* |
| 020 | 1+ | 3.49 | 020 | w | 3.45 |
| 200 | 10 | 3.29 | 200 | st | 3.32 |
| 120 | 8 | 3.10 | 120 | m | 3.11 |
| 210 | 3 | 2.98 | | | |
| 220 | 1 | 2.400 | 220 | w | 2.405 |
| 310 | 2 | 2.095 | 310 | w | 2.115 |
| 320 | 5 | 1.859 | 320 | st | 1.862 |
| 040 | 3 | 1.749 | 040 | m | 1.742 |
| 140 | 4 | 1.692 | 140 | m | 1.686 |
| 400 | 5 | 1.647 | 400 | st | 1.657 |
| 410* | 6 | 1.600 | 410, 330? | st | 1.614 |
| 240 | 2 | 1.546 | 240 | w | 1.545 |
| 340, 150† | 1 | 1.370 | 340, 150 | mst | 1.369 |
| 510* | 4 | 1.293 | 510 | st | 1.301 |
| | | | 250? | w | 1.285 |
| 520 | 2 | 1.233 | 520 | st | 1.237 |
| 440 | 1− | 1.199 | 440 | m | 1.203 |
| | | | 350 | vw | 1.180 |
| 060 | 2 | 1.169 | 060 | m | 1.164 |
| 530* | 5 | 1.148 | 530, 160 | st | 1.151 |
| 260* | 3 | 1.102 | 260, 600 | m | 1.099 |
| 610 | 5 | 1.085 | 610 | st | 1.089 |
| 450 | 2 | 1.068 | 450 | m | 1.068 |

* Indexing assured by comparison with Weissenberg pattern.

† Not observed on Weissenberg pattern.

‡ Gliszczynski lists angles, from which spacings have been derived for this table. The question marks with certain indices have been copied from Gliszczynski. The beta spots in his table are here omitted.

admixture of thorite. Brögger (1906), however, considered the $ThSiO_4$ as being a part of the monazite itself and spoke of the "homoiomorpher Verbindung $(ThO)SiO_3$," which may be considered to have been found in the new mineral huttonite.

The structure of monazite has been investigated by Kokkoros (1942) and the structure of artificial $CePO_4$ has been reported by Mooney (1948). These investigators agree as to cell dimensions, cell content and space group but arrive at different parameters. Since the original paper by Kokkoros has not been accessible to the writer and the findings of

TABLE 2. COMPARISON OF POWDER PATTERNS OF HUTTONITE AND MONAZITE

| *Huttonite* Gillespie's Beach S. Westland, N. Z. | | | | *Monazite* near Chochi-wan, southern Korea* | | |
|---|---|---|---|---|---|---|
| *Intensities estimated* | *Spacings* | | *hkl*‡ | *Spacings* | | *Intensities estimated* |
| | *obs.* | *calc.*† | | *calc.*† | *obs.* | |
| 3 | 5.29 | 5.28 | $\bar{1}01$ | 5.13 | 5.23 | 4 |
| — | — | 4.80 | 110 | 4.78 | 4.72 | 4 |
| 5 | 4.71 | 4.69 | 011 | 4.67 | | |
| 6 | 4.23 | 4.19 | $\bar{1}11$ | 4.13 | 4.17 | 6 |
| 4 | 4.08 | 4.08 | 101 | 4.11 | — | — |
| 4 | 3.53 | 3.52 | 111 | 3.54 | 3.52 | 5 |
| — | — | 3.48 | 020 | 3.50 | — | — |
| 6 | 3.29 | 3.29 | 200 | 3.29 | 3.31 | 7 |
| — | — | 3.16 | 002 | 3.12 | — | — |
| 8 | 3.09 | 3.07 | 120 | 3.08 | 3.09 | 10 |
| — | — | 3.05 | 021 | 3.05 | — | — |
| 3 | 2.98 | 2.98 | 210 | 2.98 | 2.99 | 2 |
| — | — | 2.96 | $\bar{2}11$ | 2.92 | — | — |
| — | — | 2.89 | $\bar{1}21$ | 2.88 | — | — |
| 7 | 2.89 | 2.89 | $\bar{1}12$ | 2.83 | 2.88 | 7 |
| | | 2.88 | 012 | 2.86 | | |
| — | — | 2.65 | 121 | 2.66 | — | — |
| 3 | 2.65 | 2.64 | $\bar{2}02$ | 2.57 | 2.61 | 2 |
| — | — | 2.48 | 211 | 2.45 | — | — |
| 3 | 2.48 | 2.47 | $\bar{2}12$ | 2.41 | 2.45 | 3 (*b*) |
| 1 | 2.44 | 2.44 | 112 | 2.45 | | |
| — | — | 2.39 | 220 | 2.40 | — | — |
| 4 | 2.19 | | | | 2.19 | 4 |
| 2 | 2.156 | | | | | |
| | | | | | 2.139 | 6 |
| 3 | 2.110 | | | | | |
| 4 | 1.953 | | | | 1.969 | 5 |
| | | | | | 1.963 | 1 |
| 3 | 1.893 (*b*) | | | | 1.899 | 2 (*b*) |
| 2 | 1.857 | | | | 1.875 | 6 |
| 2 | 1.810 | | | | 1.800 | 2 |
| 2 | 1.784 | | | | 1.766 | 4 |
| 4 | 1.749 (*b*) | | | | 1.746 | 6 |
| 2 | 1.692 | | | | 1.695 | 4 |
| 2 | 1.646 | | | | 1.651 | 1— |
| | | | | | 1.630 | 1— |
| 3 | 1.603 | | | | 1.605 | 1 |
| 3 | 1.550 | | | | 1.541 | 4 |

* Kindly furnished by Mr. C. W. Chesterman.

† Spacings obtained by the graphical method of Peacock (*Zeit. Kr.*, **100**, 93–103, 1938) from cell dimensions given in Table 3.

‡ The sequence of indexed lines in the table is determined from huttonite.

Mooney have been reported only in a preliminary fashion it is not easy to arrive at an opinion on the merits of the conflicting results. Nevertheless it can be asserted with great confidence that huttonite is isostructural with monazite.

TABLE 3. CELL DIMENSIONS OF SOME MATERIALS ISOMORPHOUS WITH MONAZITE AND ZIRCON

| *Material* | $a_0$ | $b_0$ | $c_0$ | $\beta$ | Cell volume | Reference |
|---|---|---|---|---|---|---|
| Huttonite, $ThSiO_4$ | 6.80 Å | 6.96 Å | 6.54 Å | 104°55′ | 299 | Pabst, 1950 |
| Monazite† | | | | | | |
| (Ce, La)$PO_4$ | 6.76 | 7.00 | 6.42 | 103 10 | 296 | Parrish, 1939 |
| $LaPO_4$ | 6.89 Å | 7.05 Å | 6.48 Å | 103 34 | 306 | Mooney, 1948 |
| $CePO_4$ | 6.76 Å | 7.00 Å | 6.44 Å | 103 38 | 296 | Mooney, 1948 |
| $PrPO_4$ | 6.75 Å | 6.94 Å | 6.40 Å | 103 21 | 292 | Mooney, 1948 |
| $NdPO_4$ | 6.71 Å | 6.92 Å | 6.36 Å | 103 28 | 287 | Mooney, 1948 |
| $BiPO_4$ | 6.78 | 6.99 | 6.45 | 104 | 297 | Zemann, 1949 |
| Crocoite, $PbCrO_4$ | 7.108 | 7.410 | 6.771 | 102 27 | 353 | v. Gliszczynski, 1939 |
| Zircon, $ZrSiO_4$ | 6.60 | | 5.88 | | 256 | Wyckoff & Hendricks, 1927 |
| Thorite,* $ThSiO_4$ | 6.315 | | 5.667 | | 226 | Boldyrev et al., 1938 |
| Xenotime, $YPO_4$ | 6.88 | | 6.013 | | 285 | Vegard, 1927 |
| $YVO_4$ | 7.126 | | 6.197 | | 314 | Broch, 1933 |
| $CaCrO_4$ | 7.25 | | 6.34 | | 333 | Clouse, 1932 |

Note:—Where units are not specified in this table they are in doubt though probably kX.

* See text for comment on the cell dimensions of thorite.

† Slightly differing cell dimensions for monazite have been published by v. Gliszczynski (1939), Machatschki (1941), Kokkoros (1942) and others.

A number of substances isostructural with monazite are listed in Table 3. According to Mooney (1948) the phosphates of lanthanum, cerium and neodymium are "dimorphic," existing also in an hexagonal form. However, she states that "the presence of zeolitic water . . . is probably necessary to stabilize the structure." Under these circumstances this is not strictly a case of dimorphism. $ThSiO_4$, on the other hand, is now known to be dimorphous, having representatives in both the monazite and zircon groups.

The more familiar tetragonal form of $ThSiO_4$, thorite, is nearly always metamict. Vegard (1916) failed to observe any $x$-ray diffraction in it. An indexed powder pattern of thorite from the Langesundfjord, Norway, has, however, been published and cell dimensions given by Boldyrev, Mikheiev, Kovalev and Dubinina (1938) as well as by Mikheev and

Dubinina (1939). In the first of these papers it is stated that "This pattern has only lines with rather weak intensity as consequence of transformation of nearly whole mass of mineral to metamict state, i.e., isotropic state of secondary origin." It will be seen from Table 3 that the cell volume of thorite given there is quite out of line with that of other members of the zircon and monazite groups. Also some of the indices assigned to powder lines by Boldyrev et al. are not in conformity with the space group $I4/amd$ and the writer has found that the published pattern does not fit well an ideal set of spacings calculated from the given cell dimensions. Hence those dimensions are to be regarded with some reserve.

It is of interest to consider a possible explanation of the fact that the tetragonal form of thorium silicate is characteristically found in the metamict condition whereas the newly recognized monoclinic form occurs entirely in clear crystal fragments showing not the slightest trace of alteration. This may be correlated with observations on the better known relatives of these two minerals. Zircon has frequently been found in the metamict state whereas monazite is rarely, if ever, found in this condition. It has been suggested by Machatschki (1941) that the metamict condition of zircon arises due to an inherent instability of the structure of zircon. In this zirconium has an 8-fold coordination, whereas the radius of $Zr^{+4}$ is near the boundary of 6 and 8-fold coordination and in many minerals $Zr^{+4}$ goes into 6-coordinated positions. It may then be that the huttonite structure is more stable than the thorite structure though it is not possible at this time to state precisely what the differences in the two structures are.

## OCCURRENCE, OPTICAL PROPERTIES AND CHEMICAL COMPOSITION OF HUTTONITE

C. Osborne Hutton

### Introduction

During a detailed study of a series of Recent and sub-Recent beach and fluvio-glacial sands and gravels from South Westland, New Zealand, the writer observed a mineral of unique properties in an assemblage that consisted in the main of scheelite, cassiterite, usually a tantalian variety, uranothorite, zircon, ilmenite, and gold. After having determined the mineral to be a thorium silicate with physical properties quite distinct from those of tetragonal thorite, the writer handed over a small sample of pure material to Professor Adolf Pabst of the University of California with the suggestion that it might be profitable to examine this more fully. Professor Pabst very kindly agreed to undertake a crystallographic study of the mineral with the result that he has found the mineral to be monoclinic with the same symmetry as monazite.

### Occurrence

Huttonite has been recognized in sands from Harihari, Saltwater Creek, Okarito, Five Mile Beach, Bruce Bay, north and south of the mouth of the Waikukupa River, and Gillespie's Beach, but it appeared to be more plentiful in the Gillespie's Beach area than elsewhere. In each of these occurrences it is concentrated in the finer size fractions and careful searching did not reveal any grains with diameters in excess of 0.20 mm., but at the same time, it showed that it was more plentiful in the $-60$ $+120$ and $-120$ $+230$—mesh screenings than in $-230$—mesh material.

### Physical Properties

In a preliminary survey of sands from South Westland the writer mistook huttonite for scheelite but after closer observation found it to differ from the associated scheelite in a number of ways, chief among which are the following:

(1) Consistent biaxial character although the optic axial angle is small.

(2) A distinct cleavage or parting nearly normal to the acute bisectrix causes preferred orientation of the anhedral grains when mounted in refractive index media. In the interference figure obtained from such a grain the point of emergence of the optic axis lay at or just outside the edge of the field of view. A second cleavage is present but its orientation relative to the first was not known; this appears to be orthopinacoidal cleavage, according to Pabst.

(3) A moderate dispersion of the optic axes with $r<v$ is a distinctive feature of huttonite. The preferred orientation with $Bx_a$ nearly normal to the microscope stage, combined with the small optic axial angle, makes the dispersion more obvious than it might otherwise be.

(4) Grains of huttonite have a profound and rapid effect on the emulsion of nuclear track plates when embedded therein.

(5) Ultraviolet light of short wave-length (2540 Å) produces a distinctive fluorescence in both minerals, a characteristic blue color for scheelite, and a dull white color with a pink tinge for huttonite.

When it was realized that some mineral quite distinct from scheelite was present, an attempt was made to isolate it and this end was achieved fairly readily since it was concentrated with scheelite, zircon, apatite, and cassiterite, when the sands containing it were fractionated first in methylene iodide and subsequently electromagnetically. By careful adjustment of field strengths huttonite may be almost entirely segregated from the associated constituents just mentioned. But it was found that an absolutely pure sample could only be prepared by hand-picking in oblique illumination beneath a binocular microscope.

Since both huttonite and scheelite have a similar aspect beneath a binocular microscope satisfactory differentiation between the two minerals may be accomplished in either of two ways:

(*a*) If the concentrate is treated with boiling HCl for two or three minutes a canary yellow coating of the trioxide is produced on the surfaces of the scheelite; huttonite is quite unaffected by such treatment. The acid-treated material is then hand-picked in oblique illumination from an ordinary light source.

(*b*) In short wave-length ultraviolet light, *viz.* 2540 Å., scheelite fluoresces with a distinctive blue color, zircon, with a golden yellow color, whereas huttonite exhibits a faint, but distinct, dull white color with a pink tinge. In this instance hand-picking may be carried out in oblique illumination from a source of ultraviolet light.

The following properties have been determined for huttonite from Gillespie's Beach:

$$\alpha = 1.898^* \pm 0.003$$
$$\beta = 1.900 \text{ (by calc.)}$$
$$\gamma = 1.922$$
$$\gamma - \alpha = 0.024$$

Dispersion: Moderate with $r<v$

$$2V = 25° \pm 1°.$$

Optic sign: Positive.

Color: Colorless to very pale cream.

$$D_{20° C.} = 7.1 \pm 0.1$$

* Refractive indices for scheelite from Gillespie's Beach.

$$\alpha = 1.919: \gamma = 1.935: \gamma - \alpha = 0.016$$

## Chemical Properties

A small sample of carefully purified material, was partially analyzed by Mr. F. T. Seelye, and subsequently a second sample with identical physical properties, and separated from the same source, was analyzed by the present writer. These analyses are combined and set out in Table 1.

Table 1. Analysis of Huttonite, Gillespie's Beach, South Westland, New Zealand

| | |
|---|---|
| $ThO_2$ | 76.6 |
| $UO_2$ | nil. |
| $SiO_2$ | 19.7 |
| $Fe_2O_3$ | 1.2 |
| CaO | nil. |
| MgO | nil. |
| MnO | trace |
| $P_2O_5$ | trace |
| $Ce_2O_3$ etc. | 2.6 |
| $H_2O$ (total) | nil. |
| | 100.1 |

The mineral appears to be completely unaffected after treatment with hot concentrated hydrochloric acid for fifteen minutes, but the very finely powdered material is slowly dissolved by repeated evaporations in concentrated sulfuric acid. A fusion with sodium carbonate must be carried out with the greatest care since a portion of the powder invariably remains after solution of the fusion cake; this residue must be reground and refused with carbonate once again.

## Provenance of Huttonite

Huttonite has not been found *in situ* but on account of the nature of the associated heavy minerals, the ultimate source could only have been the low-grade schists or the associated but sparsely distributed pegmatitic veins of the alpine range a few miles to the east of the Bruce Bay-Gillespie's Beach area. Neither huttonite nor uranothorite has been recognized so far as a constituent of these rocks but since none of the pegmatite veins examined are of the complex type, and both the schists and radioactive mineral sands have considerable lateral extent, the source for these two minerals is believed to be the schists.

## References

Boldyrev, A. K., Mikheiev, V. I., Dubinina, V. N., and Kovalev, G. A., *X*-ray determinative tables for minerals: *Leningrad, Inst. Mines, Ann.*, **11**, 1–157 (1938).

Broch, E., Die Kristallstruktur von Yttriumvanadat: *Zeit. phys. Chem.*, (B), **20,** 345–350 (1933).

Brögger, W. C., Mineralien der südnorwegischen Granitpegmatite: *Norsk Ak., Skr.*, (Mat.-Natur. Kl.) I, **6,** 1–136 (1906).

Clouse, J. H., Investigations on the *x*-ray crystal structures of $CaCrO_4$, $CaCrO_4 \cdot H_2O$ and $CaCrO_4 \cdot 2H_2O$: *Zeit. Kr.* **83,** 161–171 (1932).

von Gliszczynski, S., Beitrag zur "Isomorphie" von Monazit und Krokoit: *Zeit. Kr.*, **101,** 1–16 (1939).

Kokkoros, M. P., La structure de la monazite: *Praktika Acad. Athens*, **17,** 163, 1942. (Not seen. Cited by Zemann, 1949.)

Machatschki, F., Zur Frage der Stabilität des Zirkongitters: *Zbl. Min.* (**A**), 38–40 (1941).

Mikheev, V. I., and Dubinina, V. N., Standard powder-diagrams of some minerals of the class of oxides: *Leningrad, Inst. Mines, Ann.*, **12,** 151–167 (1939).

Mooney, Rose C. L., Crystal structures of a series of rare earth phosphates: *J. Chem. Phys.*, **16,** 1003 (1948).

Parrish, W., Unit cell and space group of monazite (La, Ce, Y)$PO_4$: *Am. Mineral.*, **24,** 651–652 (1939).

Vegard, L., Results of crystal analysis: *Phil. Mag.*, **32,** 65–96 (1916).

Wyckoff, R. W. G., and Hendricks, S. B., The crystal structure of zircon and criteria for the special positions in tetragonal space groups: *Zeit. Kr.*, **66,** 73–102 (1927).

Zemann, J., Beiträge zur Kristallchemie des Wismuts: *Tschermak's Min., pet. Mitt.* (3), **1,** 361–377 (1949).

# PETROLOGY OF THE RED RADIOACTIVE ZONES NORTH OF GOLDFIELDS, SASKATCHEWAN

Charles E. B. Conybeare and Charles D. Campbell,
*The State College of Washington, Pullman, Washington.*

Abstract

The red rocks that occur along faults and shear zones in the Precambrian granitic terrane north of Lake Athabaska are more radioactive than others in the area. They are mylonites ranging from protomylonite to ultramylonite, the latter generally forming anastomosing veinlets in the less intensely crushed types.

In the protomylonites the feldspar is deformed albite colored with hematite dust, especially along the cleavages; unstrained minerals fill the interstices. In the more intensely crushed types the hematite dust permeates most of the rock; the unstrained minerals present form scattered aggregates or may locally replace the mylonite completely.

The first of these late minerals is clear albite, which forms rims on the red albite relicts. Then follow, in variable order and with repetitions, clear subhedral quartz and albite, specularite, and penninite containing radioactive anatase grains. The latest veins contain also pitchblende, calcite, and specularite. Oxidation products of pitchblende are locally abundant in solution cavities.

The early iron and later radioactive elements were introduced probably by solutions that rose along the mylonite zones. The other elements were probably present before mylonization; and all the late minerals, excepting pitchblende and calcite, may be products of recrystallization.

The dusty hematite was probably not formed either by radioactive bombardment of ferrous minerals or by unmixing of iron-feldspars.

## Introduction

During the summer of 1948, while engaged in exploration for uranium deposits in the Goldfields area (Fig. 1), the attention of the first author was drawn to certain linear zones of brick-red radioactive rock containing stringers of pitchblende. These zones lie along or close to the surface expressions of major faults. Although the degree of radioactivity is not uniform over the exposed portions of the zones, the lowest measurements obtained with Geiger-Mueller counters were two to three times higher than those obtained over the local soda-rich granites and granodiorites. The texture of this reddish rock varies from coarse to very fine grained. Megascopically it shows a marked resemblance to reddish cherty rock associated with the pitchblende deposits at Great Bear Lake. Kidd and Haycock (1935, p. 890) have mentioned these rocks and Murphy (1948, p. 266) states: "This so-called red alteration, undoubtedly related to the quartz-hematite period of mineralization, affects the quartzose rocks most severely, but where alteration is intense there is little selectivity. The exact nature of the alteration has not been determined, but quartz, hematite, magnetite, sericite, chlorite, and carbonate are obvious constituents." Christie and Kesten (1949*b*, p. 650) suggest that the red

cherty alteration "may be due to silicification, the silica being accompanied by iron stain, or it may be due to introduction of fine-grained red-stained feldspar, or to both of these causes." No explanation for the red coloration is offered by James, Lang, Murphy, and Kesten (1950).

As no petrographic work has been carried out with these reddish rocks at Great Bear Lake, their genesis and possible relationship to the pitchblende mineralization is still open to question. The apparent similarity

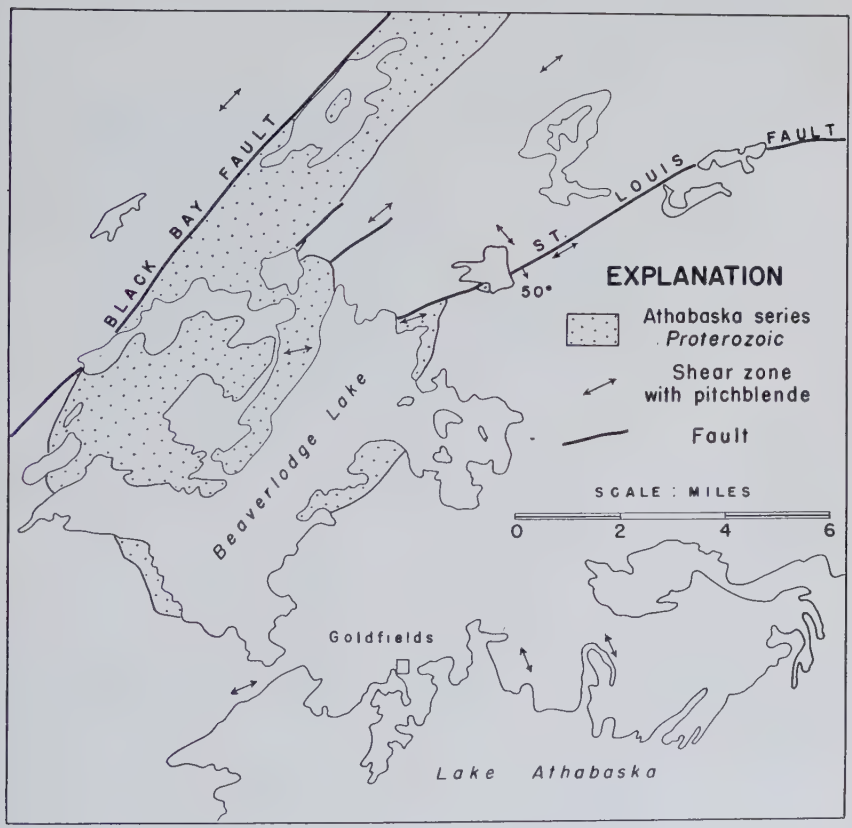


FIG. 1. Map of Goldfields area.

between these rocks and those forming pitchblende-mineralized linear zones in the Goldfields area suggests that the same genetic relationship between the rock and the pitchblende obtains in both the Great Bear Lake and Goldfields areas. For the purpose of determining the nature of this red radioactive rock and its probable genesis, the writers made a petrographic examination of about 80 thin sections, which included both coarse and fine-grained phases and the associated country rocks.

## Structural Relationships

Within a few miles north of the townsite of Goldfields there are two major faults striking northeasterly. As shown on the maps accompanying reports by Christie and Kesten (1949*a*) and James and others (1950), the Black Bay fault can be traced for twelve miles and the St. Louis fault for seven. Along both faults are zones of red radioactive rocks.

Diamond drilling across the St. Louis fault has shown that the zone of movement is marked by a 100-foot width of sheared rock. Examination of core taken from this zone indicates that the rock has not everywhere been sheared with equal intensity, as minor zones, from a fraction of an inch to a few feet wide of reddish and cherty rock are separated by rock

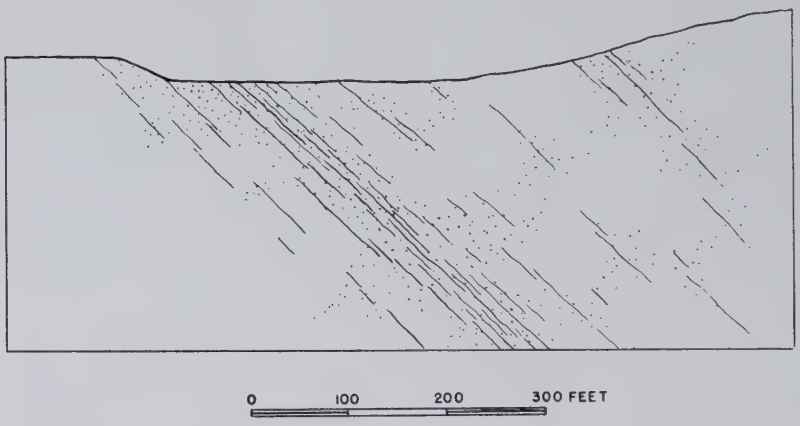


Fig. 2. Generalized section across St. Louis fault. Red rock is stippled.

which usually is much coarser grained and shattered. Microscopic examination shows the cherty rock to be ultramylonite. Its vein-like character strongly suggests that it has been squeezed into fractures in the less-crushed rock.

The St. Louis fault closely follows the strike and dip of foliation in the country rock, and movement has taken place along numerous subparallel shears which are indistinguishable within the main zone. The generalized relationship of the linear zones of red rock, which in outcrop tend to follow the strike of the foliation and shearing, is shown in Fig. 2.

## Petrology of the Red Rock

Coarse-grained varieties of this brick-red rock resemble breccia with the texture of building stucco. Close examination reveals, however, that the angular constituents are not rock fragments but subhedral feldspar crystals. These crystals, which are on the average a few milli-

meters wide, are loosely intergrown, and the interstices are filled with calcite, penninite, and quartz.

Under the microscope the feldspar crystals are seen to consist of fresh rims surrounding dark reddish and highly altered relicts (Fig. 3) with bent and broken twinning lamellae. Optical continuity between the relicts and rims suggest that the former have the same composition as the latter; that is approximately $An_{10}$. The relicts are colored with hematite dust, which has thoroughly permeated both fine and coarse-grained types of the red rock, and which is concentrated especially along microfractures and cleavages in shattered grains of feldspar (Fig. 4).

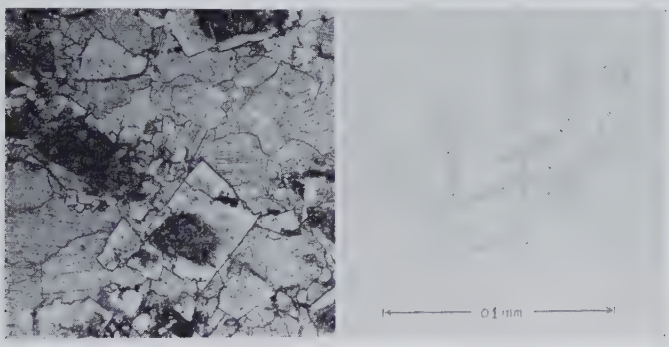


FIG. 3. Clear albite overgrowths on red albite relicts. Matrix of twinned calcite. Largest albite crystal is 0.4 mm. wide.

FIG. 4. Pattern of red alteration in feldspar porphyroclast. Camera lucida drawing.

The interstices are filled largely with twinned calcite, the lamellae of which are not bent. Variable amounts of penninite are also present in the interstices, and in places there is more penninite than calcite. Penninite also fills fractures and occurs as tiny flakes within the feldspar. These flakes, imbedded in a reddish matrix of dusty hematite and altered feldspar, are surrounded by bleached zones. It is inferred that the flakes of chlorite have chemically utilized the hematite during their growth. On the basis of this inference at least part of the chlorite has formed subsequent to the development of the dusty hematite impregnation.

Adhering to the surfaces of feldspar crystals and lining interstices filled with calcite, chlorite, and quartz are clusters of euhedral crystals of specularite. These crystals possess a platy and tabular habit and are approximately 0.05 mm. wide. A few convex forms with striated surfaces were observed. It was further observed that clusters of the crystals were sufficiently magnetic to adhere to the point of a magnetized needle. The possibility that the crystals might be pseudomorphs of magnetite after specularite was obviated by comparing their magnetic susceptibility

with that of finely powdered magnetite. Also adhering to the surfaces of feldspar crystals, and projecting into the interstices are euhedral grains of quartz up to 1.0 mm. long. Larger anhedral and subhedral grains form aggregates in the interstices. None of the quartz grains show strain shadows.

Disseminated in the calcite are euhedral crystals of anatase from 0.05 mm. to 0.2 mm. in width. Very small grains form elongated clusters along cleavages in the flakes of penninite and these clusters are surrounded by very pronounced pleochroic halos.

Finer-grained varieties of the red rock contain much less calcite and chlorite. Under the microscope they show angular fragments of dark reddish feldspar surrounded by a fine-grained matrix impregnated with hematite dust. Within the matrix are aggregates of albite, chlorite, and specularite. The albite crystals are unaltered, have a composition within the range $An_5$ to $An_{10}$ and are usually less than a millimeter wide.

The modes of this red rock could be determined only in the coarse-grained type. In general, where quartz is present there is more penninite than calcite. Also, where specularite is present in relative abundance it is usually associated with calcite. The approximate minimum and maximum percentages by volume of the various minerals are estimated as follows:

| | |
|---|---|
| Albite | 70%–80% |
| Calcite | 10%–25% |
| Chlorite | 1%–15% |
| Quartz | 1%–10% |
| Specularite | 1%– 5% |
| Anatase | trace |

## Recrystallization and Replacement of Mylonites

Along the St. Louis fault crushed granitic rocks are abundant. They are reddish from dusty hematite, and vary in texture from protomylonites (Fig. 5) through fine-grained and streaked mylonite (Fig. 6) to cherty-appearing ultramylonite. Apparently similar rocks were noted in southern Norway by Barth (1949, p. 177), who refers to granite having been "partly mylonitized and again compressed to a dense, red felsite."

Fairly evenly disseminated within the ultramylonite are rounded and amoeboid grains of albite usually less than 0.1 mm. wide. As these grains are unaltered they are considered to be the initial forms of porphyroblasts. Microcline grains of similar size are also present, and in one sample of mylonite microcline was observed to have replaced part of an augen of fine-grained quartzose-feldspathic material (Fig. 7). In places euhedral porphyroblasts, up to 10 mm. wide, of unaltered albite and microcline are so numerous that the mylonite has the appearance of a porphyry.

Whether the albite and microcline have resulted from the introduction of soda and potash into the mylonite, or from recrystallization only, is open to question. As the mylonites were originally alkali-rich granitic rocks, recrystallization alone could account for the porphyroblasts. The very high albite content of the red rock suggests, however,

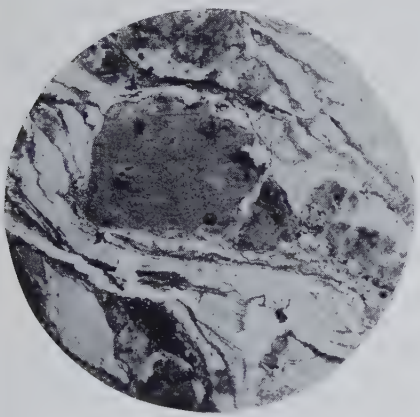

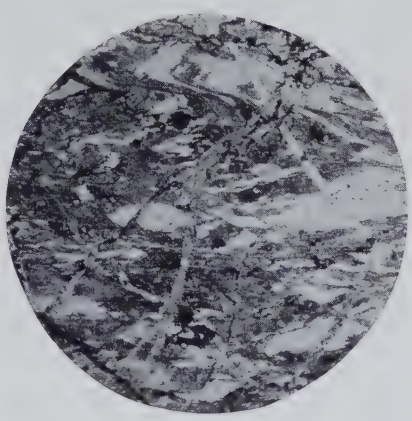

FIG. 5. Protomylonite. Red feldspar porphyroclast 0.7 mm. wide in fine flow-textured groundmass of quartz and muscovite.

FIG. 6. Mylonite. Red feldspathic material with clear lenses and swirls of quartz. Transverse veinlets of quartz-calcite are 0.05 mm. wide.

that there has been local migration of soda. It is perhaps significant that this enrichment of soda should have occurred along the zones of most intense shearing. Wiman (1932, pp. 156–157) has expressed the view that a certain amount of soda derived from crushed granite will migrate along mylonite zones.

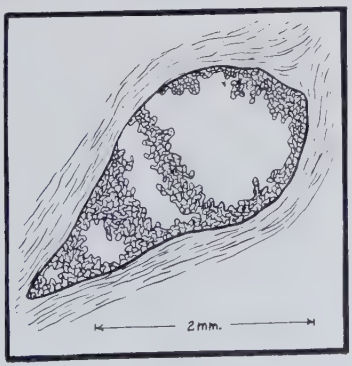


FIG. 7. Clear microcline porphyroblasts. Amoeboid forms replacing quartz-feldspar lens in mylonite.

## Paragenesis of the Minerals

The paragenesis of the minerals in the red rock is by no means clear-cut. The earliest mineral to have developed within the mylonite is albite which, in addition to the amoeboid forms mentioned above, forms fresh rims around highly altered albite relicts. Later there crystallized, in variable order and with repetitions, quartz and albite, specularite, and penninite containing anatase grains. Cutting the red rock are stringers containing pitchblende, calcite, and specularite. Oxidation products of pitchblende are disseminated locally within the red rock.

A. M. Christie[1] made a petrographic examination of stringers within a pitchblende-mineralized zone in the area and found them to be of quartz, quartz-albite, albite, chlorite-albite, chlorite, carbonate, albite-carbonate-hematite, hematite, and pitchblende. He states: "A striking feature is the lack of shearing in these veinlets and the freshness of the quartz and albite. The quartz occurs in fresh-looking equidimensional grains as contrasted with the intensely sheared and fractured lamellar quartz of the wall rock. The vein albite is also fresh, the twinning clear. The vein quartz of the main vein is fractured but by clear-cut fractures parallel to the walls of the vein which cut the grains in a straight line. The vein quartz shows no appreciable straining or strain lamellae." And further, "In one interesting case a quartz veinlet is cut by an albite-carbonate-hematite (pitchblende?) veinlet, the latter being therefore the younger. The more complex vein is banded, the albite crystals lining the walls with the metallics, carbonate and chlorite in the centre. In this case the quartz veins must be older and the complex vein the younger with albite being deposited before the other associated minerals."

It is not known to what extent the stringers of albite, quartz, chlorite, calcite, and possibly hematite represent introduced minerals, or minerals dissolved from the wall rock and re-deposited along fractures. It does seem fairly certain, however, that pitchblende was introduced at a late stage.

## The Red Coloration

There are at least three possible explanations for the presence of dusty red hematite in the feldspar porphyroclasts and the groundmass around them:

(1) The iron of the hematite was introduced by solutions or diffusion.

(2) The hematite was liberated from pre-existing iron-bearing minerals by radioactive bombardment.

(3) The hematite is an exsolution product of ferromicrocline and ferroalbite.

[1] Geological Survey of Canada, written communication.

The first of these explanations is believed to be the correct one. The iron for the hematite was probably introduced by solutions that rose along the mylonite zones before recrystallization began. Transport principally by solutions, not by diffusion, is suggested by the distribution of the red rock, which is indicated diagrammatically in Fig. 2, but without the actual intricacy of detail. In detail the limits of the red coloration are very irregular, as some foliae of the mylonites are red to a greater distance than are others. In general, the great irregularity in distribution of the red coloration suggests, though it does not prove, that the iron was distributed in solution along a network of fissures, mainly parallel to the foliation, instead of migrating as a continuous front through the unfissured rock. It is not possible to state whether it was these iron-bearing solutions or later ones that permitted recrystallization of the mylonites after the hematite was formed.

Concerning the second explanation, an examination of thin sections of pitchblende stringers in fine-grained red rock revealed no deepening of color close to the stringers, and it is therefore inferred that the brick-red color of this rock is not attributable to the proximity of pitchblende.

Frequently it has been observed that strongly radioactive minerals in pegmatite are surrounded by aureoles of reddened rock and that minute fractures radiate from the radioactive mineral. Walker and Parsons (1923, p. 26) wrote of such an occurrence: "A section of potash feldspar enclosing euxenite from Maberley, Ontario, was examined to see whether any trace of shattering could be observed. Although the shattering was not radial the feldspar was completely ruptured and the cleavages and fractures were filled with hematite, which gives a deep red colour to this feldspar in contrast to the pale colour which characterises most of the feldspar from this quarry." The hematite in this case appears to have been introduced subsequent to or during the period of fracturing. The cause of the observed fracturing around highly radioactive minerals such as euxenite, uraninite, and samarskite is not known; but it is inferred that oxidation of these minerals results in an increase of volume which produces shattering in the surrounding rock.

The third explanation, that the hematite is an exsolution product from ferric feldspars, is more probable than the second but is rejected also. Faust (1936, p. 762) has shown that iron-orthoclase definitely exists, that what is probably iron-microcline has been synthesized, and that iron-albite may exist, though its existence is doubtful. Andersen (1915) had given indirect proof of the existence of iron-plagioclase at high temperatures by showing that the hematite scales in aventurine feldspar were, at least in part, so oriented as to indicate exsolution as their origin.

The analogy between the red feldspars and aventurine feldspar is weakened when the following differences are noted:

(1) The hematite in the red feldspars forms dull-lustered granules under 0.005 mm. in diameter; but hematite scales in aventurine feldspar are transparent and shiny, and are from 0.2 to 3.0 mm. in diameter and 0.0001 to 0.0004 mm. thick.

(2) Exsolution of hematite from ferric feldspars results only from cooling, not from comminution, so far as is known. Mylonization, during which temperatures may locally rise to fusion point, might cause solution of iron in melted feldspar, which would then unmix upon cooling. But although some of the dusty hematite in the ultramylonite stringers may be of this origin, the hematite in the bent and evidently unfused feldspar relicts is not. Moreover, the hematite formed in the laboratory experiments by Faust (1936, p. 750) crystallized into translucent red and yellow flakes, as in aventurine feldspar, not dull-red granules.

## Radioactivity of the Red Rock

The relatively high radioactivity of the red rock is no doubt due in large part to the contained uranium minerals. Even where these minerals are not apparent, however, the rock has a radioactivity two to three times that of the local granite. To what extent this radioactivity may be caused by accessory minerals or included gases is not known. It is an interesting fact that the anatase within penninite is surrounded by very dark pleochroic halos, and one which suggests that the anatase is radioactive.

It has been pointed out by Piggot and Merwin (1932), Morgan and Auer (1941), Keevil, Larsen, and Wank (1944), and Sahama (1945) that more than half the radioactivity of a granite is attributable to the accessory minerals zircon, apatite, allanite, epidote, sphene, monazite, and the micas. Osborne (1939, p. 934) quotes J. W. Waters (1909, 1910) as saying that within the Cornish granite, radium is concentrated in anatase and rutile; within the Dalbeattie granite, in allanite; and within the Mourne granite, chiefly in zircon and a titaniferous mineral. Osborne found that the radioactivity of a tonalite in southern California varies directly with the albite content. In view of Osborne's findings, the high albite content of the red rock may have some bearing on the radioactivity. According to Palache, Berman, and Frondel (1944) anatase is of hydrothermal origin. It is therefore possible that both sodium and titanium have been introduced.

## Conclusions

Zones of deep-red rocks, shown by petrographic study to be mylonites, have been observed to be more radioactive than others in the Goldfields and Great Bear Lake areas of western Canada. For the Goldfields area, this relationship is considered a result of the following sequence of events, all of which took place in Precambrian time:

(1) Partial replacement of a bedded series by the minerals of albite granite.

(2) Mylonization during early movements along the St. Louis and related fault zones.

(3) Deposition of finely-divided hematite in feldspar porphyroclasts and groundmass, from solutions migrating along the mylonite zones.

(4) Widespread recrystallization of feldspar and quartz and introduction of calcite, penninite, specularite, and pitchblende.

## References


Andersen, Olaf (1915), On aventurine feldspar: *Am. Jour. Sci.*, ser. 4, **40,** 351–398.

Barth, T. F. W. (1947), The Birkeland granite, a case of petroblastesis: *Comm. Géol. de Finlande, Bull.*, No. **140,** 173–182.

Christie, A. M., and Kesten, S. N. (1949*a*), Goldfields and Martin Lake Map-Areas, Saskatchewan: *Geol. Surv. Canada, Paper* **49–17.**

——— (1949*b*), Pitchblende occurrences of the Goldfields area, Saskatchewan: *Canadian Min. Met. Bull.*, 643–651.

Faust, G. T. (1936), The fusion relations of iron-orthoclase: *Am. Mineral.*, **21,** 735–763.

James, W. F., Lang, A. H., Murphy, Richard, and Kesten, S. N. (1950), Canadian deposits of uranium and thorium: *Mining Engineering,* **187,** 239–255.

Keevil, N. B., Larsen, E. S., and Wank, F. J. (1944), The distribution of helium and radioactivity in rocks: *Am. Jour. Sci.*, **242,** 345–353.

Kidd, D. F., and Haycock, M. H. (1934), Mineragraphy of the ores of Great Bear Lake: *Geol. Soc. Am., Bull.*, **46,** 879–960.

Morgan, J. H., and Auer, A. L., (1941), Optical, spectrographic and radioactivity studies of zircon: *Am. Jour. Sci.*, **239,** 305–311.

Murphy, R. (1948), Eldorado Mine: *Can. Inst. Min. and Metall.* Symposium, "Structural Geology of Canadian Ore Deposits," 259–268.

Osborne, E. F. (1939), Structural petrology of the Val Verde tonalite, Southern California: *Geol. Soc. Am., Bull.*, **50,** 921–950.

Palache, C., Berman, H., and Frondel, C. (1944), The System of Mineralogy: vol. **1,** 834 pp., New York.

Piggot, C. S., and Merwin, H. E. (1932), Radium in rocks: location and association of radium in igneous rocks: *Am. Jour. Sci.*, ser. 5, **23,** 49–56.

Sahama, T. G. (1945), On the chemistry of the East Fennoscandian rapakivi granites: *Comm. Géol. de Finlande, Bull.*, **136,** 15–64.

Walker, T. L., and Parsons, A. L. (1923), Shattering of minerals and rocks about inclusions: *Univ. Toronto Geol. Ser.*, **16,** 25–28.

Waters, J. W. (1909), Radioactive minerals in common rocks: *Philos. Mag.*, **18,** 677–679.

——— (1910), Radioactive minerals in common rocks: *Philos. Mag.*, **19,** 903–904.

Wiman, E. (1932), Studies of some Archaean rocks in the neighbourhood of Upsala, Sweden, and of their geological position: *Geol. Inst. Univ. Upsala, Bull.*, **23,** 1–170.


*Manuscript received*
*Feb. 24, 1950*

# FURNACE ATMOSPHERE CONTROL IN DIFFERENTIAL THERMAL ANALYSIS

Richards A. Rowland and Donald R. Lewis*

Abstract

The usefulness of differential thermal analysis can be extended considerably by controlling the composition of the furnace atmosphere. The method described for securing atmosphere control is applicable to most existing differential thermal analysis furnaces. Examples are given which show the effect of a furnace atmosphere of nitrogen on differential thermal curves of clays containing organic matter and pyrite. Other curves show the effect of $CO_2$ on differential thermal curves of siderite, magnesite, dolomite and calcite. One curve follows the alternate dissociation-reconstitution of the $CaCO_3$ part of dolomite in an atmosphere of $CO_2$. The effect, on the differential thermal analysis curve, of filling the furnace with a gas which is a participant in the reaction is explained by the relation of the partial pressure to the equilibrium constant and the heat of reaction.

## Introduction

The method of differential thermal analysis consists of simultaneously heating in a furnace two substances, one of which is an inert material which undergoes no phase change or chemical reaction in the temperature range to be covered, while the other is the sample to be analyzed. As the furnace temperature is raised, the temperature difference between the two substances is measured by a dual hot-junction thermocouple, and the thermocouple *EMF* is recorded. If the unknown substance undergoes no phase changes or chemical reactions its temperature will follow that of the inert material. If a change does occur, the temperature of the substance being analyzed will lag behind, or gain over that of the inert material, and deflections of the recorded line will be produced. Conventionally, the recorded curves are oriented for study and interpretation so that endothermic reactions, during which the sample is cooler than the inert material, are shown as downward deflections, and exothermic reactions as upward deflections. The apparatus used here is similar in furnace design to that described by Grim and Rowland (1944), but with the addition of a copper tube cemented into the back plug so that a selected gas may be introduced into the furnace.

The ambient atmosphere in a differential thermal analysis furnace may be controlled in several ways depending on what the control is expected to do. First, an inert gas such as nitrogen or argon may be introduced into the furnace to eliminate oxygen and prevent oxidation reactions without changing the pressure inside the furnace. Second, an

* Publication No. 10, Exploration & Production Research Division, Shell Oil Company, Houston, Texas.

active gas which will be evolved by the expected reaction, such as $CO_2$ for the carbonate minerals, may be introduced to maintain at one atmosphere the partial pressure of the gas to be evolved. Third, with the usual method of differential thermal analysis, air at atmospheric pressure may be allowed in the furnace so that oxidation proceeds at will within the limits of access of air to the sample, and the partial pressure of an evolved gas may increase during the heating cycle. Fourth, with a special furnace, equipped for either vacuum or moderate pressures, the effects of pressure changes may be followed in air, an inert gas, or an active gas.

For several years this laboratory has regularly introduced various gases into the furnace in differential thermal analyses of geological materials, and recently Whitehead and Breger (1950) have described vacuum equipment for pressure control below one atmosphere. Different commercially available gases can be introduced into the furnace of most existing differential thermal analysis apparatus with the simple addition of a tube in the porous plug generally used to close the end of the furnace opposite that into which the sample holder is inserted. Some of the results obtainable by this simple technique will be described here.

## Inert Atmospheres

The presence of organic matter in the fine fraction of soil and clay materials has long made difficult the identification of the mineral content of these materials. When viewed under the petrographic microscope the organic matter obscures the small particles and often partially dissolves in the immersion oil, changing its refractive index. On *x*-ray diffraction photographs the effect of organic material in the sample is a general scattering of the beam which produces over-all darkening of the film, especially in the critical region where the Bragg angle is small. In differential thermal analysis the exothermic loop resulting from the oxidation of the organic material is often so large by comparison with the dehydration loops of the minerals that the latter, of prime interest in interpretation, are frequently completely obscured up to at least 650° C.

Chemical treatment to remove the organic material either by solution in appropriate solvents or by oxidation has met with only partial success. When various organic solvents are used the liquid sometimes dissolves the unwanted organic material, but as frequently as not it simply displaces the organic matter and is itself held by the clay. The various oxidizing agents are generally ineffective until their concentration is such that the action is vigorous enough to disrupt the clay mineral lattice.

This problem is especially critical in differential thermal analysis and can be partly solved by the rather obvious technique of controlling the composition of the ambient furnace atmosphere so that oxidation is

either suppressed or allowed to proceed so slowly that the heat effect is negligible. This may be accomplished by allowing a stream of nitrogen to flow into the furnace through a porous plug of insulating firebrick inserted in the furnace tube from the end opposite that containing the sample holder. The required rate of nitrogen flow will vary with different apparatus and should be large enough to suppress oxidation but not so large as to affect the heating rate appreciably. For the apparatus here employed the optimum rate is about 0.25 cubic feet per minute.

Although water-pumped nitrogen (usual compressed cylinder nitrogen) contains some oxygen, no exothermic oxidation reactions are recorded when this nitrogen makes up the furnace atmosphere. When the sample is removed from the furnace before cooling, as is standard practice, only the upper crust is oxidized and then only after contact with the air. The bulk of the sample contains black particles of carbon.

Since oxidation of the organic matter is prevented by displacing the oxygen in the furnace atmosphere with nitrogen, the organic material may pyrolize or vaporize. The process of pyrolysis involves the breaking up of large unsaturated molecules into smaller molecules which then vaporize. Both of these reactions are endothermic. They are not recorded, however, because the organic matter contains only a very small amount of many different molecules which undergo pyrolysis over a wide temperature range. Furthermore, the heat of vaporization of the products is only about $\frac{1}{6}$ to $\frac{1}{10}$ that of water, and is not sufficient to change the sample temperature relative to the inert material.

## Effect on Organic Matter

In Fig. 1 are four curves of the same clay from near Brenham, Texas. The first curve was obtained from the raw sample ground to pass 100 mesh and exhibits no recognizable clay characteristics. Its outstanding feature is a broad exothermic deflection starting at 200° C. and ceasing abruptly at 800° C. The second curve was made from the same material with nitrogen streaming through the furnace. This curve resembles kaolinite except for the endothermic loop between 50° C. and 200° C. The abrupt break at 800° C. has disappeared. It is thought that this break coincides with the completion of burning of an organic constituent. The third curve was made from the minus-two-micron fraction of the same sample. As is generally the case, the minus-two-micron fraction contains more clay mineral and a concentration of some of the organic matter. That the organic constituent responsible for the abrupt endothermic break in the first curve has been eliminated suggests that it is associated with particles larger than two microns. The fourth curve represents the minus-two-micron fraction when heated in an atmosphere

of nitrogen. This curve indicates that the clay mineral is chiefly kaolinite mixed with a small amount of a three-layer lattice clay. The *x*-ray diffraction pattern indicates kaolinite with about 15 per cent illite.

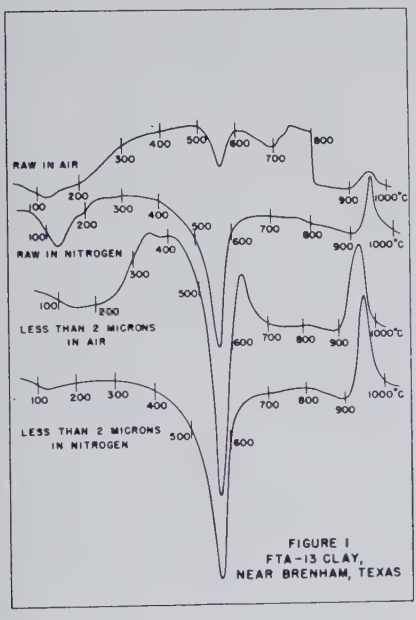


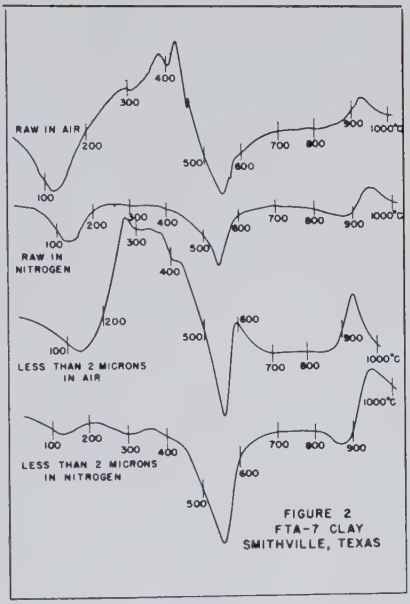


Figure 2 presents a similar series for a clay sample from a bentonite horizon exposed under the bridge where State Highway 71 crosses the Colorado River at Smithville, Texas. The clay portion of the curve for the raw clay and the minus-two-micron fraction heated in air are partially obscured by the exothermic deflections accompanying the burning of organic matter. In an atmosphere of nitrogen, however, both the raw and minus-two-micron fractions produce curves with identifiable clay mineral loops. The curve for the minus-two-micron fraction in nitrogen is similar to curves obtained from montmorillonites of sedimentary origin. *X*-ray diffraction identification shows the clay mineral to be a well organized montmorillonite, which can be expanded with ethylene glycol.

A series of four curves for the well-known Kentucky Ball Clay is presented in Fig. 3. The curve for the raw clay exhibits a large exothermic deflection on which is superimposed the dehydration loop of kaolinite. This is followed by an endothermic deflection between 700° C. and 800° C., and finally at 950° C. the exothermic loop associated with mullitization

appears. When the same material is heated in an atmosphere of nitrogen, the exothermic effect between 200° C. and 500° C. is eliminated as is the endothermic deflection between 700° C. and 800° C. The minus-two-micron fraction heated in air shows that some of the organic matter and the clay mineral have been concentrated. When the minus-two-micron material is heated in nitrogen a typical, uninterrupted kaolinite curve is obtained.

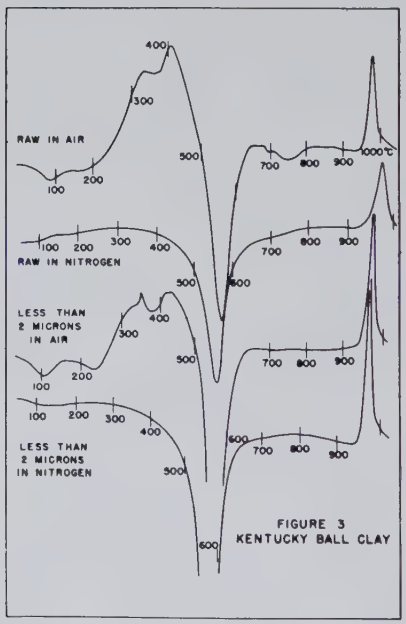


FIGURE 3
KENTUCKY BALL CLAY

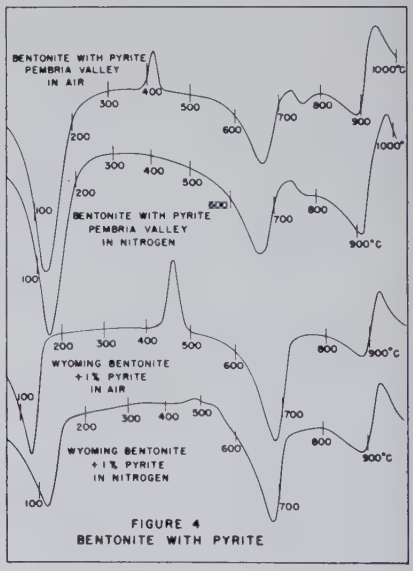


FIGURE 4
BENTONITE WITH PYRITE

Figure 5 presents three curves from the Green River Oil Shale which contains more than 25 per cent organic matter. The first is in air, the second in nitrogen, and the third in argon. The first is recorded on a scale which represents temperature differences at about $\frac{1}{8}$ the scale for the second and third. On the first curve the oxidation of organic material is represented by a broad exothermic deflection between 150° C. and 700 °C. This deflection is interrupted by endothermic loops between 400° C. and 500° C. and between 700° C. and 800° C. These two loops remain when the sample is heated in an inert atmosphere. The minor difference between the nitrogen and argon curves is attributed to a small amount of oxygen in the nitrogen, since water-pumped nitrogen contains about 4

per cent air. The significance of the two endothermic loops is not known and the curves are presented to show the effectiveness of the method even when large quantities of organic matter are present.

## Effect on Pyrite

Figure 4 presents two bentonites containing pyrite. The one from Pembria Valley is a natural mixture. The other is a prepared mixture of 1 per cent pyrite in Wyoming bentonite. As can be seen from the

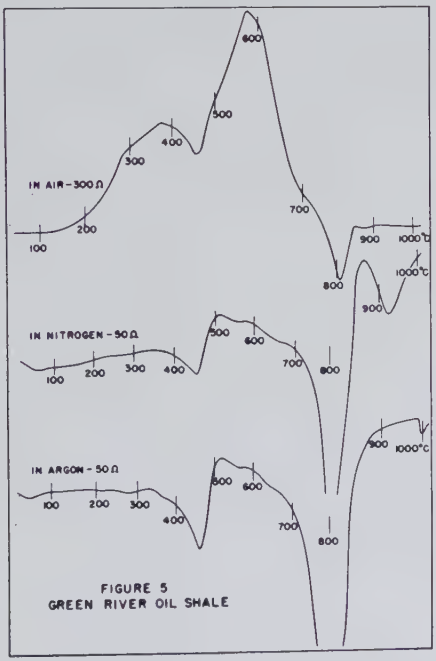


FIGURE 5
GREEN RIVER OIL SHALE

curves, heating in a furnace atmosphere of nitrogen eliminates the exothermic effect beginning at 390° C. in the Pembria Valley sample, and at 450° C. in the prepared mixture, and spreads out the approach to the endothermic loop at 900° C. The inert atmosphere has little effect on the endothermic deflection between 700° C. and 800° C. on the curve for the Pembria Valley sample. It is thought that in each case both the sulfur and the iron are oxidized, since the final product proves to be hematite. When the sample is heated in air this oxidation takes place between the temperatures indicated by the exothermic loop. In a nitrogen atmosphere

the sulfur is vaporized and removed from the furnace by the stream of nitrogen, and the iron is oxidized only when, after the run is finished, the hot sample is withdrawn and exposed to the air.

### Carbon Dioxide Atmosphere

In addition to the use of inert gases to suppress the oxidation reaction of materials associated with clays, differential thermal curves of the carbonate minerals can be improved by introducing an atmosphere of $CO_2$ in the furnace. When calcite is heated in air in the differential thermal apparatus, its dissociation begins to be registered at about 650° C. and the reaction progressively becomes more vigorous until a peak is reached at about 925° C. When the reaction starts, the $CO_2$ content of the air surrounding the $CaCO_3$ is very low but progressively increases as $CO_2$ is evolved from the sample. If the furnace is filled with $CO_2$ at approximately one atmosphere pressure, the reaction does not begin until a temperature of 925° C. is reached, whereupon it proceeds vigorously until completion.

These phenomena may be interpreted in terms of the basic thermodynamics of the calcium carbonate-calcium oxide-carbon dioxide system. For the reaction:

$$CaCO_3 \rightleftarrows CaO + CO_2$$

the equilibrium constant may be written as

$$K_p = \frac{p_{CO_2} \times p_{CaO}}{p_{CaCO_3}}.$$

The general case of a gas reacting with a solid is treated by MacDougall (1939). Since the partial pressure of the solid phase is constant, this can be written as

$$K_p = p_{CO_2}.$$

The equilibrium constant at a given temperature is determined only by a function of the partial pressure of the carbon dioxide evolved, which will, in turn, depend on the pressure of the $CO_2$ in the surrounding atmosphere. The pressure of a mixture of gases is equal to the sum of the partial pressure of each of its constituents. In an ideal gas the partial pressure of each constituent is equal to the pressure that constituent would exert if it occupied the entire volume of the mixture or to its mol fracton times the pressure of the mixture. Since the mol fraction of $CO_2$ in air is about 0.0003, then the partial pressure of $CO_2$ in air is about 0.0003 atmosphere. According to various investigators, the temperature corresponding to this equilibrium partial pressure should be between 500° C. and 600° C. Before attaining this temperature, $CO_2$ has not been dis-

sociated from the solid $CaCO_3$. In this temperature range and at higher temperatures, the system in which all three phases CaO, $CaCO_3$ and $CO_2$ are present continuously attempts to adjust to equilibrium conditions by releasing more $CO_2$ and forming more CaO at the expense of $CaCO_3$. As the furnace temperature increases, the partial pressure of $CO_2$ continues to rise until it approaches atmospheric pressure, which it cannot exceed since the sample is not enclosed. At this point the rate of dissociation becomes a maximum, and the heat absorbed allows the thermocouple junction in the sample to lag in temperature behind the temperature of the junction in the inert material, which produces a strong endothermic loop on the diagram. When the furnace atmosphere consists entirely of $CO_2$ at approximately one atmosphere pressure, little or no dissociation takes place until a temperature is reached at which the equilibrium partial pressure becomes equal to that prevailing in the furnace. Delays involving the transfer of heat through the sample to the thermocouple junction and the simultaneous increase, at a regular rate, of the furnace temperature make the recorded endothermic deflection of the D.T.A. curve appear at a higher temperature than the temperature at which the reaction takes place.

A similar explanation applies to the dissociation of all carbonate minerals although the effect may not be as evident as with calcite because the dissociation temperature $-p_{CO_2}$ relation may not extend over so wide a temperature range below one atmosphere. The effect of dissociation in $CO_2$ rather than in air may be estimated by comparing the heat of reaction with that of calcite. The relation between the equilibrium constant and heat of reaction is stated by the expression

$$\left(\frac{\mathrm{d}\ln K_p}{\mathrm{d}T}\right)_2 = \frac{\Delta H}{RT^2}$$

in which $\Delta H$ is the heat of reaction, $T$ the absolute temperature, and $R$ the gas constant. This equation shows that the effect of the increase in $p_{CO_2}$ on the temperature at which the dissociation loop will occur will be greater for carbonates with $\Delta H$ larger than calcite and less for carbonates with $\Delta H$ smaller than calcite. An example is afforded by comparing calcite, $\Delta H_{18°C} = 43.2$ kilocal/mole, and magnesite, $\Delta H_{18°C} = 27.4$ kilocal/mole. The magnitude of the shift for calcite is considerably greater than for magnesite, Fig. 6.

Figure 6 shows the dissociation of several carbonates the curves for which are reproduced only in the range of dissociation. The upper curves were prepared in an atmosphere of air, while the lower curves represent dissociation in a $CO_2$ atmosphere. Calcite dissociation is illustrated by the two curves at the right side of the figure.

The dissociation of siderite in air and in $CO_2$ has been discussed previously (Rowland and Jonas, 1949). Briefly, the curve indicates that between 450° C. and 530° C. the endothermic effect of the dissociation of $CO_2$ is accompanied by oxidation of FeO, so that the first part of the curve is a compromise. When a temperature of 530° C. is attained, sufficient $CO_2$ is liberated to prevent the oxidation of the FeO, and a modified endothermic loop is registered. At about 570° C. the evolution of $CO_2$ decreases enough so that the FeO can oxidize, and an exothermic loop is recorded. The small exothermic mound between 750° C. and 850° C.

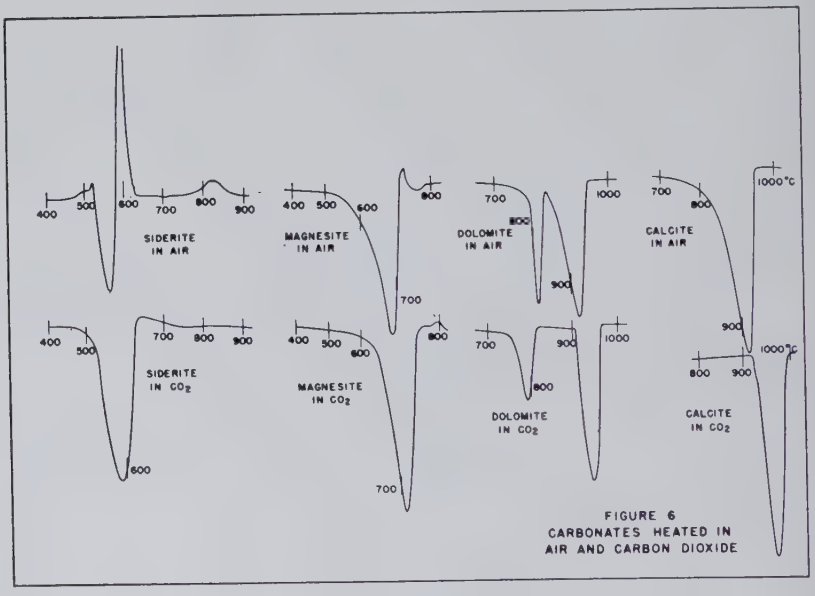


FIGURE 6
CARBONATES HEATED IN AIR AND CARBON DIOXIDE

is registered when the iron oxide becomes hematite. In a $CO_2$ atmosphere the iron is not oxidized and a larger, uninterrupted endothermic loop is obtained.

Differential thermal curves for magnesite from Stevens Co., Washington, also showed a marked difference between dissociation in air and in $CO_2$. The endothermic deflection, when the sample is heated in air, begins at about 380° C. and becomes quite sharp at 515° C. The peak is reached at 690°C. after which there is a light exothermic deflection. When the sample is heated in $CO_2$, the endothermic deflection also begins at about 380° C. but does not bend sharply until about 650° C. It peaks at 710° C. and returns to the base line without an exothermic loop. The endothermic loop in $CO_2$ encloses a larger area than that enclosed by the

curve obtained in air. The absence of the exothermic loop in $CO_2$ suggests that an oxidation takes place towards the end of the dissociation when the sample is heated in air. *X*-ray diffraction and spectrochemical analyses indicate that the sample contains a small quantity of iron (2% Fe) as siderite ($FeCO_3$). Oxidation of the FeO dissociated from the $CO_2$ would account for the small exothermic loop and the subsequent wiggles at about 800° C. Beck (1950) has shown that a sample of bruenerite from Gustine, California, produces a curve of the same character, and Gruver (1950) discusses a similar curve obtained from magnesite from Chewelah, Washington. According to Dana, magnesite and siderite form a continuous series without definite intermediate compounds.

Perhaps the differential thermal curve of dolomite (Fig. 6) is benefited more by a furnace atmosphere of $CO_2$ than is any other carbonate. When this mineral is heated in air, the endothermic loop which accompanies the loss of $CO_2$ by the $MgCO_3$ begins its sharp deflection at about 780° C., more than two hundred and fifty degrees higher than the beginning of the sharp deflection for magnesite alone. The peak occurs at 820° C. and before the loop is completed it is interrupted by an endothermic deflection accompanying the loss of $CO_2$ by the $CaCO_3$ portion of the mineral. Frequently this interruption takes place considerably before the first loop is completed. When the same material is heated in an atmosphere of $CO_2$, the $MgCO_3$ part of the curve begins at 750° C., peaks at about 790° C., and is complete at 820° C. The $CaCO_3$ part does not start until 910° C. and is clearly separated from the $MgCO_3$ loop.

The use of a $CO_2$ atmosphere in the furnace likewise affords an opportunity to observe the reversibility of the reaction, $CaCO_3 \rightleftarrows CaO + CO_2$ by alternately heating and cooling the sample through the temperature range of dissociation-reconstitution. For this purpose a Bureau of Standards sample of dolomite was heated in $CO_2$ to 1000° C. then cooled to 200° C. and reheated to 1000° C. This cycle occurs four times without removing the sample from the furnace atmosphere of $CO_2$. Those parts of the curve on which there was a deflection are reproduced in Fig. 7. On the first heating, the expected dissociation loops for dolomite were obtained. When the sample was cooled, only one loop formed, and successive heating and cooling dissociated and reformed only the compound responsible for this loop. *X*-ray diffraction patterns indicate the presence of CaO and MgO in the product above 1000° C., and MgO, calcite, and some CaO in the material after cooling in $CO_2$. It should be noted from the position of the 900° C. mark on the dissociation loops that dissociation took place at a progressively lower temperature as the cycle was repeated. Also the size of the reconstitution loops decreased as the cycle was repeated. It is of some interest to compare the areas under the

reconstitution loops with the corresponding dissociation loops since presumably exactly the same amount of material is dissociated as has been previously reconstituted, and the net heat involved in the reaction should be the same. During dissociation, an endothermic reaction, the sample takes up heat and tends to remain at the same temperature until the reaction is complete. While this is happening, the thermocouple in the sample is maintained at a temperature lower than the furnace temperature. When reconstitution takes place, the reaction is exothermic and the sample heats the thermocouple. During this process the thermo-

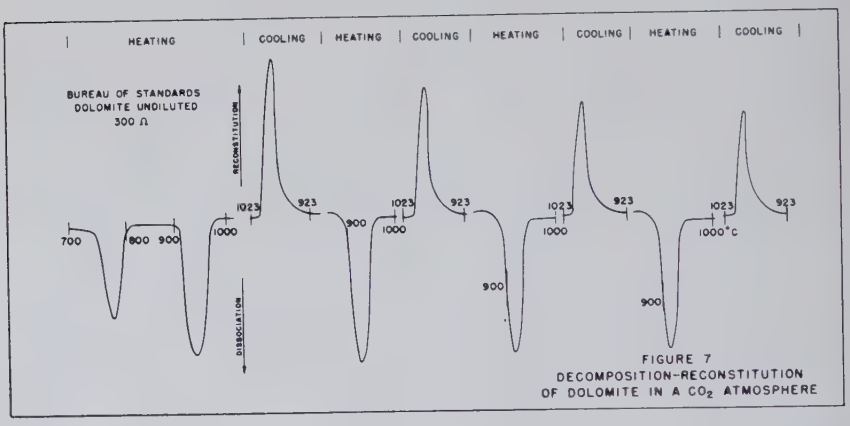


FIGURE 7
DECOMPOSITION-RECONSTITUTION
OF DOLOMITE IN A $CO_2$ ATMOSPHERE

couple is maintained at a temperature higher than that of the furnace. Since the furnace heating and cooling rates are essentially the same, then a comparison of the areas enclosed by the loops and an extended base line should indicate the relative efficiency with which exothermic and endothermic reactions are recorded. For the four reversals shown here, the ratio of the area under the reconstitution loop to the area under the following dissociation loop lies between 0.68 and 0.72, indicating that the apparatus more faithfully records endothermic effects than exothermic effects.

## Conclusions

It is apparent from the foregoing discussion that the usefulness of existing differential thermal analysis apparatus can be extended considerably by controlling the composition of the furnace atmosphere. Adequate control to take advantage of the method may be obtained by simply passing a gas from commercially available pressure cylinders through the furnace. When it is desirable to suppress the oxidation of organic matter or sulfides, water-pumped nitrogen may be used. If a more completely

inert atmosphere is required, purified nitrogen and argon are available. When it is desired to control the partial pressure of a gas being evolved in the reaction, the participating gas, such as $CO_2$ in the dissociation of the carbonates, may be introduced into the furnace. In each case confusing aspects of curves obtained in air are eliminated, and inflection points are sharpened considerably.

## References


Beck, C. (1950), Differential thermal analysis curves of carbonate minerals: *Am. Mineral.*, **35,** 985–1013.

Grim, R. E., and Rowland, R. A. (1944), Differential thermal analyses of clays and shales, a control and prospecting method: *Jour. Am. Ceramic Soc.*, **27,** 65–76.

Gruver, R. M. (1950), Characteristic heat effects of some carbonates: *Jour. Am. Ceramic Soc.*, **33,** 96–101.

MacDougall, F. H. (1939), *Thermodynamics and Chemistry*, John Wiley, N. Y. p. 228 ff.

Rowland, R. A., and Jonas, E. C. (1949), Variations in differential thermal analysis curves of siderite: *Am. Mineral.*, **34,** 550–558.

Whitehead, W. L., and Breger, I. A. (1950), Vacuum differential thermal analysis: *Science*, **III,** 279–281.


*Manuscript received*
*Aug. 1, 1950*

# A USEFUL METHOD FOR DETERMINING APPROXIMATE COMPOSITION OF FINE GRAINED IGNEOUS ROCKS

W. H. Mathews, *University of California, Berkeley, California.*

Abstract

The refractive indices of glasses formed by artificial fusion of samples from *selected* suites of igneous rocks show a close correlation with chemical composition. Each of three suites studied has its own characteristic curves relating refractive index to composition of chemically analyzed samples, and these curves can be used to establish the approximate composition of other rocks from the same suites for which no chemical analyses are available. Similar relationships can be expected for the igneous rocks of many other suites and petrographic provinces.

Complete fusion of the powdered rock can be effected in a carbon arc using a small but representative sample. The glass formed from this fusion is crushed and its refractive index determined in immersion oils.

That the refractive index of a glass is determined by its chemical composition has long been known. Michael Stark (1904) and Walter George (1924), recognizing this relationship, attempted to correlate refractive indices of natural glasses with the content of their major constituent, silica, but with comparatively little success. According to their own observations two glasses with the same index might differ in silica content by as much as 14 per cent, or conversely two glasses with the same silica content might differ in index by as much as 0.065. Thus, although they demonstrated that indices are generally low if the silica content of the glass is high, and vice versa, they did not demonstrate a relationship sufficiently precise to provide a means of determining composition with any assurance of accuracy. The early work on refractive indices and composition, of which Stark and George were well aware, makes it clear that the proportion of any one constituent, even the major constituent, does not alone determine the refractive index of the glass, but instead each constituent contributes according to its abundance and to its specific properties. Thus, although the silica content of two natural glasses may be the same, as in a phonolite and an andesite, the proportion of other constituents may be markedly different and the refractive indices may, therefore, show no similarity. However, the application of Harker's variation diagrams (Harker, 1909, pp. 118–125) to *selected* groups of igneous rocks, of one general locality and age, does show that within such groups two rocks with similar silica contents have similar bulk compositions and, if glassy, can be expected to have similar refractive indices. Thus had Stark and George confined their studies to glasses of a single petrographic province or magmatic suite they could have expected a much closer distribution of plotted points on the silica-refractive

index diagram along a smooth curve than anything they obtained (Fig. 1 lower left).

Few completely glassy rocks, suitable for refractive index determinations, are encountered in the field; but there is no reason, as Tesch indicated in 1903, why partly or wholly crystalline rocks could not be fused artificially to produce glasses suitable for composition-refractive index studies. The significant changes brought about in the composition of rocks as a result of artificial melting are essentially loss of the most volatile constituents, notably water, and change in the state of oxidation of iron. The presence of variable quantities of water in natural glasses may well have contributed to the deviations from George's silica-refractive index curve, for, as shown by Tilley (1922), this constituent even in small amounts can have a significant influence on refractive index.[1] Similarly, differences in the degree of oxidation of lavas during and after extrusion may also create deviations from the composition-refractive index curves for a particular suite. By artificially eliminating water and bringing iron to a uniform state of oxidation, however, a comparison of indices with composition in the suite may thus be aided.

Combining the two concepts outlined above, it would appear possible to correlate compositions of the members of a particular magmatic suite with the refractive indices, not merely of the naturally glassy rocks within the suite, but also with any artificially fused specimens of partly or wholly crystalline rocks. It would appear necessary only that the anhydrous compositions of the members of the suite can be expressed in terms of a single variable, that is that rocks representing comparable degrees of magmatic differentiation would contain similar amounts not merely of silica but also of alumina, iron, lime, and other essential constituents. The process of artificial fusion must be one that does not significantly alter the anhydrous composition of the specimens by faulty sampling, by contamination, by selective melting, or by differential boiling. If a reasonably close relationship can be established between composition and refractive index of the artificial fusion for a representative group of rocks from the magmatic suite in question, then the relationship can, in turn, be utilized in determining the approximate composition of other rocks from the same suite for which no chemical analyses are available. The degree of accuracy obtainable in the latter determinations is indicated by the scale of discrepancies between the mean curves on the composition-refractive index diagrams and the individual points corresponding to the analyzed rocks.

[1] According to Tilley the index rises, other things being equal, at a rate of about 0.0033 for each additional per cent water up to at least 3.3 per cent; the density falls with increasing amounts of water.

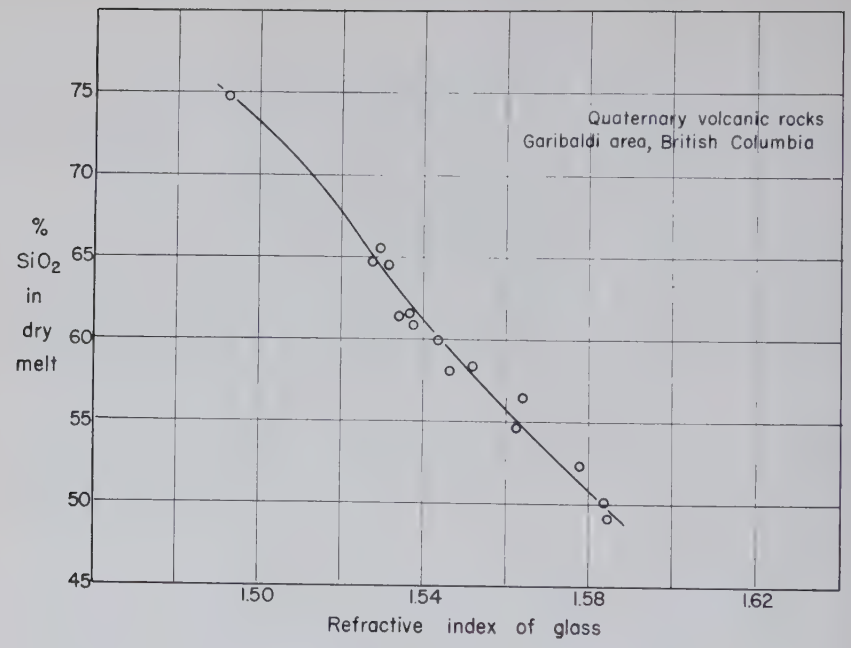


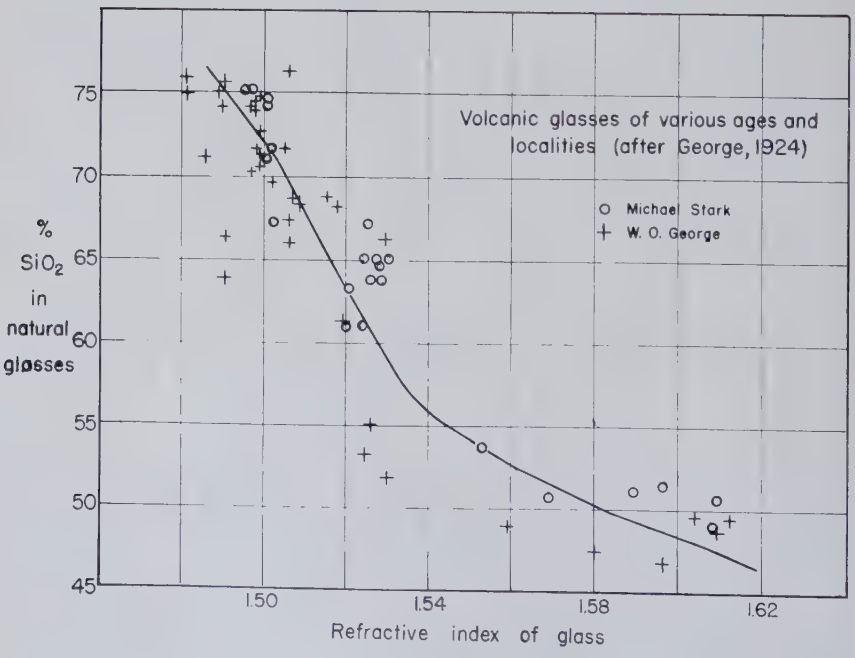


FIG. 1. Four compositio

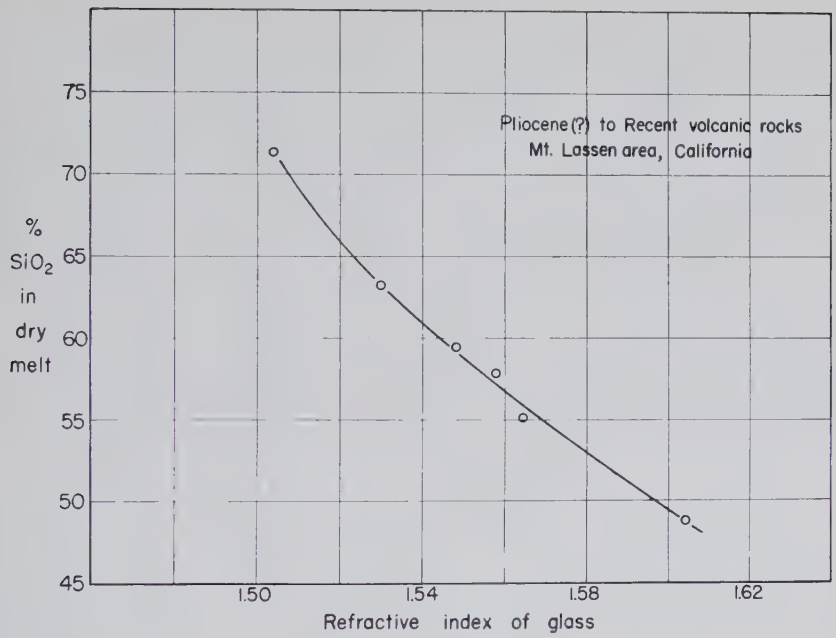


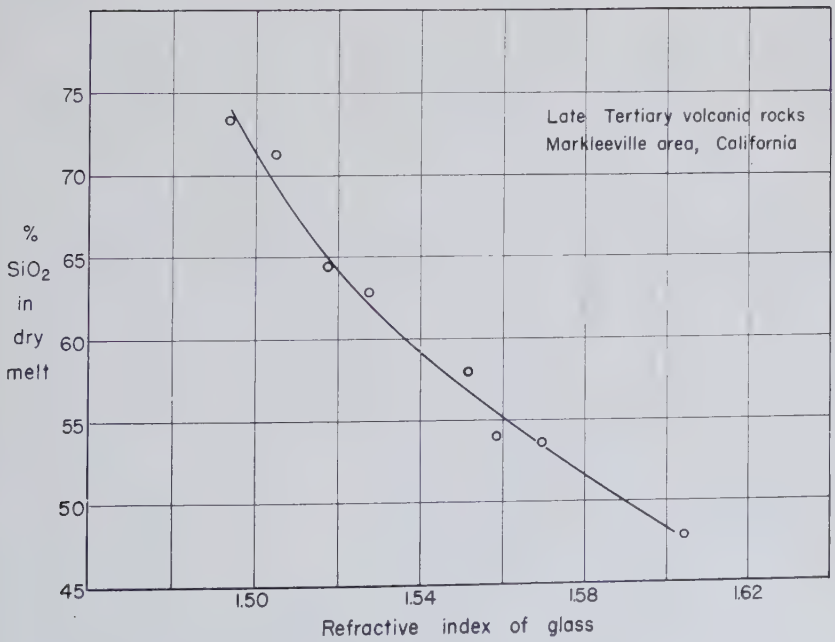


active index diagrams.

As a test of the idea, 16 unaltered Quaternary volcanic rocks from the Garibaldi area of southwestern British Columbia were fused, and the refractive indices of the resulting glasses compared with the rock analyses. The analyses had already indicated that composition could be expressed, with but a small error, in terms of a single variable. The results of the test are indicated in Fig. 1 (upper left.) The maximum departure of any point from a smooth mean curve on the silica-refractive index diagram is 0.007 in index and 1.8 per cent in silica content. The maximum departure from a smooth alumina-refractive index curve is 1.6 per cent alumina, and from a potash-refractive index curve only 0.25 per cent potash for 15 of the 16 analyzed rocks, and 0.40 for the 16th. The accuracy of the results, though by no means perfect, was far superior to any obtained by George and was sufficient to justify the effort involved in making the observations.

Similar refractive index measurements have been made by Messrs. G. H. Curtis and D. B. Slemmons of the University of California for two other volcanic suites, one of late Tertiary rocks from the Markleeville area (Fig. 1 upper right) in the northern Sierra Nevada, and one of Pliocene (?) to Recent rocks from Mount Lassen (Fig. 1 lower right). For both suites a close relationship is indicated between refractive index and the silica content of the water-free glass as calculated from the chemical analyses of the original rocks.

A comparison (Fig. 2) of the four available silica-refractive index diagrams[2] shows (1) that the mean curve for the Garibaldi suite diverges appreciably over a part of its range from the curve for the Markleeville lavas, (2) that for glasses of the same refractive index those from the Lassen area are regularly about 2 per cent richer in silica than those from the Markleeville area, and (3) that not one of the three curves corresponds to the one derived by George from a large but indiscriminately chosen set of volcanic glasses. The volcanic suites of the Garibaldi, Markleeville, and Lassen areas are all calcic (Peacock, 1931). Had alkaline suites been included in the studies we might expect to find other curves differing markedly from those already established, and in all probability lying on the opposite (left) side of the average curve prepared by George. Such variations show clearly how unsafe it is to assume that a composition-refractive index curve for one suite of rocks should necessarily apply for a suite of some other locality or age.

It should be emphasized that for each of the three suites so far studied

[2] Note, however, that the diagrams for the rocks from the Garibaldi, Markleeville, and Lassen areas are based on the silica content of *water-free* glasses, whereas George's diagram is based on the silica content of natural glasses, many of which may be rich in water. The last mentioned diagram is not, therefore, strictly comparable with the other three.

it had been established by at least 8 chemical analyses that composition of the rocks could be expressed, with but a minor error, in terms of a single variable, such as silica content. Where more than one process of magmatic differentiation operated simultaneously and at independently varying rates in the development of these magmatic suites such a relationship might fail to develop. Had solfatarized, weathered, or otherwise metasomatized rocks been included in the suites, again no such relationship

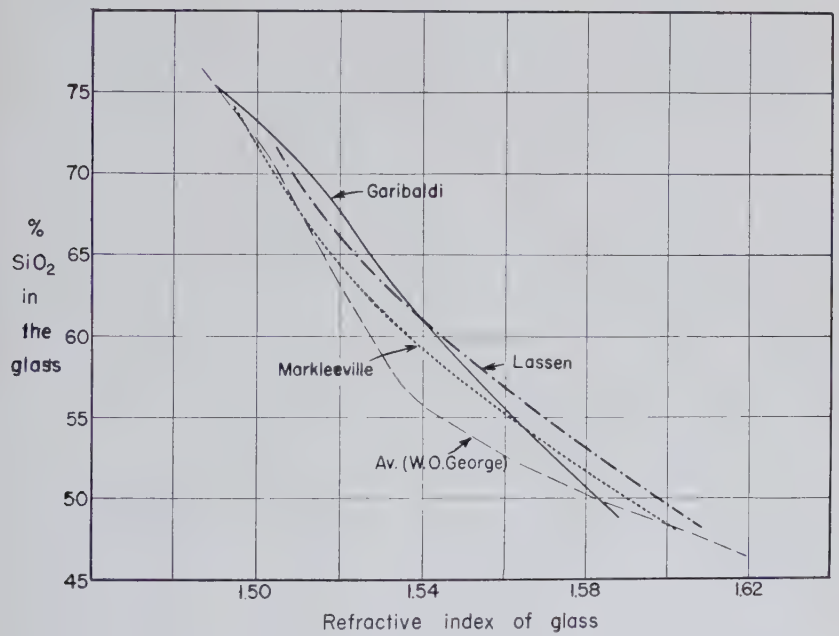


Fig. 2. Four composition-refractive index curves superimposed.

could be expected to hold, and the observations plotted on a silica-refractive index diagram would, almost certainly, have been widely scattered. Should the rocks have been metamorphosed without alteration of chemical composition, however, the close distribution of points along the silica-refractive index curves would have been unaffected.

Any technique for the complete fusion of a representative sample of the rock without affecting its anhydrous composition is suitable for the application of the principles discussed above. The fusion temperatures of most igneous rocks are, however, so high that complete melting calls for special facilities; the ordinary Bunsen burner, Meeker burner, or blowpipe flame is inadequate. Reaction between sample and container might,

moreover, render unsatisfactory the slow melting of the sample in a high-temperature oven. Tesch (1903) found it possible to fuse rock samples in bone ash cupels using a gas-oxygen flame, but he did not eliminate the dual problem of complete fusion of sample without reaction with the container. I found it possible to melt completely small quantities of the powdered rock in a crater cut in the lower electrode of a carbon arc lamp. During the early part of the arcing cycle the molten bead rests in the electrode like water on a hot stove, and the contact between melt and container is so slight and the carbon so inert that contamination of the glass by reaction can be neglected. The technique thus adopted overcomes the difficulties mentioned above and necessitates only such facilities as are commonly present in a well equipped petrographic laboratory. One drawback exists, however, with this method: the amount of material that can be treated in the arc, perhaps 10 milligrams at a time, though sufficient for the determination of refractive index by oil immersion technique, is so small that extreme care is necessary to obtain accurate sampling. Experience in quantitative spectrochemical analysis shows, however, that sampling with the desired degree of accuracy is possible after fine grinding of the original rock and thorough mixing.

For the first step in this technique a rock chip of sufficient size to be representative within the limits of accuracy desired, *i.e.* yielding an error of less than 1 per cent in composition, is broken from the hand specimen. If the rock is homogeneous and fine grained or glassy a very small chip, weighing perhaps a couple of grams, is adequate; if, however, the rock is coarse grained or porphyritic the chip must be considerably larger, preferably of a size such that the addition or subtraction of a single grain or phenocryst would not materially affect the composition. The chip is then pulverized in a mortar until a fineness and degree of mixing is obtained such that any 10 mg. sample would differ from the mean composition of the mix by less than 1 per cent. At such a stage, again depending on the homogeneity and grain size of the original rock, most if not all the powder should be -200 mesh. It is desirable to split the sample, using an approved sampling technique, at several stages in the grinding in order to minimize the time and effort involved. A "diamond" mortar has proved better for pulverizing hard volcanic rocks than a cast iron mortar in which sufficient iron filings can be produced during the grinding of a single chip to contaminate the sample effectively. An agate mortar, though unsuited for coarse grinding, is well adapted for the later stages of grinding and permits a more thorough mixing than does the diamond mortar. At first, until this part of the technique has been perfected, it is advisable to repeat determinations using different chips off the same hand specimen to establish the accuracy of sampling.

The powdered sample is introduced into a broad crater cut with the point of a penknife to a depth of about 2 mm. in the upper end of the lower electrode of the carbon arc lamp. Uncored carbons, 7 mm. in diameter, are used after their ends have been tapered to about one half the original diameter by means of a pencil sharpener to reduce both the wandering of the arc and the heat loss from the vicinity of the crater. With this modification the powdered rock can be completely melted in the arc within several seconds, whereas with the full 7 mm. diameter persisting to the end of the electrode complete fusion can be obtained only with prolonged arcing. It is important to watch through a dark filter the powder in the process of melting to recognize the time at which fusion has reached completion and after which the arc should be switched off. If fusion is incomplete and the less fusible constituents remain undissolved, the glass will not have the composition of the anhydrous rock. If fusion is unnecessarily prolonged differential boiling may lead to a loss of volatile constituents other than water and again the composition of the glass will not be that of the anhydrous rock. After prolonged heating, moreover, the melt is absorbed into the electrode and on cooling the glass is badly clouded with opaque grains of carbon. The composition of the glass itself is unaffected but the impurities make the refractive index determination difficult.

The glass bead which forms in the crater of the electrode after the arc has been switched off is then crushed on a metal plate and the index of the glass fragments determined by the ordinary immersion methods (Johannsen, 1914, p. 249 et seq.) in oils of known refractive index. Inasmuch as a maximum error of about 0.004 is permissible in routine determinations of the index of the glass, and as still greater accuracy is needed in the preparation of standard curves from analyzed samples, monochromatic light is virtually essential. Either a sodium vapor lamp or appropriately filtered white light can be used; unfiltered white light is unsatisfactory because of the vague color fringes it produces in place of the sharp Becke line when oil and glass have nearly the same index. Inasmuch as the refractive indices of oils change with age and vary with temperature they should be checked at the time of use with a refractometer to ensure the most accurate results.

The time involved in grinding and fusing a sample, determining the index of the resulting glass, and cleaning mortar, pestle, electrodes, and slides preparatory to a new determination can be as little as 10 to 15 minutes in routine work. If the fusion and index determinations of the powdered sample are repeated to obtain greater accuracy a few more minutes are required for each rock. In the preparation of the standard composition-refractive index curves from analyzed samples greater care

is necessary and the determinations should be made in triplicate; such determinations involve correspondingly greater periods of time. A large number of determinations can, nonetheless, be completed in an uninterrupted day's work and the information provided by these determinations seems well worthy of the time spent.

Applications of the results of this technique are at once apparent. The correlation of two igneous rocks having similar chemical composition but different cooling histories, and hence distinct textures and possibly distinct mineralogical compositions, can be facilitated without the time and expense of additional chemical analyses; conversely the recognition of dissimilarity of two rocks of different chemical composition but alike in physical appearance is aided. The volumetric or stratigraphic distribution of acid to basic igneous rocks within a volcanic succession can be determined without resort to a large number of chemical analyses, or to tedious and commonly uncertain microscopic determinations. In the selection, from some igneous suite, of rocks for chemical analysis the technique can be of material assistance for it permits the recognition of the most acid rocks, the most basic, and a representative group of intermediate types.

This technique is not offered as a substitute for, but rather as an adjunct to, the microscopic examination of fine grained igneous rocks. The refractive index of a glass yields a minimum of information on the petrogenesis of the rock from which it has been made, and information on petrogenesis as well as on composition is the objective of petrographic studies. The technique is not offered, moreover, as a suitable one for the study of the coarser grained igneous rocks. For these the time and effort of grinding a representative chip sample minimizes the advantages of the method, and other techniques are better adapted for the solution of the problems. Specific gravity of non-vesicular samples, for example, can be obtained with greater ease than refractive index of a fusion and can be used in precisely the same way for the determination of approximate composition of holocrystalline rocks. In such rocks, moreover, mineralogical composition is a fairly reliable guide to chemical composition and the essential minerals of the rock can be recognized with ease and assurance with the naked eye or with low magnifications after the staining of a sawn section (Keith, 1939). For the coarse grained rocks, therefore, these other methods are simpler and more satisfactory, but for the finer grained and especially for the partly glassy rocks they form no substitute for the refractive index of glass from artificial fusions as a guide to composition.

## References

George, W. O. (1924), The relation of the physical properties of natural glasses to their chemical composition: *Jour. Geol.*, **32,** 353–372.

Harker, A. (1909), The Natural History of Igneous Rocks; Macmillan Co., New York.

Johannsen, A. (1914), Manual of Petrographic Methods; McGraw-Hill Book Co., Inc., New York.

Keith, M. L. (1939), Selective staining to facilitate Rosiwal analysis: *Am. Mineral.*, **24,** 561–565.

Peacock, M. A. (1931), Classification of igneous rock series: *Jour. Geol.*, **39,** 54–67.

Stark, M. (1904), Zusammenhand des Brechungsexponenten natürlicher Gläser mit ihrem Chemismus: *Tsch. min. i. petr. Mitt., Neue Folge,* **23,** 536–552.

Tesch, P. (1903), On the refractive index of rock-glasses: *Proc. Sci., K. Acad. Wetens., Amsterdam,* **5,** 602–605.

Tilley, C. E. (1922), Density, refractivity, and composition relations of some natural glasses: *Min. Mag.*, **19,** 275–294.

*Manuscript received*
*March 28, 1950*

# PRECISION LATTICE MEASUREMENTS OF GALENA

B. Wasserstein, *Geological Survey, Mines Dept.,* Pretoria, Union of South Africa.*

Abstract

Precision lattice determinations of galena are virtually lacking; this paper partly rectified this deficiency. The cube-edge for pure galena at 25° C. was found to be 5.9240 ±0.0004 kX units. The process of pulverizing galena preparatory to *x*-ray examination causes crystal distortion which, however, is removed by gentle heating. The resultant sharp lines with very large Bragg angles enabled precision data to be obtained for the first time from *x*-ray powder photographs of galena. Such data made it clear that bismuth can substitute for lead causing a shrinkage of the unit cell.

Apparently identical galena specimens can readily be differentiated spectrochemically by means of their minor element content and to a lesser extent by the variation in their cube-edges. Some of the biggest differences were found in the galenas of the "Rand" gold mines. This information should prove useful to geologists in their investigations.

## Introduction

The writer recently drew attention to the work of others which indicated that pyrite could conceivably assume the role sometimes of an "indicator fossil" (1); both duplication and differences in the values of the cube-edges of pyrite provided criteria. It was also stated there that other cubic minerals warranted attention; among them is galena. Fortunately, a collection of very small galena fragments was available from a previous, as yet unpublished, study of the minor elements in galena, as determined spectrographically. It was therefore decided to utilize some of these specimens in the determination of the cube-edge of galena; at the same time it was hoped to demonstrate that at least some of the minor elements did in fact occupy lead positions in the galena framework.

An added incentive was the thought that there was a possibility of recognizing the different geological origins of the samples by means of laboratory investigations of a modern kind. In this respect the work has probably not progressed sufficiently and a handicap is the lack of geological interpretation of the lead deposits. A start has, however, herewith been made and new data have been obtained that justifies publication at this stage. It is hoped hereby to interest geologists in a novel attack on their field problems. There is clearly a need for the accumulation of similar data on relatively common minerals, comparable to the work by Smith on pyrite (2). It is the writer's contention that modern laboratory methods are as yet not fully appreciated by field geologists in their academic as well as economic studies. In South Africa where

* Published by permission of the Honourable the Minister of Mines.

geological correlation follows lithological lines, where particularly "gold reefs" are identified according to their disposition to certain "markers," varietal features of relatively common minerals deserve special study and take on a new significance.

## Previous Work

The new "Dana," volume I (3), quotes an averaged value for the cube-edge of galena which is derived from results of about 20 years ago, collected in the "Strukturbericht," viz:

$$a_0 = 5.93 \pm 0.02.$$

This result which has no pretensions to high accuracy is adopted also by Strunz in his "Mineralogische Tabellen" (4).

For PbS—no value for galena is listed—the well known "Handbook of Chemistry and Physics, 30th Edition" (5), gives the value 5.97.

In the A.S.T.M. set of $x$-ray diffraction cards, there is one precision result, obtained with Mo-radiation on a galena specimen whose origin is not given, viz:

$$a_0 = 5.9195 \text{ (Temp.?)}.$$

The relative smallness of the "back-reflection" angles obtainable with Mo-radiation, added to the relatively high absorption of lead, would tend to give a rather low result in this instance, as comparison with the results in Table 1 would suggest. Of course, an impure specimen could also cause a lowering of the cube-edge—it is not known what precautions were adopted in this determination and this result is not acceptable as representing the true cube-edge of pure galena.

In any event one has to choose between this value and that given by von Zeipel (6) who selected his specimen with some care but failed to test it chemically in any way. He reports:

*Galena, Přibram, at 18° C.*

$$a_0 = 5.923_{34}$$

with the last two digits doubtful. This result is the only one that could be found in the literature which deserves serious consideration, and, as will be shown later, is correct as far as can be judged, to within the errors indicated, *i.e.*, to four significant figures.

Although all these results are reported in Ångstroms, they are actually in kX units.

It is evident that there is need for reliable and accurate data on the lattice parameter of such a common mineral as galena. It is surprising to find that, despite the comparative simplicity of procuring such measurements on cubic minerals, there are probably no more than a half

dozen or so precision cube-edge determinations in the literature—apart from those on diamonds which have been the subject of more intensive investigations.

## Distortion in Powdered Galena

At the start of the investigation it seemed likely that at best a result with four significant figures could possibly be achieved if the conventional powder $x$-ray technique was to be used. Although the low $\theta$ values were indicated by sharp lines, the important large angle ones, *i.e.*, the back-reflections, were very diffuse. This is commonly encountered in minerals with a more complicated structure and in the so-called metamict

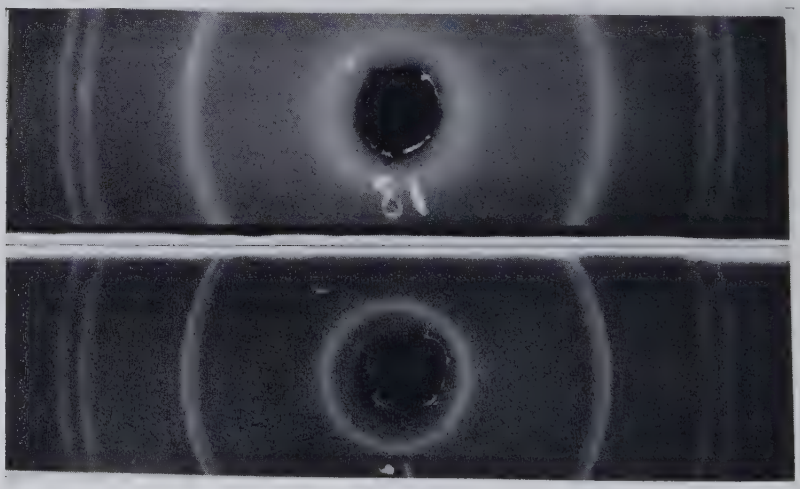

Fig. 1. *Top:* Back-reflection lines of galena before being heated. *Bottom:* The same, after gentle heating.

minerals. The writer at first assumed the cause of this phenomenon to be inherent in the galena samples; it was thought to be largely due to small variations in composition coupled with zonal arrangement. When, however, the rather pure sample from Joplin, No. 1 in Table 1, also yielded fuzzy lines, it seemed possible that the cause lay in induced distortion or strain of the crystal structure as is found commonly in metals. Guided by metallurgical practice—the writer received much of his practical training in $x$-rays in the Metallurgical Department at M.I.T. under Professor T. J. Norton—and also with the knowledge that radioactive minerals yield better $x$-ray photographs after being heated, the powdered sample was heated to between 300 and 400° C. for a few minutes. The remarkable improvement in definition is apparent from Fig. 1 which shows the same sample before and after "annealing."

It could readily be established that it was the grinding process which mainly, if not wholly, always caused the lattice distortion for, if the annealed powder was again ground, the sharp lines gave place to diffuse ones in the $x$-ray pattern. Although such phenomena are normally encountered in metals, they have apparently not been reported in minerals. It is of course known, even if not well known, that radioactive minerals also respond to annealing but they cannot then rapidly be made to revert to the previous strained condition. It seems likely that other minerals are affected by grinding in the same way as galena and would also respond to gentle heating to yield better defined $x$-ray powder patterns.

Discussing these observations in a letter to Professor Martin Buerger, the writer said. " . . . I found it was necessary to 'anneal' the powdered sample. . . . I take it that this is glide-translation phenomena for even around 200° C. the distortion is somewhat rectified. I am wondering whether relief of strain may also give sharper definition in single crystal work sometimes? . . . I do not think one has here the grain-growth as with your work on fluorite" (7). The writer is grateful to Prof. Buerger for the following comments in his reply: "Your remarks on galena are certainly interesting. The effect you have mentioned is a well-known one for plastic materials. When these are ground for powder samples they deform and this always results in lack of definition of the diffraction lines. This results from curved planes chiefly, and is an indication of the internal strain . . . it seems to me that I had read some place that when platinum is deformed it increases slightly in lattice constant. But I believe that the change is less than you have detected in galena. . . . Whether you recognize the effect as such or not, the decrease in fuzziness on annealing is equivalent to a recrystallization. I know that this annealing is customarily done to metallurgical powder samples to make the powder photographs readable. Incidentally, you can't do this to single crystals which have been bent and get a single crystal back. Instead you get an aggregate back. Furthermore you can't recrystallize a single crystal by annealing if it hasn't been deformed mechanically. Anyway, not in reasonable time. If one could, no single crystal would show lineage structure or other deviation from perfection if it had been grown at elevated temperatures."

## Apparatus and Method

A Picker $x$-ray unit was used with unfiltered copper radiation. The $x$-ray tube was run at 35 KV and 20 MA, and exposures were usually for about 2 hours. The change of temperature of the camera during this period did not exceed 2° C. under operating condtions; the room in which the apparatus was housed was well ventilated. The temperature of the

sample was taken as the temperature of the camera, which was determined by placing a thermometer in contact with it; readings were taken at the beginning, during, and at the end of the exposure. The air temperature was also noted during this period. All the results were obtained in the narrow temperature range from 22° to 26° C. and these were corrected to correspond to a temperature of 25° C. Errors in temperature are considered to be less than one degree, which, in terms of the final cube-edge figure means that this source of error is less than 0.0001 kX units. Some crude insulation helped to reduce the heating of the camera due to the operation of the $x$-ray unit.

A Debye-Scherrer camera, as designed by Buerger (8), which had a diameter of 114 mm., was available. Kodak No-Screen $x$-ray film was used and, after processing, was allowed to dry and approach normalcy for a week before being measured. This was done by means of a commercial viewing box fitted with a fluorescent bulb, which did not create undue heat, and a measuring scale with vernier. By interpolation, measurements to a precision of 0.02 mm. could be duplicated. Films were at first measured twice using different parts of the scale but no added accuracy resulted nor were any real variations in results found.

The diffraction rings were measured on either side of the $x$-ray beam's exit and entrance holes; the determination of the centers of these holes on the scale gave two valuable check-points, one of which could be used for each pair of measurements. The difference between these two points enabled the "shrinkage correction" to be applied accurately and simply because of the Straumanis (9) method of film mounting in the camera used.

After the calculation of the cube-edge derived from the higher angles, the results were plotted graphically according to the method of Bradley and Jay (10) for the elimination of systematic errors, and the extrapolation gave the value for the cube-edge of that sample at the temperature at the time of determination. The correction which had to be added or subtracted from this value for each degree centigrade was taken as 0.000115 kX units;* the positive correction for refractivity for galena is 0.0001 kX units, calculated according to the method of Lipson and Wilson (11), and, in common with other workers, has been neglected.

The wave-length values used, were:

| | |
|---|---|
| $CuK\alpha_1$ | 1.537395 kX |
| $CuK\alpha_2$ | 1.541232 kX |
| $CuK\beta$ | 1.38935 kX |

The following seven points proved most useful in plotting the graph for

* The average of the slightly differing values of the coefficient of linear expansion for galena given in refs. 5 and 17 was used in this calculation.

the extrapolation to zero error, according to the method of Bradley and Jay, and are given in terms of $(h^2+k^2+l^2)$ and relevant copper radiation:

(59) $K\alpha_1$
(56) $K\alpha_1$
(56) $K\alpha_2$
(52) $K\alpha_1$
(52) $K\alpha_2$
(51) $K\alpha_1$
(51) $K\alpha_2$

The point corresponding to (64)K$\beta$ was sometimes useful when its reflection was of sufficient intensity, for the precision in measuring was directly dependent on this factor. Points corresponding to (44)$K\alpha$ and (40)K$\alpha$ usually showed the straight line relation of the graph to change—often steeply—to a curve. These points because of the absence of resolution in the $K\alpha_1$, $K\alpha_2$ doublet, are not highly accurate and show the systematic errors due to eccentricity and absorption more markedly. Great care was taken in trying to place the small rods as centrally as possible; in order to counteract the effect of absorption these rod-like samples were kept as thin as was practicable viz. 0.2 mm. in diameter.

To ascertain with what accuracy the apparatus could operate with the technique employed, parallel determinations of the lattice constants of gold and silver were carried out. These serve as a basis of comparison in assessing the cube-edge determination of the galenas. Both metals were obtained from the South African Mint and were of exceptional purity; the gold had a fineness of 999.99 and the silver, 999.9. The procedures were exactly the same including the temperature observations.

There are slight differences in the published results of the lattice constants of the metals; those given in the new "Dana," Volume I, correspond to the values listed by Barrett (13), when reduced to the same temperature, and these have been used here in order to compare with the writer's determinations. The constants are given for 18° C. as:

| | As Published | This Work |
|---|---|---|
| Gold | $4.0699 \pm 0.0003$ kX | 4.0701 kX |
| Silver | $4.0772 \pm 0.0002$ kX | 4.0777 kX |

This agreement is highly satisfactory and incidentally demonstrates with what accuracy Debye-Scherrer cameras with Straumanis film mounting can be used. Some published results of the lattice constant for silver suggest that the writer's value is perhaps not unduly high. In any event it is hardly beyond the combined limits of error, and the correction for temperature adds a slight uncertainty to the last digit. In such work it is reasonable to assume that the writer's error is comparable to those of other workers.

The diffraction patterns of the metals yielded somewhat sharper lines than those obtained with galenas. If this tended to increase the error, this effect must have been more than counteracted by the fact that galena yielded a higher Bragg angle. It must be exceptional that such a high angle, $85\frac{1}{2}°$, could be utilized in the determination of a lattice constant.

The seven points plotted corresponded to angles from $85\frac{1}{2}°$ to 68° for galena subjected to copper radiation. Taking into consideration factors of thermal expansion, $x$-ray absorption, elimination of strain, line sharpness and the like, it seems reasonable to assess these as not too different in respect of accuracy between the metals and galena as to increase the over-all limits of error unduly. It is believed that this can be safely taken as 0.0004 kX and probably, in most determinations, as less. The cube-edge results of galena are given in this paper subject to this limit of error, viz. $\pm$ 0.0004 kX and therefore may be regarded as precision determinations.

## Spectrographic Examination

Small cleavage fragments of selected material—often from polished, ore-sections which had previously been checked for homogeneity under the microscope—were placed on flat copper electrodes which were made the cathode, and arced for 20 seconds at 5 amps. before a large Hilger Littrow type spectrograph set for the range 2800 to 5000 Å.

To assess roughly the amounts of the more important minor components, lead sulfide was precipitated which contained 1% respectively of the metals Bi, Sb, Cd, and Sn, also in the form of sulfides. This precipitate was diluted with pure lead sulfide to give the lower concentrations. These mixtures served as standards in determining the order of magnitude of the four elements present in individual galena samples, by comparing visually the intensities of element lines in the spectra. The quantitative results listed in Table 1 should not be interpreted too rigidly. A number of other elements were found—some of these appear in Table 2—but either they could not be used diagnostically or they were conceivably derived from contaminants. Here the role of silver could not be assessed and its great sensitivity in the spectrographic examination did not allow the estimation of even very approximate amounts in the samples. It did allow the detection of the extremely small amounts of silver in the Joplin sample. Very small amounts of thallium were frequently found, usually at the threshold sensitivity of the method used and special refinements of technique would be necessary to obtain quantitative information.

The spectrographic method used here, as stated earlier, was never intended for this particular study; as always it represents a compromise. It is considered adequate for the present purpose and enabled the selec-

tion of suitable material for the determination of the cube-edge. There was not much difficulty in duplicating results; different samples from the same locality showed very little variation in results—a factor, which is relevant in comparing von Zeipel's determination (6) on the galena from Přibram, Bohemia, with that of the writer's. This is discussed below.

The value of linking spectrographic tests with $x$-ray work deserves emphasis and certainly helps to complete the picture—especially in the absence of any chemical examination. Such tests however are not exhaustive; for example, they would not indicate a sulfur deficiency in the galenas.

## Results

The tabulated findings in Table 1 briefly summarize the results of the present investigation; the arrangement is such as to show some of the influences of geological origin and locale. Eight South African specimens were selected as the spectrographic work dealt primarily with local ores; the two overseas samples were included, as one, Joplin (No. 1), is the purest, while the other from Přibram, No. 3, was examined in order that

Table 1. Spectrographic and $X$-Ray Results on Galena

| Sample No. | Locality: Farm or mine | Geological Environment | | Sn | Sb (Per cent) | Cd (Per cent) | Bi (Per cent) | $a_0$@25° C. (kX units) |
|---|---|---|---|---|---|---|---|---|
| (1) | Joplin area | Replacement of flat-lying Limestones. | | 0 | 0 | 0 | 0 | 5.9240 |
| (2) | Bokkraal 300, W. Transvaal | Replacement of flat-lying Limestones. | | Tr | 0.1 | 0.02 | Tr | 5.9232 |
| (3) | Přibram, Bohemia | Quartz Veins | (in Granite) | Tr | 0.1 | 0 | 0 | 5.9236 |
| (4) | Langlaagte, 1693 N. Transvaal | Quartz Veins | (in Granite) | 0 | 0 | 0.01 | 0.01 | 5.9230 |
| (5) | Union Lead and Silver Mine, Pretoria Distr. | Quartz Veins | (in Diabase) | 0 | 0.02 | Tr | 0 | 5.9233 |
| (6) | Balloch, 0.136, N.W. Cape Province | Quartz Veins | (in Jaspers) | Tr | 0.05 | 0.05 | Tr | 5.9235 |
| (7) | Zaaiplaats Tin Mine, Transvaal | Late hydrothermal accessory in "tin pipes" of the Bushveld Granite | | Tr | 0.1 | 0.01 | 0.01 | 5.9240 |
| (8) | City Deep Gold Mine, Johannesburg | Minor accessory in the auriferous conglomerates of the Witwatersrand System | | 0 | 0.05 | Tr | 0 | 5.9235 |
| (9) | C.M.R. Gold Mine, West Rand. | Minor accessory in the auriferous conglomerates of the Witwatersrand System | | Tr | 0.02 | .02 | 1.0 | 5.9223 |
| (10) | New Modderfontein Gold Mine, Benoni | Minor accessory in the auriferous conglomerates of the Witwatersrand System | | 0.02 | 0.1 | Tr | >1.0 | 5.9190 |

its result could be compared with the work done by von Zeipel on a similar specimen.

The geological grouping throws little light on the results and this may be attributed to the fact that galena forms over a wide range of temperature and conditions as may be learnt from the recent "Symposium on the Geology, Paragenesis, and Reserves of the Ores of Lead and Zinc" of the last International Geological Congress held in London (1948). Too few results are presented to cover this aspect, but among the groups, it appears, that locality exercises an influence: Galenas of the same origin tend to differ rather than to agree in minor element content and the concept of mineral provinces finds support. It is clear how readily galenas from different localities can be differentiated—although apparently identical even after microscopic examination. The results on the galenas from the South African gold mines, Nos. 8–10, indicate how unfortunate it is that galena is a relatively rare constituent of the auriferous conglomerates of the Witwatersrand system, as the mineral here shows promising possibilities to serve as an indicator in "reef" correlation problems.

The frequency with which certain elements occur in 60 galena specimens tested spectrochemically is given in Table 2; it must be noted that the sensitivity of detection for the different elements is not the same. However, spectrographic sensitivity is not a controlling factor for the order of the elements in the table; elements that were less frequently detected are by no means those of poorer sensitivity. An interesting by-product of this investigation was the conclusion that vanadium, despite certain opinions to the contrary, hardly if ever is found in galena (14); the limit of detection for this element was less than 0.005% $V_2O_5$.

Table 2. Frequency of Occurrence of Minor Elements in 60 Galena Samples

| | |
|---|---|
| Ag | 100% |
| Sb | 80% |
| Cd | 70% |
| Bi | 50% |
| Sn | 40% |
| Fe | 40% |
| Tl | 35% |
| Mn | 30% |
| Sr | 20% |
| V | tr? |

Apart from silver, the four elements listed in Table 1, viz. Bi, Sb, Cd, and Sn, are the only ones that occur in "chemical amounts" in galena, and only bismuth in possibly major amounts. Only this element occurs in sufficient quantity to affect noticeably the cube-edge value, while such elements as Sr, Tl, Fe, and Mn probably never exceeded 0.01% in any

galena sample. No sympathetic or antipathetic relationship of the minor elements could be observed.

TABLE 3. IONIC RADII OF ELEMENTS (VARIOUS AUTHORITIES)

| $Pb^{+2}$ | $Ag^{+1}$ | $Bi^{+3}$ | $Bi^{+5}$ | $Sb^{+3}$ | $Sb^{+5}$ | $Sn^{+2}$ | $Cd^{+2}$ | $Sr^{+2}$ | $Tl^{+3}$ |
|---|---|---|---|---|---|---|---|---|---|
| 1.18–1.32 | 1.13–1.26 | 1.20 | 0.74 | 0.90? | 0.62 | 1.02 | 0.97–1.3 | 1.13–1.27 | 0.95–1.05 |

Table 3 lists the ionic radii which, of course, can vary with coordination and are not too accurately known. Nevertheless, it is clear that the size of the ions is in keeping with the common substitutions found; such elements as manganese and iron are too small for substitution and the extreme minuteness of the amounts found are best explained by contamination, especially when one considers the frequency, in this country, of the association of lead deposits and wad.

There is no difficulty in correlating size of ion with isomorphous replacement of $Pb^{+2}$ by $Ag^{+1}$, or $Bi^{+3}$, or even such unusual elements as $Tl^{+3}$ and $Sr^{+2}$, in galena. The chalcophile nature of lead is in conflict with the lithophile one of strontium, and this precludes any high degree of isomorphism in nature despite the close similarities of the two ions. $Cd^{+2}$ and $Sn^{+2}$ fall just within the 15% limit of tolerance for size suggested by V. M. Goldschmidt and it is, therefore, not surprising to find that they also only occur in very limited amounts in galenas.

The fact that antimony occurred so frequently in local galenas—and then in "chemical amounts"—suggests that the rather doubtful size of $Sb^{+3}$ has been taken at too low a value. This explanation is suggested because of the relative rarity of the antimony-bearing minerals, boulangerite and tetrahedrite, in South African lead deposits (15). Most of the galenas were tested under the ore microscope for homogeneity; tetrahedrite would have revealed itself by its common accessorial elements, such as zinc and arsenic, during the spectrochemical examination. Galenas showing the presence of zinc, of which there were very few, were discarded as the zinc was due to contaminating sphalerite: this also could be deduced from the increase in such elements as cadmium, iron, indium, etc. It is, therefore, concluded that $Sb^{+3}$ can substitute fairly readily for the metal in galena. There is thus a certain uniformity in behavior of the similar elements bismuth and antimony: their analogues of galena are bismuthinite and stibnite, and here the metals are trivalent. It is the trivalent ion that can replace $Pb^{+2}$ because of the size relationship between the ions; the higher charge is also a favorable factor in aiding such replacement.

There is an alternative consideration in explaining the introduction

of cadmium, which may operate with other elements also. One has to consider that there are two known forms of CdS: one is greenockite which has the crystal structure of wurtzite; the other is CdS ($\beta$), which has the same cubic structure as the commonest associate of galena, viz. sphalerite. It is true that its cubic structure differs from the one of galena but the parameters are very close: 5.92 and 5.82. The unit cell in each case contains four formula weights. Miscibility between these compounds is a likely explanation of the presence of cadmium in galena. In contrast, argentite could not conceivably enter such substitution as its cube-edge differs markedly, viz. 4.88. A zonal distribution of silver in some galena specimens has been reported (16). As the role of silver in galenas will be tested by synthesis, the question is not further elaborated here.

The replacement of lead by bismuth in galena has been commonly accepted; it has probably never been so clearly demonstrated as here, in the cube-edge variations that result from this element entering the galena lattice. In Table 1 the cube-edge results show a remarkable uniformity from Nos. 1 to 8: the variations hardly exceed the maximum limits of errors that have been assumed. On the other hand, the only samples that contain a foreign element in appreciable amounts, Nos. 9 and 10, are characterized by a marked and progressive reduction of the unit cell, corresponding to the amount of bismuth found in the samples. Both Wahlstrom (17) and Oftedal (18) have reported the presence of bismuth up to about 2% in galenas and have discussed the effect of this element on octahedral cleavage and parting in such galenas.

The ionic radii involved suggest that a shrinkage could have been predicted by a replacement of $Pb^{+2}$ by $Bi^{+3}$. In the absence of any evidence that galena, like pyrite, may sometimes have a deficiency of sulfur, it must be concluded when weighing the results obtained on galenas from ten different localities, that isomorphic substitution does in fact take place as suggested and that substitution causes the unit cell to become measurably smaller.

The way is now opened to synthesize galenas and substitute bismuth in the lattice in increasing amounts and measure the resultant shrinkage of the cube-edge; such findings may find application in the field investigations of lead silver deposits.

In determining the parameter for galena one could take the average of the values from samples No. 1 to No. 8 and this is 5.9235 kX. In view of the fact that No. 1, *i.e.*, the sample from Joplin, was the purest galena examined here, it is proposed to take its value, as representative of pure natural galena until such time as a purer specimen is measured:

*Galena, Joplin, Mo., at 25° C.*
$a_0 = 5.9240 \pm 0.0004$ kX

Actually this value is the result of a duplicate determination: when doing the first, the temperature was not noted but it can be assumed to lie, with the other determinations, in the range of 22° to 26° C. The first determination gave the result of 5.9239 kX—which, despite a small possible error, demonstrates with what precision results can be duplicated.

It became interesting to compare the proposed value for the cube-edge of galena with that determined by von Zeipel (6), mentioned earlier. At the same time it was desirous to work on a similar specimen to the one examined by him. A number of different specimens of galena from Přibram, Bohemia, were obtained from museum collections and subjected to spectrographic examination for minor elements. They all gave rather similar results and one of these, No. 3, in Table 1, was used for a cube-edge determination. The following results, neglecting errors, show a very satisfactory agreement:

*Galena, Přibram, at 25° C.*

$a_0 = 5.9241$ kX..... von Zeipel, 1936 (6)
$a_0 = 5.9236$ kX..... This work, 1950

These results by two different workers using different methods certainly support the proposed cube-edge value of galena.

The determination with precision of the galena parameter now allows a check of the "*d*-spacings" given in the A.S.T.M. *x*-ray cards; Table 4

TABLE 4

| Calculated, $a_0 = 5.9240$ kX | A.S.T.M. Card II—1452 | A.S.T.M. Card II—3992 |
|---|---|---|
| 3.500 | 3.42 | 3.42 |
| 2.962 | 2.96 | 2.960 |
| 2.095 | 2.08 | 2.093 |
| 1.786 | 1.785 | 1.785 |
| 1.710 | 1.710 | 1.709 |
| 1.481 | 1.480 | 1.480 |
| 1.359 | 1.360 | 1.358 |
| 1.325 | 1.325 | 1.324 |
| 1.2093 | 1.220 | 1.2083 |
| 1.1401 | 1.140 | 1.1392 |
| 1.0472 | 1.049 | 1.0464 |
| 1.0014 | 1.004 | 1.0006 |
| 0.9874 | 0.989 | 0.9866 |
| 0.9367 | 0.938 | 0.9360 |
| 0.9034 | 0.905 | 0.9027 |

shows the fairly good agreement obtained between the calculated and observed spacings recorded on two of the cards.

## Summary

(1) The crystal distortion resulting from the process of grinding galena intended for powder $x$-ray work, can be removed by gentle heating of the ground powder.

(2) The resultant sharply defined pattern with exceptionally high Bragg angles for copper radiation enabled precision cube-edge determinations of galena to be made on samples of various origins and of differing purity.

(3) The purest galena found after spectrochemical analysis gives the following result which is suggested as the best known value for this parameter:

*Galena, Joplin, Mo., at 25° C.*
$a_0 = 5.9240 \pm 0.0004$ kX

(4) Apart from the ubiquitous silver, the common minor constituents of galena, in "chemical amounts" are antimony, bismuth, cadmium and tin. Their substitution for lead is discussed briefly, chiefly from the viewpoint of similar ionic radii.

(5) Only bismuth was found to substitute for lead to any appreciable extent in galena; the effect was to lower the value of the cube-edge so that differences were easily measurable.

(6) Apparently similar specimens of galena show diagnostic differences but these cannot at present be correlated with geological origin; the spectrograph rather than the $x$-ray unit discovers these differences readily.

(7) Among galenas of similar origin the minor element content tends to support the concept of "mineral provinces."

(8) The calculated "$d$-spacings" are compared with the data furnished by the A.S.T.M. $x$-ray cards.

(9) This laboratory approach to geological field problems is considered worthy of the attention of both academic and economic geologists.

## Acknowledgments

The writer was introduced to $x$-ray work while at M.I.T. as guest visitor during the period 1946–1947; certain facilities were provided by the Mineralogical Department at Harvard, also. It is with pleasure that the writer records his indebtedness to the authorities and teachers who so generously provided a foreigner an opportunity to study in the U.S.A.

Several colleagues of the U. S. Geological Survey, Messrs. Christ,

Murata, and Fleischer, sought useful references and read through the writer's manuscript critically—these labors are gratefully acknowledged.

The work was done almost wholly in the laboratories of Mines Department in Pretoria and Johannesburg; here the writer wishes to thank Mr. Hardy for the use of equipment.

## References

1. Wasserstein, B., *Am. Mineral.*, **34,** 731 (1949).
2. Smith, F. G., *Am. Mineral.*, **27,** 1 (1942).
3. Dana's System of Mineralogy, 7th Ed., Vol. **1,** pp. 201, 204 (1944).
4. Struntz, Hugo, Mineralogische Tabellen, 2nd Ed. (**1949**); Akad. Verlag Gesellschaft, Giest u. Portig, p. 79.
5. Handbook of Chemistry and Physics, 30th Ed. (**1947**), p. 2040; Chemical Rubber Publishing Co.
6. von Zeipel, E., *Arkiv. Mat. Astron. Fys.*, **25,** (1936).
7. Buerger, M. J., *Am. Mineral.*, **32,** 296 (1947).
8. Buerger, M. J., *J. Applied Physics*, **16,** 501 (1945).
9. Straumanis, M. E., *J. Applied Physics*, **20,** 726 (1949).
10. Bradley, A. J., and Jay, A. H., *Proc. Phys. Soc.*, **44,** 563 (1932).
11. Lipson, H., and Wilson, A. J. C., *J. Sci. Instruments*, **18,** 146 (1941).
12. Handbook of Physical Constants, *Geological Soc. Am.*; *Special Papers* #**36**
13. Barrett, C. S., Structure of Metals, McGraw-Hill (**1943**).
14. Wasserstein, B., *Proc. Geol. Soc. S. Africa* (**1945**), p. 1, xxxii.
15. Willemse, J., Schwellnus, C. M., Brandt, J. W., Russell, H. D., and van Rooyen, D. P., *Union S. Africa Dept. Mines, Geol. Survey, Memoir* **39** (**1944**).
16. Frondel, C., Newhouse, W. H., and Jarrell, R. F., *Am. Mineral.*, **27,** 726 (1942).
17. Wahlstrom, E. E., *Am. Mineral.*, **22,** 906 (1937).
18. Oftedal, I., *Norsk Geol. Tids.*, **22,** 61–68 (1942).

*Manuscript received*
*April 13, 1950*

# SPHALERITE-DOLOMITE ORIENTATION RELATIONS AT THE RENFREW ZINC PROSPECT, ONTARIO

FORBES ROBERTSON, *Montana School of Mines, Butte, Montana.*

ABSTRACT

The orientation of dolomite and metasomatic sphalerite in slightly foliated, coarsely crystalline dolomite from the Renfrew Zinc Prospect, Ontario, shows the following features: The crystallographic axes $C_v$ of dolomite are normal to the foliation. There is a remarkable development of $(02\bar{2}1)$ twin doublets which, with the crystal axis orientation, fixes the position of the grains. The orientation pattern supports Fairbairn's assumption of a direction-sense of twinning in dolomite which is the reverse of that known for calcite, and also the hypothesis that the chief stress acted approximately normal to the foliation. Measurement of the dodecahedral cleavage planes of scattered sphalerite grains reveals a high degree of orientation of their isometric axes, one being parallel to the *S*-surface, the other two inclined at 45 degrees on either side of the *S*-surface. The sphalerite is, in part, elongated parallel to the foliation as a result of movement along cleavage planes. The marked symmetrical relations between the dolomite and later sphalerite suggests an inherited orientation modified by deformation.

## INTRODUCTION

Dark brown sphalerite grains are disseminated throughout coarsely crystalline dolomite at the Renfrew Zinc Prospect in Ontario. The dolomite shows inconspicuous *S*-surfaces in which the dark sphalerite plays a conspicuous role in emphasizing this megascopic structural feature.

By the use of especially thin rock slices and intense illumination, it was possible to transmit light through the sphalerite grains, and measure the cleavage planes by routine petrofabric methods. The dolomite exhibited twinning, the orientation of which served to fix the position of the dolomite crystals in space.

By correlating the petrofabric data of the sphalerite, which showed a high degree of orientation, with the dolomite, a new field of ore mineral —country rock fabric relations has been initiated (1). This study represents statistical data on these relations, only. That there is a definite mutual orientation relation is established.

## DESCRIPTION OF SPECIMENS

The sphalerite at the Renfrew Zinc Prospect occurs in small, dark brown, sub-metallic, slightly elongated, disseminated grains from 0.5 to 2 mm. in diameter in a massive, coarsely crystalline, slightly foliated dolomite. The dolomite grains range from two to five mm. The hand specimens show a fairly distinct banding due to the concentration of small deformed sphalerite grains in planes which were tentatively desig-

nated $S$-surfaces. Evidence of foliation due to dimensional relations of the dolomite grains themselves is very inconspicuous. What evidence there is, plus the indication that the sphalerite was formed by replacement of the dolomite, suggest that the $S$-surface is actually in the position designated. In some specimens, there was not sufficient evidence to determine the $S$-plane megascopically.

Due to the large size of the dolomite grains, it was not possible to get the orientation relations on as large a number of individual grains as is usually thought necessary. On the other hand, the orientation proved to be so marked that a relatively small number of grains clearly indicate the relations. Determination of the position of low angle cleavage or twin planes is relatively more difficult the flatter the cleavage. Measurements from 90 to 30 degrees are possible, but below that point these are not obtainable on the universal stage. Sections cut at right angles to the $S$-surface were employed in one instance to furnish the desired data on the low angle cleavage planes in sphalerite.

## Petrofabric Analysis

Standard universal stage techniques were employed to measure the crystal axes and deformation twins in the dolomite and the cleavage planes in the sphalerite. These data were plotted on an equal area net using the lower hemisphere projection (2).

The dolomite hand specimen $R$ 13—2 in which the sphalerite orientation appeared most noticeably, was given the greatest amount of attention. Figure 1 represents the orientation of the crystallographic $c$ axes for the grains which have twin doublets. The axes are essentially normal to the foliation. Figure 2 shows the position of the $(02\bar{2}1)$ twin poles for the same dolomite grains. The distribution of the maxima does not fix the position of the dolomite grains in space as well as might have been expected. The theoretical positions which were substantiated by the work of Fairbairn and Hawkes (3) are shown in Fig. 3 at the $T$ positions. These positions were much more nearly reproduced in Fig. 9 which represents an additional diagram of dolomite from the same locality. Figure 4 is constructed from the data in Figs. 1 and 2, and shows the orientation of the assumed glide line for the formation of the dolomite twins. The ideal position of these glide lines is shown in Fig. 3 by the dashed line and the $G$ points. The maxima in Fig. 4 do not correspond too closely to the theoretical positions, but indicate a definite tendency to lie on the small circle indicated. The erratic orientation of the twin poles is probably responsible for the erratic results.

The sphalerite orientation is indicated in Fig. 5, which is a composite diagram derived from two thin sections cut at right angles to each other

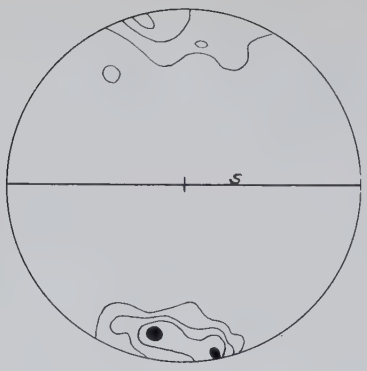


FIG. 1

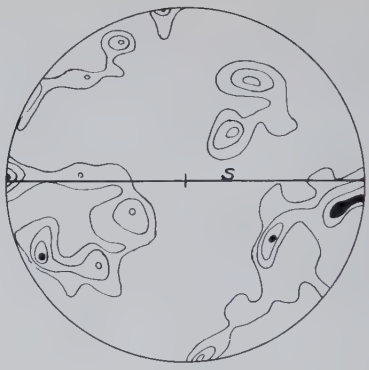


FIG. 2

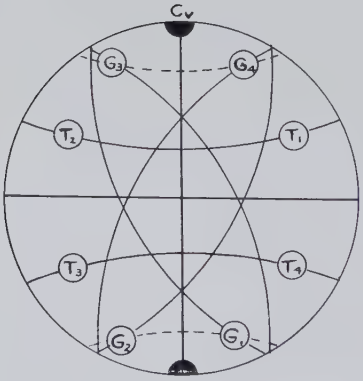


FIG. 3

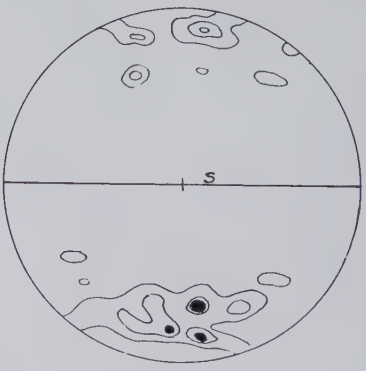


FIG. 4


FIG. 5

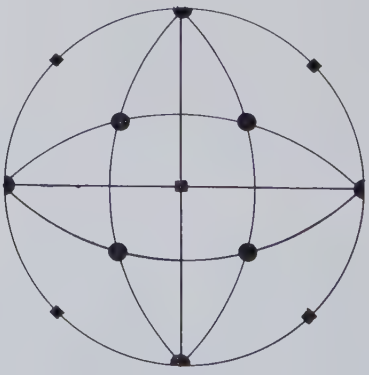

FIG. 6

PLATE I

so that the concentrations in the center of the diagram could be indicated. The orientation of the sphalerite with respect to the rock fabric is indicated in Fig. 6. The squares are the crystallographic axes, whereas the dodecahedral cleavage poles are indicated by circles. The strongest maxima are on the periphery of the diagram and removed from each other by 90 degrees. They show a remarkable degree of orientation, especially when it is considered that there are six possible positions for each grain. The lineation of the sphalerite grains is due to elongation in the *b* direction by fracture along the cleavage planes on the circumference of the diagram. No account was taken of the relative development of a given set of cleavage planes in the individual grains, but it is clear, from a purely statistical analysis, that the maximum deformation took place along these best developed planes.

In specimen *R* 15-4, there were very few sphalerite grains, but the *S*-surface in the dolomite was fairly well indicated. Fig. 7 shows the vertical crystallographic axes of the dolomite grains showing twin doublets. The maxima are slightly inclined to the *S*-surface, presumably more so than could be accounted for in cutting the section. (See also Fig. 10.) Figure 8 shows the position of the poles of the twin planes. These maxima agree rather closely with the *T* positions in Fig. 3. Figure 9 was compiled from Figs. 7 and 8 to show the position of the assumed "glide" line of the dolomite deformation twins. These data correspond rather closely to the *G* positions in Fig. 3.

Specimen *R* 15-5 contained an appreciable amount of sphalerite, but the *S*-surface was not readily distinguishable. The vertical axes are shown in Fig. 10 and the twin plane poles are shown in Fig. 12. Figure 11 shows the orientation of the sphalerite cleavage poles. The cleavage poles of the sphalerite indicate a marked girdle around the periphery of the diagram, the whole tilted with respect to the horizontal plane of the lower hemisphere by about 10 degrees. The relations of the fixed positions of dolomite

---

Fig. 1. Dolomite from Renfrew Zinc Prospect, Ontario. *R* 13—2. 75 crystallographic axes of dolomite having twin doublets. *S*=foliation. 8, 6, 4, 2, 0%.

Fig. 2. The same. 125 Dolomite twin doublet poles. 4, 3, 2, 1, 0%.

Fig. 3. Schematic diagram to illustrate dolomite orientations. $C_v$=vertical crystallographic axis. $T_1$, $T_2$, $T_3$, $T_4$ are the twin pole positions. $G_1$, $G_2$, $G_3$, $G_4$ are the corresponding dolomite "glide" lines of the Figure after Fairbairn and Hawkes Plate I, Fig. 6. (2).

Fig. 4. The same. Dolomite "glide" lines of the doublet twins. Constructed from Fig. 2. 4, 3, 2, 0%.

Fig. 5. The same. 194 sphalerite dodecahedral cleavage poles. Composite diagram from two thin sections cut at right angles to each other.

Fig. 6. Schematic diagram to illustrate sphalerite orientation. Squares=crystallographic axes, circles=dodecahedral cleavage poles.

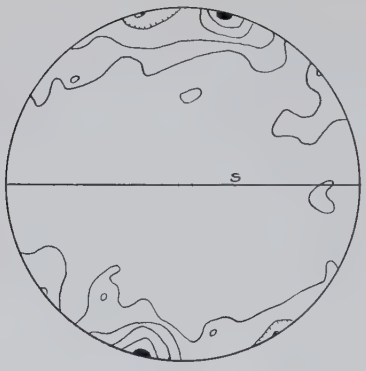


FIG. 7

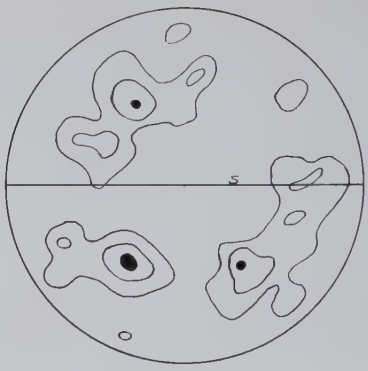


FIG. 8

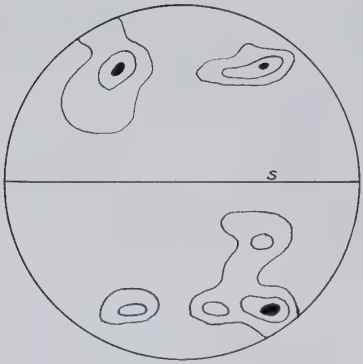


FIG. 9

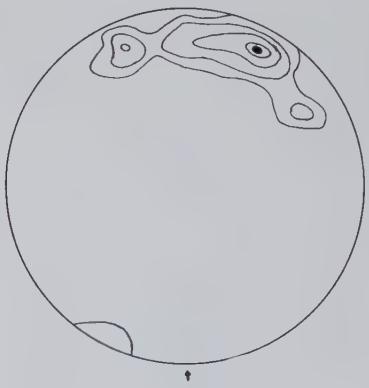

FIG. 10

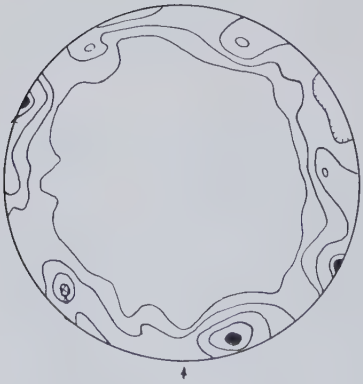

FIG. 11

FIG. 12

PLATE II

and sphalerite are not so clear in these off-centered diagrams (which could not be positively related to an *S*-surface); however, the geometry is very nearly the same. Significantly, the sphalerite is well oriented. The true *S*-surface is not delimited by the planar arrangement of sphalerite grains, but at about 45 degrees from the horizon of the diagram.

## Discussion

These data indicate distinct preferred arrangement in space for the dolomite and the sphalerite grains. The hand specimens were not oriented in the field so that no correlation with field relations can be attempted. The emphasis is placed on the fact that mutual orientation relations exist, a conclusion heretofore not demonstrated for these two minerals. It appears clear that the sphalerite was introduced into the dolomite as a hypogene mineral by metasomatic replacement of the dolomite. The replacement was controlled, to a large degree, by the pre-existing fabric of the dolomite country rock. The "ore" has been subsequently deformed to a slight extent. In the deformation, the dolomite twins and the elongation of the sphalerite grains occurred, both phenomena serving to fix the spacial relations of the two minerals.

These data on dolomite deformation, and the assumed "glide" lines, serve to further substantiate the work of Fairbairn and Hawkes (2) in establishing that the direction-sense of the "glide" lines, which produce the dolomite twin, is fundamentally different from the direction-sense for the formation of similar twins in calcite.

## Conclusions

1. The orientation pattern of the deformation twin doublets of dolomite adds further evidence in support of Fairbairn and Hawkes' assumption that the direction-sense for producing the twins is the reverse of the direction-sense for calcite. In other words, the chief stress acted approximately normal to the foliation.

2. The sphalerite grains in the dolomite are well oriented, based on the measurement of the dodecahedral cleavage planes. The axes are thought to be oriented; one parallel to the *S*-surface and the other two inclined at 45 degrees on either side of the *S*-surface.

---

Fig. 7. Dolomite, Renfrew Zinc Prospect, Ontario. *R* 15-4. 75 crystallographic axes having twin doublets. *S*=foliation. 10, 8, 6, 4, 2, 0%.

Fig. 8. The same. 72 dolomite twin doublet poles. 4.5, 3, 1.5, 0%.

Fig. 9. The same. Dolomite "glide" lines constructed from Fig. 8.

Fig. 10. The same. *R* 15-5. 85 crystallographic axes having twin doublets. 7, 5, 3, 1, 0%.

Fig. 11. The same. 67 sphalerite dodecahedral cleavage poles. 13, 10, 7, 4, 0%.

Fig. 12. The same. 100 dolomite twin doublet poles. 5, 3, 1, 0%.

3. The sphalerite is, in part, elongated parallel to the foliation as a result of movement along cleavage planes.

4. The marked symmetrical relations between the dolomite and sphalerite suggest that the sphalerite was introduced after the dolomite had formed (probably by metasomatic replacement of the dolomite) and inherited its orientation from the dolomite country rock. The rock was subsequently subjected to minor deformations at which time the dolomite twins were formed and the elongation of the sphalerite grains took place.

## Acknowledgments

The author acknowledges the interest of Dr. W. H. Newhouse in whose laboratory the ideas for this paper evolved, and to Dr. H. W. Fairbairn in whose laboratory the work was done, and who critically reviewed the data for this paper.

## References

1. Korn, Doris, Zur Lagebestimmung opaker Erze, etc.: *Neues Jahrb., B.B.* **67 A,** 428 (1933).
2. Knopf, E. B., and Ingerson, Earl, Structural Petrology: *G.S.A. Memoir* **6** (1938).
3. Fairbairn, H. W., and Hawkes, H. E., Jr., Dolomite orientation in deformed rocks: *Am. Jour. Sci.*, **239,** 617–623 (1941).

*Manuscript received*
*Jan. 14, 1950*

# SETTING A GIVEN DIRECTION PARALLEL TO THE AXIS OF A GONIOMETER HEAD

D. Jerome Fisher, *University of Chicago, Chicago, Illinois.*

Abstract

Certain problems require that an unusual crystal direction rather than an ordinary crystal axis be made parallel the axis of the goniometer head. This is the case when a triclinic crystal is worked out by the precession method; it is also not uncommon in crystal structure or disorder studies. The stereographic technique here described permits easy visualization of the situation in any individual case, whether working with a euhedron and the optical goniometer or an anhedron and purely *x*-ray techniques. The method makes an unusual application of the stereogram since the principle employed involves the use of small circles not parallel to the equator of the stereonet.

The introduction includes a description of the goniometer head, together with brief remarks on crystal mounting and handling on the optical goniometer. The next section outlines the method of preparing a stereogram showing the necessary minimum data to obtain the new arc readings when the desired crystal direction is parallel the axis of the goniometer head. This is followed by a section explaining the theory of the method. Brief general remarks conclude the paper.

## Introduction

A goniometer head is a gadget which supports a crystal in suitable orientation on some axis of an optical or *x*-ray goniometer. For ordinary work it is desirable that this instrument (Fig. 1) includes two sledges and two arcs. The arcs permit circular movements in the planes determined by the axis of the head (shown by a line terminated by an arrow at each end near the top of the figure) and the direction of motion of each of the sledges. The arcs have a common center; the radius of the small arc $S$ of the instrument shown is about 23 mm.; that of the large arc $L$ is about 35 mm. The sledges ($Sl_L$ parallel the large arc and $Sl_S$ parallel the small arc) allow movements in two mutually-perpendicular directions, both normal to the axis of the head.

The crystal may be mounted on the head as follows. A small cork with a hole bored in it is used to support a brass rod about one cm. long in vertical position; this rod is of a size to fit a hole in the flat end of the $S$ arc. A short glass capillary tube is fastened in parallel position to the upper end of the brass rod by means of a thermoplastic cement (such as Cementyte *C*), or by a mixture of about 50-50 beeswax and rosin, or even by Apiezon sealing compound or a gob of plasticine. Now put a blob of Apiezon N grease or Duco cement on the end of the glass capillary and place one end of the crystal in this. The crystal may be picked up with a match stick which has a pointed tip of plasticine stuck on one end of it. Working under the binocular the crystal may be lined

up so that the desired zone is approximately parallel the glass capillary. When the cement has set, it may be advisable to add a bit more of it at the glass-crystal contact to make a firm union. The cork may now be inserted in a glass vial to protect the crystal while setting continues for a few hours.

Using pointed pliers to hold the brass rod, the crystal may be transferred to the goniometer head and adjusted in azimuth under the binocu-

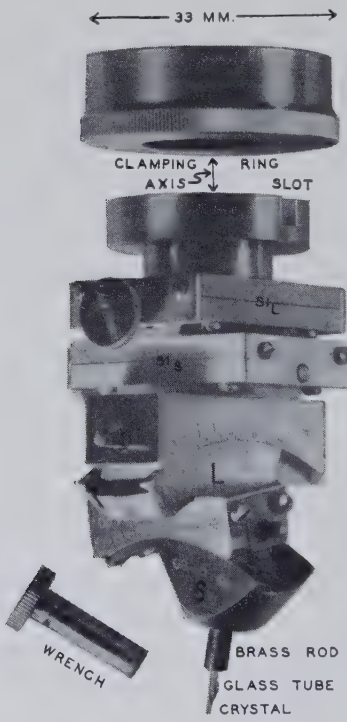


FIG. 1. The goniometer head, with crystal attached. The clamping ring normally covers the slot in the ring-base. $L$ = large arc, $S$ = small arc, $Sl$ = sledges (parallel $L$ or $S$ respectively).

lar so that the desired directions are parallel the sledges. The set-screw clamping the brass rod in the end of the goniometer head is then tightened when the part of the crystal through which the $x$-ray beam should go is at the center of the arcs; this is 12 mm. beyond the flat end of the small arc for the instrument shown in Fig. 1.

The head is now fastened to the optical goniometer where its orientation is fixed by the slot in the ring-base which engages with a pin on the

goniometer axis. The slot is shown in Fig. 1, although it normally would be hidden by the clamping ring had this not been detached from the ring-base when the photograph was taken. The crystal is now adjusted on the optical goniometer so the desired direction, generally the [$c$]-axis, is parallel the goniometer axis (axis of the $V$-circle of the Goldschmidt two-circle instrument). The technique required to accomplish this is in the text-books. When oriented, the $S$ and $L$ readings are noted. These are recorded as right ($r$) or left ($l$) as seen when looking from the crystal towards the goniometer head. This position is adopted because it is the normal one used in viewing a crystal and its gnomonogram or stereogram, assuming the (+) end of the axis (which is set parallel to the axis of the goniometer head) is the one extending out from the head; the one pointing towards the observer in this case. Thus the readings for the head shown in figure 1 are $L = 10°00'\ l$ and $S = 20°00'\ r$; it is unfortunate that the numbers engraved on the arcs are upside down from this point of view. The goniometric readings for the various faces on the crystal may now be obtained and from these a gnomonogram may be prepared and the face-poles indexed, at least in preliminary fashion. Of course on this the $\phi = 0°$ azimuth (generally the direction of [$b^*$]) may be shown; also the positions of the $L$ and $S$ arcs, and which side of each is the engraved one.

## Tilting the Arcs to a New Position

This problem is most easily grasped from the working of an actual example. Suppose that it is desired that a random direction $R$ be made parallel the axis of the goniometer head. $R$ may represent [$c^*$] of a triclinic case in a typical precession camera problem, or it may represent some zone [$u\ v\ w$] in a rotation-oscillation problem. In any case the position angles for $R$ may be obtained from the gnomonogram just prepared.

Figure 2 is a stereogram to fit a case in which the [$c$] -axis of a crystal is parallel the axis of the goniometer head when the arc readings are $S = 26°.5\ r$ and $L = 16°.0\ r$. Also from the gnomonogram mentioned it may be ascertained that $\phi_S = 25°$ and $\phi_L = 115°$ with the engraved side of $S$ towards $\phi = 115°$ and that of $L$ away from $\phi = 25°$. It will be noted that normally these $\phi$ readings would be close to 0° and 90°, but a completely general case is here assumed. The problem is to make $R$ parallel the axis of the goniometer head where $\phi_R = 65°$ and $\rho_R = 60°$.

The stereogram shows the cyclographic projection of $R$, as well as $L^c$ (the cyclographic projection of the large arc) and $S^c$. Note that $L^c$ is fixed, but that $S^c$ is represented by a series of great circles having a common diameter while the $S$ arc is being tilted by movement of the $L$ arc. In short any movement of $L$ also moves the whole $S$ arc (see Fig. 1)

but the reverse is not true. When $L = 16°.0$ *r*, then in Fig. 2 the cyclographic projection of the $S$ arc is at $S_1^c$, the first or starting position of $S^c$. This is 16° off $S_0^c$, the position of $S^c$ when the reading on the $L$ arc is 0°; i.e., in the stereogram $c\,e = 16°.0$. Note that *r* or *l* is plotted while facing towards the engraved side of the arc concerned.

Let $P_1$ be the pole of $S_1^c$. Pass a great circle through $P_1$ and $R$ locating $d$ on $S_1^c$; this great circle (like all those through $P_1$) is normal to $S_1^c$. Measure $d\,R (= 23°.5)$ and $d\,e (= 46°.3)$. Then the required tilts on the

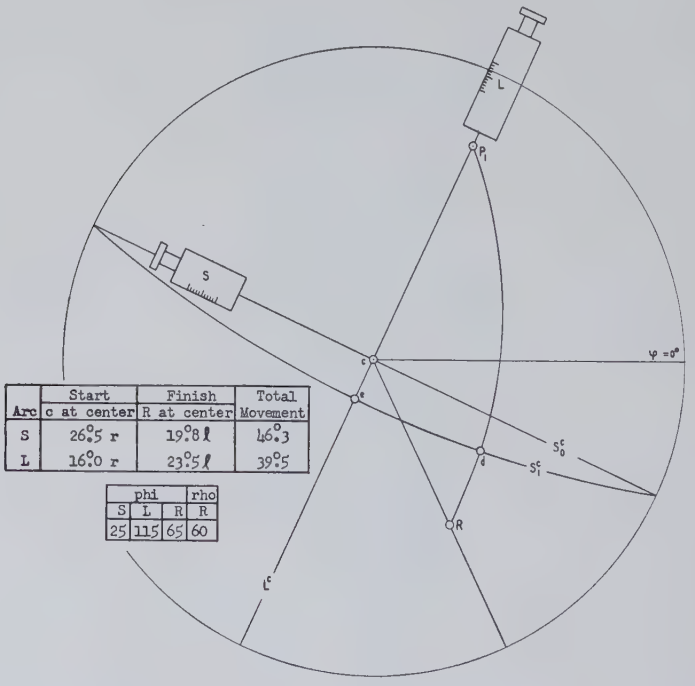


| Arc | Start c at center | Finish R at center | Total Movement |
|---|---|---|---|
| S | 26°.5 r | 19°.8 l | 46°.3 |
| L | 16°.0 r | 23°.5 l | 39°.5 |

| phi | | rho | |
|---|---|---|---|
| S | L | R | R |
| 25 | 115 | 65 | 60 |

FIG. 2. Stereogram to explain motion of $R$ (a random direction) to $c$ in terms of arcs $L^c$ and $S_1^c$, the cyclographic projections of $L$ and $S$ (the latter in its first position). $P_1$ is the pole of $S_1^c$.

two arcs to place $R$ at the center of the stereogram (so that it is parallel to the axis of the goniometer head) are 46°.3 on the $S$ arc and 39°.5 (16°.0 + 23°.5) on the $L$ arc. This leads to final arc readings of $S = 19°.8$ *l* and $L = 23°.5$ *l*. Using a meridian stereonet with a radius of 20 cms. (the writer has one of these mounted on a sheet of bakelite) this problem may be solved quickly to the nearest 0°.1 or 0°.2. Of course in actual practice the great circle $P_1R$ is not drawn; in fact only a small part of $S_1^c$ need be traced, and along this a tick locates *d*.

## Explanation of the Method

If $B$ is located on $S_1{}^e$ so that $e\,B = 26°.5$ (the first reading on the $S$ arc) as is shown on the stereogram of Fig. 3, it represents the cyclographic projection of the brass rod; i.e., it is a normal to the flat end of the $S$ arc in its first position. As $S$ is moved 46°.3 from 26°.5 $r$ to 19°.8 $l$, $B$ moves to $B_1$; as $L$ is moved 39°.5 from 16°.0 $r$ to 23°.5 $l$, $B_1$ follows a small circle normal to $S_1{}^e$ and so goes to $B_2$. Or if $L$ is moved before $S$, $B$ goes to $B_3$, then to $B_2$. $B_3\,B_2$ defines $S_2{}^e$, the second or final position of $S^e$, where $ch = 23°.5$.

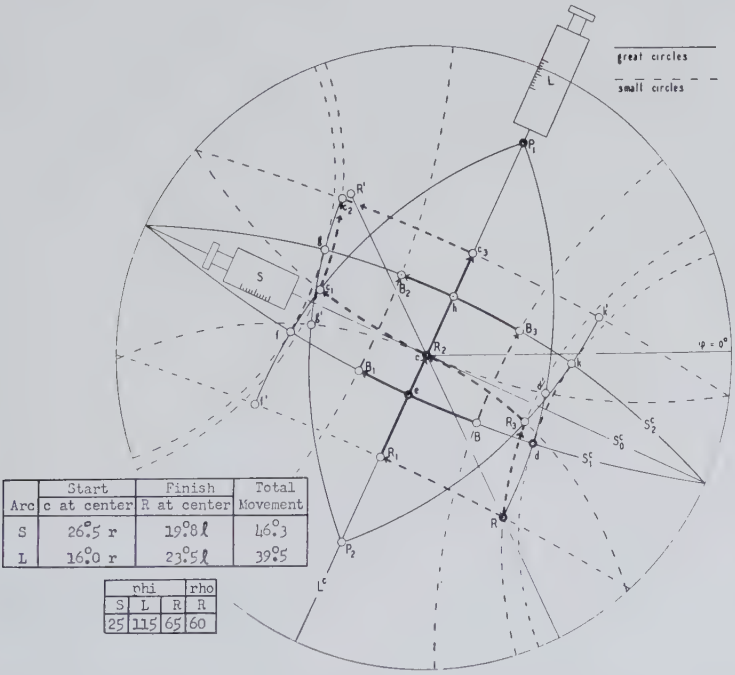


| Arc | Start c at center | Finish R at center | Total Movement |
|---|---|---|---|
| S | 26°.5 r | 19°.8 l | 46°.3 |
| L | 16°.0 r | 23°.5 l | 39°.5 |

| phi | | rho | |
|---|---|---|---|
| S | L | R | R |
| 25 | 115 | 65 | 60 |

Fig. 3. Stereogram as in Fig. 2 showing in addition the small circles along which $R$, $B$ (the brass rod; see Fig. 1), and $c$ travel while tilting the two arcs. $S_2{}^e$ is the second position of the small arc; its pole is $P_2$.

If one now mentally passes a great circle through $B$ and $R$, and thinks of $R$ as being tied by a rigid pin $B\,R$ to $B$, then as $B$ moves to $B_1$, $B\,R$ becomes $B_1\,R_1$; likewise it becomes $B_3\,R_3$, and from either $B_1$ or $B_3$ becomes $B_2\,R_2$. However this is more simply carried out in terms of a rigid pin $d\,R$ which is normal to $S_1{}^e$, and which goes to $e\,R_1$ or $k\,R_3$ and thence to $h\,R_2$. Similarly a pin like $e\,c$ goes to $f\,c_1$ or $h\,c_3$ and thence to $g\,c_2$; this is simpler than to imagine a pin $B\,c$ going to $B_1\,c_1$ or $B_3\,c_3$ and thence to $B_2\,c_2$.

The details of construction are as follows: $d$, $k$, $f$, and $g$ lie along small circles 46°.3 from but parallel to $L^c$; $d$ and $f$ lie along $S_1{}^c$ while $k$ and $g$ are on $S_2{}^c$. $R$, $R_1$, and $f'$ lie along great circles through $P_1$ and $d$, $e$, and $f$, respectively, at 23°.5 from the latter; they establish a small circle $R\ R_1\ f'$ parallel to but 23°.5 from $S_1{}^c$; this is the 82° small circle of the stereonet, counting down from its poles. Of course to draw this circle the center of the tracing paper can no longer coincide with the center of the stereonet. Similarly $d'$, $c$, and $c_1$ are on great circles through $P_1$ and $d$, $e$, and $f$, respectively, at 16°.0 from the latter; they fix the 61° small circle parallel to and 16°.0 from $S_1{}^c$. Likewise $R_3$, $R_2$, and $g'$ are on great circles through $P_2$ (the pole of $S_2{}^c$) and $k$, $h$, and $g$, respectively; they define small circle $R_3\ R_2\ g'$ parallel to and 23°.5 from $S_2{}^c$; this is the 49° small circle. Also $k'$, $c_3$, and $c_2$ are on great circles through $P_2$ and $k$, $h$, and $g$, respectively; they determine the 83° small circle parallel to and 16°.0 from $S_2{}^c$. The four small circles here described which are parallel to $S^c$ in either its first or second position, represent the paths of $R$ or $c$ as tilt occurs on $S$.

The point $R'$ lies on diameter $c\ R$; moreover, $R$ and $R'$ are equidistant from $c$. It will be noted that while tilting along the two arcs causes $R$ to move to $R_2$, it results in $c$ going to $c_2$ and not to $R'$.

## General Remarks

This stereographic technique, besides permitting a ready solution with satisfactory accuracy of what at times may be an obstinate little problem, has the added advantage of such graphical methods that it permits easy visualization of the set-up. Thus from quick inspection of a hastily-drawn small stereogram ($r = 5$ cms.), one can decide whether it is possible to orient a given direction of a crystal without first remounting it. While the arcs of the head shown in Fig. 1 are graduated to only 20° each way, by making use of the vernier graduations it is possible to tilt up to 31° each way, though with reduced accuracy of reading. If the crystal must be remounted, one gets a good picture of how this should be done.

Of course it is not necessary to have a euhedron or subhedron to make use of the method described. One may orient and prepare an indexed gnomonogram (similar to the first level of the reciprocal lattice to a suitable scale) by purely $x$-ray techniques, rather than by the use of the optical goniometer as here outlined in the Introduction. Thus from an $x$-ray picture of any orientation in which two or three directions can be recognized, one may use the method to compute the new arc settings for any desired orientation.

*Manuscript received*
*July 30, 1950*

# THORITE FROM CALIFORNIA, A NEW OCCURRENCE AND VARIETY

D. R. George*

Abstract

The occurrence of green thorite is not recorded in the literature nor has thorite from California been previously described. The mineral is widely distributed in the major gold placers of California and is probably derived from the weathering of Jurassic granites. Physical and optical properties and a chemical analysis are presented.

## Introduction

Thorite ($ThO_2 \cdot SiO_2$) has been described from several localities in the United States, notably from Henderson Co., N. C. (auerlite) (1), Llano Co., Texas (mackintoshite and thorogummite) (2), and from Blueberry Mountain, near Boston, Massachusetts (organite) (3). In addition it has been reported from the Lake Champlain district of New York (4) and from the old Trotter Mine at Franklin Furnace, New Jersey (5). The purpose of this paper is to describe and record a variety of green thorite which is widely distributed in California. As far as is known, the existence of green thorite has not been previously recorded nor has thorite from California been described.

## Occurrence

Thorite occurs in California as a very minor constituent in the gold placers of the central part of the state, but particularly along the Feather, Yuba, American, Mokelumne, Tuolumne and Merced Rivers which lie between Oroville in Biggs Co. on the north and Snelling in Merced Co. on the south, a distance of approximately two hundred miles.

The writer's field work and sample collecting have been confined to this area, but samples of black sand concentrates from other placer gold mining operations ranging from the Scott River near Callahan in Siskiyou Co. to Atolia in San Bernardino Co. have been examined, and in all cases thorite is present. In addition thorite occurs along the beaches near Monterey, and after very severe storms it is reported† that a thin layer of the mineral is sometimes found concentrated on the surface of the beach just above the water line.

## Source

In all of the placers in which thorite has been found, the watersheds of the streams contain exposures of granitic rock which is identified by

* Division of Industrial Cooperation, Massachusetts Institute of Technology.

† Personal communication from R. D. Nininger.

the California Geological Survey as Jurassic. This is the only formation which is common to all of the watersheds, and based upon a limited amount of field work, there appears to be a general correlation between the area of Jurassic granite exposed and the concentration of thorite in the placers. Thus even though there is no direct evidence that thorite is present in the Jurassic granite, it is strongly inferred that this formation is the source of the thorite. The age of the mineral as calculated from the approximate formula,

$$\text{Age} = \frac{\text{Pb}}{\text{U} + 0.36\text{th}} \times 7600 \times 10^6 \text{ years}$$

is only twenty-one million years, and it is assumed that the comparatively young calculated age is the result of the removal of lead by leaching.

## Associated Minerals

The principal minerals in the heavy mineral (black sand) concentrates from all of the areas from which samples have been examined to date include magnetite and ilmenite, which generally account for over 90 per cent, the balance, besides thorite, consisting chiefly of garnet, chromite, hematite, ferromagnesian minerals, zircon, rutile, monazite, and pyrite. Locally, as for example in the Inyo and Atolia districts, scheelite is present in small amounts, and one sample from the Scott River district contained cinnabar and a mineral tentatively identified as thorianite.

## Description of Thorite

The thorite occurs mostly as small rounded grains and broken fragments although partially rounded, but clearly recognizable tetragonal crystals of both long and short prismatic habit are not uncommon. The grains vary in size from less than 0.1 mm. to about 0.6 mm. and are typically translucent and light to dark bluish-green. A small proportion are in whole or part yellow-green, greenish-yellow, greenish-orange, and reddish-orange (orangite), and it is believed that the yellow and orange colors are the result of hydration and oxidation. The specific gravity of the mixed grains is 6.36.

In transmitted light, grains having a thickness of 0.03 to 0.07 mm. vary in color from nearly colorless to pale yellow, pale green, and various shades of greenish-yellow and orange yellow. The typically bluish-green grains are isotropic (metamict) whereas the altered yellow and orange grains are in part isotropic and in part anisotropic with a finely fibrous internal structure. The indices of refraction are extremely variable even within the same grain. Measurements made in white light with a recently calibrated set of high-index liquids showed that most of the grains had indices of refraction ranging from 1.82 to 1.86, but a few of

the yellow and orange grains had indices of refraction as low as 1.76 to 1.79, whereas some of the darker green grains were as high as 1.87. The maximum birefringence is 0.005 to 0.015.

## Chemical Composition

A small amount of a nearly pure thorite was separated from a black sand concentrate obtained from the LaGrange Gold Dredging Company which operates on the Tuolumne River near LaGrange, California. The thorite was separated from the bulk of the associated minerals with a hand magnet and Frantz isodynamic separator. The resulting product consisted almost wholly of thorite, zircon and rutile, all of which are essentially nonmagnetic or diamagnetic. This concentrate was then further separated by placing it in a beaker containing hot, concentrated Clerici solution and allowing the solution to cool and solidify. As a result the zircon and rutile which have a specific gravity of approximately five or less floated to the top as the density of the liquid gradually increased. The thorite remained at the bottom. The thorite was finally recovered by breaking the beaker and shaving off the bottom of the solidified mass. This final thorite concentrate contained a very small amount of zircon and rutile and was cleaned to final purity by hand picking.

A chemical analysis of the clean thorite concentrate was made by the National Bureau of Standards, the results of which are shown in Column 1 of the following tabulation. Column 2 shows the analysis given in Column 1 after recalculating the $U_3O_8$ to $UO_2$ and the $Fe_2O_3$ to FeO. A recalculation of the analysis shown in Column 2 to 100 per cent is given in Column 3.

| | 1 | 2 | 3 |
|---|---|---|---|
| CaO | nil | — | — |
| MgO | 0.01 | 0.01 | 0.01 |
| PbO | 0.09 | 0.09 | 0.10 |
| FeO | — | 0.57 | 0.59 |
| $Fe_2O_3$ | 0.63 | — | — |
| $Al_2O_3$ | 1.25 | 1.25 | 1.29 |
| $ZrO_2$ | 0.07 | 0.07 | 0.07 |
| $TiO_2$ | 0.10 | 0.10 | 0.10 |
| $ThO_2$ | 69.36 | 69.36 | 71.61 |
| $UO_2$ | — | 8.10 | 8.36 |
| $U_3O_8$ | 8.43 | — | — |
| Rare Earths | 0.52 | 0.52 | 0.54 |
| $SiO_2$ | 15.96 | 15.96 | 16.47 |
| $H_2O$ | 0.82 | 0.82 | 0.86 |
| Total | 97.24 | 96.85 | 100.00 |
| Sp. G. | 6.36 (20°/45° C.) | | |

The summation of the analysis in Column 1 is low. A spectrographic analysis failed to disclose the presence of elements other than those shown in the chemical analysis in more than trace amounts, and based upon analyses of other samples of thorite as recorded in the literature, it seems probable that the silica determination is low. The state of oxidation of the uranium and iron was not determined, but in view of the predominantly green color of the thorite, it is believed that these elements are chiefly present in their lower valence form. Hence the mineral is *uranoan* thorite. The high specific gravity is probably attributable to the absence of appreciable water of hydration.

## Acknowledgments

The writer wishes to express his appreciation to Dr. C. J. Rodden and his group at the National Bureau of Standards for making the analysis. Thanks are also due to Mr. F. A. Gonyer of Harvard University for assistance in making the heavy liquid separation.

## References

1. Dana, J. D., and E. S., The System of Mineralogy, John Wiley and Sons, Inc., New York, N. Y., 6th Ed., pp. 488–489 (**1914**).
2. *Idem.*, p. 893.
3. Richmond, W. E. Paragenesis of the minerals from Blueberry Mt., Woburn, Mass.: *Am. Mineral.*, **22,** 293–294 (1937).
4. Dana, *op. cit.*, p. 488.
5. Palache, Charles, The Minerals of Franklin and Sterling Hill, New Jersey: *U.S.G.S. Prof. Paper,* **180,** 96, (1935).

*Manuscript received*
*March 25, 1950*

# THE ROLE OF YTTRIUM AND OTHER MINOR ELEMENTS IN THE GARNET GROUP[1]

HOWARD W. JAFFE[2]

ABSTRACT

Several minor and trace elements, notably yttrium, scandium and zinc, are very common in garnets. The frequent occurrence of several of these in particular varieties of garnet suggests isomorphism. Yttrium, heretofore considered to be a rare constituent of garnets, is very prevalent in spessartites. It has been found to occur in concentrations of greater than 2 per cent $Y_2O_3$ in a few manganese-rich garnets. The frequent association of yttrium and manganese in spessartites suggests that ions of $Y^{+3}$ with an ionic radius of 1.06 Å have replaced ions of $Mn^{+2}$ having an ionic radius of 0.91 Å, the radii being those of Goldschmidt. The substitution scheme is $Y^{+3}Al^{+3}$ for $Mn^{+2}Si^{+4}$. Scandium is most abundant in pyropes, and $Sc^{+3}$ with an ionic radius of 0.83 Å may substitute for ions of divalent Mg (0.78 Å) or possibly for divalent Fe (0.83 Å) if enough almandite is present. Zinc is a common trace element in manganese, iron and magnesium-rich garnets and ions of divalent Zn (0.83 Å) may proxy for those of divalent iron. Other trace constituents detected in garnets include, Ga, Ti, Cr, Na, Li, Dy, Gd, Ho, Yb, Er, La, Ce, Nd, Pr, Sr, F, V, B, Be, Ge, Sn, Pb, Cu and Nb. Their hypothetical isomorphous relations to the major constituents are discussed. Included in the data are 7 new quantitative yttria determinations, visual spectroscopic analyses of more than 70 garnets, and spectrographic analyses of 2 yttria precipitates obtained from spessartites.

## INTRODUCTION

The garnets form a well-defined group of minerals with respect to their essential chemistry, physical constants and geological environment. Ford (1915), Stockwell (1927), Winchell (1933), Menzer (1928), Fleischer (1937) and Levin (1949) have discussed the relationships between the chemical composition and the physical constants within the group. Heritsch (1926) and Wright (1938) have emphasized the unique association of the different garnets with particular geological environments. However, relatively little information has been published on the minor and trace element chemistry of the garnets. The present investigation was undertaken to determine (*a*) the prevalence of yttrium and other minor and trace elements in garnets; (*b*) the hypothetical isomorphous relationships, if any; and (*c*) the consequent relationships to the rock types in which they occur. The accessory constituents detected in garnets, during the present investigation, include: Y, Sc, Zn, Ga, Ti, Na, Li, Cr, Dy, Gd, Ho, Er, Yb, La, Ce, Nd, Pr, Sr, V, B, Ge, Be, Sn, Pb, Cu, F and Nb. Yttrium, heretofore considered to be a rare or uncommon

[1] Not subject to copyright.

[2] Petrographer, Metallurgical Division, College Park Branch, Bureau of Mines, College Park, Maryland.

TABLE 1. VISUAL SPECTROSCOPIC ANALYSES OF GARNETS

Determinations by H. W. Jaffe

*Key*

Major constituents.....M.....More than 5 per cent
Minor constituents.....m.....0.5 to 5 per cent
Trace constituents.....t.....Less than 0.5 per cent
—.....Absent

GROUP I—MANGANESE-RICH GARNETS

| Sample | Ca | Mg | Fe | Mn | Al | Si | Zn | Cr | Ti | Y | Sc | Li | Na | Sr | V | F | Ga | Nb |
|---|---|---|---|---|---|---|---|---|---|---|---|---|---|---|---|---|---|---|
| 1. | t | m | M | M | M | M | t | — | t | t | — | — | t | — | — | — | t | — |
| 2. | m | M | M | M | M | M | t | — | t | t | t | — | t | — | — | — | t | — |
| 3. | t | t | M | M | M | M | t | — | t | m | t | t | — | — | t | t | t | — |
| 4. | t | t | M | M | M | M | t | — | t | t | t | t | — | — | — | t | t | — |
| 5.* | m | t | m | M | M | M | t | — | t | t | — | t | t | — | — | t | t | — |
| 6. | m | m | M | M | M | M | t | — | t | m | t | — | t | — | — | — | t | — |
| 7. | m | m | M | M | M | M | t | — | t | t | — | — | t | — | — | — | t | — |
| 8. | m | t | M | M | M | M | t | t | t | t | t | t | t | — | — | — | t | — |
| 9. | t | m | M | M | M | M | t | — | t | t | — | t | t | — | — | — | t | — |
| 10. | t | m | M | M | M | M | t | — | t | t | — | — | — | — | — | — | t | — |
| 11. | t | M | M | M | M | M | t | — | t | t | t | — | t | — | — | — | t | — |
| 12. | m | t | M | M | M | M | t | — | t | m | t | t | t | — | — | — | t | — |
| 13. | t | m | M | M | M | M | t | — | t | m | t | — | — | — | — | — | t | — |
| 14. | m | t | M | M | M | M | t | — | t | m | t | t | t | — | — | — | t | — |
| 15. | m | t | M | M | M | M | t | — | t | — | — | — | t | — | — | — | t | — |
| 16. | t | m | M | M | M | M | t | — | t | t | — | t | t | — | — | — | t | — |
| 17. | t | m | M | M | M | M | t | — | t | t | t | t | t | — | — | — | t | — |
| 18. | t | t | M | M | M | M | t | — | t | t | t | t | t | — | — | — | t | — |
| 19. | t | m | M | M | M | M | t | — | t | t | — | — | t | — | — | — | t | — |
| 20. | m | m | M | M | M | M | t | — | t | t | — | — | t | — | — | — | t | — |
| 21. | m | t | M | M | M | M | t | — | t | t | t | — | t | — | — | — | t | — |
| 22. | t | m | M | M | M | M | t | — | t | t | t | — | t | — | — | — | t | — |
| 23. | m | m | M | M | M | M | t | — | t | t | — | t | t | — | — | — | t | — |
| 24. | t | M | M | M | M | M | t | — | t | t | — | t | t | — | — | — | t | — |
| 25. | m | m | M | M | M | M | t | — | t | t | t | t | t | — | — | — | t | — |
| 26. | t | t | M | M | M | M | t | — | t | t | — | t | t | — | — | t | t | — |
| 27. | m | m | M | M | M | M | t | — | t | t | — | — | — | — | — | — | t | — |
| 28. | m | m | M | M | M | M | t | — | t | t | — | — | t | — | — | — | t | — |
| 29. | m | m | M | M | M | M | t | — | t | t | t | t | t | — | — | — | t | — |
| 30. | m | m | M | M | M | M | t | t | m | t | t | t | t | — | — | — | t | — |
| 31. | m | m | M | M | M | M | t | — | t | t | — | — | t | — | — | — | t | — |
| 32. | m | m | M | M | M | M | t | — | t | t | t | — | t | — | — | — | t | — |
| 33. | m | m | M | M | M | M | t | t | t | t | — | — | t | — | — | t | t | — |
| 34. | m | m | M | M | M | M | t | — | t | t | t | t | t | — | — | t | t | — |
| 35. | m | m | M | M | M | M | t | — | t | t | t | t | t | — | — | — | t | — |
| 36. | t | t | M | M | M | M | t | — | t | t | — | t | — | — | — | — | t | — |
| 37. | t | m | M | M | M | M | t | — | t | t | t | t | t | — | — | t | t | — |
| 38. | m | m | M | M | M | M | t | — | t | t | — | t | — | — | — | — | t | — |
| 39. | m | m | M | M | M | M | t | — | t | t | — | t | — | — | — | — | t | —† |
| 40. | t | m | M | M | M | M | t | — | — | m | t | — | — | — | — | — | t | — |

Note: 2 garnets from pegmatite, Pala, Calif., also contained spectrographic traces of Ge, Sn, B and Zn, G. Steiger, U. S. Geol. Survey files.

| Sample | Ca | Mg | Fe | Mn | Al | Si | Zn | Cr | Ti | Y | Sc | Li | Na | Sr | V | F | Ga | Nb |
|---|---|---|---|---|---|---|---|---|---|---|---|---|---|---|---|---|---|---|
| | | | | | | | | GROUP II—MAGNESIUM-RICH GARNETS | | | | | | | | | | |
| 41. | m | M | M | m | M | M | t | — | t | t | t | — | t | — | — | — | — | — |
| 42. | m | M | M | m | M | M | t | — | t | t | t | — | — | — | — | — | t | — |
| 43. | m | M | M | m | M | M | t | — | t | t | t | — | t | — | t | — | — | — |
| 44. | m | M | M | m | M | M | t | — | t | — | — | — | t | — | t | — | — | — |
| 45. | m | M | M | m | M | M | t | — | t | — | t | — | t | — | — | — | — | — |
| 46. | m | M | M | m | M | M | t | t | t | t | t | — | t | — | — | — | — | — |
| 47. | m | M | M | m | M | M | t | — | t | t | t | — | — | — | — | — | t | — |
| 48. | m | M | M | t | M | M | t | — | t | — | t | t | t | — | — | — | — | — |
| 49. | m | M | M | t | M | M | t | — | t | — | t | — | t | — | — | — | — | — |
| 50. | M | M | M | m | M | M | t | — | t | t | t | t | t | — | — | — | t | — |
| 51. | m | m | M | m | M | M | t | — | t | t | — | — | — | — | — | — | — | — |
| 52. | m | m | M | m | M | M | — | t | t | — | — | — | t | — | — | — | t | — |
| 53. | M | M | M | m | M | M | — | t | t | — | t | — | — | — | — | — | t | — |
| 54. | M | M | M | m | M | M | t | — | t | — | — | — | t | — | — | — | t | — |
| 55. | m | M | M | m | M | M | — | — | t | — | — | — | — | — | — | — | — | — |
| 56. | m | M | M | t | M | M | — | t | t | — | t | — | — | — | — | — | — | — |
| 57. | t | M | M | m | M | M | — | t | m | t | — | — | t | — | — | — | — | — |
| 58. | m | M | M | t | M | M | — | — | t | t | t | — | t | — | — | — | — | — |
| 59. | m | M | M | m | M | M | t | t | t | t | t | t | t | — | t | — | t | — |
| 60. | m | M | M | t | M | M | — | t | m | — | — | — | t | — | — | — | — | — |
| 61. | m | M | M | m | M | M | t | t | t | t | t | — | t | — | — | — | t | — |
| 62. | M | M | M | m | M | M | t | t | t | — | — | — | — | — | — | — | — | — |
| 63. | m | M | M | m | M | M | t | t | t | — | t | — | — | — | — | — | — | — |
| 64. | m | M | M | m | M | M | t | t | t | — | t | t | — | — | — | — | t | — |
| 65. | t | M | M | m | M | M | t | t | t | t | t | — | — | — | — | — | t | — |
| | | | | | | | | GROUP III—CALCIUM-RICH GARNETS | | | | | | | | | | |
| 66. | M | t | M | t | m | M | — | — | t | — | — | — | — | — | — | — | — | — |
| 67. | M | t | M | m | m | M | t | — | t | — | — | — | t | — | — | — | t | — |
| 68. | M | m | M | m | M | M | t | t | t | t | — | — | t | t | — | t | t | — |
| 69. | M | t | M | m | M | M | t | — | t | — | — | — | t | — | — | — | — | — |
| 70. | M | M | M | m | m | M | t | — | M | — | — | — | t | — | — | — | — | t |
| 71. | M | t | m | t | M | M | t | t | t | — | — | — | t | t | — | — | t | — |
| 72. | M | M | M | m | M | M | — | m | t | — | t | — | t | — | — | — | — | — |
| 73. | M | m | M | m | t | M | — | — | t | — | — | — | t | — | — | — | — | — |
| 74. | M | m | m | t | M | M | — | M | m | — | — | — | — | — | t | — | t | — |
| 75. | M | m | m | m | M | M | — | t | t | — | — | — | t | — | — | t | — | — |
| 76. | M | t | M | m | M | M | — | — | t | — | — | — | — | t | — | — | — | — |
| 77. | M | t | M | m | m | M | t | — | t | — | — | — | — | — | — | — | — | — |
| 78. | M | t | M | t | t | M | — | — | m | — | — | — | — | — | — | — | — | — |

Note: Andradite, Beemerville, N. J., showed "Si, Al, Ca, Fe, Ti above 1%; Mg, Mn 0.X%; Y, Yb, Be 0.0X–0.00X%; Pb, Cu traces," spectrographic, A. T. Myers, U. S. Geol. Survey.

* + spectrographic traces of Sn and Ge, G. Steiger, U. S. Geol. Survey files.

† Cu, less than 0.5%.

INDEX TO TABLE 1

| Locality | Occurrence | Refractive Index |
|---|---|---|
| 1. Brown Derby mine, Gunnison County, Colo. | Pegmatite | $n=1.821$ |
| 2. Hackettstown, N. J. | Granite-gneiss | $n=1.820$ |
| 3. Wildomar, Calif. | Pegmatite | $n=1.820$ |
| 4. New Mexico | do | $n=1.805$ |
| 5. Amelia Courthouse, Va. | do | $n=1.803$ |
| 6. Brazil | do | $n=1.814$ |
| 7. Zionville, N. C. | do | $n=1.826$ |
| 8. Gotta Walden mine, Portland, Conn. | do | $n=1.812$ |
| 9. Bergdorff, Idaho | Heavy sand | $n=1.819$ |
| 10. Unaweep Canyon, Mesa Co., Colo. | Granite | — |
| 11. Ober Creek, Alaska | Au placer | — |
| 12. Gunnison Co., Colo. | Pegmatite | $n=1.820$ |
| 13. North Carolina | do | — |
| 14. Kiarfvet, Sweden (U.S.N.M. C6780) | — | — |
| 15. Broken Hill, New South Wales (U.S.N.M. R3437) | — | — |
| 16. Haddam, Conn. (U.S.N.M. 4459) | Pegmatite | — |
| 17. Raymond, Maine (U.S.N.M. 2756) | do | — |
| 18. Ramona, Calif. (U.S.N.M. R3438) | do | — |
| 19. Aschafferburg, Bavaria (U.S.N.M. R3442) | — | — |
| 20. Guilford Courthouse, Conn. (U.S.N.M. 96819) | Pegmatite | — |
| 21. Nathrop, Colo. (U.S.N.M. 80457) | Rhyolite | $n=1.820$ |
| 22. Maine | Pegmatite | $n=1.810$ |
| 23. Montgomery County, Md. | do | — |
| 24. Yancey County, N. C. (U.S.N.M. 80219) | do | — |
| 25. Spruce Pine, N. C. (*U.S.G.S. Bull.* 878) | do | $n=1.808$ |
| 26. Moneta, Va. (*U.S.G.S. Bull.* 878) | do | $n=1.803$ |
| 27. Union Pt., Ga. (*U.S.G.S. Bull.* 878) | do | $n=1.803$ |
| 28. West Hawley, Mass. (*U.S.G.S. Bull.* 878) | do | $n=1.800$ |
| 29. West Cunningham, Mass. (*U.S.G.S. Bull.* 878) | do | — |
| 30. King's Mt. Dist., S. C. (*U.S.G.S. Bull.* 878) | do | — |
| 31. Bald Knob, N. C. (*U.S.G.S. Bull.* 878 | do | — |
| 32. Gossan Lead, Va. (*U.S.G.S. Bull.* 878) | do | — |
| 33. Macon County, Ga. (*U.S.G.S. Bull.* 878) | do | — |
| 34. Geoffrey, S. C. | do | — |
| 35. Shooting Creek, Va. | do | — |
| 36. Striegen, Silesia (U.S.N.M. 7525) | — | — |
| 37. New Mexico | Pegmatite | — |
| 38. Fairfax Quad., Va. | — | — |
| 39. North Carolina | Pegmatite | — |
| 40. Do | do | — |
| 41. Burlington, Vt. | Mica schist | — |
| 42. Locality unknown | Chlorite schist | — |
| 43. Avalanche Lake, Essex County, N. Y. (*Jour. Geol.*, 54, pp. 105–116, 1946) | Gabbro | $n=1.780$ |
| 44. Gore Mtn., N. Y. | Massive garnet | — |

| Locality | Occurrence | Refractive Index |
|---|---|---|
| 45. Locality unknown | Granite-gneiss | — |
| 46. McCall, Idaho | Heavy sand | — |
| 47. Wyoming | Glaucophane schist | — |
| 48. California | Mica schist | — |
| 49. North Carolina | do | — |
| 50. Chester, Vt. | do | — |
| 51. St. Maries, Idaho | Placer | — |
| 52. Burnsville, N. C. | — | — |
| 53. Locality unknown | Mica schist | — |
| 54. Do | Gneiss | — |
| 55. Fort Wrangel, Alaska (*Am. Mineral.*, **12,** p. 343, 1927) | — | $n=1.807$ |
| 56. Hawk, N. C. | Schist | — |
| 57. Lumpkin County, Ga. | — | — |
| 58. New York, N. Y. | Manhattan schist | — |
| 59. Meronitz, Czechoslovakia | Serpentine | — |
| 60. Locality unknown | — | — |
| 61. 5 miles NE of Dillard, Ga. | Biotite gneiss | — |
| 62. Avery Quad., Idaho (U.S.N.M. 95679) | — | — |
| 63. Mitchell County, N. C. (U.S.N.M. R3444) | — | — |
| 64. New Mexico | — | — |
| 65. Georgia | Schist | — |
| 66. Essex County, N. Y. | Diopside, wollastonite tactite | — |
| 67. Sierra Mts., Calif. | Tactite | — |
| 68. West Adirondacks, N. Y. | Pyroxene skarn | — |
| 69. Chula Vista, Calif. | Tactite | — |
| 70. Colorado Springs, Colo. | — | — |
| 71. Xalostoc, Mexico (*Am. Mineral.*, **12,** p. 343, 1927) | — | $n=1.742$ |
| 72. Santa Fe, Ariz. (Dana's System, p. 441) | — | — |
| 73. Prince Rupert Island, B. C. | Tactite | — |
| 74. So. California Desert (*Am. Mineral.*, **32,** p. 640, 1947) | Diopside, idocrase tactite | — |
| 75. Democrat, N. C. | — | — |
| 76. California | Tactite | — |
| 77. Fairfield, Idaho | — | — |
| 78. Sierras, Calif. | Tactite | — |

element in garnet, is actually a very persistent trace or minor constituent of spessartite garnets where it may occur in concentrations of more than 2 per cent $Y_2O_3$.

## Analytical Data

During the present investigation, more than 70 garnets were studied. All of these were subjected to visual spectroscopic analysis, using the equipment and methods described by Peterson, Kauffman, and Jaffe (1947), Gabriel, Jaffe and Peterson (1947) and Jaffe (1949). Major, minor, and trace constituents determined by this method and reported in this paper are defined as follows:

Major constituents (M).....More than 5%
Minor constituents (m).....0.5 to 5%
Trace constituents (t).....Less than 0.5%
Absent (—).....Less than 0.1% for those elements listed below:

The following elements have been detected in garnets in concentrations at least as low as 0.1% by means of visual spectroscopy:

Fe, Mn, Ca, Mg, Al, Cr, V, Ti, Sc, Y, Ga, Na, Li, Zn, Sr, Cb and F.

Yttrium, found to be a common trace constituent of spessartites, may be detected spectroscopically in concentrations lower than 0.01%.

Table 2. $Y_2O_3$ in Spessartite Garnets

| Sample (Numbers from Table 1) | Geological occurrence | $\%Y_2O_3$ |
|---|---|---|
| 2. Hackettstown, N. J. | Granite-gneiss | 0.29 |
| 3. Wildomar, Calif. | Pegmatite | 2.48 (*a*) |
| 4. New Mexico | do | .10 |
| 8. Portland, Conn. | do | .14 |
| 12. Gunnison County, Colo. | do | 1.36 (*b*) |
| 37. New Mexico | do | .26 |
| Elk Mt., near Las Vegas, N. Mex. | do | 2.01 (*c*) |
| Schreiberhau | No data | 2.64 ("YO") |
| Iisaka, Japan | Pegmatite | 2.45 ("Rare Earths") |

Analyses 2, 3, 4, 8, 12 and 37 by A. M. Sherwood (new data).
Analysis of Elk Mt., N. M. spessartite by Charles Milton (new data).
Analysis of Schreiberhau spessartite by Websky (1868) as quoted in Dana's *System*.
Analysis of Iisaka, Japan spessartite by Takeo Iimori (1938).
(*a*) + spectrographic traces of (Sc, Gd, Dy, La, Ce, Nd, Pr)$_2O_3$.
(*b*) + spectrographic traces of (Dy, Gd)$_2O_3$.
(*c*) + spectrographic traces of (Yb, Dy, Er, Ho)$_2O_3$.

Quantitative $Y_2O_3$ determinations were made of 7 garnets, according to the method of Minami (1935). The sample is dissolved in concentrated hydrofluoric acid to remove the silica, and the residue is digested with very dilute hydrofluoric acid. The residue is dissolved and precipitated with strong potassium hydroxide solution, dissolved in hydrochloric acid and reprecipitated with ammonia. The precipitate is dissolved, the solution evaporated to a very small volume and the rare earths precipitated with oxalic acid. After standing for 12 to 24 hours the rare-earth oxalates are filtered off and ignited. For an evaluation of this method, the reader is referred to a paper by Sahama and Vähätalo (1939).

In addition to the visual spectroscopic and quantitative analytical determinations, spectrographic analysis was employed in two instances. Semiquantitative spectrographic analyses were made of two ignited oxalic acid residues obtained from spessartites in order to determine their purity as $Y_2O_3$ and to detect any additional rare earths that were coprecipitated. By this means of enrichment, traces of the Y earths, Dy and Gd, were detected in both instances. In one of the samples, traces of the Ce earths, La, Ce, Nd, and Pr, were also detected.

The visual spectroscopic analyses are given in Table 1, the quantitative analytical yttria determinations in Table 2, complete analyses of four yttrian garnets in Table 3 and the semiquantitative spectrographic determinations of two yttria precipitates in Table 4. The writer is indebted to Charles Milton of the U. S. Geological Survey for the unpublished complete analysis of the yttrian garnet from New Mexico given in Table 3.

## Relations Between the Composition and Occurrence of Garnets

The unique relationships between the five major garnet molecules—spessartite, almandite, pyrope, grossularite, and andradite—and the rock types in which they occur have been noted by numerous investigators, particularly Wright (1938) and Heritsch (1926). Before considering any hypothetical isomorphism that may exist in the garnet group, a review of Wright's conclusions is necessary. Wright selected 223 garnets for which both complete quantitative analytical data and geological occurrence were given in the literature. The data are representative of a world-wide distribution of garnets composed essentially of the five major molecules. He converted the analytical values to spessartite, almandite, pyrope, grossularite, and andradite and showed that, with few exceptions, different combinations of the garnet molecules were associated with particular rocks. This is illustrated in Table 5.

TABLE 3. COMPLETE ANALYSES OF FOUR YTTRIAN SPESSARTITES

| | Schreiberhau | Elk Mt., N. M. | Gunnison Co., Colo. | Iisaka, Japan |
|---|---|---|---|---|
| $SiO_2$ | 35.83 | 34.99 | 36.84 | 34.95 |
| $Al_2O_3$ | 20.65 | 20.76 | 20.75 | 14.80 |
| $B_2O_3$ | — | — | — | 0.15 |
| $Fe_2O_3$ | — | — | — | 16.60 |
| $Y_2O_3$ | 2.64 ("YO") | 2.01 (*b*) | 1.36 (*a*) | 2.45 ("R.E.") |
| MnO | 8.92 | 29.60 | 16.80 | 22.28 |
| FeO | 31.52 | 10.76 (total Fe) | 21.51 | — |
| MgO | — | 0.17 | tr | — |
| CaO | 0.76 | 1.17 | 1.95 | 4.52 |
| BeO | — | — | — | 0.39 |
| $Na_2O$ | — | — | tr. | 1.67 |
| $K_2O$ | — | — | — | 0.16 |
| $H_2O$ | — | 0.75 | 0.76 | 0.45 |
| $CO_2$ | — | — | — | 0.41 |
| Total | 100.32 | 100.12 | 99.97 | 98.83 |

Schreiberhau, analyzed by Websky as quoted in Dana's *System of Mineralogy*, 6th ed.' p. 442 (1892).

Elk Mt., N. M., analyzed by Charles Milton (new data).

Gunnison Co., Colo., analyzed by A. M. Sherwood (new data).

Iisaka, Japan, analyzed by Takeo Iimori, *Sci. Pap. Inst. Phy. Chem. Res., Tokyo*, No. 805, Vol. **34,** p. 836 (1938).

(*a*) + spectroscopic traces of (Sc, Dy and Gd)$_2O_3$.

(*b*) + spectrographic traces of (Yb, Dy, Er, Ho)$_2O_3$.

It is significant to note that the pegmatite and granite garnets are essentially spessartite and almandite. Shand (1943), in a reference to garnets in eruptive rocks, also notes, "Garnet is sometimes prominent in aplite and pegmatite veins, and occasionally in acid lavas. The variety is almandine or spessartite." He notes further that the magnesian garnet, pyrope, is an unsaturated mineral and incompatible with quartz in eruptive rocks. Shand writes, "The magnesian garnet, pyrope, is restricted to very basic rocks such as peridotites, pyroxenites and serpentines, which are generally free from feldspar. There is nothing in the known facts of distribution of either melanite (andradite) or pyrope to suggest that these minerals are capable of forming in presence of an excess of silica." Pegmatite garnets were also investigated by Mosebach (1938), who determined that these garnets are all spessartite containing up to 40% almandite, some grossularite and occasionally pyrope. Five additional garnets analyzed by Milton (1937) are very representative of the pegmatitic-granitic environment. These show major amounts of spes-

sartite and almandite, trace to minor amounts of pyrope and grossularite and only trace amounts of andradite.

The results obtained by the author and given in Table 1 are in accord with those obtained by Heritsch (1926), Wright (1938) and Mosebach (1938) for pegmatite and granite garnets. Of the 40 garnets from pegmatitic-granitic rocks listed in Table 1, all contain major amounts of manganese and iron and only trace to minor amounts of magnesium and calcium. Inasmuch as no chemical analyses were made for $Fe_2O_3$, it is not possible to state whether any appreciable amounts of andradite are present. All previous analytical data in the literature, however, indicate that andradite is the least abundant of the five major garnet molecules

TABLE 4. SPECTROGRAPHIC ANALYSES OF TWO $Y_2O_3$ PRECIPITATES FROM SPESSARTITES

| Constituent | No. 12 Gunnison County, Colo., Per cent | No. 3 Wildomar, Calif. Per cent |
|---|---|---|
| $Y_2O_3$ | >10 | >10 |
| $Sc_2O_3$ | — | .1 –1. |
| $Pr_2O_3$ | — | .02 – .2 |
| $Nd_2O_3$ | — | .05 – .5 |
| $La_2O_3$ | — | .02 – .2 |
| $Ce_2O_3$ | — | .01 – .1 |
| $Dy_2O_3$ | .05 –.5 | .08 – .8 |
| $Gd_2O_3$ | .005–.05 | .005–.05 |
| M. J. Peterson, spectrographer | | |

NOTE: The yttria precipitate from the Elk Mt., N. Mex., spessartite (tables 2 and 3) was spectrographed by K. J. Murata who found Yb, Er, Dy and Ho to be present.*

* Fleischer, M., Private communication, 1949.

in garnets found in pegmatitic and granitic rocks. Wright concluded that "Spessartite and almandite constitute 85–90% of the molecules of garnets from pegmatites and granites. In general, if one of the major constituents is known, either spessartite or almandite, the other can be estimated within a reasonable error, with 5–15% left for the remaining molecules." From the data given in Table 1, it is evident that a correlation exists between manganese-rich garnets, pegmatitic environment and yttrium-enriched garnets. This will be elaborated further in the following sections of this report.

## TRACE AND MINOR CONSTITUENTS OF GARNETS

That certain trace and minor elements are characteristic of particular varieties of garnet is not surprising in view of the associations of the

different garnets with particular rock types as proposed by Wright and Heritsch and verified during the present investigation. This affinity of particular accessory elements for the various garnets suggests isomorphism, which may be explained on the basis of similarities of ionic radii, using the values given by Goldschmidt (1929). The garnets studied during this investigation fall conveniently into three groups, categorized as follows:

| *Group* | *Diagnostic major elements* | *Association* |
|---|---|---|
| I | Mn, Fe | Pegmatite, granite |
| II | Mg, Fe | Schist |
| III | Ca, Fe | Tactite |

Although all garnets will not fit into one of the above groups, particularly a low-iron grossularite, a survey of the literature and the results of the present study suggest that the vast majority of garnets will fit this generalized grouping. While some schist garnets may contain major amounts of Mn and Ca, these elements are *not diagnostic*, as are Mg and

Table 5. Average Proportion of Five Major Garnet Molecules in Different Rock Types (Adapted from Wright (1938))

| Rock Types | Spessartite | Almandite | Pyrope | Grossularite | Andradite |
|---|---|---|---|---|---|
| Pegmatites | 47.1 | 41.8 | | | |
| Granites | 36.0 | 56.8 | | | |
| Garnets assoc. with contact action on siliceous rocks | 30.7 | 56.4 | | | |
| Biotite schists | | 73.0 | 13.8 | 6.0 | |
| Amphibole schists | | 53.6 | 20.3 | 20.7 | |
| Eclogites | | 18.5 | 37.4 | 39.1 | |
| Kimberlites and peridotites | | 13.4 | 72.3 | 9.0 | |
| Various basic rocks | | 34.4 | 20.7 | 28.7 | 15.6 |
| Calcareous contact rocks | | | | 51.5 | 40.8 |

Fe, which will invariably be present in major amounts. Similarly, a pegmatite garnet will invariably contain major amounts of the diagnostic elements, Mn and Fe, and may in *unusual examples* also contain major amounts of Mg or Ca. There follows a discussion of the minor and trace elements characteristic of Groups I, II and III and their possible relationships to the major cations.

### Group I. Accessory Elements Associated with Garnets of Pegmatites and Granites

Yttrium in garnets was reported as early as 1868 by Websky, as noted in Dana's *System of Mineralogy* (1892). Websky found 2.64% of

"YO" in a garnet that is listed under the almandites in Dana's *System*. It is interesting to note, however, that the analysis (Table 3) shows major amounts of MnO. Magnesium and ferric iron are absent and calcium is only sparingly present. Dana also refers to another questionable yttrian garnet which yielded 6.6% of $Y_2O_3$, but a second analysis showed only a trace of yttria. The "yttergarnets" mentioned by Dana are erroneously listed with the andradites. This is surprising, in view of the fact that the only yttrian garnet listed by Dana—the one analyzed by Websky—is clearly an almandite-spessartite. The only other analysis of an yttrian garnet published to date is that described by Iimori (1938). The garnet was found in a pegmatitic environment in Iisaka village, Fukushima Prefecture, Japan, where it is associated with feldspar, tengerite, yttrialite, fergusonite, thorogummite and xenotime. The garnet, which contains 2.45% of rare earths (Table 3), is referred to as a "spalmandine" by Iimori, although all of the iron is reported in the analysis as $Fe_2O_3$. Calcium is present in minor amounts, and magnesium is absent. The garnet occurs as partly hollowed shells in which tengerite, the yttrium carbonate, is deposited. The rare earths found in the garnet are not listed, but the dominant earth in the intimately associated tengerite is yttrium. Minor amounts of Gd, Dy, and Er are reported as being next in abundance. It is unfortunate that Iimori did not identify the rare earths found in the garnet. The validity of this analysis will be discussed later.

Goldschmidt and Peters (1931) detected spectrographic traces of yttrium in several garnets but did not find more than trace amounts in any sample. The spectrographic values listed by these investigators also show that the largest traces of yttria occur in spessartites from plumasitic granite-pegmatite. These data are given in Table 6.

Sahama and Vähätalo (1939) also noted spectrographic traces of yttria in garnets. Sahama concludes "that an appreciable part of the yttrium earths in rocks remains outside the minerals orthite and monazite."

Yttrium has also been noted in garnets by van der Lingen (1928). He detected this element in garnets but did not estimate the amounts present. It is interesting to note that this investigator detected the element by use of visual spectroscopy in the same manner as the author. Van der Lingen writes, "From a large series of observations the conclusion can be drawn that yttriferous garnets are not rare in South Africa. For this type of garnet, namely a spessartine containing yttrium, I propose the name emildine, the limitation being that the molecules of uvarovite must be absent, and that the molecule of pyrope is either wholly absent or only present as a trace." For garnets containing a trace of yttrium associated with pyrope and uvarovite, he proposed the name, erinadine.

Table 6. Spectrographic Traces of Yttrium and Scandium in Garnets Reported by Goldschmidt and Peters (1931)

| Sample | Geological occurrence | $\%Y_2O_3$ | $\%Sc_2O_3$ |
|---|---|---|---|
| Garnet, spessarite, Tveit, Norway | Granite-pegmatite | 0.01 | 0.01 |
| Garnet, spessartite, Sigdal, Norway | do | .01–.1 | .0005 |
| Garnet, mangan-grossularite, Arvold, Norway | — | .0001 | — |
| Garnet, andradite, Kalkofen, Norway | — | <.0001 | — |
| Garnet, almandite, Fort Wrangel, Alaska | — | <.0001 | .0005 |
| Garnet, Silberbach, Bavaria | Eclogite | .001 | .01 |
| Garnet, pyrope, Bohemia | do | <.001 | .01 |
| Garnet, Piedimonte, Italy | do | .001 | .01 |
| Garnet, Almeklovdalen, Norway | do | <.001 | .01 |
| Garnet, Tafjord, Norway | do | .001 | .005 |
| Garnet, Grytingvag, Noway | Eclogite-pegmatite | <.001 | .001 |
| Garnet, Kimberley, S. Africa | Kimberlite | <.001 | .01 |

A further reference to yttrium in garnets was found in a paper by Björlykke (1937) on the granite pegmatites of southern Norway. Björlykke notes that, "The minerals which occur in both the magmatic and in the hydrothermal-pneumatolytic pegmatites generally are present in different habits, and with different compositions in the two types of occurrences. Spessartite and apatite of the cleavelandite-quartz pegmatites usually occur in ill-defined crystals intersected by blades of cleavelandite. They contain no detectable amount of Y-elements, while those of the magmatic pegmatites usually contain these elements in considerable amounts." He also states that spessartite occurs in the magmatic pegmatites "in euhedral crystals containing small amounts of Y-elements." In the hydrothermal-pneumatolytic pegmatites, spessartite occurs, "mostly in anhedral crystals without detectable amounts of Y-elements." His usage of the terms, "considerable amounts" and "small amounts" on two different pages is not clear. No percentages are given, and there is no indication, therefore, of the amounts present. It is noteworthy, however, that the yttrium detected by Björlykke is in manganese-rich garnets found in pegmatite. It is assumed that his "Y-elements" embrace the yttrium group: Y, Gd, Tb, Dy, Ho, Er, Tm, Yb and Lu.

The present writer found that yttrium is an especially common trace constituent of spessartite garnets. It was detected in 39 out of 40 spessartites studied (Table 1). It is less common in magnesium-rich garnets and uncommon in calcium-rich garnets (Table 1). In the course of the present investigation, seven quantitative yttria determinations were

made of spessartites, all associated with pegmatites. These are given in Table 2, along with the two analytical values of Websky and Iimori. Two new complete analyses of yttrian spessarittes are given in Table 3 and are offered for comparison with those of Websky and Iimori. These represent the only four yttrian garnets that have been completely analyzed. The occurrence of the Japanese garnet has already been mentioned. The garnet from New Mexico, analyzed by Charles Milton, was submitted by V. Leon Guy of Las Vegas, New Mexico. It is reported to occur in pegmatite at Elk Mountain, northwest of Las Vegas. The garnet from Colorado, analyzed by A. M. Sherwood, was submitted by A. M. Crawford, Delta, Colo. Crawford states that it occurs "on the western slope in Gunnison County near Little Blue Creek, not far from the Black Canyon of the Gunnison River where there are a good many pegmatite dikes and feldspar deposits."

All four of the analyzed yttrian garnets (Table 3) are rich in manganese and ferrous iron and conversely impoverished in magnesium, calcium and ferric iron. $Y^{+3}$ has an ionic radius of 1.06 Å and $Mn^{+2}$, an ionic radius of 0.91 Å. Divalent iron ions (0.83 Å) are too small to be expected to serve as hosts for the larger yttrium ions. Goldschmidt (1945) notes that the host mineral should have some main constituent with an ionic radius similar to the minor elements associated with it. This suggests that $Y^{+3}$ may occupy $Mn^{+2}$ positions in the garnet lattice due to similarities of ionic radii. Substitution of this type is not to be unexpected, according to Goldschmidt (1945), who writes, "Generally the possibility of large scale isomorphous substitution in minerals from magmas will be limited to such pairs of ions, the radii of which agree within a tolerance of 10–15 per cent of the larger radius of the pair. Divalent magnesium (0.78 Å) and ferrous iron (0.83 Å) freely replace each other in ionic crystals, but not magnesium and calcium (1.06 Å). Divalent manganese occupies a position intermediate between magnesium and calcium, having an ionic radius of 0.91 Å and entering into isomorphous substitution either for magnesium, or in many cases, for calcium. . . . Comparable to divalent calcium (1.06 Å) are—to a certain degree the divalent manganese (0.91 Å) . . . the trivalent ions of yttrium (1.06 Å) and all the trivalent lanthanide elements from lanthanum (1.22 Å) to luctecium (0.99 Å)."

Close inspection of the chemistry of the minerals associated with the yttrian spessartite from Californa (Tables 2 and 7) affords further illustration of the substitution of the yttrium for manganese. Table 7 includes visual spectroscopic analyses of all of the minerals present in the rock, a simple pegmatite, and Table 8, the ionic radii of the possible host and substitute ions. It is significant to note that the garnet is the only mineral of the assemblage that contains both yttrium (2.48% $Y_2O_3$)

and major amounts of manganese. Hence, it is reasonable to assume that all of the yttrium has entered the garnet lattice substituting for manganese on the basis of similarities of ionic radii. Scandium, on the other hand, is present in the muscovite and tourmaline as well as in the garnet (Table 7). Triply charged ions of scandium (0.83 Å) may proxy for divalent magnesium (0.78 Å) or iron (0.83 Å) according to Goldschmidt and Peters (1931), who state that trivalent scandium ions commonly proxy for either of these divalent ions. This is further emphasized by Sahama (1936). In the California garnet, muscovite and tourmaline (Table 7) scandium probably proxies for divalent iron as the pegmatite is impoverished in magnesium. Gallium is present in four of the five

Table 7. Visual Spectroscopic Analyses of an Yttrian Spessartite and Associated Minerals from a California Pegmatite
($Y_2O_3$ in the spessartite = 2.48%)

| | Ca | Al | Fe | Mn | Mg | Si | Y | Na | Li | K | Zn | Ti | V | Sc | Rb | Tl | Ga | B | F |
|---|---|---|---|---|---|---|---|---|---|---|---|---|---|---|---|---|---|---|---|
| Spessartite | t | M | M | M | t | M | m | — | t | — | t | t | t | t | — | — | t | — | t |
| Muscovite | t | M | m | t | t | M | — | m | t | M | — | t | t | t | t | t | t | — | t |
| Tourmaline | t | M | M | t | m | M | — | m | t | — | t | — | — | t | — | — | t | M | t |
| Albite | m | M | t | — | — | M | — | M | — | — | — | — | — | — | — | — | t | — | — |
| Quartz | — | — | t | — | — | M | — | — | — | — | — | — | — | — | — | — | — | — | — |

Determinations by H. W. Jaffe.

minerals of the assemblage and this element may replace aluminum, the sizes of the respective trivalent radii being (0.62 Å) and (0.57 Å). Vanadium found in the garnet and the mica may supplant ions of aluminum as quadrivalent V (0.61 Å) ions. Titanium (0.64 Å) may similarly replace aluminum. Zinc (0.83 Å) present in the garnet and tourmaline may substitute for ferrous iron. Lithium (0.83 Å) found in the garnet, muscovite, and tourmaline may similarly proxy for divalent iron. Fluorine, found in the garnet, mica, and tourmaline should proxy for oxygen or hydroxyl.

To determine whether any additional rare earths were present in garnets, the yttria precipitates obtained from the California and the Colorado spessartites (Table 2) were subjected to spectrographic analysis. It was assumed that any additional rare earths present in the garnet would be coprecipitated with yttrium and therefore concentrated many fold. The results of these spectrographic analyses are given in Table 4. The ignited oxalic acid residues obtained from both garnets showed traces of the Y-elements gadolinium and dysprosium. These were not detected in the original visual spectroscopic analyses because of their low concentrations in the garnets. Traces of the Ce-elements—cerium, lanthanum, neodymium, and praseodymium—were also detected in the residue

of the California garnet. According to Sahama,* the cerium earths had not been previously detected in garnets probably because enough material was not available for chemical enrichment. If all group precipitations, particularly those of the difficultly separable rare earths, were subjected to spectrographic analysis our geochemical knowledge would be greatly enriched.

TABLE 8. IONIC RADII IN ANGSTROMS (GOLDSCHMIDT 1929) AND SUGGESTED ISOMORPHISM

| $Ca^{+2}$ | $Al^{+3}$ | $Fe^{+2}$ | $Mn^{+2}$ | $Mg^{+2}$ | $Si^{+4}$ | $Y^{+3}$ | $Na^{+}$ | $Li^{+}$ | $K^{+}$ | $Zn^{+2}$ | $Ti^{+4}$ | $V^{+4}$ | $Sc^{+3}$ | $Rb^{+}$ | $Tl^{+}$ | $Ga^{+3}$ | $B^{+3}$ | $F^{-}$ | $O^{-2}$ |
|---|---|---|---|---|---|---|---|---|---|---|---|---|---|---|---|---|---|---|---|
| 1.06 | 0.57 | 0.83 | 0.91 | 0.78 | 0.39 | 1.06 | 0.98 | 0.83 | 1.33 | 0.83 | 0.64 | 0.61 | 0.83 | 1.49 | 1.49 | 0.62 | 0.20 | 1.33 | 1.32 |

| | | | | | |
|---|---|---|---|---|---|
| Spessartite Mn(Y, Ca) | Fe(Zn, Sc, Mg, Li) | | Al(Ga, V, Ti) | O(F) | |
| Muscovite | Fe(Mn, Mg, Sc, Li, Na) | | Al(Ga, V, Ti) | O(F) | K(Rb, Tl) |
| Tourmaline | Fe(Mn, Zn, Mg, Sc, Li, Na) | | Al(Ga, Ti) | O(F) | |
| Albite | | | Al(Ga) | | Na(Ca) |

## SUBSTITUTION OF YTTRIUM FOR MANGANESE

The substitution of ions of $Y^{+3}$ for those of $Mn^{+2}$, as postulated, obviously upsets the neutrality of the crystal owing to higher positive charge of the former. This might be balanced, however, by a corresponding substitution of $Al^{+3}$ ions for $Si^{+4}$ ions in tetrahedral coordination. Al ions are known to proxy for Si ions in tetrahedral coordination in the amphiboles (Warren, 1929), micas (Jackson and West, 1930), clinopyroxenes (Hess, 1949) and in many other minerals. That Al may occupy Si positions in garnet has already been suggested by Alderman (1935). The substitution scheme in the yttrian spessartites might then be:

$$Y^{+3}Al^{+3} \text{ for } Mn^{+2}Si^{+4}.$$

A similar substitution scheme involving yttrium is offered by Sahama (1946) in explanation of the sphene-keilhauite series. According to Sahama, the isomorphism is:

$$Y^{+3}Al^{+3} \text{ for } Ca^{+2}Ti^{+4}.$$

In the sphene lattice, however, the Al and Ti ions are believed to be in octahedral rather than tetrahedral coordination (Zachariasen 1930).

Based upon the suggested substitution of $Y^{+3}Al^{+3}$ for $Mn^{+2}Si^{+4}$, a theoretical yttrian spessartite containing 8.89% $Y_2O_3$ should be a stable garnet with the ideal composition calculated as shown at the top of the next page.

A garnet of this composition has recently been synthesized by H. S. Yoder at the Geophysical Laboratory. He has also been able to synthesize yttrian spessartites containing more than 8.89% yttria. Based upon

* Sahama, Th. G., Personal communication 1948.

| Composition | | Atomic Ratios | | | Cations to Twelve O |
|---|---|---|---|---|---|
| $SiO_2$ | 30.73 | Si | 512 | 592 | Z=3 |
| $Al_2O_3$ | 24.08 | | | | |
| $Y_2O_3$ | 8.89 | Al | 472 | 80 | |
| MnO | 36.30 | | | 392–392 | Y=2 |
| | 100.00 | Y | 80 | 592 | X=3 |
| | | Mn | 512 | | |
| | | O | 2362 | | |

Formula: $(Mn_{3-x}Y_x)Al_2(Si_{3-x}Al_x)O_{12}$, where x=0.4.

the substitution scheme suggested by the author, $Y^{+3}Al^{+3}$ for $Mn^{+2}Si^{+4}$ Dr. Yoder has suggested the following formula for yttrian spessartites:

$$(Mn_{3-x}Y_x)Al_2(Si_{3-x}Al_x)O_{12}.$$

The end members of the substitution series may then be expressed as:

1. $Mn_3Al_2Si_3O_{12}$ (spessartite).
2. $Y_3Al_2Al_3O_{12}$ ( ? ).
   or
   $Y_3Al_5O_{12}$

The compositions of these calculated from the formulas, give:

| | 1 | 2 |
|---|---|---|
| $SiO_2$ | 36.40 | — |
| $Al_2O_3$ | 20.60 | 42.93 |
| $Y_2O_3$ | — | 57.07 |
| MnO | 43.00 | — |
| | 100.00 | 100.00 |

No yttrium aluminate of the composition of the end member is known to occur naturally. If it can be synthesized, in order for it to retain the garnet structure it would require the Al ions to be present in two coordinations. The garnet structure (orthosilicate) requires independent $SiO_4$ tetrahedra which are linked by $AlO_6$ octahedra. Therefore, an end member garnet of the composition, $Y_3Al_2Al_3O_{12}$, would require independent $AlO_4$ tetrahedra linked by $AlO_6$ octahedra with yttrium in the interstices, probably in eightfold coordination. Whether such a continuous substitution series is possible will soon be determined by Dr. Yoder's work on synthetic yttrian garnets.

The substitution of Y and Al ions for Mn and Si ions, respectively, should expand but not excessively distort the garnet lattice. The ionic radii of $Y^{+3}$ (1.06 Å) and $Al^{+3}$ (0.57 Å) are both larger than those they replace, $Mn^{+2}$ (0.91 Å) and $Si^{+4}$ (0.39 Å). Menzer (1928) has shown that the large Ca ions (1.06 Å) in grossularite are surrounded by extremely

distorted oxygen polyhedra. Further, it is generally believed that in the titanian andradites, most and in some cases all of the $Ti^{+4}$ ions (0.64 Å) replace the much smaller $Si^{+4}$ ions (0.39 Å) expanding the unit cell (Zedlitz 1933 and 1935). A good example is the titanian andradite from Oberweisenthal quoted in Dana's *System* (analysis 32 under andradites). The atomic ratios indicate that most, if not all, of the Ti has replaced Si.

| Composition | | Atomic Ratios | | Cations to Twelve O |
|---|---|---|---|---|
| $SiO_2$ | 29.15 | Si | 483 } 620 | Z=3.11 |
| $TiO_2$ | 10.84 | Ti | 137 } | |
| $Al_2O_3$ | 6.50 | Al | 127 } 401 | Y=2.01 |
| $Fe_2O_3$ | 21.92 | Fe | 274 } | |
| MgO | 0.98 | Mg | 24 } 548 | X=2.75* |
| CaO | 29.40 | Ca | 524 } | |
| | 98.79 | O | 2390 | |

* (The low value for X may be a reflection of the low summation and possibly the failure to determine FeO and MnO.)

Accordingly, if the $Ti^{+4}$ ions (0.64 Å) and the Ca ions (1.06 Å) can occupy Z and X positions, respectively, in the garnets, and in large amounts, the lattice should be no more distorted by the acceptance of ions of $Al^{+3}$ (0.57 Å) and $Y^{+3}$ (1.06 Å). That 2.48% $Y_2O_3$ does not appreciably alter the spessartite lattice is shown by the *x*-ray data in Table 9. The differences in spacings shown in these patterns are due essentially to the relative amounts of almandite and spessartite present rather than the small amount of yttria. In any event, the amount of expansion of the lattices of garnets containing small amounts of yttrium would be hidden by the much more important variable, the ratio of almandite to spessartite. That yttrian spessartites have a larger lattice than pure spessartite (never found in nature) will be illustrated by Dr. Yoder in his report on synthetic yttrian spessarittes. The garnet lattice, then, like that of the micas, appears to be quite elastic and capable of housing ions of a wide range of size in large amounts.

To date, only four naturally occurring yttrian garnets have been completely analyzed (Table 3). Calculating the atomic ratios of the yttrian garnets from Schreiberhau, Elk Mt., N. Mex., and Gunnison County, Colo. (Table 3), on the basis of $Y^{+3}Al^{+3}$ proxying for $Mn^{+2}Si^{+4}$, the following ratios are obtained (Table 10).

The fourth analysis of an yttrian garnet from Iisaka, Japan (Table 3), is questionable, as the atomic ratios for garnet cannot be satisfactorily calculated. The analyst, Iimori (1938), refers to the garnet as a "spal-

TABLE 9. *X*-RAY DIFFRACTION PATTERNS OF SPESSARTITES

| 3 *d* | 4 *d* | 5 *d* | 8 *d* | 16 *d* | *hkl* | *I* |
|---|---|---|---|---|---|---|
| 2.90 | 2.91 | 2.92 | 2.92 | 2.90 | 400 | m |
| 2.60 | 2.60 | 2.61 | 2.61 | 2.60 | 420 | vs |
| 2.48 | 2.48 | 2.49 | 2.49 | 2.48 | 332 | w |
| 2.37 | 2.37 | 2.38 | 2.38 | 2.38 | 422 | w |
| 2.28 | 2.29 | 2.29 | 2.29 | 2.28 | 510 | w |
| 2.12 | 2.13 | 2.13 | 2.13 | 2.12 | 521 | m |
| 2.07 | 2.06 | 2.06 | 2.07 | 2.06 | 440 | w |
| 1.888 | 1.890 | 1.895 | 1.890 | 1.884 | 611 | s |
| 1.734 | — | — | — | — | 622 | w |
| 1.678 | 1.680 | 1.686 | 1.684 | 1.678 | 444 | s |
| 1.613 | 1.615 | 1.618 | 1.615 | 1.613 | 640 | m |
| 1.556 | 1.558 | 1.558 | 1.558 | 1.554 | 642 | s |
| 1.492 | 1.488 | — | — | — | | w |
| 1.453 | 1.457 | 1.455 | 1.461 | 1.457 | 800 | w |
| 1.301 | 1.304 | 1.305 | 1.305 | 1.301 | 840 | w |
| 1.269 | 1.272 | 1.272 | 1.274 | 1.268 | 842 | m |

| | % $Y_2O_3$ |
|---|---|
| #3—Wildomar, Calif. | 2.48 |
| #4—New Mexico | 0.10 |
| #5—Amelia Courthouse, Va. | tr. |
| #8—Gotta Walden mine, Portland, Conn. | tr. |
| #16—Haddam, Conn. | tr. |

vs—very strong
s—strong
m—medium
w—weak
Determinations by G. E. Ashby.

mandine" and paradoxically reports all of his iron as $Fe_2O_3$. All attempts to calculate the atomic ratios of this garnet have been unsatisfactory, whether the iron is claculated entirely as $Fe_2O_3$ or as FeO. The presence of 1.67% $Na_2O$ and some $CO_2$ and $K_2O$ is not clear, and the sample may not have been pure. The best ratios are obtained by assuming that both ferrous and ferric iron are present and that $Na^{+1}Y^{+3}$ replaces $2Mn^{+2}$. Recasting the analysis on this basis the ratios may be as shown at the top of the next page.

In view of the questionable validity of this analysis, the unwarranted recasting of the iron, and the assumptions regarding the various substitutions, the isomorphism of $Na^{+1}Y^{+3}$ for $2Mn^{+2}$ in spessartites is purely speculative. However, in fairness to Iimori, who made a very detailed examination of the associated tengerite, his analysis of the yttrian garnet

| Reported Composition | | Fe recasted | Atomic Ratios | | Cations to Twelve O |
|---|---|---|---|---|---|
| $SiO_2$ | 34.95 | | Si | 582.....582 | Z=2.98 |
| $Al_2O_3$ | 14.80 | | Al | 290 | |
| $B_2O_3$ | 0.15 | | B | 4 | |
| BeO | 0.39 | | Be | 16 .....401 | Y=2.06 |
| $Fe_2O_3$ | 16.60 | 7.30 | $Fe^{+3}$ | 91 | |
| FeO | — | 9.30 | $Fe^{+2}$ | 129 | |
| $Y_2O_3$ | 2.45 ("R.E.") | | Y | 22 | |
| MnO | 22.28 | | Mn | 314 .....600 | X=3.08 |
| MgO | — | | Ca | 81 | |
| CaO | 4.52 | | Na | 54 | |
| $Na_2O$ | 1.67 | | | | |
| $K_2O$ | 0.16 | | O | 2341 | |
| $H_2O$ | 0.45 | | | | |
| $CO_2$ | 0.41 | | | | |
| | 98.83 | | | | |

$n$=1.830
G=4.21

(If $Na^{+1}Y^{+3}$ replaces $2Mn^{+2}$ there remains an excess of Na ions.)

should not be discredited until such time as we have more data regarding the role of the various minor constituents in garnets. Although the garnets have been studied by numerous investigators, there are several aspects of their constitution that have not been sufficiently clarified. For example, Fermor's work (1926) on some Indian garnets, suggesting the presence of $Mn_2O_3$, has been regarded with some skepticism, perhaps unjustly so. Unless the presence of trivalent manganese is assumed satisfactory atomic ratios cannot be calculated for the garnet from Chargoon, India (Fermor 1926), one from Amelia, Va. (Dana 1892 and Shannon 1927), and another from Nathrop, Colo. (Dana 1892). Similarly, the role of titanium in garnets has not been well defined. Apparently it plays a dual role, proxying both for silicon in the Z group and aluminum in the Y group. The answers to these and other problems pertaining to the chemistry of the garnets can best be obtained by synthesizing the various garnets and their possible analogues.

### Group II. Accessory Elements Associated with Garnets of Schists

As previously stated, this group usually contains major amounts of magnesium and iron and may also contain appreciable amounts of calcium and to a lesser extent manganese.

Scandium is a very characteristic trace element in the pyrope-rich garnets of this group. In all probability, it substitutes for magnesium and possibly for divalent iron. Goldschmidt and Peters (1931) note that

TABLE 10. ATOMIC RATIOS OF ANALYZED YTTRIAN GARNETS CALCULATED ACCORDING TO SUBSTITUTION, $Y^{+3}Al^{+3}$ FOR $Mn^{+2}Si^{+4}$

| Composition | | Atomic Ratios* | | | Cations to Twelve O |
|---|---|---|---|---|---|
| | | *Schreiberhau* | | | |
| $SiO_2$ | 35.83 | Si | 597 | 620 | Z=3.08 |
| $Al_2O_3$ | 20.65 | | 23 | | |
| $Fe_2O_3$ | — | Al | 405 | | |
| $Y_2O_3$ | 2.64 | | 382 | 382 | Y=1.90 |
| MnO | 8.92 | $Fe^{+3}$ | — | | |
| FeO | 31.52 | | | | |
| MgO | — | | | | |
| CaO | 0.76 | Y | 23 | | |
| $H_2O$ | — | Mn | 126 | | |
| | | Fe | 439 | 602 | X=2.99 |
| | 100.32 | Mg | — | | |
| | | Ca | 14 | | |
| | | O | 2414 | | |
| | | *Elk Mt., New Mexico* | | | |
| $SiO_2$ | 34.99 | Si | 583 | 601 | Z=3.01 |
| $Al_2O_3$ | 20.76 | | 18 | | |
| $Fe_2O_3$ | — | Al | 407 | | |
| $Y_2O_3$ | 2.01 | | 389 | 389 | Y=1.95 |
| MnO | 29.60 | $Fe^{+3}$ | — | | |
| FeO | 10.76 | | | | |
| MgO | 0.17 | Y | 18 | | |
| CaO | 1.17 | Mn | 417 | | |
| $H_2O$ | 0.75 | Fe | 150 | 610 | X=3.05 |
| | | Mg | 4 | | |
| | 100.12 | Ca | 21 | | |
| | | O | 2395 | | |
| | | *Gunnison County, Colorado* | | | |
| $SiO_2$ | 36.84 | Si | 613 | 625 | Z=3.09 |
| $Al_2O_3$ | 20.75 | | 12 | | |
| $Fe_2O_3$ | — | Al | 407 | | |
| $Y_2O_3$ | 1.36 | | 395 | 395 | Y=1.95 |
| MnO | 16.80 | $Fe^{+3}$ | — | | |
| FeO | 21.51 | | | | |
| MgO | tr | Y | 12 | | |
| CaO | 1.95 | Mn | 237 | | |
| $Na_2O$ | tr | Fe | 299 | 583 | X=2.88 |
| $H_2O$ | 0.76 | Mg | — | | |
| | | Ca | 35 | | |
| | 99.97 | Na | — | | |
| | | O | 2426 | | |

* In calculating the atomic ratios, all of the yttrium must be placed in the X group of cations. When this is done, a corresponding amount of aluminum must be removed from the Y group and added to the Z group in order to achieve crystal neutrality. Thus, the substitution is $Y^{+3}Al^{+3}$ for $Mn^{+2}Si^{+4}$.

scandium follows magnesium and ferrous iron and concentrates in the ultrabasic rocks in garnet, olivine, and augite. Sahama (1936) also notes that scandium is abundant in several Finnish garnetiferous peridotites. The author found traces of scandium in 18 out of 26 garnets of this group (Table 1). Zinc was detected in 18 of these garnets and may proxy for ferrous iron as suggested in the previous group. Chromium was observed in 10 of these garnets and may replace aluminum, the respective trivalent ionic radii being 0.64 Å and 0.57 Å. Faint traces of yttrium were detected in 12 of these garnets. In this group, it may proxy for either calcium or manganese, the former, however, is generally more abundant. There are no instances where yttrium becomes more than a trace constituent of the garnets of schists. Yttrium, then, is the most characteristic trace constituent of the pegmatite garnets whereas scandium may occur in both pegmatite and schist garnets, but is more at home in the latter environment.

### Group III. Accessory Elements Associated with Garnets of Tactites

This group invariably contains major amounts of calcium and iron and may also contain appreciable amounts of chromium. Schorlomite, the titanium-rich garnet also belongs here. Calcareous contact metamorphic rocks or tactites are the type environment for this group. Wright (1938) notes that grossularite and andradite represent over 90% of the garnet molecules in these rocks and that it is possible to estimate the composition by determining the index of refraction alone. It is interesting to note that manganese was detected in all of the garnets of this group in small amounts (Table 1). The author has not found any variety of garnet that is entirely free of manganese.

Chromium and titanium are the most characteristic accessory elements found in this group and may produce the less common uvarovites and schorlomites. Strontium was observed in a few of the garnets of this group and may replace calcium, the respective radii being 1.27 Å and 1.06 Å.

One sample, a schorlomite from Colorado, contained a trace of niobium. Pentavalent Nb has an ionic radius of 0.69 Å and should proxy for quadrivalent Ti possessing a radius of 0.64 Å. Inasmuch as only one true schorlomite was studied, the prevalence of niobium in schorlomites is not significant. However, the presence of this element in garnet has been noted by Rankama (1949) who has emphasized the affinity of niobium for titanium minerals.

### Conclusions

1. A survey of the literature plus independent visual spectroscopic analyses of more than 70 garnets reaffirms Wright's study of the associations of certain garnets with particular rock types.

2. Yttrian garnets are not as rare as previously suspected and are characteristically associated with pegmatites. They are not to be classed with the andradites as indicated by Dana but rather with the spessartites.

3. Yttrium occurs in some pegmatite garnets in concentrations of greater than 2% $Y_2O_3$ where it may proxy for manganese. The substitution appears to be $Y^{+3}Al^{+3}$ for $Mn^{+2}Si^{+4}$.

4. Traces of the other rare earths, particularly Dy, Gd, and to a lesser extent Ho, Er, Yb, Ce, La, Nd, and Pr, not previously detected in garnets were found in spessartite.

5. Scandium is a characteristic trace constituent of the magnesium and iron rich schist garnets and to a lesser extent of pegmatite garnets.

6. Traces of Ga, Ti, Li, Na, F, Zn, Cr, Sr, Nb, V, Be, B, Ge, Sn, Pb and Cu are present in garnets.

## Acknowledgments

This investigation was conducted under the general direction of P. M. Ambrose, Chief, Metallurgical Division, College Park Branch, Bureau of Mines, and under the supervision of H. F. Carl, Chief, Chemical and Physical Section, of the same agency.

The author is especially indebted to Charles Milton, U. S. Geological Survey, for supplying an unpublished analysis of an yttrian garnet, for furnishing several samples of garnets, and for valuable criticisms; to H. S. Yoder, Geophysical Laboratory, for synthesizing yttrian spessartites and for valuable criticisms and suggestions; to A. M. Sherwood, formerly of the Bureau of Mines, for making most of the chemical analyses without which this investigation would not have been successful; to M. J. Peterson and G. E. Ashby, both of the Bureau of Mines, for making spectrographic and *x*-ray analyses, respectively, of several yttrian garnets; to Alton Gabriel, Bureau of Mines, for a critical review of the manuscript; and to Michael Fleischer, U. S. Geological Survey, for furnishing pertinent references and helpful suggestions during the course of the investigation. Several of the samples described in this paper were furnished through the courtesy of E. P. Henderson of the U. S. National Museum.

## References

Alderman, A. R. (1935), Almandine from Botallack, Cornwall: *Mineral Mag.*, **24,** 42–48.

Benedicks, C. (1906), Yttriumhaltiger Mangangranat: *Bull. Geol. Inst. Upsala*, **7,** 271–277.

Björlykke, H. (1937), The granite pegmatites of southern Norway: *Am. Mineral.*, **22,** 241–255.

Dana, E. S. (1892), A System of Mineralogy, 6th Ed. 440–444.

Fermor, L. L. (1926), On the composition of some Indian garnets: *Records Geol. Surv. India*, **59,** 191–207.

Fleischer, M. (1937), The relation between chemical composition and physical properties in the garnet group: *Am. Mineral.*, **22,** 751–759.

Ford, W. E. (1915), A study of the relations existing between the chemical, optical and

other physical properties of the members of the garnet group: *Am. Jour. Sci.*, 4th Ser., **XL,** 33–49.

Gabriel, A. G., Jaffe, H. W., and Peterson, M. J. (1947), Use of the spectroscope in the determination of the constituents of boiler scale and related compounds: *Proc. A.S.T.M.*, **47,** 1111–1120.

Goldschmidt, V. M. (1929), Crystal structure and chemical constitution: *Trans. Farad. Soc.*, **XXV,** 258, 282.

——— and Peters, C. (1931), Zur geochemie des scandiums: *Nachr. Gess. Wiss, Göttingen, Math-Phys., Kl,* pp. 264–267.

——— (1945), The geochemical background of minor element distribution: *Soil Sci.*, **60,** No. 1, 1–7.

Heritsch, F. (1926), Studien über den chemismus der granaten: *Neues Jahrb. Mineral., Geol.*, Band **55A,** 60–91.

Hess, H. H. (1949), Chemical composition and optical properties of common clinopyroxenes: *Am. Mineral.*, **34,** 621–667.

Iimori, T. (1938), Tengerite found in Iisaka and its chemical composition: *Sci. Papers, Inst. Chem. Res., Tokyo,* **34,** 832–841.

Jackson, W. W., and West, J. (1930): *Zeit. Krist.*, **76,** 211.

Jaffe, H. W. (1949), Visual arc spectroscopic detection of halogens, rare earths and other elements by use of molecular spectra: *Am. Mineral.*, **34,** 667–675.

Levin, S. B. (1949), The physical analysis of polycomponent garnet; Presented, 30th Annual Meeting, Mineral Soc. Amer., El Paso, Texas.

Menzer, G. (1928), Die Kristall Struktur von granat: *Zeit. Krist.*, **69,** 300–396.

Milton, C. (1937), in *U.S.G.S., Bull.* **878,** Analyses of Rocks and Minerals, p. 101.

Minami, E. (1935), Gehalte an seltenen Erden in europaischen and japanischen Tenschiefern: *Nachr. Gess. Wiss, Göttingen, Neue, Folg.*, Band **1,** No. 14, 155.

Mosebach, R. (1938), Pegmatites and their minerals: *Senckenbergiana*, **20,** 443–462; (1939), *Neues Jahrb. Mineral., Geol.*, Ref. **1,** 548–549.

Peterson, M. J., Kauffman, A. J., and Jaffe, H. W. (1947), The spectroscope in determinative mineralogy: *Am. Mineral.*, **32,** 322–335.

Rankama, K. (1948), On the geochemistry of niobium: *Suom. Tied. Toim. Ann. Acad. Sci. Sarja,* Ser. A. **III,**, 22–34.

Sahama, Th. G. (1936), Akzessorische Elements in den Granulitin von Finnisch-Lappland: *Bull. Geol. de Finl.*, **IX,** *Bull., Comm. Geol. de Finl.*, **115,** 267.

——— and Vähatälo, V. (1939), *X*-ray spectrographic study of the rare earths in some Finnish eruptive rocks and minerals: Extrait des *Compt. rend. de la Soc. Geol. de Finl.*, **XIV,** 79–80.

——— (1946), On the chemistry of the mineral titanite: *Bull. Comm. Geol. de Finl.*, **138,** 88–118.

Shand, S. J. (1943), Eruptive rocks, 2d ed. Ch. VIII, 127–136.

Shannon, E. V. (1927), Blythite: *J. Wash. Acad. Sci.*, **17,** 444.

Stockwell, C. H. (1927), An *x*-ray study of the garnet group: *Am. Mineral.*, **12,** 327–344.

*U.S.G.S., Bull.* **878,** (1937), Analyses of Rocks and Minerals, 101.

Van der Lingen, J. S. (1928), Garnets, South Afr.: *Jour. Sci.*, **XXV,** 10–15.

Winchell, A. N. (1933), Optical Mineralogy, Part II, 3rd Ed. 174–183.

Wright, W. I. (1938), The composition and occurrence of garnets: *Am. Mineral.*, **23,** 436–445.

Zachariasen, W. (1930), *Zeit. Krist.*, **73,** 7.

Zedlitz, O. (1933), Lime-iron garnets rich in titanium: *Centr. Mineral. Geol.*, 225–239.

——— (1935), Titaniferous calcium-iron garnets. II. *Centr. Mineral., Geol.*, 68–78.

*Manuscript received*
*May 31, 1950*

# NOTES AND NEWS

## MINERALS OF THE EASTERN SANTA MONICA MOUNTAINS, LOS ANGELES CITY

GEORGE J. NEUERBURG, *Department of Geology, University of California, Los Angeles.*

Mineral occurrences in the eastern Santa Monica Mountains are for the most part unrecorded. Some of these occurrences are of interest, and attention will be brought to them here. The more interesting localities are marked on the map (Fig. 1). The map shows that part of the Santa Monica Mountains north of Los Angeles from the University of California to the Los Angeles River on the east end of the mountains. The geology of the region has been described by Hoots (1931). The writer has a detailed investigation of this area in progress.

ZEOLITES. Zeolites and related minerals are common in the basalts of the Middle Miocene section, and have 3 types of occurrence. Amygdules, wholly or partly filled, comprise the most common type. Veins occur in a few localities. Zeolites and associated minerals occur interstitial to and replacing peripheral portions of the pillows in the pillow basalt exposed in Cahuenga Pass.

Most of the amygdaloidal basalts are intrusive; amygdules are irregularly distributed within any one intrusive with no evident relation to the shape of the intrusive. All of the vesicular basalts in this area contain amygdaloidal fillings.

The three modes of occurrence show some differences in mineralogy. Amygdules contain mostly natrolite with later analcite. Pyrite, pectolite, and griffithite occur, but are rare. Griffithite was first described from the basalts at the south end of Cahuenga Pass (Larsen and Steiger, 1917) (locality 1). This chlorite mineral also occurs in the Pacific Electric quarries in Brush Canyon (locality 2). Large, weathered, allotriomorphic amygdaloidal fillings of leonhardite, a variety of laumontite, occur at the south end of Caheunga Pass (locality 3) and along Mulholland Drive just west of Cahuenga Pass (locality 4).

Groups of radial natrolite crystals completely fill vesicles in a sill at the head of Brush Canyon (locality 5). The core of each radial natrolite group is colored a uniform pink. The contact between the pink and the outer white natrolite is sharp. There is a considerable disparity in grain size between the two colored varieities of natrolite, the pink variety being much finer grained. The color fades to disappearance after exposure for a few weeks. The color is suggestive of one of the oxidation states of

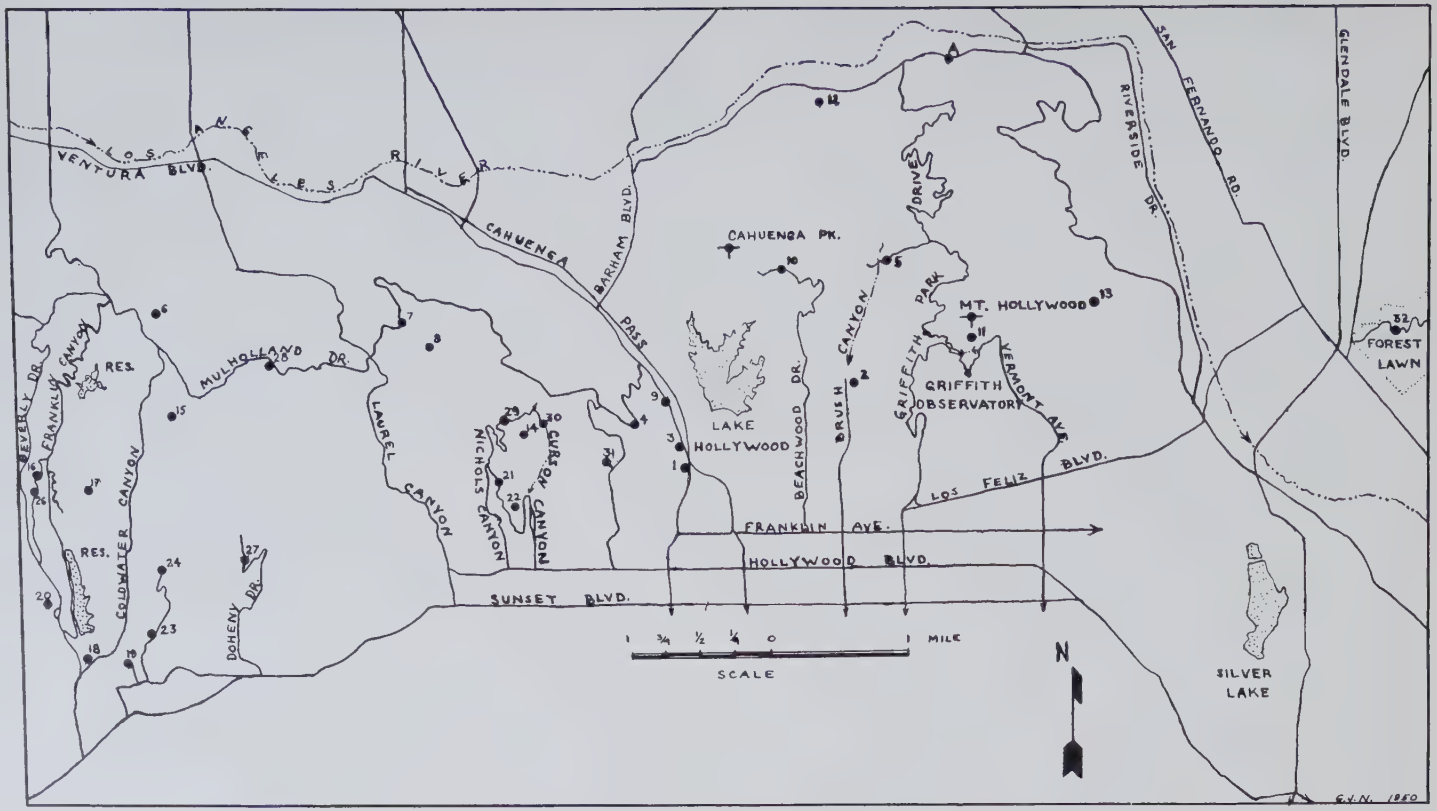


FIG. 1. Index map showing mineral localities of the Eastern Santa Monica Mountains.

manganese. In some places films of manganese oxides cover fracture surfaces in the basalt.

Incompletely filled amygdules in a pillow basalt at the head of Coldwater Canyon (locality 6) contain sheaf-like aggregates of tabular stilbite (?) crystals. Some of the amygdules are much larger and contain, in place of stilbite(?), cotton-like aggregates of a very fine fibrous white unidentified zeolite.

Veins with zeolites were found in only three localities, the Pacific Electric quaries in Brush Canyon (locality 2), the south end of Cahuenga Pass (locality 3), and on Mulholland Drive just east of Laurel Canyon (locality 7). The veins in Brush Canyon are thin, discontinuous, and vuggy. Prehnite occurs as deep sea-green, reniform crusts and as white fibrous aggregates pseudomorphous after tabular barite(?); the pseudomorphous crystals are perched on the reniform prehnite. One side of a large vuggy vein is exposed on a quarry wall. In this vein the most common mineral is trapezohedral analcite with natrolite and a minor amount of apophyllite perched on the analcite. Veins of pure apophyllite and natrolite also occur. The apophyllite crystals in these veins are tabular, pseudohexagonal, and up to about the size of a silver dollar. A single irregular veinlet of platy thomsonite was found at locality 2.

The veins at the south end of Cahuenga Pass contain calcite scalenohedrons and green prehnite. They occur in the basalt containing the leonhardite amygdules.

Rosettes of aragonite occur on fracture surfaces and in veins in an amygdaloidal basalt agglomerate just west of Laurel Canyon (locality 7). Associated minerals are natrolite, analcite, calcite, and several unidentified zeolites. Near here, amygdules of natrolite the size of a hen's egg occur in a basalt flow (locality 8).

In the pillow basalt of Cahuenga Pass (locality 9), pink heulandite occurs as selvages on the pillows. Veins and stringers of opaline and chalcedonic quartz occur in the interstices of the nested pillows and as replacements of basalt along the peripheries of the pillows and on either side of veinlets within the pillows. Crystal cavities with shapes suggestive of calcite rhombohedrons occur in many of these veins and are partly filled with clusters of capillary crystals of ptilolite and/or mordenite. Calcite, natrolite, pyrite, hematite pseudomorphs after pyrite, and an unidentified dull brownish black tabular mineral were found in the central parts of some of these quartz veins.

Zeolites are abundant in the many exposures of basalt on the northern side of the mountains west of Cahuenga Pass. This area of basalt exposure has not been investigated by the writer and many localities have probably been overlooked.

Sulfates. A sandy conglomerate just east of Cahuenga Peak (locality 10) contains a minor proportion of altered pyritiferous diabase boulders. These boulders are in various stages of alteration and contain pyrite, halotrichite, melanterite, jarosite(?), adularia, gypsum, and calcite.

The fresh diabase is a fine-grained bluish black rock. The altered boulders consist of a soft clay-like material in the center surrounded by hard shells of light yellow and red-brown, altered diabase. The clay-like center is of two types, a soft, yellow waxy material containing mostly gypsum and calcite and a dark bluish gray material containing the greater quantity of sulfates.

Pyrite occurs in the fresh material and in the dark blue-gray clayey material as small shiny grains. Halotrichite is limited to the bluish material, and fills abundant veinlets, $\frac{1}{8}$ to $\frac{1}{4}$ inch wide, in which the fibers are perpendicular to the walls. A small amount of halotrichite has been redeposited by ground waters in the form of loose, "corroded" crystals on the surfaces of diabase boulders. Melanterite is found as small clusters of colorless and light greenish crystals in cavities in the yellow waxy material and on the weathered surfaces of the boulders containing the bluish material. Jarosite(?) occurs as minute dust-like, orange-colored grains on fracture surfaces in both the yellow and bluish clay material.

Other Minerals. Massive and drusy veins of calcite are common in the region. East of Cahuenga Pass, massive veins of coarse colorless calcite are found in all rock types. A vein just south of Mt. Hollywood yields fluorescent specimens (locality 11). Calcite from the veins along the Los Angeles River (locality 12) was mined by the early Spanish settlers who had a lime kiln nearby (locality A). Similar veins are found near the east end of the mountains (locality 13).

West of Cahuenga Pass, calcite veins are mostly confined to shear zones in quartz diorite. These veins are vuggy with flat rhombohedral calcite crystals having an iridescent coating of limonite. These crystals make quite showy specimens. They are found at the head of Nichols Canyon (locality 14), at the head of Coldwater Canyon (locality 15) and in Franklin Canyon (localities 16 and 17).

Abundant crystals of chiastolite occur in intensively sheared spotted slates and in some unsheared spotted slates at the mouth of Coldwater Canyon (localities 18 and 19). The crystals show no preferred orientation and were formed after the shearing. They are largely pseudomorphs composed of fine fibrous aggregates of muscovite.

Cubes of fluorite, averaging half an inch on a side, occur with calcite and milky quartz in cavities in a fault breccia on the west side of Higgins Canyon (locality 20). The fluorite cubes are partly replaced by calcite and have a thin crust of fine calcite crystals.

A single large platy crystal of molybdenite was found with pyrite in a quartz vein in the chiastolite spotted slates at the mouth of Coldwater Canyon (locality 18).

Thin acicular crystals of black tourmaline occur in small patches of fine-grained chlorite in quartz veins along shear zones in quartz diorite on the east side of Nichols Canyon (locality 21). Farther south on the same side of Nichols Canyon (locality 22), similar crystals occur in a quartz-feldspar-muscovite pegmatite vein in quartz diorite. Similar pegmatitic veins of black tourmaline, quartz, and feldspar occur in phyllite on the east side of Coldwater Canyon (localities 23 and 24), and at the head of Peavine Canyon (locality 25). Dravite occurs in a quartz vein in phyllite on the west side of Franklin Canyon (locality 26).

A bed of calc-silicate hornfels, consisting of wollastonite, diopside, and garnet also occurs at locality 26.

Small, white, dense, very fine-grained veinlets of zoisite occur in albitized malchite intrusions and in albitized quartz diorite in Doheny Canyon (locality 27), along Mulholland Drive (locality 28), in Nichols (locality 29), Curson (locality 30), and Outlook (locality 31) Canyons, and in Forest Lawn just east of Griffith Park (locality 32). These veinlets would appear to have originated as a consequence of the albitization of the malchite and surrounding quartz diorite.

Localities 2, 10, 16 and 18 are listed by Murdoch and Webb (1948).

### References

Hoots, Harold W. (1931), Geology of the eastern part of the Santa Monica Mountains, Los Angeles County, California: *U. S. Geol. Surv., Prof. Paper*, **165-C.**

Larsen, Esper S., and Steiger, G. (1917), Mineralogic notes: *Jour Wash. Acad. Sci.*, **7,** 11.

Murdoch, Joseph, and Webb, Robert W. (1948), Minerals of California: *Calif. Div. of Mines, Bull.* **136.**

## A NOTE ON THE FLUORESCENCE OF WYOMING BENTONITE

H. R. Samson*

A recent paper[1] describes a method which differentiates swelling clays of the montmorillonite group from kaolinite, illite, attapulgite and halloysite, and, futhermore, provides an estimate of certain physical proper-

* An officer of Division of Industrial Chemistry, Commonwealth Scientific and Industrial Research Organization, Melbourne, Australia.

[1] Brown, B. W., A fluorescence study of Wyoming bentonite: *Am. Mineral.*, **34,** 98, (1949).

ties of bentonites. The technique consists of moistening the dry clay with a solution of zinc uranyl acetate and exposing it to ultra-violet light. Under these conditions, it is stated, swelling bentonites fluoresce immediately, whereas other clays do not. The explanation advanced is "interfacial dehydration of the zinc uranyl acetate and ultra-violet fluorescence of the anhydrous salt." This phenomenon arises from "the dehydrating powers of the clay involving free energy levels of the order chemisorption."

It may be readily demonstrated, however, that such fluorescence could be due to sodium zinc uranyl acetate, a strongly fluorescent material, which is precipitated by the exchangeable $Na^+$ of the clay mineral. Since the reagent contains a quantity of $Zn^{++}$ in excess of that required for precipitation of $NaZn(UO_2)_3(C_2H_3O_6)_9 \cdot 6H_2O$, the original $Na^+$ would presumably be replaced by $Zn^{++}$.

Naturally occurring montmorillonites, e.g. Wyoming bentonite, generally contain appreciable quantities of $Na^+$, as well as $K^+$, $Ca^{++}$, $Mg^{++}$ as exchangeable ions. Consequently, they fluoresce more or less intensely, depending upon the quantity of $Na^+$ present. If, however, a sample of Wyoming bentonite is leached with $CaCl_2$ solution to remove all cations excepting $Ca^{++}$, no fluorescence is observed.

Further, since the solid sodium zinc uranyl acetate fluoresces intensely, even a coarse-grained kaolinite, if its exchange positions are saturated with $Na^+$, should give a positive test.

To verify this, a sample of kaolinite (cation exchange capacity = 3.8 milliequivalents/100 gm.) was treated with just sufficient NaOH to ensure saturation, the pH of the resultant suspension being 7.0. When a dried specimen of this clay was moistened with the reagent and irradiated with ultra-violet light, an intense fluorescence was observed.

The correlation between intensity of fluorescence and gell strength, green compressive strength, etc., follows from the fact that such properties are largely controlled by the nature and amount of exchangeable ions present.

If a positive test is obtained, it may be assumed that the clay mineral contains adsorbed $Na^+$. This cannot, however, be taken as an indication of the presence of montmorillonite, nor indeed of any particular clay mineral. Brown mentions that "the part the sodium plays has not been determined, but it may prove to be considerable." It is not clear whether this refers to the actual fluorescence, or to the hydration of the montmorillonite. In any case, precipitation of sodium zinc uranyl acetate seems a more likely explanation of the fluorescence than a process of "interfacial dehydration."

## A GRAPHICAL SIMPLIFICATION OF THE RELATIONSHIP BETWEEN 2V AND Nx, Ny AND Nz

C. P. Gravenor, *University of Wisconsin, Madison, Wisconsin.*

This diagram like those of F. E. Wright (3) and H. T. U. Smith (2) yields the value of 2V if the three refractive indices of a biaxial crystal are known, or yields the value of the third refractive index if 2V and the other two indices are known. The advantage offered: that the sign of the crystal is automatically indicated and no sliding scales are needed. It is the graphic solution of the same equation,

$$\text{Tan}^2 \text{V} = \frac{\text{Nz} - \text{Ny}}{\text{Ny} - \text{Nx}}$$

in simplified form.

The use of the diagram is expressed in the key inserts. Abscissa and ordinate scales are the partial birefringences, the ordinate being the larger and the abscissa the smaller of the two. Nz−Ny is found on the right side and Ny−Nx on the left of the diagram, the larger as the ordinate. The radial through the point of intersection gives 2V and the side of the diagram on which the point of intersection falls gives the sign.

Two examples will illustrate:

| | | |
|---|---|---|
| (1) | Nx=1.596 | 2V is unknown |
| | Ny=1.600 | Ny−Nx=.004 |
| | Nz=1.612 | Nz−Ny=.012 |

.012, the larger of the partial birefringence values, is found on the right hand ordinate scale—the right hand since it is Nz−Ny and the ordinate since it is the larger. .004, the smaller value is found on the left hand abscissa scale. The radial through the point of intersection indicates a 2V of 60° and the sign is positive.

| | | |
|---|---|---|
| (2) | Nx=1.582 | Nz is unknown |
| | Ny=1.590 | Ny−Nx=.008 |
| | 2V=70° (−) | |

As in the above case the larger value is again applied to the ordinate scale. Hence, it must be reasoned out as follows: generally, Ny is above the midpoint between Nz and Nx in a negative mineral and below in a positive mineral. Therefore, in a negative mineral Ny−Nx is the larger and Nz−Ny the smaller partial birefringences. In this case then, .008 is the ordinate. This intersects the 2V radial at the abscissa value .004 which is Nz−Ny. Hence, Nz=1.594.

In laboratories which take advantage of the dispersion of the Becke line, by using immersion media of high rather than low dispersion (1), a special advantage accrues. Such laboratories ordinarily use the Hart-

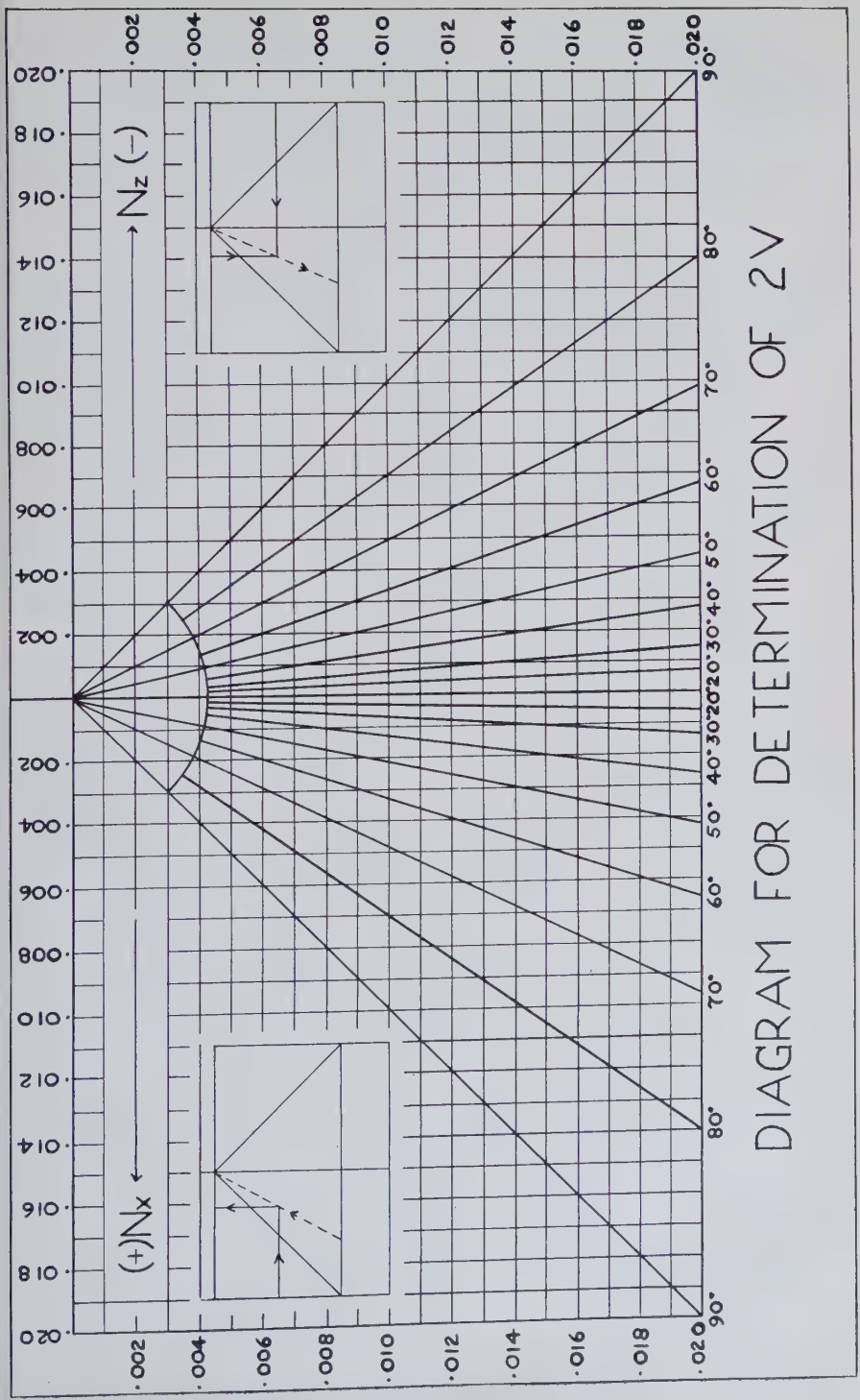
DIAGRAM FOR DETERMINATION OF 2V
(+)Nx
Nz (-)
.002
.004
.006
.008
.010
.012
.014
.016
.018
.020
90°
80°
70°
60°
50°
40°
30°
20°

mann net for the speed and accuracy it affords. For this use the coordinate scale divisions should agree with those of the net. Then, the D line of the net is made to coincide with these scales, the Ny value being 0. Nz−Ny and Ny−Nx are used directly without subtraction. For minerals of high birefringence the scale divions may be multiplied.

The diagram is constructed as follows: use the approximate formula

$$\text{Tan V} = \frac{\text{Nz} - \text{Ny}}{\text{Ny} - \text{Nx}}.$$

Allow Nz−Ny to equal unity and vary the value of V from 0° to 45°; obtain values for Ny−Nx ranging from 0 to 1 and varying in a function of $\text{Tan}^2$. If the value of Nz−Nx is then increased in arithmetic progression, corresponding values of Ny−Nx can be obtained for any value of V.

### References

1. Emmons, R. C., and Gates, R. M., *Am. Mineral.*, **33,** 612–618 (1948).
2. Smith, H. T. U., *Am. Mineral.*, **22,** 675–681 (1937).
3. Wright, F. E., *Carnegie Inst. Publ.* **158,** Washington, 142–200 (1911).

## AN IMPROVED "DIAMOND" MORTAR

William C. Oke, *California Institute of Technology, Pasadena, California.*

While the conventional "Diamond" mortar is efficient for grinding or crushing, it is almost impossible to clean it effectively so that no particle of the material ground is left to contaminate the next grinding.

The writer designed, and first made about ten years ago, an improved mortar which is cleaned very easily. Instead of a hole in the mortar it has a projection and the grinding hole is obtained by a close fitting sleeve around the projection. The pestle is a close working fit in the upper part of the sleeve as in the conventional mortar. After grinding, the sleeve is removed and the ground up material is shaken or brushed from the top. The face of the projection, which does the grinding, is cleaned very easily, but if any material adheres to the face it may be rubbed lightly over a sheet of fine sand paper. The face of the pestle is cleaned in the same manner.

The mortar proper is made from $1\frac{3}{4}$ inch round machine steel turned to the dimensions shown in the drawing. The sleeve is $1\frac{1}{8}$ inch by 10 gauge Shelby tubing, the inside bored, or drilled and reamed, to exactly $\frac{3}{4}$ inch, and both inside edges slightly chamfered so as to allow it to fit down tight on the mortar. The pestle is made from a piece of $\frac{3}{4}$ inch round machine steel, turned as shown in the drawing. The top part may be knurled or left plain as desired.

Both pestle and mortar should be sent to a commercial heat treating house to be carburized to a depth of at least $\frac{1}{8}$ inch and hardened to 62–64 Rockwell C. It is not necessary to harden the sleeve although it may be cyanided.

After heat treating the mortar is chucked in the lathe and the diameter of the projection is ground with a tool post grinder to a tight, but re-

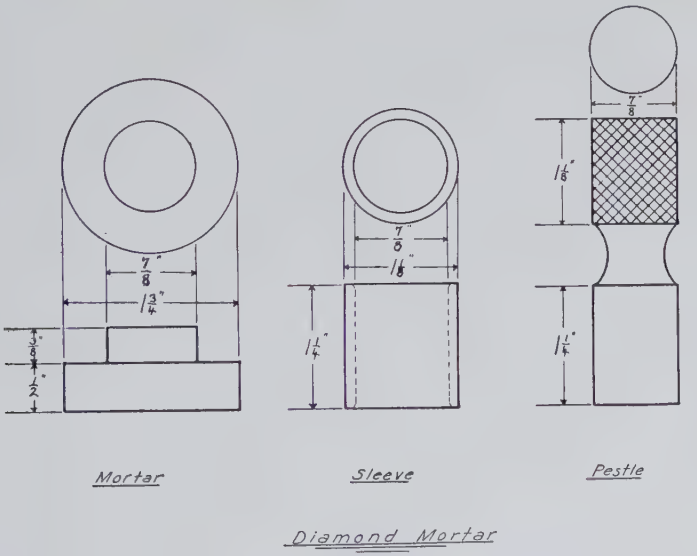


Fig. 1

movable, fit to the sleeve. The face of the projection should be ground true to the side at the same chucking. The pestle is also chucked and the diameter of the grinding end reduced about .005 inch, or a working fit in the sleeve. The face of the pestle should also be ground true with the side.

## A NEW LOCALITY FOR GREENOCKITE CRYSTALS IN BOLIVIA

Frederico Ahlfeld, *Cochabamba, Bolivia.*

Greenockite is a rare mineral in the Bolivian tin deposits. It has been described only from Llallagua by S. Gordon (1). The mineral forms coatings of minute red crystals, resembling vanadinite in colour, upon quartz, marcasite, cassiterite and on the wall rock, almost always associated with wavellite. The crystals are exceedingly minute, rarely measuring as much as 0.1 mm. They vary greatly in habit from pyramidal to thick tabular and prismatic. Cyclic twins are common. Gordon ascribes the formation of the mineral to supergene solutions. The source of the cadmium may have been from the wurtzite or sphalerite which has relaced pyrrhotite.

Recently I found a second occurrence of greenockite in Bolivia, which is remarkable for the larger size and the rich red colour of the crystals. The crystals are probably the finest ever found of this rare mineral.

The crystals were found in the Asunta tin-silver mine, 4 kms. northeast of San Vicente, a silver district in the Sud Chichas province, Department of Potosi. Here, lode-like bodies of a mineralized breccia in Ordovician metamorphosed shales pass in depth into real veins. In a first stage of mineralization, quartz, yellowish fine-grained cassiterite, and pyrite have been formed. In a second stage, the "Veta Chica," a small silver vein cutting the breccia, was formed. The vein has a complex mineralization with pyrite, dark grey fine-grained cassiterite, stannite, alunite, miargyrite, canfieldite(?), barite, franckeite, and greenockite. Franckeite is the most common mineral of the second stage. It is also found in the vugs and fissures of the brecciated shales outside of the vein.

In the fissures and small vugs the greenockite crystals form coatings upon pyrite, franckeite, canfieldite(?), and on the wallrock. They are 0.5 to 2 mm. in size, have a strong adamantine luster, and are generally of a deep red, garnet-like colour, but I also found crystals resembling realgar in colour. Some of them are covered by earthy orange greenockite and partially replaced by it.

All crystals are dihexagonal pyramids, sometimes twinned with twin plane parallel to (0001). Cyclic twins are absent.

I found the mineral in the 56 m. and 150 m. levels. It is obviously a hypogene mineral, the latest in the paragenesis. The source of the cadmium has not been determined. Sphalerite and wurtzite do not occur in the vein which contains the greenockite crystals.

### Reference

1. Gordon, Samuel G., Greenockite from Llallagua, Bolivia: *Notulae Naturae of the Acad. of Nat. Sci., Philadelphia*, No. **1** (1939).

# BOOK REVIEWS

X-RAY OPTICS. The Diffraction of X-rays by Finite and Imperfect Crystals, by A. J. C. Wilson (Department of Physics, University College, Cardiff), pp. viii+128, 4½ by 7 inches, 33 figs. Cloth. Methuen & Co., Ltd., 36 Essex St., London, W.C. 2. **1949**. Price 6s.

This is the forty-fifth of "Methuen's Monographs on Physical Subjects" (B. L. Worsnop, ed.), among which crystallographers still remember "X-Ray Crystallography" by R. W. James and "X-Rays" by Worsnop and Chalklin. As stated on the flap of the jacket, this series is intended for readers of "average scientific attainment," such as "the Honours student and the research worker in other branches of physics."

The book deals with the effect on $x$-ray reflections of crystal size and of such crystal imperfections as are due to strain, structural mistakes, distortion, and thermal motion. This, the first connected account to appear in the field, is very satisfying in most respects. The interpretation of $x$-ray diffraction patterns rests on the reciprocal lattice (Ch. II). The reciprocal space corresponding to small crystals is studied (Ch. III) as a prerequisite for the treatment of line broadening (on powder patterns) as a function of crystal size and shape (Ch. IV). In faulty crystals the structure amplitude has different values in different cells, which vary in cell contents. The general calculation is given for mistakes in layer structures—the most common case (silicates, cobalt, graphite); as to the (much rarer) mistakes "in three dimensions" ($AuCu_3$), their effect on powder patterns is treated like that of crystal size (Ch. V–VI). Complex quantities are then introduced, briefly but adequately (Ch. VII), in order to cope with the more difficult problems encountered in the preceding two chapters and with the added complication of crystal distortion (cells varying in size and shape as well as in contents). The latter is illustrated (Ch. VIII) by $Cu_4FeNi_3$ and by copper aluminum alloy (4 wt.% Cu). A discussion of the effects of thermal agitation (Ch. IX) completes the book.

The presentation is condensed, yet lucid and elegant. Professor Wilson uses no more mathematics than he needs (probabilities, integral calculus, complex quantities, but no vectors) and introduces it gradually, "the earlier chapters requiring little more than elementary trigonometry." Having done considerable research himself on almost all the problems he covers, he knows whereof he speaks.

The book has been reviewed by H. Jagodzinski (*Acta Crystallographica*, **2,** 340, 1949), by F. A. Bannister (*Min. Abs.*, **10,** 504, 1949), and by A. R. Stokes (*Science Progress*, **37,** 749, 1949).

J. D. H. Donnay
*The Johns Hopkins University*

ECONOMIC MINERAL DEPOSITS by Alan M. Bateman, second edition, John Wiley & Sons, Inc., New York, 1950. Pp. 916, Illus. 308. Price $7.50.

The first edition of this excellent text was published in 1942 (*Am. Mineral.*, **28,** 340–341). In the second edition, the outline of the first is retained and the material is divided into three parts: (I) Principles and Processes (415 pages), (II) Ore Deposits (213 pages), and (III) Nonmetallic Mineral Deposits (245 pages). Following an introduction and interesting historical review, the principles relating to the formation of mineral deposits are covered in the following chapters: Materials of Mineral Deposits and Their Formation; Magmas, Rocks and Mineral Deposits; Processes of Formation of Mineral Deposits; Controls of Mineral Localization; Folding and Faulting of Mineral Deposits; and Classifications of Mineral Deposits. Important revisions in this part of the text have eliminated cer-

tain duplications evident in the earlier edition and have permitted a more comprehensive review of the major topics without greatly increasing the size of the book.

The author gives a clear outline of the crystallization and differentiation of the magma and an impartial summary of the prevailing views as to the origin of the ore fluid. He attributes the formation of contact silicates and certain deposits of the contact metasomatic type to an early vapor phase but regards most hydrothermal deposits as the product of late residual fluids which may leave the magmatic environment either as liquids or as gases which later condense to liquids.

In the important chapter on the formation of mineral deposits, nine processes are distinguished and each is clearly explained. Outstanding are the sections on Magmatic Concentration, Residual and Mechanical Concentration, and Oxidation and Supergene Enrichment. Proper emphasis is given to hydrothermal deposition with a detailed description of both open filling and replacement. Sublimation, Contact Metasomatism, Sedimentation, Evaporation, and Metamorphism complete the list of nine processes.

Bateman presents a genetic classification of mineral deposits with nine major divisions, each corresponding to a process of mineral formation. In the classification of the hydrothermal deposits, he emphasizes processes and structural control rather than intensity of deposition and recognizes two subdivisions, deposits due to open filling and those due to replacement. The major classes proposed by Lindgren, hypothermal, mesothermal and epithermal, are reviewed briefly and the terms are used by the author to define the intensity range of many individual deposits.

From the standpoint of teaching, a more extended discussion of wall-rock alteration, intensity and geologic environment of ore deposition, and hypogene zoning might be desired. However, this is largely a matter of personal opinion, and on the whole the basic subjects are adequately covered, clearly presented and in proper balance.

Additional chapters in Part I are devoted principally to mineral resources, geophysical prospecting and extraction of metals.

Part II gives a concise summary of representative ore deposits arranged by metals. Pertinent information is given on production, distribution, uses and technology of each metal, and this is followed by a survey of the geologic occurrence with a list of the major deposits arranged by genetic type. The individual districts are well selected and the descriptions, although necessarily brief, give the essential facts as to the ore deposits. The information is up-to-date and the major post-war developments have been noted. A more detailed description of certain significant deposits might be included, such as the iron ores of the Lake Superior district, the Tri-State zinc deposits and the mixed ores of the San Juan region.

Part III, comprising ten chapters, covers the nonmetallic products grouped according to their principal use. Eight chapters give an up-to-date, systematic review of the industrial minerals, with an account of important technological as well as geological features. The section also includes a summary of coal (18 pages), petroleum and gas (41 pages) and ground-water supplies (19 pages).

A few inaccurate statements were noted as well as a few typographical errors, but these are of minor importance. The material, which covers a wide field, is well organized and the illustrations are exceptionally good. The book is outstanding as a text for the first courses in economic geology and it constitutes a valuable reference book for engineers and geologists in the field.

F. S. TURNEAURE
*University of Michigan*

A ROMAN BOOK ON PRECIOUS STONES, including an English modernization of Pliny's 37th book of his HISTORY OF THE WORLD BY SYDNEY H. BALL, pp. xii+338, octavo, Gemological Institute of America, Los Angeles, **1950**. Price $6.75.

This book is a very important and informative contribution to the literature of gemology. It is the result of a labor of love by Dr. Sydney H. Ball, a noted economic geologist, who for many years was intensely interested in the history of gems, their occurrence, mining and superstitions concerning them. Dr. Ball's many contributions on gems include the authoritative chapters on gemstones in the *Minerals Yearbook*, and on precious stones in *Industrial Minerals and Rocks;* also the annual reviews of the diamond industry published by the *Jewelers' Circular Keystone.*

Unfortunately, Dr. Ball died before the manuscript was ready for the printers. Great credit is due Miss Kay Swindler of the Gemological Institute of America for completing the text and seeing the book through the press, which she has done very successfully.

The volume is based upon the 37th book of the *Natural History of the World* by Pliny the Elder, 23 to 79 A.D., as translated into English by Philemon Holland and printed in London by Adam Islip in 1601. In Section I, 108 pages, Dr. Ball discusses the life of Pliny and his standing as a mineralogist and gem expert. Roman jewelry, jewelers and lapidaries, geographical sources of gems, ancient commerce in gems, their value and relative rank, gem mining, treated and false stones, and industrial uses of gems in Pliny's time are described in subsequent chapters. These are followed by two comprehensive and very helpful tables, which identify Pliny's gems and minerals with their modern equivalents.

In Section II ninety-two pages are devoted to the Holland translation with a foreword by Miss Swindler. Section III contains Dr. Ball's very extensive notes, 125 pages, which explain and amplify many of Pliny's statements and allusions, or correct his errors. There is also a comprehensive index.

That Dr. Ball had been engaged for many years in preparing this volume, which involved much painstaking research, is recognized at once by the extensive documentation of Pliny's sources, and the author's many comments and references to ancient and recent publications. There can be no doubt whatever concerning Dr. Ball's very comprehensive knowledge of the literature on gems from the earliest time to the present.

A ROMAN BOOK ON PRECIOUS STONES now makes available to all mineralogists and dealers and lovers of precious stones a wealth of information, which thus far has not been readily accessible. The volume adds materially to Sydney H. Ball's reputation as an authority on gems. The Gemological Institute of America deserves great credit for publishing this volume, which is well printed and attractively bound.

EDWARD H. KRAUS
*University of Michigan*

LEITFADEN FÜR DIE EXAKTE EDELSTEINBESTIMMUNG BY K. SCHLOSSMACHER, pp. 174, 21 illustrations and 8 tables in the text, and 3 plates with 18 microphotographs, 6″×9″, E. Schweizerbart'sche Verlagsbuchhandlung, Stuttgart, Germany, 1950. Price 13.60 German marks.

The author of this manual for the determination of gemstones, Dr. K. Schlossmacher, was formerly professor of mineralogy at the University of Königsberg. He is now director of the Gemstone Research Laboratory at Idar-Oberstein. Dr. Schlossmacher is the well-known author of the third edition of Max Bauer's *Edelsteinkunde* published in 1932.

The purpose of this manual is to make available to the German gemstone industry, collectors, and lovers of gems information concerning the progress made in gemology during recent decades. The various properties which are essential in gemstone determination are discussed in an easily understood manner. These properties include specific gravity, optical properties, methods, and instruments, and hardness. The principal gems, pearls, corals, synthetics, imitations, and doublets are then briefly described. Twenty pages are devoted to a discussion of methods and tables for the determination of gemstones. Three plates con-

tain excellent microphotographs of a selected list of gems showing structural features and inclusions. These illustrations were furnished by Dr. E. Gübelin of Lucerne, Switzerland, who is a specialist in this field.

The book is well printed. It is hoped that it may appeal strongly to the German public interested in gemology.

EDWARD H. KRAUS
*University of Michigan*

## CORRECTION

(1) Vol. 33, page 344, Table I, 1948:

| *As is:* | | *As should be:* | |
|---|---|---|---|
| Number of Run | Factor | Number of Run | Factor |
| C-60 | 40.92 | C-60 | 40.78 |
| C-158 | 40.78 | C-158 | 40.64 |

(2) Vol. 35, page 221, par. 3, 1950:

*As is:*

The value of the heat of the reaction, $\Delta H$, . . . as follows 9,680 joules at 800°C.; 8,132 joules at 1,000°C.; and 8,654 joules at 1,200°C. The value of $\Delta H$ at 898.6°C. . . . is 9,426 joules.

*As should be:*

The value of the heat of the reaction, $\Delta H$, . . . as follows 169,452 joules at 800°C.; 160,498 joules at 1,000°C. and 151,503 joules at 1,200°C. The value of $\Delta H$ at 898.6 . . . is 165,017 joules.

G. T. FAUST

---

Martin Alfred Peacock, professor of crystallography and mineralogy at the University of Toronto, and past president of the Mineralogical Society of America, died on Oct. 30, 1950, at the age of 52 years.

---

Otto C. von Schlichten, associate professor of geology at the University of Cincinnati, died on Oct. 4, 1950, of a heart attack. His special fields of interest included mineralogy, petrology and the geology of southwestern Ohio.

---

The Editorial Board of the new geochemical journal, *Geochimica et Cosmochimica Acta*, consists of the following:

Professor C. W. Correns (Göttingen)
Dr. Earl Ingerson (Washington)
Dr. S. R. Nockolds (Cambridge)
Professor F. A. Paneth (Durham)
Professor L. R. Wager (Oxford)
Professor F. E. Wickman (Stockholm)
Professor Paneth will be responsible for the cosmochemical part.

The Editors will be assisted by an honorary Advisory Board, the names of its members are given on the cover of the journal. The journal will be published every second month, six numbers form one volume, and the subscription price for one volume is $9.50.